Theory of Vibrating Lifting Tools of Sugar Beet Harvesters

Volodymyr Bulgakov, Simone Pascuzzi,
Ivan Holovach, Jüri Olt, Valerii Adamchuk
and Francesco Santoro

MDPI

Theory of Vibrating Lifting Tools of Sugar Beet Harvesters

Volodymyr Bulgakov, Simone Pascuzzi, Ivan Holovach, Jüri Olt,
Valerii Adamchuk and Franceso Santoro

Theory of Vibrating Lifting Tools of Sugar Beet Harvesters

AUTHORS

Volodymyr Bulgakov and Ivan Holovach
National University of Life and
Environmental Sciences of Ukraine
Kiev
Ukraine

Simone Pascuzzi and Francesco Santoro
University of Bari Aldo Moro
Bari
Italy

Jüri Olt
Estonian University of Life Sciences
Tartu
Estonia

Valerii Adamchuck
National Scientific Centre
Kiev
Ukraine

For citation purposes, cite each article independently as indicated below:

Bulgakov, Volodymyr, Simone Pascuzzi, Ivan Holovach, Jüri Olt, Valerii Adamchuck and Francesco Santoro. *Theory of Vibrating Lifting Tools of Sugar Beet Harvesters*; MDPI: Basel, Switzerland, 2022.

Cover image by Prof Volodymyr Bulgakov, 2011, used with permission.

Contents

V

List of Figures

List of Tables

1. Introduction

The cultivation and harvesting of sugar beets (roots and leaves) is one of the most labour and energy consuming work processes in the agricultural industry.

The most important task in sugar beet farming is to improve the quality of sugar beet root crop harvesting and reduce energy costs for harvesting. This primarily concerns reductions in losses and damage of root crops, as well as a reduction in their contamination; in this case, the loss of fertile soil will be excluded, which will be removed from the fields together with the contaminated root crops. These issues present a multifaceted scientific and technical problem, which must be solved by searching for new working elements of sugar beet harvesting machines. Despite the modern level of construction of beet harvesters and their working bodies that has been achieved, there is a need to find further ways to improve them. Further research should deal with the improvement of general constructional schemes of new beet harvesters, with thorough theoretical justification of their constructions and technological parameters. The newly developed theories of functioning of improved constructions of sugar beet harvesters and their working bodies require thorough experimental verification. This will give grounds to use the obtained theoretical dependences for the final goal—analysis and generalisation of their rational parameters.

Theoretical research must play a fundamental role in the mechanical and technological substantiation of the root lifting process. It must be used as the basis for developing rational kinematic and dynamic operation conditions in order to achieve the required quality of the performed work process as well as streamlined energy consumption.

At the modern stage of the development of agricultural mechanisms, the methods of mathematical model generation based on the use of the theoretical and analytical mechanics and the application of up-to-date mathematical tools and computer technology have to be employed in the analysis and synthesis of the parameters of implements and agricultural machines overall.

Thus, the modern methods of theoretical research into the implements of sugar beet harvesters have to be based, first, on the state-of-the-art perception of the principles of the processes that take place when the roots are lifted from the soil and, second, on the possibility of describing these processes more comprehensively and systematically with the use of modern mechanical and mathematical methods. Undoubtedly, such a description only has to be provided for the principal and essential moments of the mentioned processes, while the insignificant and incidental factors must be completely neglected. Further, on the basis of the analytically determined

rational parameters of the lifting implements of sugar beet harvesters, which are subsequently experimentally validated and refined, highly reliable prototypes must be designed, which then have to be widely used by the agricultural engineering plants and companies.

Therefore, this treatise presents the fundamentals of a new theory of the lifting tools of sugar beet harvesters—in particular, vibrational lifters based on the modern methods of mechanics and mathematics.

It has been a long time since the first attempts were made (in the 1970s) to analytically describe the oscillating processes that take place during the vibrational lifting of sugar beet roots from the soil. The theory of the vibrational lifting of root crops has, overall, not been developed to a sufficient extent; the mathematical model specifically used for the process of root extraction from the soil by the vibrational lifter has not been devised. Until recently, it had been assumed that the experimental methods of determining the amplitude and frequency of oscillation of the vibrational faces—which could only have relatively limited values, subject to the reliability of the vibrational actuator—completely ensured the optimality of this whole process. However, at the present time, under the conditions of significant improvements in the reliability of designs and changes in the kinematic parameters of harvesting (for example, the increase in the travel speed to levels of up to 2.5 m·s^{-1}), the obtained values of the parameters of vibrational lifters can by no means be considered optimal. Therefore, a goal has been set to develop, first of all, a new theory of vibrational root lifting based on the generation of mathematical models, which would describe the interaction between the digging shares on the one hand and the root's body and the soil on the other hand. At the same time, the theory has to provide the mathematical descriptions of all stages of said interaction, starting from the stage of the lifter approaching the root body fixed in the soil (as in elastic medium), proceeding to the interaction of the root body with only one digging share of the lifter (asymmetric gripping of the root), followed by the interaction with both the share surfaces (symmetric gripping), and finally the eventual translation of the root along the lifting tool's throat towards the level of the soil surface. Additionally, as a matter of principle, the theory needs to consider different (possible) directions of the oscillating motions of the digging shares of the vibrational attachment—i.e., the longitudinal and transverse ones.

2. Lifting Implements of Sugar Beet Harvesters

2.1. Analysis of Existing Theoretical Studies on Sugar Beet Root Lifting Process and Lifting Implements of Sugar Beet Harvesters

Fundamental research into the work processes of agricultural machines has been carried out in the studies by P.M. Vasilenko [1–6], L.V. Pogorely [7,31,41,188,234–240], E.S. Bosoy [8], V.A. Khvostov [11,12], P.M. Zayika [27,28], V.M. Bulgakov [54–108], V.P. Goryachkin [125,161], G.D. Petrov [232,233] and others [16,18,20,29,43,46,48–53,110–114,120–126,160,164–166,169–172,179–185,187,189–197,242–261,265–270,281–286].

The general theoretical basis of the investigation, development and engineering of implements for sugar beet root harvesting machinery and the methods of substantiation of the design and process schematic models of beet harvesters as well as major agricultural practice are presented in scientific papers by Yu.B. Avanesov [1,47], P.M. Vasilenko [5,6], V. Brei [6,7,186], L.V. Pogorely [6, 7,31,41,235,237,239], N.V. Tatyanko [7,31,186], B.M. Gevko [9,10,19,115–117], S.V. Siny [10], V.A. Khvostov [12,163], V.M. Bulgakov [15,59,61,106,108,241,271–280], N.M. Zuyev [37,119,167,168], Ya.I. Kozibroda [61,177,178], A.P. Gurchenko [106,162], A.A. Vasilenko [109], V.S. Glukhovsky [118,119], S. Pascuzzi [127–159], Yu.I. Kovtun [173–186], A.G. Tsimbal [186], F. Santoro [198–231], M.L. Pogorely [240], and N.M. Khelemendik [262–264].

The theoretical studies on the operation of a majority of agricultural machines are concerned with the investigation of their motion or the motion of their implements. The most thorough studies with regard to the problem of developing mathematical analytical models of the motion of agricultural machines and mechanisms have been written by P.M. Vasilenko [1–6]. The results of these studies have to be used in the research into the motion of roots under the action of the work faces of sugar beet harvesters' lifting implements.

The fundamental paper under the editorship of academician L.V. Pogorely [7] represents the results of diverse studies on the issues of beet harvesting mechanisation. The paper presents the analysis and the principles of substantiation of parameters of beet harvester implements such as topping tools, root top cleaners, lifting implements, and transferring and loading conveyors, which can be applied in the investigation of the work processes of new root harvesters and the development of their implements.

Lifting tools are among the primary implements of beet harvesters since they almost entirely determine the level of quality of the whole process of root gathering, effectively generate the tractive power of the harvesting units, and generally consume

a large overwhelming majority of the energy in the work process, which have a substantial effect on all their performance indicators.

In the initial period of the development of beet root harvesting machinery, the lifting tools of beet harvesters were just basic passive means that solely facilitated the disruption of bonds between the roots and the soil during their translational motion in the soil at a certain depth. However, in the course of time, they transformed into rather complex pieces of hardware equipped with rotation or oscillation drives and auxiliary equipment, which facilitated achieving the best operating conditions. Despite the great number of various designs, all digging implements of beet harvesting machines perform, in essence, the same operations, the total combination of which is what ensures the accomplishment of the work process of lifting roots from the soil. The operations combined in one integrated process include: translational motion in the soil at a certain depth along the row of roots, breaking up the bonds between the roots and the soil (by cutting out the whole soil layer on both sides of the root body or crushing it as a consequence of compression and following dislodgement) and applying extracting vertical forces to the roots (while holding and dragging or even not holding the very bodies of the roots), which cause their eventual translation upwards to the soil surface level. To achieve such a number of operations, different solutions are available. This can be achieved with the use of a simple passive share lifter design, but rather complex arrangements exist as well—for example, the rotary prong lifter, in which a special drive is used to create the counter-rotational motion of two digging cones set at an angle to each other and travelling at a certain depth in the soil, while a power-actuated root pick-up attachment installed above the cones also travels partially in the soil.

Meanwhile, the large diversity of the design solutions for the lifting implements stems not only from the intensive search for the ways to ensure the fulfilment of the above-said requirements to ensure performance quality, but also from the great variation in the environment and climate conditions in which they have to operate, the varied size and mass parameters of the roots, their statistical layout in the soil (irregular distribution of the depths and positions along the row), etc. The lifting implement adjustments (presetting some average values of the parameters) are performed mostly with regard to setting up the mean depth of sitting in the soil and the velocity of translation.

Since the design of a lifting tool that could adapt to the digging out of each individual root would admittedly be prohibitively sophisticated and ineffective, urgent need arises to optimise the design and kinematic parameters of the simpler designs of digging tools, which could provide a sufficiently high level of their performance quality within a wider range of variation of random parameters. The development of such adaptable digging tools is too complicated a problem, as minimising the damage inflicted on the roots and their loss in the field on the one

hand and minimising the energy consumption and securing high productivity rates on the other hand are two incompatible targets—for example, increasing the depth of travel of the lifting parts in the soil in order to avoid breaking off the beet root tails during their lifting from stiff soil will inevitably result in a considerable increase in tractive resistance.

Despite the wide variety of beet harvester lifting implement designs, they can be classified in accordance with the preceding block diagram (Figure 2.1).

A great assortment of designs have also given rise to a considerable number of theoretical and experimental studies of the implements as well as dedicated tests, which has made it possible to determine a large majority of the required parameters. The obtained parameter values have been used in the designs of the root harvesters produced by the machine engineering industry in many countries.

Attempts to generate a unified general theory of lifting roots from the soil can be found in [7], which should be regarded as not quite successful since the generation of the simple differential equation of the motion of the root body (its centre of mass) in the vertical and longitudinal plane, in general, by no means represents the real process of breaking up the bonds of the soil around the root or applying the vertically vectored extraction forces or the specific motions (velocities and accelerations) of the root body inside the implement. The authors further elaborate on the probabilistic representation of the vertical and horizontal components of the forces that extract the beet root from the soil, which also, in practice, does not reveal the mechanical and technological essence of the root lifting process. As a consequence, the principal theoretical propositions stated in said study are rather difficult to utilise, as the analytical expressions obtained in the study do not contain any specific design and kinematic parameters of the digging tool and the extraction process (for example, the velocity of translation of the share lifter, which defines the horizontal component of the extraction force). At the same time, such an approach also precludes carrying out numerical experiments with the use of the PC, which would enable determining the optimum (rational) parameters. Thus, the large majority of the sugar beet harvester lifting tools' design parameters presented in said study have actually been determined solely on the basis of the data from the authors' long-term tests and experimental studies.

Classification by type

Discs

Shared

Forked

By the number of shares

1 share

2 share

By way of oscillations

Disks across the row

Drive along the row

With fluctuations of the digging leg

Shares across the row

Synchronous oscillating plowshares along the row

Asynchronous oscillating plowshares along the row

Shares in different planes

Forks across the row

Forks in the plane of row

With spiral rotors

By the number of disks

One disc

Two discs

One disc

Two discs

By way of self-assignment on row

With shared oscillations on the axis of suspension across row

With flat-parallel movement of shares across the row

Active (with rotation)

Passive (without rotation)

By the form of forks

Conical

Triangular prism

Cylinder

Stepped

Elastic

Spiral-shaped

By direction of oscillation

Up - Down

Forward down - back up

Forward and back

Symmetric

Asymmetric

With air supply

By type of drive mechanism

Four tight links

Four links with elastic element

Slide mechanism

Debalance vibration exciter

Figure 2.1. Classification of digging tools of sugar beet harvesters. Source: Prof. Volodymir Bulgakov, 2011.

As the digging tools for beet roots, including the vibrating type, must move in the soil, destroy it and create conditions for lifting up the bodies of roots, they must have working planes inclined at an angle to each other. In this case, these planes will work as triangular wedges—i.e., working bodies of tillage machines. In this case, there is every reason to use the main provisions of the theory of movement in the soil of a trihedral wedge when creating the theory of vibration digging of sugar beet roots out of the soil. Therefore, based on this theory the theories of digging working tools, of the usual ploughshare type, for sugar beet root crops were created [8], allowing, for the most part, the real process of the digging shares moving in the soil to be described, as these theories describe the interaction between the soil and the lifter's two coupled trihedral wedges with sufficient accuracy, which impart the respective extraction forces on the root body. Nevertheless, this approach again does not focus on the particular process of the root body extraction from the soil, since the authors from the beginning make the assumptions that the complete extraction of the root from the soil takes place without any direct contact between the root body and the share surfaces, but solely acts via the deformed soil layers. However, this scenario is applicable only in the case of the sugar beet harvester's digging tools operating being under very favourable conditions: the soil must be soft and loose, with an average moisture content (which implies the absence of strong bonds between the roots and the soil), foreign bodies are to be absent, all roots must be of average size and shape and positioned symmetrically with respect to the centreline of the share digging tool, etc. Meanwhile, under the real harvesting conditions, the root lifting process most frequently involves direct contact between the root body and the digging tool's surface, and the gripping of the root by the implement is most frequently asymmetric; moreover, at a rather high velocity of the lifter's translation, the shares of the digging tool actually hit the body of the root fixed in the soil. This study also does not provide any analytical mathematical model specifically for sugar beet root extraction from the soil.

A significant part of [9] discusses the issues of root harvesters' wheel lifter implements. In this study, and in [10], the main conditions of operation of wheel-type digging implements, their interaction with the soil, etc., are examined in detail. The bulk of theoretical research into the wheel lifter issues in the mentioned studies comes down to the search for the analytical expressions of the wheels' kinematic and design-and-power parameters—in particular to find the linear velocity of any point of the wheel and the normal component of the force of the soil's pressure on the wheel, which are subsequently used (in terms of the projections on the coordinate axes) for determining the power-and-force parameters of operation of the wheel lifter implements. Later in these studies, the geometrical parameters of the wheel lifters (angles of tilt, attack and flare of the wheels as well as the sifting holes in the wheels' surfaces) are optimised with the use of the multicriterion nonlinear

7

programming problem. Unfortunately, the root itself as a subject matter of the mechanical and mathematical models is not discussed here and the study does not offer any mathematical model specifically for the root extraction from the soil by the wheel lifter.

Fundamental research into the root lifting implements is presented in the studies [11] and [12]. These consider, in detail, the processes of lifting roots from the soil by share and wheel lifters on the basis of finding the principal conditions and forces that arise during them. The fullest detailing is provided in said study for the process of the root extraction from the soil by wheel lifter implements. This includes drawing the schematic model of the force interaction between the root body and one of the lifting wheels. For this purpose, on the inner surface of one of the wheels a surface element dS was selected, which is the source of the following forces imparted on the root body: dN—force of normal pressure, dT—elementary friction force and P_b—lateral force. At the next stage, when all the forces were projected on the X axis that passes through the lifter's line of symmetry, and on which the root is situated, the $\overline{P}_C$ shear force that acts along the line of translation of the wheel lifter produces the root body deflection and the $\overline{P}_B$ extraction force allow for the eventual extraction of the root body from the soil. Under the assumption of leaving intact (not chipping off) the root body, the respective analytical constraint (the resultant shear force must be equal to zero), which defines the extraction of the root from the soil and is written in terms of the design and kinematic parameters of the wheel lifter, is generated.

Thereby, the described treatise also contains a special case of the theory of the root extraction from the soil by a wheel lifter in the case of symmetrical positioning, which is examined with sufficiently detailed specification and description of all the forces that can arise in such a case. The differential equations of motion of the root body during digging out by a wheel lifter are not generated in the study and the motion of the root under the action of the above-mentioned system of forces specifically during its extraction is not considered.

Attempts to analytically describe the conditions and specifically the process of extraction of roots from the soil are represented in [13]. However, the authors only take as a basis the geometry analysis and the methods of geometric design of the new working faces for the digging tools of root harvesters. Again, the mathematical model of the sugar beet root extraction from the soil is not provided in the study, while the analysis of the forces that arise during the interaction between various types of digging tools (with shares, wheels, prongs) and the root body contains the functional relations that were obtained earlier by other authors and published in the papers [7,11], etc. The above-said information leads to the conclusion that without focusing on the main subject of research, i.e., the sugar beet root, and without a thorough examination of its interaction with specific digging surfaces and a detailed investigation of the root body motion at every stage of its extraction from the soil,

in general the geometric designing of digging tools for root harvesters will be of little effect. Unfortunately, it appears impossible to use the results obtained by such geometric designing for finding the optimum process and design parameters of the process of extracting roots from the soil.

The work of [14] can be noted as one of the first solid analytical studies on the process of vibrational digging of sugar beet roots. It offers an analysis of up-to-date engineering solutions of vibrational digging tools and experimental investigations of the first vibrational lifters, as well as the equation of oscillating motions of digging shares. The study does not take into consideration the sugar beet root in the soil as an elastic oscillating system.

2.2. Physical–Mechanical Properties of Sugar Beet

The operation of beet harvesters can be efficient only in case their implements are designed and adjusted for harvesting with due consideration of the main mass and dimension specifications and physical–mechanical properties of the sugar beet roots. Despite the differences between the existing cultivars of sugar beet, the variation of the natural and operational conditions of cultivation and the stochastic nature of the parameters at the time of gathering, it is possible to determine the main physical–mechanical properties of the roots. In Figure 2.2—Dimension specifications of sugar beet root, the principal dimension specifications of the sugar beet root as well as the parameters of its position in the soil relative to the soil surface are shown [7].

As can be seen in Figure 2.2., it has a conical shape and the main part of it sits in the soil. The upper part of the root is called the "top" and is normally situated above the soil surface level (sometimes it can have a position below the soil surface level—by up to 30 mm).

The bulk of the sugar content (over 90%) is localised in the body of the root. The distribution of the root's mass between its parts and the sugar content in the parts of a sugar beet root are shown in Table 2.1 [15].

The total length (height) of the root can reach 1 m, but in harvesting its tail usually breaks off (at the diameter of 8–10 mm) and remains in the soil; therefore, in practice, the root's length is defined by the parameter l_k. The leaves that shoot from the root's top, the number of which can be from 10 to 30, make up a bunch, which generally also has (provisionally) the shape of a cone. Sometimes, by the time of harvesting several leaves, situated for the most part outside the main leaves cone, fall over or completely dry out and also fall over onto the surface of the soil.
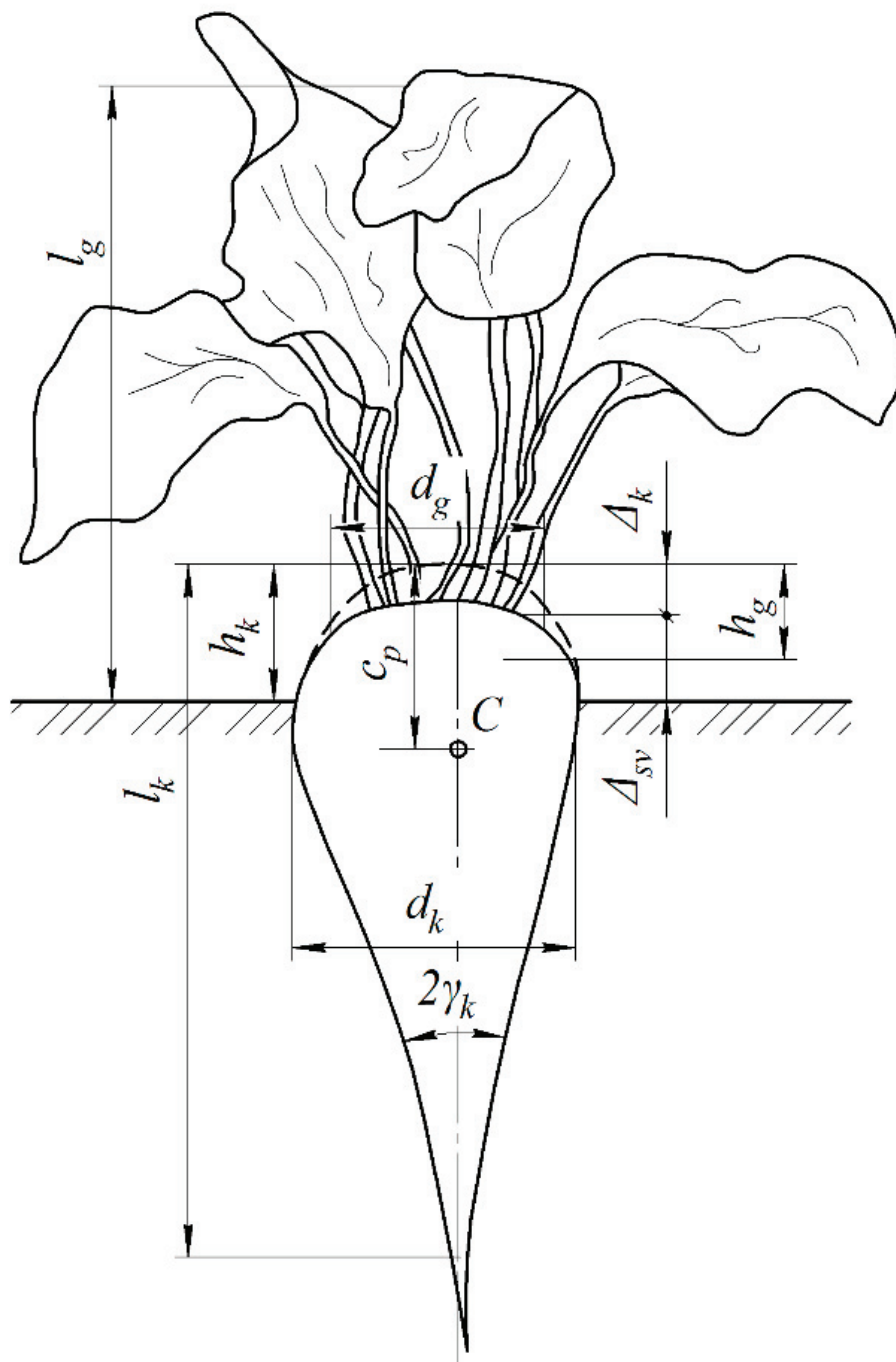
Figure 2.2. Dimension specifications of sugar beet root. Source: Prof. Volodymir Bulgakov, 2011.

Table 2.1. Shares of different parts of sugar beet root in mass and sugar content.

	Name of Root's Part		Mass Share (%)	Net Sugar Content (%)
Top	Crown		5–7	–
	Dormant eye zone		6–18	9.7
	Body		76–88	90.3
	Tail		1	–

Source: Prof. Volodymir Bulgakov, 2011.

Table 2.2. Dimension and mass specifications of sugar beets.

Description	Unit	Value
Length of root, l_k	mm	230–280
Diameter of root, d_k	mm	67–122
Mass of root, Q_k	kg	0.3–1.6
Angle of taper of root, γ_k	deg	9–19
Height of top of root, h_g	mm	10.4–32.4
Height above soil surface level, h_k	mm	18.4–42.4
Coordinate of centre of mass, C, c_p	mm	90–100
Lengths of leaf stalks, l_g	mm	300–400
Diameter of leaf bunch, d_g	mm	50–60
Mass of leaves, Q_g	kg	0.12–0.80
Thickness of crown, Δ_k	mm	13.2–16.2
Thickness of dormant eye section, Δ_{sv}.	mm	8.0–21.4
Mass of crown, q_{kor}	kg	0.055–0.096
Mass of dormant eye section, q_{cg}	kg	0.062–0.123

Table 2.2 contains the average dimension and mass specifications of the roots and leaves of sugar beets [7] in accordance with the results of computational observations, special measurements as well as on the basis of the processed long-term statistical data.

The principal strength features of the root and leaves of a sugar beet are the bonding force between the root and the soil, the specific gravity of the roots and the leaves and the bending failure stress of the root. The main physical–mechanical properties of the root and leaves of a sugar beet are shown in Table 2.3 [16].

Table 2.3. Physical–mechanical properties of sugar beet.

Description	Unit	Value
Specific gravity of root	kg·m^{-3}	550–650
Specific gravity of leaves	kg·m^{-3}	140–160

Bending failure stress of root:
    static load
    dynamic load
	MPa	1.80
		1.15

Elastic modulus of root	MPa	18.40
Force of root extraction from soil	N	50–770
Force of separation of leaves from root top	N	50–650

Coefficient of friction of root on steel:
    static
    dynamic
		0.50–0.70
		0.45–0.70

Specific cutting resistance of root	kN·m^{-1}	3–6
Specific cutting resistance of leaves	kN·m^{-1}	1–4

Angle of repose:
    in quiescence
    in motion
	deg	35–40
		25–30

Specific resistance factor of leaves	N·mm^{-1}	2.26–2.65
Specific resistance factor of root	N·mm^{-1}	2.10–3.50
Work of lifting root by horizontal force	J	17.80–25.30
Work of extracting dug root from soil	J	15.20

Tearing resistance of leaf stalks:
    outer
    inner
	MPa	0.94
		1.21

Work of failure of bonds between leaf stalks and root top in the case of tangential application of force	J	33.90

Force of root's resistance to action of force of:
    angular displacement (up to 10°)
    extraction
	N	185–432
		227–522

The most important specification of sugar beets is their positioning in the sugar beet plantation at the moment of harvesting. It is common knowledge that these

features depend first of all on the sugar beet cultivar, the technology of its mechanised cultivation, environment and climate conditions and some other random factors. For example, it is assumed on average that the optimum population of sugar beet plants in the sugar beet plantation is 80,000–150,000 pcs·ha^{-1}.

The second important feature of a sugar beet is the shape of the root body, which is defined by the density of the soil around the beet root. For example, in the case of the mechanised cultivation of sugar beets, if the soil density is within the range of 1.20–1.30 g·cm^{-3} (as a result of the ploughing, sowing, care for the seedlings and inter-row tillage), the roots acquire the most productive conical shape (the same as that shown in Figure 2.2).

In the case of an excessive density of the soil (1.32–1.70 g·cm^{-3}), the roots have shortened circumferences and barrel-like shapes and their tops project excessively above the soil surface level. When the soil density is below the normal range , and lower), the sugar beet roots can have undeveloped, arbitrary shapes. The variation of the soil density against the depth of sitting of the conical sugar beet root is shown in Figure 2.3 [16]. As can be seen, at the depth of travel in the soil of a majority of digging tools (0.06–0.1 m), the density of soil around the root almost reaches its maximum values.
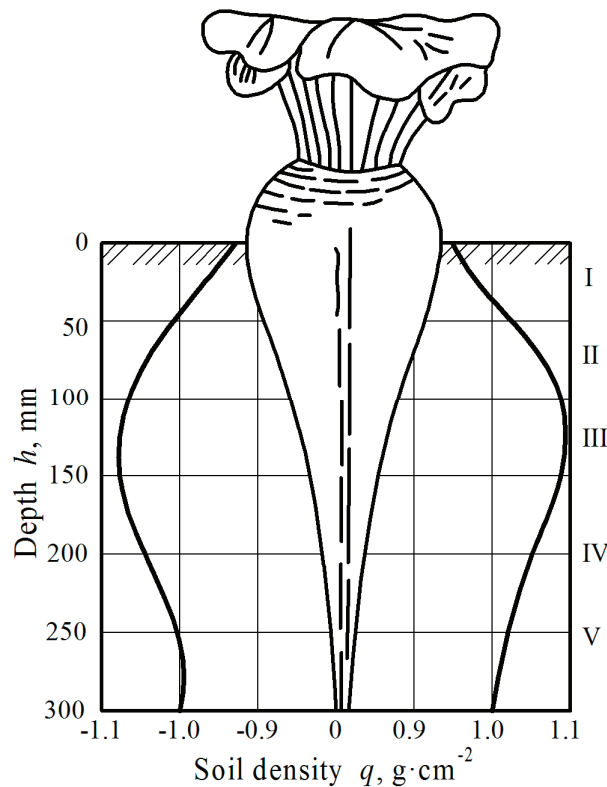
Figure 2.3. Variation of density of soil around the root against the depth. Source: Prof. Volodymyr Bulgakov, 2011.

The third key feature of sugar beet root positioning in the beet field is the distance between two proximate roots in the planted row. Taking into account the fact that this parameter is completely random, it is assumed that the spacing between the centres of sugar beet roots in the row within the range of 0.16–0.23 m ensures the optimum yield. Under such a condition, one running metre of the planted sugar beets has to contain 4–6 pcs of roots. This kind of distribution of beet roots in the row is the factor that defines some other features of the beet roots as the object of harvesting: the positions of root tops relative to the soil surface level (heights of the tops), sizes and shapes of the tops, degree of development of the leaves, overall dimensions of the roots, etc.

The offset of sugar beet roots from the provisional centreline of the planted row to one or the other side that does not have a substantial impact on the quality of harvesting is within 0.02–0.04 m. The increase in said parameter to a level of 0.05 m and higher results in the sharp rise of the root losses.

Thus, taking into account the above-mentioned physical–mechanical properties of sugar beet roots and the soil around the roots, the following general conditions and basic assumptions can be laid down for the analytical treatment of the work process of the root extraction from the soil.

For the analytical investigation of the process of extracting a root from the soil, the following fundamental provisions, which are quite widely applied in the scientific literature, but undoubtedly need clarification and updating, are assumed.

First, it is believed that the root body can be approximated by a geometrical body with the shape of a regular cone, the apex of which points downwards. Irrespective of the fact that the uppermost part of the root (its top) can be situated either above the soil surface level or strictly at this level, or even below the soil surface level, the depth of sitting of the root in the soil is determined by the distance from the cone apex to the soil surface level. The height of the root is designated as h_k, the cone apex angle—$2\gamma_k$, the root radius, i.e., the cone base radius—r_k. The total vertical resistance reaction of the soil acting on the root is conventionally applied to the apex of the cone, vectored vertically downwards and designated as $\overline{R}_z$.

The root is an elastic solid specified by the Young modulus E (N·m^{-2}), specific gravity ρ (kg·m^{-3}) and mass m (kg).

The soil surrounding the root is also an elastic medium specified by its elastic stiffness C (N·m^{-3}), bulk specific gravity $\gamma_{ob.}$ (N·m^{-3}), specific resistance in loose condition $k_{ud.}$ (Pa), etc.

2.3. Share Lifters

Share lifter implements comprise two symmetrically positioned shares (wedges), which are set at certain angles to each other and to the line of travel so that their front

ends are drawn apart from each other and their rear parts are drawn near to each other, thus arranging the narrowing lifting throat of the tool (Figure 2.4) [12].
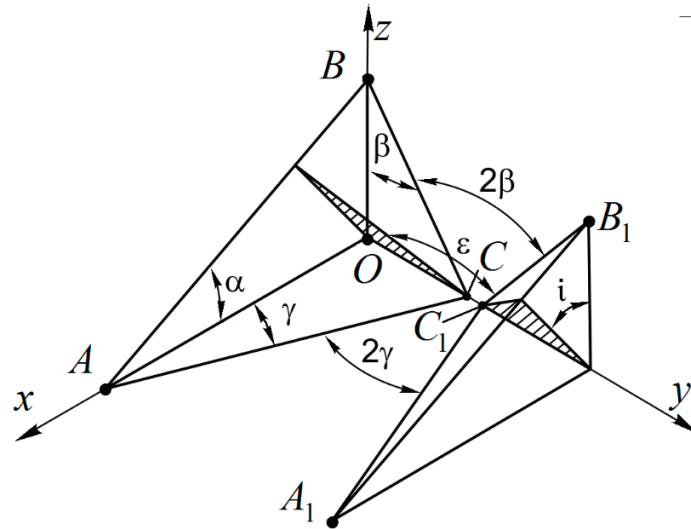
Figure 2.4. Schematic model of share lifter.

In the following pages, the existing analytical studies on this type of digging tool are discussed. First, consideration is given to the research into the geometrical parameters of share lifters. For this purpose, the trihedral wedges, which have been studied in sufficient detail in the science of tillage, are employed and the basic geometrical relations provided in [11] are used. The vertices of the angles between the edges of the inner faces of the wedges, which form the digging throat of the share lifter, are designated as A, B, C and A_1, B_1, C_1, respectively. The working face of the trihedral wedge is referenced to the three-dimensional coordinate system O_{xyz} in such a way that axis O_x coincides with the line of translational motion of the wedges, axis O_y is oriented from the right to the left and axis O_z is oriented vertically upwards and passes through point B. Lines AB, BC and AC, which result from the intersection of the working plane of one of the wedges (ABC) with the coordinate planes xOz, yOz, xOy, respectively, form the respective angles α, β and γ. Evidently, the same angles are formed in the case of wedge $A_1B_1C_1$.

If both the wedges are intersected by the horizontal plane xOy, the angle 2γ is formed, which is the angle of attack of the share lifter; the intersection with the transverse and vertical plane yOz gives the angle of flare 2β; the intersection with the vertical and longitudinal plane xOz produces the angle of cutting α. Overall, the values of these angles define the quality of performance of the work process of lifting sugar beet roots from the soil. The dihedral angle between planes ABC and $A_1B_1C_1 - \varepsilon$ is the angle of maximum opening of the inner surface of the lifter, while i is the angular displacement of the share lifter's maximum opening plane from the vertical line.

In the schematic model shown in Figure 2.4, there are respective correlations between the mentioned angles, which are as follows [12]:

$$tan\beta = tan\frac{\varepsilon}{2} \cdot cosi,$$
$$tan\gamma = tan\frac{\varepsilon}{2} \cdot sini, \quad\quad\quad (2.1)$$
$$tan\alpha = tani = \frac{tan\gamma}{tan\beta}.$$

It has been found in the numerous experimental studies that the optimum values of these angles are [17]: $\beta = 50 - 55°$, $\gamma = 14 - 15°$ and $\alpha = 10 - 15°$.

Further, it is necessary to examine the work process of digging sugar beet roots with the use of a share lifter in detail. When moving along the row of sugar beet roots, the wedges first break down the soil layers, initially at a certain distance from the root sitting in the soil, using their separated front parts. Next, the digging channel reaches the root and partially pushes it forward. After this, the root, together with the soil surrounding it, moves inside the lifter's narrow throat formed by the rear inner faces of the wedges and moves through it. As the wedges are set at certain angles, the initial and following interactions between the soil layer together with the beet root and the wedges' working faces during the latter's translational motion proceed in such a way that the layer is compressed on the sides and strained and then, during the further movement of the beet root between the necking working faces, the corresponding forces are generated for its extraction from the soil. However, the forces that directly extract the sugar beet root from the soil will be generated in the share lifter only subject to the unconditional presence of the backup forces exerted by the soil and vectored opposite to the translation of the digging tool. Otherwise, the share lifter will just push the root forward. These backup forces are the factor promoting the secure advancement of the beet root inside the digging tool along the wedges' faces through the narrow throat with the subsequent corresponding secure movement upwards. It should be noted that the presence of sufficient backup forces exerted by the soil and the pressure on the upper part of the root applied by the translationally moving digging tool cause a certain bending of the root body in the direction of the lifter's progression. This bending must not result in the chipping-off of the tail part of the root. Within the limits of the elastic properties of the sugar beet root body, its certain forward motion, even in some bent conditions, under the action of the pressure applied by the share lifter will not cause the chipping-off of the root body, as in a very short period of time its bonds with the soil will be completely disrupted. Overall, the above-described position of the share lifter working faces during their translational motion in the soil will certainly promote the upward migration of the parts of the soil and solid bodies (that is, root bodies) that have entered the lifter's throat (since the motion trajectories within the throat, except its central part, are directed upwards). The generation of sufficient backup forces by the soil depends

on the physical–mechanical properties of the same soil that surrounds the sugar beet root. It is quite obvious that in the case of high moisture content in the soil, the provision of such forces is impossible in general. At the same time, if the soil is stiff and the moisture content in it is low, the operation of share lifter implements also becomes impossible due to the accumulation of firm soil formations in its throat and the high probability of chipping-off the tail parts of the roots due to the high magnitude of the bonding forces between the roots and the soil throughout the whole depth at which they sit in the soil.

Based on the above, the physical model of digging a sugar beet root out of the soil by a share lifter is as follows. The gradual advancement of the forepart of the wedges causes the cutting off of a block of soil (of conical shape) on both sides of the root body. The further translation of the lifter produces the compression of the upper soil layer on both sides of it and its following displacement inside the working channel. The presence of the sufficient backup force exerted by the intact soil ahead of the lifter ensures, for a while, the vertical position of the root and even its slight bending forward, until the bonds between the root and the soil are completely disrupted and the root becomes fully contained inside the working channel of the lifter (at the beginning of its throat). Next, contact takes place and the root body slides along the surfaces of both wedges, resulting from the continuing action of the backup forces exerted by the parts of the soil inside the working channel of the lifter and leading to the complete extraction from the soil to its surface.

The described sequence of events in the process of digging the root from the soil is facilitated by the action of two coupled trihedral wedges travelling in the soil at a certain depth. Hence, the process of interaction between the working faces of the share lifter and the soil can be identified with the operation of the dihedral wedge, which has extensive coverage in the studies on tilling machinery. With the angle of cutting α, the soil grains move on the right lines that are parallel to the right lines AB and A_1B_1. If the coefficient of friction of the soil on the working face of a dihedral wedge is equal to f, then, in the case of the share lifter, its reduced value appears as follows [11]:

$$f' = \frac{f}{sin\left(\frac{\varepsilon}{2}\right)}. \tag{2.2}$$

The rear part of the share lifter contains the clearance CC_1, the magnitude of which has to be set taking into account the minimum diameters of sugar beet roots (especially of their tail parts, which have to pass the clearance without being damaged); hence, to be within the range of 30~40 mm. The length of the lifter's working channel must not be less than l where:

$$l \geq CC_1 cot\gamma \tag{2.3}$$

The distance between the tips of the shares AA_1 must be as short as possible as this determines the width of the soil layer that is dug under and, hence, in effect determines the amount of soil conveyed into the root harvester together with the beet roots. However, the same distance also has an effect on the likelihood of damaging roots in the case of deviation of their positions from the row centreline; therefore, its unreasonable reduction will make the steering of the root harvester along the rows of beets more difficult.

The design distance between the tips of the shares must comply with the following formula:

$$AA_1 = d_k + 2\Delta_o + 2m \tag{2.4}$$

where d_k—maximum diameter of the sugar beet root; Δ_o—allowed offset of the root from the row centreline (assumed to be equal to up to 60 mm); m—probable deviation of the lifter from the row centreline due to the steering inaccuracies.

The maximum opening of the shares, i.e., the distance AA_1, must be within the range of 180~220 mm.

The pattern of the soil deformation during the operation of share lifters depends on various factors, such as, for example, the angle of cutting α, properties of the soil, etc. It is quite obvious that with the increase in said angle the deformation of the soil increases as well. However, the increase in the angle α also leads to the growth of the horizontal dislocation of parts of the soil, which can result in the beet roots breaking during their extraction. For this reason, the limiting value of the angle of cutting is to be determined with the use of the following formula [18]:

$$\alpha \frac{1}{2} atan \frac{f}{sin\left(\frac{\varepsilon}{2}\right)_{max.}} \tag{2.5}$$

When the angle of cutting α exceeds the above-said value, the vertical displacement of parts of the soil grows smaller, but the horizontal displacement sharply rises, which causes the loss of and damage to beet roots during harvesting.

The depth of travel of share lifters in the soil must stay within the range of 110–120 mm [12]. Thus, the analytical studies that have been carried out up to date on the topic of share-type digging tools do not contain the mathematical model of the specific interaction between the digging shares and the root body. The overall process of the root body extraction from the soil (interaction with the root fixed in the soil, analysis of the forces in this interaction, motion of the root within the lifter's throat) has not been given analytical consideration.

2.4. Wheel Lifters

Wheel lifters are more complex and metal-intensive implements in comparison with share lifters. Nevertheless, they perform the work process of lifting beet roots

from the soil more efficiently, deform the soil layer more intensively and, at the same time, lift 2–3 times less soil together with the roots.

Wheel lifters also represent, in effect, the same two coupled wedges, the working faces of which rotate about the wheels' centres, and which are set at respective angles to each other and to the line of travel.

Wheel lifters fall into the groups of passive types (the rotation of the wheels is due solely to the interaction with the soil and grip on it during the translational motion) and active designs (i.e., those with the forced rotation of one or both of the wheels). In the first case, the wheels' rotation rate is determined by the translational velocity of the root harvester, in the second case the rate of rotation can be preset. Design-wise, the wheels in the lifters can be flat or spherical. They comprise the rim, the spokes and the hub. The outer surface of the rim can be smooth (in the case of driven wheels) or equipped with lugs (grousers), which are necessary in the case of passive wheels. The depth of travel of wheel lifters in the soil is 80–100 mm.

The work process of digging beet roots with the use of wheel lifters flows is as follows: after undercutting the soil layer together with the beet root, the wheels break the layer and clamp the root in the necking throat. Further, the pressing on the soil layer results in its broken part pouring through the windows between the spokes, while the root is extracted from the soil by the rotating wheels together with a small amount of soil, goes up and is thereafter thrown by the beater over onto the cleaning unit.

Since wheel lifters also represent coupled trihedral wedges (Figure 2.5), the same angles are taken into consideration as in the case of share lifters: α—angle of cutting; 2γ—angle of attack; 2β—angle of flare [17].
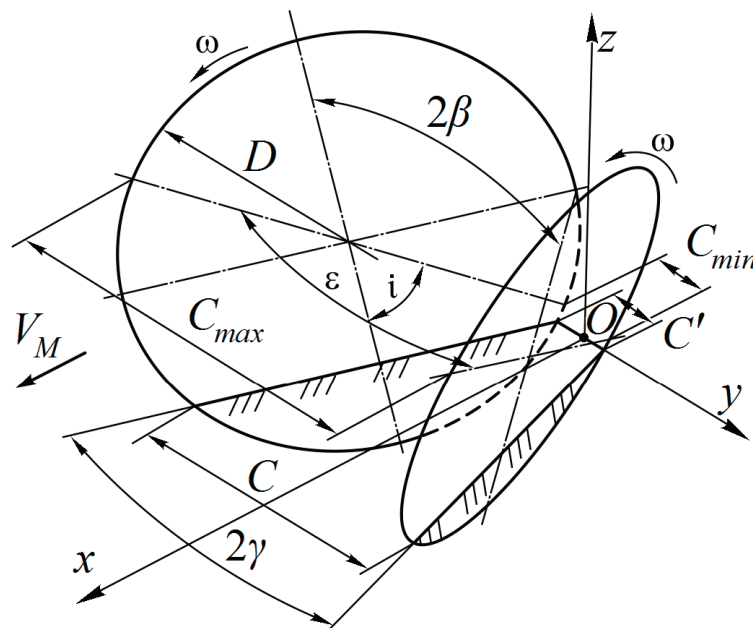
Figure 2.5. Schematic model of wheel lifter.

In the schematic model, the three-dimensional Cartesian coordinate system *Oxyz* is shown, in which the origin of coordinates *O* is the point in the middle of the shortest distance between the wheels. Hence, various points of the wheels move in the space (due to the rotational motion of the wheels and the translational motion of the implement) along the trajectories defined by the following parameters [17]:

$$\left.\begin{array}{rcl} x &=& \frac{r}{\cos\gamma}(\omega t - \lambda\sin\omega t), \\ y &=& \rho[1 - \cos(\omega t - i)]\sin\frac{\varepsilon}{2}, \\ z &=& r\cos\beta(1 - \lambda\cos\omega t), \end{array}\right\} \tag{2.6}$$

where *r*—radius of the wheel's moving centroid; $\lambda = \frac{\rho}{r}$; ρ—distance from the arbitrary point of the wheel to its centre.

There are many factors that have an effect on the quality of the work process of the sugar beet root lifting from the soil with the use of wheel lifter implements. They include, first of all, the lifter's design parameters. Wheel lifters are employed in multiple-row root harvesters, which imposes certain limitations on their design dimensions. For example, the diameter of the wheels shall be within the range of 700–750 mm. When this value decreases, the completeness of the beet root lifting from the soil decreases and the engineering solutions for the wheel rotation drive become more complicated. Greater diameters of the wheels complicate the structural configuration of the root harvester lifting implements and increases their steel intensity.

The same constraints are also applied to the setting angles of the wheels, as the allowed values for the angle between two wheels are limited by the width of the spacing between the rows of planted sugar beet roots. Hence, the angle ε of the maximum opening of the wheels must comply with the following condition:

$$\sin\frac{\varepsilon}{2} = \frac{C_{max} - C_{min}}{2D} \tag{2.7}$$

where $C_{max.}$—distance between the wheel edges in the area of maximum opening (mm); $C_{min.}$—minimum distance between the wheels (mm).

In its turn, the maximum wheel opening distance C_{max} must not exceed the following value:

$$C_{max} \leq S - 2\Delta b - \Delta s \tag{2.8}$$

where *S*—width of inter-row spacing (mm); Δb—thickness of wheel rim (mm); Δs—distance between the wheels of adjacent lifters (mm).

Based on the above-said information, the values of C_{max} can be substituted into (2.8), and the following formula is obtained:

$$sin\frac{\varepsilon}{2} \leq \frac{S - 2\Delta b - \Delta s - C_{min.}}{2D} \qquad (2.9)$$

If the values of the design parameters of the wheel lifter are assumed to be within the following range: $S = 450$ mm; $\Delta b = 5$ mm; $\Delta s = 15$ mm; $D = 750$ mm, then the value $sin\frac{\varepsilon}{2} \leq 0.243$ is obtained, which corresponds to an angle of $\varepsilon \leq 28°$.

The correlation between the angles 2γ and 2β at a constant value of angle ε is defined by angle i, which shows the displacement of the maximum opening plane from the vertical line—that is, the greater the angle i is, the greater the angle 2γ is and the better the conditions for steering the root harvester along the planted rows of sugar beets are. Nevertheless, increasing the angle i (or, what is the same, the angle of cutting α) to a level of above $45 \sim 50°$ impairs the transportation of parts of soil along the inner surfaces of the wheels, which also increases the loss and damage of beet roots.

In multiple-row root harvesters, at an inter-row spacing width of 45 cm, an angle of $i = 50°$ is assumed in order to increase the working width of the wheel lifters. At angles of $i = 50°$ and $\varepsilon = 28°$, with the use of Formula (2.1), angles of $2\beta = 18°$ and $2\gamma = 22°$ are obtained.

It has been established in numerous studies that the optimum values of the above-mentioned angles of wheel lifters, which ensure the high quality of performing the work process of digging roots from the soil and the minimum power consumption, are as follows: $2\beta = 25 \sim 30°$, $2\gamma = 20 \sim 25°$ and $\alpha = 40 \sim 45°$.

In the case of the single-row configuration, it is acceptable to increase the value of the angle i to $i = 45°$. Then, the sufficient working width of the wheels is achieved by raising the diameters of the wheels D to 800 mm and the angle ε to 38°.

Since one of the wheels can be actuated by a drive, the kinematic behaviour factor (i.e., the ratio between the wheel's circumferential velocity and its translational velocity) is $\lambda = 2.0 \sim 2.5$.

The wheels of such digging implements can be flat or spherical. Moreover, the appearance of the wheel is defined by the radius of the wheel sphere R_c, which, in turn, depends on the specific features in the performance of the work process.

The geometric elements of the wheel can be examined by giving consideration to its section by the plane drawn through its axis of rotation (Figure 2.6). For the normal operation of the wheel, it is necessary to ensure that the rear angle of cutting of the wheel γ has a positive value, which will prevent any interaction between the back part of the blade and the furrow wall. This condition is fulfilled when:

$$\gamma \geq \vartheta + \Delta \qquad (2.10)$$

where $\vartheta = asin\frac{D}{2R_c}$—semisector angle (deg); R_c—radius of the wheel sphere; Δ—angle of taper of the wheel's blade (deg).
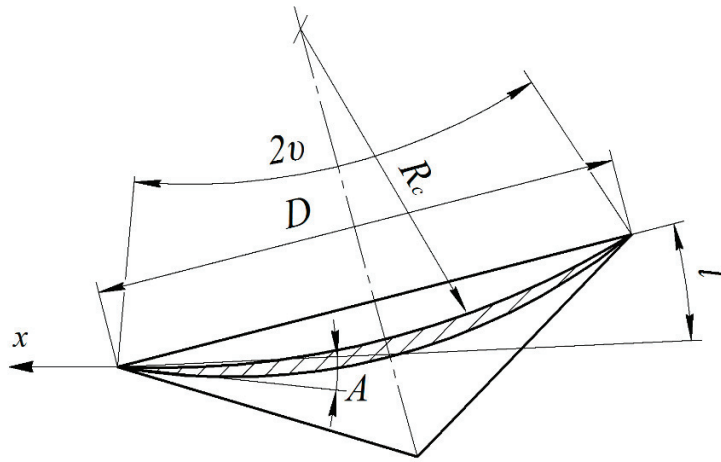
Figure 2.6. Geometric elements of wheel in its section by plane drawn through its axis of rotation.

The magnitude of the sum angle $\vartheta + \Delta$ does not remain constant in different sections of the wheel but becomes smaller as the section moves away from the wheel's centre. In view of this fact, it is necessary to find the relation between the minimum permissible sphere radius and the wheel's parameters. First, the value of said sum angle $\vartheta + \Delta$ will be found for the section of the wheel by the horizontal plane that is situated at a distance of h from the furrow bottom. For this section, the relation between all the above-mentioned angles, γ, ϑ and Δ, is as follows:

$$\vartheta + \Delta \leq atan\frac{tan\gamma}{\sqrt{2a - a^2}} \tag{2.11}$$

where $a = \frac{2h}{Dcos\beta}$; β—angle of setting of the wheel, h—depth of the wheel's travel in the soil.

After analysing (2.11), it becomes evident that the greater the angle γ of wheel setting in the horizontal plane is and the lower the ratio between the depth of the wheel's travel in the soil h and its diameter D is, the greater the maximum wheel sector apex angle 2ϑ is.

For the wheel lifters on root harvesters, angle γ must not exceed $11 \sim 13°$, while coefficient a has to stay within the range of 0.2~0.3. Hence, by substituting said values of the angles into (2.11) the relation $\vartheta + \Delta \leq 17\ldots20°$ is obtained. When this condition is not met, the self-extraction of the wheels occurs during their advancement in stiff soil. In order to prevent this from happening, it becomes necessary to additionally load the wheels with a vertical force, sometimes of rather great magnitude.

The quality of performance of wheel lifters also depends on the shape of the blades. Thus, when the blades are smooth, the beet roots are extracted from the soil most fully and without damage. Smooth blades act on the beet roots via the soil layer and displace them without damaging them, especially those ones that are situated outside the bounds of the row. Moreover, smooth blades are desirable in the sense that the wheel lifters are not clogged with plant residues, even when working on rather weedy areas of the field.

The next step is to investigate the force interaction between the wheel lifter on the one hand and the soil and the beet root on the other hand. For this purpose, the schematic model of the forces acting on the soil and the beet root during the movement of the wheel lifter is to be drawn up (Figure 2.7).

In the schematic model, two lifting wheels travelling in the soil at a depth of h are shown. The midpoint of the rear part of the lifter (the narrowest place between the wheels) is taken as point O—the origin of the three-dimensional Cartesian coordinate system $Oxyz$, axis Ox of which coincides with the lifter's line of travel; axis Oz is a vertical line.
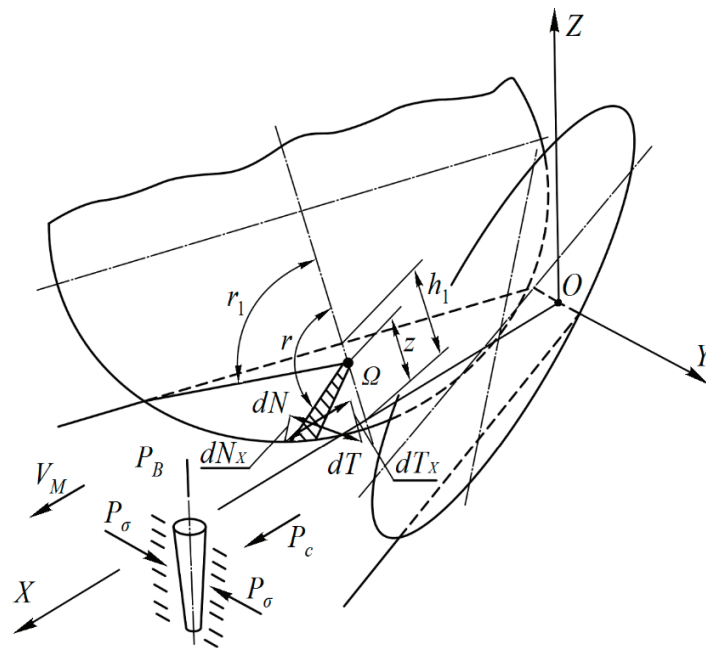
Figure 2.7. Force interaction between wheel lifter and soil and beet root.

On the inner surface of one of the wheels, a surface element dS (shaded), which rotates together with the wheel and has its own instantaneous centre of rotation Ω, is selected. For the specified instant of time, the position of the surface element dS on the wheel is determined by the angular displacement ξ about the axis of the wheel itself. The position of the instantaneous centre of rotation Ω on the wheel is determined by the distance z—i.e., its distance from the edge of the wheel's blade and the angular displacement ξ_1 (i.e., the angular displacement about the axis of the

wheel itself). h_1 denotes the distance of the wheel's part submerged in the soil. This distance is equal to:

$$h_1 = \frac{h}{\cos\beta} \qquad (2.12)$$

Further, the beet root that sits in the soil between the lifter's wheels is introduced in the schematic model. In the case under consideration, the vertical axis of symmetry of the root intersects axis Ox. When the sugar beet root is extracted from the soil, it will be under the action of several forces. These forces can be divided into three types. They are:

(1) Horizontal forces $\overline{P}_\sigma$ acting in the plane that is perpendicular to the lifter's line of travel;
(2) Force of extraction of the root from the soil $\overline{P}_B$ applied vertically upwards;
(3) Shear force $\overline{P}_C$ applied along the lifter's line of travel.

The forces of the first two types ($\overline{P}_\sigma$, $\overline{P}_B$) perform the useful work of breaking up the soil and extracting the beet roots. The force of the last type ($\overline{P}_C$) is one of the causes of major damage to the roots—it contributes to the chipping-off of their tail parts.

The next step is to examine the forces imparted on the root by the lifter's wheel during the latter's motion relative to the soil. Within the above-mentioned surface element dS, the elementary forces of pressure at a right angle $d\overline{N}$ and the elementary forces of friction $d\overline{T}$ come into action. Moreover, the elementary forces of pressure at a right angle $d\overline{N}$ are perpendicular to the plane of the wheel itself and vectored the same way as the lifter's motion (which will be true as long as the condition $2\gamma > 0$ is met), while the elementary forces of friction $d\overline{T}$ acting within the plane of the wheel itself can be vectored two ways: either the same way as the lifter's motion (applicable in the case of passive lifters, which behave the same as share lifters, or in the case of part of the wheel being submerged in the soil, which is situated above the instantaneous centre of rotation) or opposite to the lifter's motion vector (i.e., the elementary forces of friction of all the wheel's surface elements situated below the instantaneous centre of rotation Ω will be vectored that way).

Further, in order to find the shear force $\overline{P}_C$ acting on the root, the elementary forces of pressure at right angle $d\overline{N}$ and the elementary forces of friction $d\overline{T}$ will be projected on axis X. It is assumed that the minimum rate of damage to beet roots is achieved when:

$$\sum_{dS} dN_X + \sum_{dS} dT_X = 0 \qquad (2.13)$$

where dN_X—projection of the elementary forces of pressure at right angle on axis X; dT_X—projection of the elementary forces of friction on axis X.

This assumption can also be set down in the following form:

$$\frac{tan\gamma}{f} = \frac{2(1-b)^2\left(sin\xi_1 - \frac{sin^3\xi_1}{3}\right) + (2b-b^2)sin\xi_1 - (a-b)^2 ln\left[tan\left(\frac{\pi}{4} + \frac{\xi_1}{2}\right)\right] - 2I}{cos\beta\left(\frac{4}{3}a\sqrt{2a-a^2} + \frac{a^3}{4\sqrt{2a-a^2}}\right)}$$ (2.14)

where $I = (1-b)\int_{\xi_1}^{\pi} cos^2\xi\sqrt{(1-b)^2cos^2\xi + 2b - b^2}\,d\xi$; $b = \frac{z}{R}$;

$\xi_1 = arctan\frac{\sqrt{R^2-(R-h_1)^2}}{h_1-z}$; f—coefficient of friction.

In order for Expression (2.14) to become appropriate for practical use, it is necessary to solve it for the coefficient b, taking into account the kinematic behaviour factor λ, which in the case under consideration is equal to:

$$\lambda = \frac{1}{1-b} = \frac{V_o}{V_M cos\gamma}$$ (2.15)

where V_o—circumferential velocity of the wheels; V_M—translational velocity of the wheel lifter.

The solution of the Equation (2.15) is presented in the form of a nomogram (Figure 2.8).
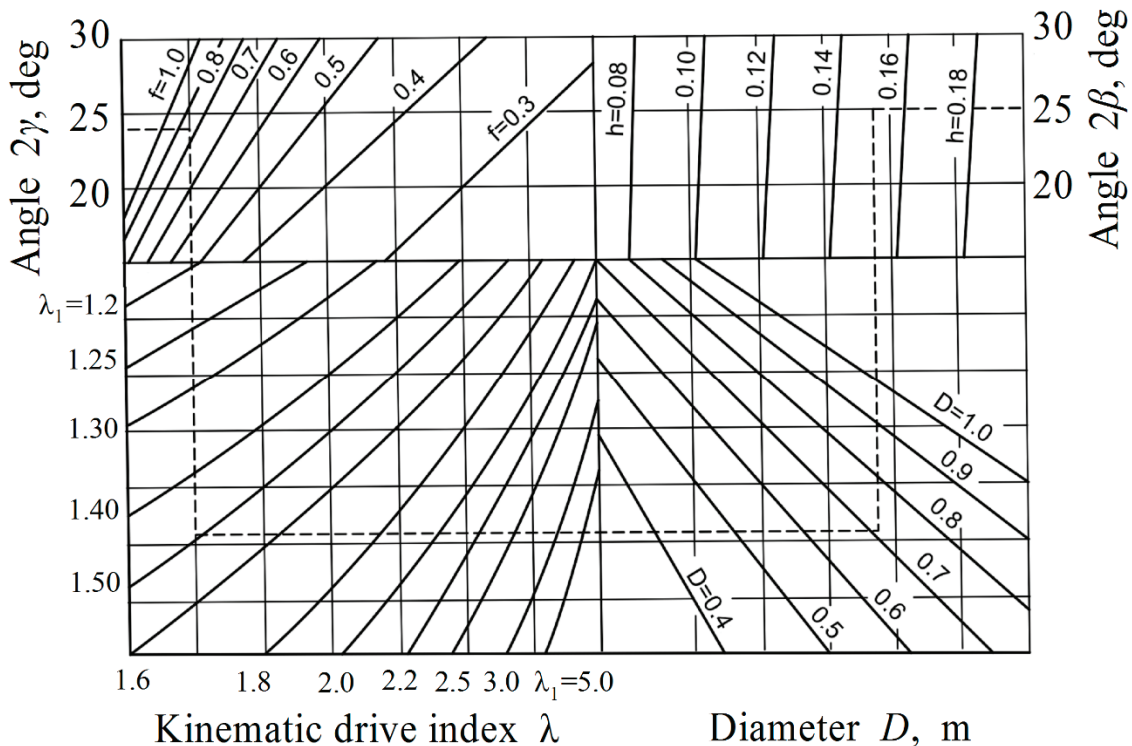
Figure 2.8. Nomogram for determination circular speed of digging disks.

To use the nomogram, it is necessary at an angle of $2\beta = 25°$ to choose $h = 150$ mm and $D = 710$ mm; on the other hand, at an angle of $2\gamma = 24°$ and $f = 0.85$, the kinematic drive index λ will be 1.48. However, using Expression (2.15) we finally find that $\lambda = \frac{V_o}{V_M} = 1.45$.

Profound theoretical research has been undertaken in [19]. The main theoretical results obtained in the study are: analysis of the interaction between the wheel implement and the soil; finding out the distribution of contact stresses over the surfaces of the wheels; establishing the effects that various factors have on the energy consumption during digging; determining the rational design and process parameters of the wheels and the optimum dimensions of their soil separating surfaces.

The interaction between the soil and the lifter's wheel is investigated in the study. As a result, the resultant of the normal components of the forces applied by parts of the soil over the whole surface of contact S has been determined. Its magnitude can be found from the following expression:

$$\overline{N} = \iint\limits_{S} P_{xyz}\overline{n}_{xyz}dS \tag{2.16}$$

where S—area of contact, P_{xyz}—normal force of pressure, $\overline{n}_{xyz}$—normal line to the spherical surface of the wheel at the point with the coordinates x, y, z.

Additionally, the coordinates and velocities of any point of the wheel during its movement in the soil have been determined.

The pattern of distribution of contact stresses during the operation of wheel lifters has been determined by way of selecting the appropriate deformation model, verifying it for adequacy in comparison with the experimental data and the following estimation of the overall stress and strain state and the distribution of contact stresses. The process of a wheel lifter deforming the soil has been investigated thoroughly, and the differential equations have been obtained for the elongation, expansion and angular displacements of an elementary volume of soil by solving which the laws of the soil deformation by the wheel lifter have been deduced. Moreover, the differential equation that allows the determination of the motion trajectory of an arbitrary point of the soil in the process of the wheel lifter cutting out a soil layer has been generated. Thus, the developed deformation model allows the deformation components at any point of the compression zone to be determined and establishes the relation with the stresses that are part of the equation of equilibrium for an elementary volume of soil of variable thickness, which is compressed between the wheels in the case of Hooke's elastic rheological model. When the roots are dug out with the use of passive lifters, the soil in front of the wheels is compacted and the von Mises model, in which a relation exists between the stresses and the rates of deformation, is more appropriate for the space between the wheels.

It has been established that the pattern of distribution of contact stresses on the wheels depends primarily on the type of lifter (active or passive), the physical condition of the soil and, less significantly, on the variation of the positions of the wheels (within their operating range).

It has also been proved theoretically that the rotational torque of the drive of the active wheel substantially depends on the physical–mechanical properties of the soil, the distribution of contact stresses and the redistribution of friction forces on the surfaces of the wheels.

It has been proved analytically that the difference between the translational velocity of the machine and the linear velocity of the wheel's rim is the principal factor that defines the redistribution of the energy consumption for the actuation of the implements and the tractive power of the beet harvester.

Thus, it becomes evident from the analysis of the theoretical studies on the wheel lifter implements that sound mathematical models describing the motion of roots inside the lifting implements have not been developed in this area of research as well.

2.5. Vibrational Digging Tools

The vibrational digging of sugar beet roots has gained wide use in many beet-growing countries. It has a number of advantages in comparison to other methods of digging. In particular, the soil accumulates to a lower extent in the lifter's working channel and the process of shaking off the soil stuck on the surface of the root is improved significantly.

It should be noted that the research into the process of vibrational digging of roots has, for the most part, been of experimental nature. Only in three studies [6,7,20] has separate theoretical research into the process of vibrational digging of roots with the oscillations generated in the transversely horizontal plane been carried out.

As suggested in [7], when the root is shaken by a horizontal force applied to the root's upper part or alternating-sign impacts, its bonds with the soil are actively broken. As alternating-sign impulse loads are applied time and again, the root starts moving vertically upwards, which contributes to the process of its extraction from the soil. Different roots require different numbers of periodic loads to be applied for the complete disintegration of the bonds with the soil.

If the root is made to oscillate in the transversely horizontal plane (Figure 2.9) by law of $\tau = \tau_0 cos\omega t$, the root, according to [7], will be extracted from the soil under the following condition:

$$l_c\omega_k^2\tau_0 > g\left(1 + \frac{R_c}{Q}\right) \tag{2.17}$$

where l_c—coordinate of the root's centre of gravity; ω_k—frequency of the root's oscillations; τ_0—angular displacement of the root from the vertical axis; R_c—force of the root's bond with the soil; Q—weight of the root; g—acceleration of gravity.

The condition of not damaging the root during its oscillatory motion appears as follows:

$$\left| \frac{l_c}{z_s} \left[(C_k l_c - Q) sin\tau_0 - \frac{I_x \omega_k^2 \tau_0}{l_c} \right] cos\tau_0 + \frac{Q l_c \omega_k^2 \tau_0}{g} - (C_k l_c - Q) sin\tau_0 \right| < [N]_{dop}, \quad (2.18)$$

where C_k—stiffness of the root at the point of fixation; z_s—coordinate of perturbing force application point; I_x—moment of inertia of the root about the horizontal axis that passes through the point of fixation; $[N]_{dop}$—bending load, which causes breaking of the root body.
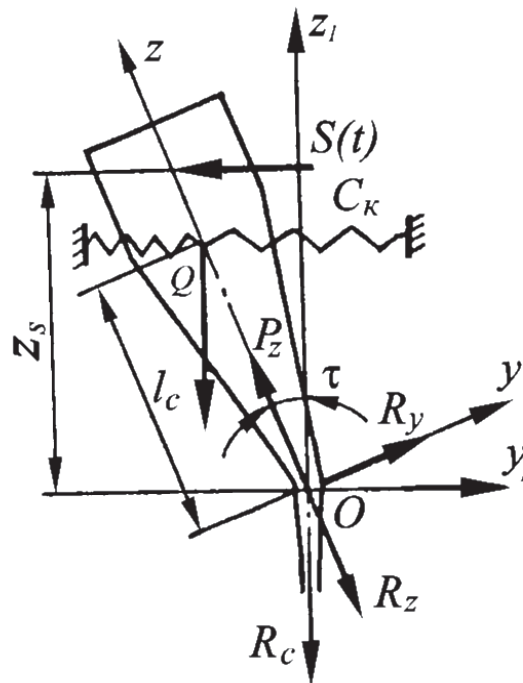
Figure 2.9. Schematic model of forces acting on root during its vibrational lifting.

As indicated in [7], the analysis of the process of the root extraction under the action of a horizontal perturbing force has shown that, in order to allow an efficient extraction process, it is necessary to make each root oscillate at its specific values of frequency and amplitude, which is impossible in practice, since the parameters of roots are random quantities. Therefore, the fulfilment of the conditions (1.17) and (1.18) have to be considered in the probabilistic sense and, for the purpose of describing the situations with the most probable outcome of extracting the root without damaging it, it is reasonable to generate the oscillations within a certain spectrum of frequencies and amplitudes. However, it follows from (2.17) and (2.18)

that the most efficient course of the process of the root extraction from the soil can be achieved by making the roots oscillate at an increasing amplitude and the constant frequency that is specific for the selected mode of operation. In order to avoid substantial damage to the sugar beet roots during their extraction, the amplitude of oscillations must not exceed 0.25–0.35 rad, with a frequency of –20 Hz. Based on the investigation of the process of the root moving under the action of the horizontally applied alternating-sign force $\overline{S}(t)$, the following expressions are suggested in [7] for the computation of the forces acting on the root (Figure 2.9):

$$R_z = \frac{Ql_c\tau^2}{g} + S(t)sin\tau - Qcos\tau \qquad (2.19)$$

$$R_y = S(t)cos\tau - (C_k l_c - Q)sin\tau - \frac{Ql_c\dot{t}}{g} \qquad (2.20)$$

where R_z, R_y—vertical and horizontal components, respectively, acting on the root at the point of fixation; Q—weight of the root; τ—trajectory of the root's motion under the action of force $\overline{S}(t)$; l_c—coordinate of the root's centre of gravity.

In [7], the maximum probability of extracting the roots combined with the limited probability of damaging them is recommended as the criterion of optimisation of the lifter's parameters—i.e.,

$$maxP\{P_z \geq R_z + Q\}, \ P\big(P_y > \big[R_y\big]\big) \leq \xi, \qquad (2.21)$$

where ξ—permissible value of the probability of damaging the roots; P_z—force of the root extraction from the soil; P_y—horizontal (lateral) force; $\big[R_y\big]$—minimum force that can cause damage to the root. The probabilities (2.21) are calculated on the PC by a statistical test.

In [7], the schematic model of the vibrational digging tool that performs angular oscillations in the horizontal plane transversely to the line of the lifter's translational motion is offered (Figure 2.10).

The principle of its operation is as follows: when the wheel (5) rotates, the shaft (4) periodically turns through angles of $\pm\theta$. The horizontal plates that form the working channel of the lifter and are connected with the shaft by the vertical bars (2) also periodically turn about point O through the same angle $\pm\theta$. For the purpose of reducing the tractive resistance and facilitating the extraction of roots from the soil with a minimum amount of soil, the axis of the oscillating shaft (3) is situated on the centreline of the front ends of the fork, obliquely or perpendicularly to its plane. In consequence of such a situation of the working channel, as the shaft periodically turns, the points of the front part of the lifter perform lengthwise oscillations, while the points of the rear part perform crosswise oscillations.

It ought to be noted that, in the process of extracting the root from the soil by a usual share lifter, an important role is played by the backup forces exerted by soil, under the action of which the soil layer is compressed in the tapering channel of the lifter and during the lifter's translational motion with the further breaking of the soil layer the vertical extraction forces needed for lifting the root are generated. Hence, the presence of the backup forces exerted by soil is a necessary condition for the operation of a conventional share lifter.

When the roots are lifted with the use of a vibrational digging tool, the soil in the area of the lifter's working channel becomes loose to a significant extent due to the oscillatory motion of the lifter's shares. In view of this, in the case of a vibrational lifter the above-mentioned forces of backing up the root do not play such an important part as in the case of a share lifter, as the necessary soil compression strain in the lifter's working channel does not arise during the lifter's translational motion and its contact with the root. As indicated in [7], the presence of soil in the vibrational lifter's working channel is not the principal condition of generating the force of the root extraction from the soil. Said circumstance embodies the essential difference between vibrational lifters and other types of digging tools as regards the performance of the work process of root digging. In this case, the required vertical forces of the root extraction are generated by the vertical motions of the lifter's shares that are three-dimensionally inclined at respective angles, which facilitates capturing of the roots by the necking channel and entraining them in the joint upward motion. The working faces of the shares of the vibrational lifter, which feature, as mentioned earlier, respective three-dimensional inclinations and form the throat of the lifter, also impart vertical extraction forces on the roots. It is also noted in [7] that, while the root in the channel of a usual wheel or share lifter in the presence of backup forces exerted by the soil bends rather appreciably along the line of travel, in the channel of a vibrational lifting tool the centreline of the root during its extraction from the soil for the most part retains the initial position that is almost vertical and perpendicular to the row centreline or deflects from said position through small angles (which depends mostly on the stiffness of the soil around the root).

This operation feature of the vibrational lifting tool establishes a situation where the root chipping-off rate is considerably reduced as a result of the slight inclination of the root's centreline along the lifter's line of translation. In the case of vibrational digging, the roots are also actively freed from the stuck soil in the process of intensive breaking of the soil in the front part and then during the gripping and forced vertical displacement of the roots due to the strong acceleration imparted on them.

Thus, the extraction of the root from the soil in the case of vibrational digging takes place under the action of the perturbing force supplied by the drive mechanism by means of direct grasping of the root by the shares of the vibrational lifting tool

and its further advancement across the shares' inner faces that have respective three-dimensional inclinations and form the throat of the lifter.
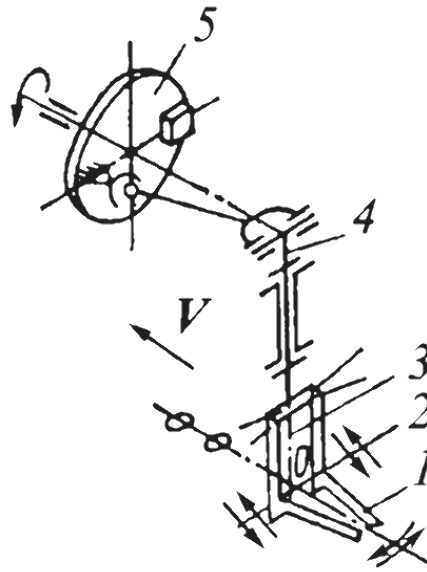
Figure 2.10. Schematic model of vibrational digging tool, which induces oscillations of root in transversely horizontal plane.

The first fundamental analytical treatment of the transverse oscillations of the body of a root fixed in the soil was undertaken and published in [6]. In this study, the sugar beet root is modelled as a cone-shaped body, one point at the bottom of which is fixed and which has elastic properties. That said, the transverse oscillations of the root are described with the use of a fourth-order partial differential equation. The solution of said equation makes it possible to determine the natural frequencies of the free transverse oscillations of the root body. Specifically, the process of sugar beet extraction from the soil is then studied with the use of additionally generated kinetostatic equations, which allow the conditions of the complete extraction of the root from the soil to be found.

In [20], which, in effect, is an extension of [6], the Hamilton–Ostrogradsky functional, which describes the root's free transverse oscillations when it is fixed in the soil at its bottom end and applies perturbing forces to it in the transversely horizontal plane along the line that is perpendicular to the line of the lifter's translational motion, is set up. Using the Ritz method and based on the conditions of time invariance of the mentioned functional, the Ritz equation of frequencies is generated to find the first, second and third natural frequencies of the free transverse oscillations of the root body.

The above-mentioned fundamental analytical treatment [7] presents the fundamental provisions and assumptions with regard to the vibrational digging of roots introduced in the earlier papers of the same authors [6,20]. However, no

mathematical model of the vibrational lifting of sugar beet root from the soil can be found in this study.

It ought to be remarked that, despite the mentioned fundamental analytical treatments of the process of vibrational lifting of sugar beet roots (by applying perturbing forces to them in the transversely horizontal plane), the accomplishment of full-scale engineering projects, the industrial production of several pilot units and the performance of elaborate experimental studies and official tests, such vibrational digging tools have not gained any ground. It is assumed (and it has been fully proved during the thorough tests under different conditions) that one of the main reasons for this is the failure to ensure a sufficiently high rate of travel of the vibrational lifters in such a design (and, accordingly, the sufficiently high rate of work subject to retaining the required harvesting quality indicators), which results from the fact that applying the perturbing forces to the beet roots in the plane that is perpendicular to the line of the lifter's translational motion leads to the constant plugging of its working channel with root bodies and soil, chipping-off of the roots' tail parts and deterioration of the implement's performance up to its complete breakdown. The power consumption rate of this process was also too high.

As has been established, said negative phenomenon can be completely avoided by switching the line of action of the perturbing forces from the transversely horizontal plane and the alignment perpendicular to the line of the lifter's translational motion into the vertical and longitudinal plane. Implementation of this change brought about good performance in the harvesting of sugar beet roots. Virtually all world leading manufacturers of beet harvesting machines started producing vibrational lifting tools, which operated based on the principle of imparting perturbing forces on the roots.

Nevertheless, for a long time there were no further profound analytical studies on the oscillation of the root body fixed in the soil and the process of its vibrational lifting with the use of perturbing forces in the longitudinal and vertical plane. Apparently, it was assumed that the investigations carried out in the fundamental papers [6,7,20] fully described the oscillation process under consideration. All further research into the process of vibrational root digging was predominantly experimental. Meanwhile, the change in the line of action of the perturbing forces entails not only alterations in the design implementation of the vibrational lifting tools, but essential adjustments in the theory itself as well, especially in its end results.

In its crucial new form, the theory of vibrational root lifting in the case of applying the perturbing forces to the roots specifically in the vertical and longitudinal plane has been published in the studies [21–23]. A case of transverse free and forced oscillations of the root body, in which the line of action of the perturbing forces coincides with the line of translational motion of the vibrational lifting tool, has been considered in the papers [24,25]. Said case is of considerable interest both from the

theoretical and practical points of views. For example, with this line of action of the perturbing forces the bonds between the root and the soil are broken more effectively (the so-called loosening effect occurs) and at the later stages, when the root body is finally lifted from the soil, it is not under the action of stretching forces. In this case, the accumulation of roots and soil in the vibrational lifter's working channel will not take place. Moreover, the design of the vibrational lifting tool that operates on the described principle will consume less energy and metal, etc.

It is also worth noting that in the case of the vibrational digging of sugar beet roots at the up-to-date velocities of translational motion of digging tools, it is quite probable that a phenomenon takes place where the digging shares hit the root body in the process of the vibrational lifting tool running in on the root. This issue has not been given analytical consideration. Accordingly, an urgent need has arisen to develop a theory of impact interaction between the vibrational lifting tool and the root body, with the purpose of substantiating the rational design parameters of the digging tool and the kinematic modes of performance of the work process of vibrational lifting of sugar beet roots under the condition of their not chipping-off at impact.

2.6. Agrotechnical Requirements for Harvesting of Sugar Beet Roots

With any combination of the techniques and technologies of harvesting sugar beets, the harvesters under operation must provide high quality gathering of the roots in compliance with the agrotechnical requirements. The characteristic values of that quality are specified by DSTU 2258-93 (GOST 7496-93) "Sugar beet harvesting machinery. General specifications", as well as the ISO guidelines. In particular, in the mentioned regulatory document and other technical guidelines, the following requirements are indicated.

The operating rate of travel of sugar beet combines must be at least 6.0 km·h^{-1} and the transport rate must be about 20 km·h^{-1}. The performance rate per hour of productive time should be at least 0.54 ha hectares for two-row combines, at least 0.81 ha for three-row ones and at least 1.62 ha for six-row harvesters. The work process performance reliability factor must be at least 0.98; the shift time utilisation factor must be at least 0.75.

The sugar beet combines must ensure collection of 98.5% of the roots (i.e., the losses cannot exceed 1.5%). In the pile of gathered roots, the extraneous material contents cannot exceed 8.0%, including plant residues at a rate of no more than 0.20%. The damaged roots may not amount to more than 10%, including the heavily damaged ones at a rate of no more than 5%.

The specific fuel consumption rate must be limited in the case of two-row machines by 24.0 kg·ha^{-1} and in the cases of three- and six-row ones by 30.0 kg·ha^{-1}. The mean time between failures is at least 50 h of productive time; the availability

factor in the productive time is at least 0.95. The specific total labour intensity of the emergency maintenance in operation may not exceed 0.08 man-hour·hour^{-1}. The mean shift running time for maintenance should be limited by 0.40 h and the specific total labour intensity of the running maintenance should be limited by 0.09 man-hour·hour^{-1}. The specific structural mass for the performance of a process operation must be no more than 4400 kg·m^{-1} in the case of two-row combines, no more than 5100 kg·m^{-1} for three-row ones and no more than 6500 kg·m^{-1} for six-row machines. The specific material intensity may not exceed 9700 kg·ha^{-1}·h^{-1} in the case of two-row harvesters, 11,000 kg·ha^{-1}·h^{-1} for three-row ones and 14,400 kg·ha^{-1}·h^{-1} for six-row ones. The labour input for changing from the transport position into the operating one and vice versa should not be more than 0.10 man-hours. The required road clearance is at least 300 mm. The sugar beet harvesters must comply with the requirements of DSTU 2189-93: "Mounted and towed agricultural machines. General safety requirements". A combine harvester should be operated by one tractor operator, whose labour input should be no more than 2.44 man-hours·ha^{-1} in the case of two-row combines, no more than 1.64 for three-row ones and no more than 0.82 man-hours·ha^{-1} for six-row ones. The annual utilisation rate is at least 160 h. The operating life of a combine harvester is equal to eight years.

2.7. Conclusions

In summary, the following conclusions can be drawn on the basis of the analytical review of the main studies concerned with the theoretical research into the process of lifting roots from the soil:

1. The existing studies of the process of vibrational lifting of sugar beet roots from the soil are predominantly of experimental nature, which does not allow for a comprehensive and thorough investigation of said work process.

    a. It is necessary to undertake fundamental theoretical research into the process of vibrational root lifting based on the application of up-to-date mechanical and theoretical methods of analysis, which would enable a more consistent and comprehensive investigation and analysis of said process.

2. The comprehensive and multivariate analysis of the vibrational root lifting process will provide the basis for finding the rational design parameters and kinematic modes of performance of vibrational digging tools, which will allow reducing of the root loss and damage rates and lower the energy consumption.

3. Hence, a need arises to individually generate the respective mathematical models of lifting roots from the soil with the use of the vibrational lifting tool for all stages of extraction: from the initial gripping of the root by the digging shares to the final lifting from the soil. In this process, it is necessary to first set

up the schematic models of the force interaction between the root body and the digging faces of the implement. Further, the differential equations of motion of the root body have to be generated with the use of the general principles of the dynamics. It is imperative to include in the equations the condition of not damaging the root body.

4. On the basis of solving the obtained systems of differential equations of motion of the root body, the rational kinematic and design parameters of vibrational lifting tools have to be determined.

5. The results of the theoretical research are to be used for the development of new designs of vibrational lifting tools for root harvesters as well as the specific recommendations on their efficient use in accordance with the environment-and-climate and working conditions.

3. Theory of Share-Type Lifting Tool

3.1. Analysis of Force Interaction between Share Lifter and Soil around Root

The principal correlations between the geometrical parameters of share-type lifting tools are presented in Section 2.

The next step is to explore the force interaction between the share lifter and the soil with the use of the main provisions of [8]. For this purpose, the schematic model of forces is set up with an element of soil layer *KL* containing in its centre the root approximated by a conically shaped solid (Figure 3.1). Under the action of the soil backup forces represented by a uniformly distributed load with an intensity of $\overline{q}$, the soil layer element *KL* is contained in the share lifter's working channel between its working faces and is continuously compressed during the translational motion of the lifter. The soil backup force applied directly to the root is designated as $\overline{Q}$. A state of stress sets in in the soil layer *KL* as a result of the action of the normal forces $\overline{N}$ and forces of friction $\overline{F}$ at points *K* and *L* of its contacts with the working faces of the wedges. As a consequence of this, the part of the root contained within the layer *KL* (the lower part of the root continues to be constrained in the unstrained layer of the soil) falls under the action of force $\overline{Q}$, resulting from the soil backup forces $\overline{q}$. From the opposite side, this part of the root is under the direct action of forces $\overline{P}'_{xi}, \overline{P}'_{yi}, \overline{P}'_{zi},$ ($i = 1, 2$) applied by the wedges' working faces, on which the corresponding forces $\overline{P}_{xi}, \overline{P}_{yi}, \overline{P}_{zi}$, ($i = 1, 2$) arise.

Each of the above-mentioned forces applied by the shares' working faces is shown in Figure 3.1 with a respective index. Thus, the forces applied by the working face $A_1B_1C_1$ to the soil layer are denoted by index 1—$\overline{P}_{x1}, \overline{P}_{y1}, \overline{P}_{z1}$—while the forces applied by this face to the root itself—$\overline{P}'_{x1}, \overline{P}'_{y1}, \overline{P}'_{z1}$. The forces acting on the soil layer from the working face $A_2B_2C_2$ are labelled with index 2—$\overline{P}_{x2}, \overline{P}_{y2}, \overline{P}_{z2}$; the forces applied by this face to the root itself and, respectively $\overline{P}'_{x2}, \overline{P}'_{y2}, \overline{P}'_{z2}$. The effect the mentioned forces have on the root is defined by their generation on the wedges' working faces and the mode of their transfer in the strained layer of the soil. The force of the bonds between the root and the soil is designated as $\overline{R}$, and it acts conventionally along the centreline of the root itself and is, in the general case, vectored vertically down, but when specifically considering the process of extraction of the root from the soil, it can be decomposed along the respective coordinate axes (in Figure 3.1, it is represented by the projections R_x and R_z).

The above-mentioned forces have to be determined. In the general case, as is shown in Figure 3.2, (1, 2, 3), forces $\overline{P}_{xi}, \overline{P}_{yi}, \overline{P}_{zi}$ ($i = 1, 2$) in vector notation are as follows:

For plane $A_1B_1C_1$:

$$\overline{P}_{x1} = \overline{N}_{x1} + \overline{F}_{x1}, \overline{P}_{y1} = \overline{N}_{y1} + \overline{F}_{y1}, \overline{P}_{z1} = \overline{N}_{z1} + \overline{F}_{z1}. \tag{3.1}$$

Similarly, for plane $A_2B_2C_2$:

$$\overline{P}_{x2} = \overline{N}_{x2} + \overline{F}_{x2}, \overline{P}_{y2} = \overline{N}_{y2} + \overline{F}_{y2}, \overline{P}_{z2} = \overline{N}_{z2} + \overline{F}_{z2}. \tag{3.2}$$

where $\overline{N}_{xi}, \overline{N}_{yi}, \overline{N}_{zi}$, ($i = 1, 2$)—normal forces of reaction of the wedges' working faces projected on the respective coordinate axes; $\overline{F}_{xi}, \overline{F}_{yi}, \overline{F}_{zi}$, ($i = 1, 2$)—forces of friction of the soil layer on the wedges' working faces, also projected on the respective coordinate axes.

The first step is to analyse the action of each of the forces entered into (3.1) and (3.2) and constituting the forces imparted directly on the root. To begin with, the vertical forces $\overline{P}'_{z1}$ and $\overline{P}'_{z2}$ generated by the share faces try to dislodge the root (especially that part of it, which is fixed in the soil) out of the soil; the horizontal transverse forces $\overline{P}'_{y1}$ and $\overline{P}'_{y2}$ also promote squeezing of the root as a tapered body out of the soil. The horizontal forces $\overline{P}'_{x1}$ and $\overline{P}'_{x2}$ (in Figure 3.1 they are denoted as the total force $\overline{P}'_{x1,2}$), which act in the direction of the share lifter's motion, also try, together with force $\overline{Q}$, to force the root out of the soil, while the direction, in which force $\overline{Q}$ acts, is opposite to that of the lifter's motion. However, depending on the properties of the soil and some other factors, the backup force $\overline{Q}$ can be insignificant, and subsequently $P'_{x1,2} > Q$, and the root will move forward under the action of the horizontal force $R_{\Gamma} = P'_{x1,2} - Q$, possibly resulting in the break-off of the root in the area of its fixation in the unstrained soil layer. Therefore, a high quality of operation of a share lifter is secured in case the lifter generates significant amounts of forces $\overline{P}_{zi}$ and $\overline{P}_{yi}$ and, vice versa, insignificant amounts of force $\overline{P}_{xi}$.

The magnitudes and lines of action of forces $\overline{N}_i$ and $\overline{F}_i$, which define forces $\overline{P}_{xi}, \overline{P}_{yi}, \overline{P}_{zi}$, ($i = 1, 2$), depend on many factors: the properties and condition of the soil, the magnitudes of the bonding forces between the root and the soil $\overline{R}$, the geometrical parameters of the lifter's wedges and the angles of their setting with respect to the line of travel, the velocity of translation, etc.
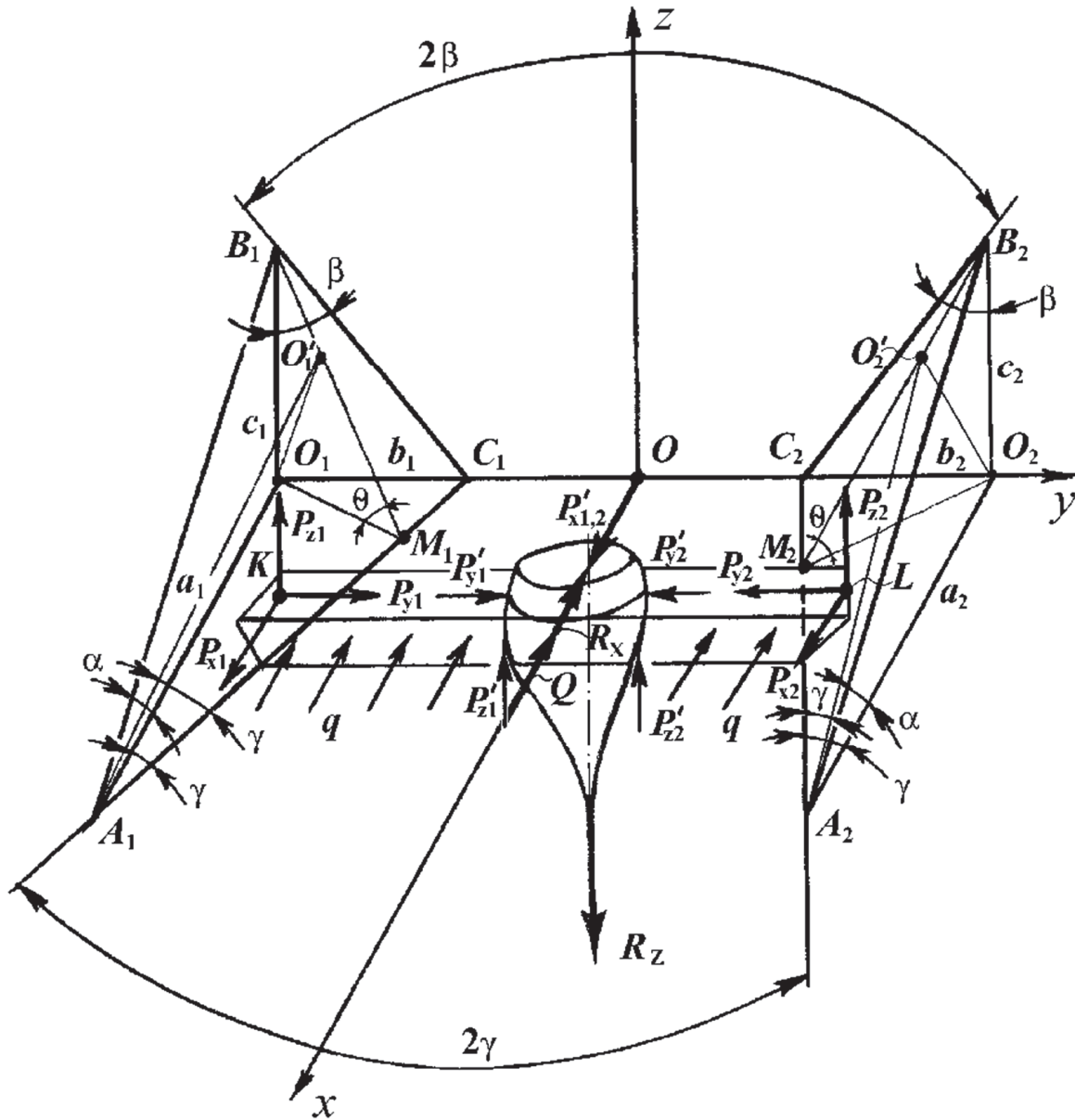
Figure 3.1. Interaction between the share lifting tool and the soil.

Further, consideration should be given to the effect that the angles α, β and γ have on the magnitudes of forces $\overline{P}_{xi}, \overline{P}_{yi}, \overline{P}_{zi}$ ($i = 1, 2$), which produce the pressure of the working face of the wedge on the soil layer and the root. This can be examined by taking one of the faces of the share lifter as an example, assuming that the second face is in a similar situation. As can be seen in Figure 3.2 (1), the point of contact L is under the action of the normal reaction $\overline{N}_2$, which can be represented by its projections on the respective coordinate axes—N_{x2}, N_{y2}, N_{z2}. After the mentioned projections of the normal reaction are found, it becomes possible to also find the force of friction $\overline{F}_2$, which in its turn can also be represented by its projections on the same coordinate axes—F_{x2}, F_{y2}, F_{z2} (Figure 3.2 (2)).
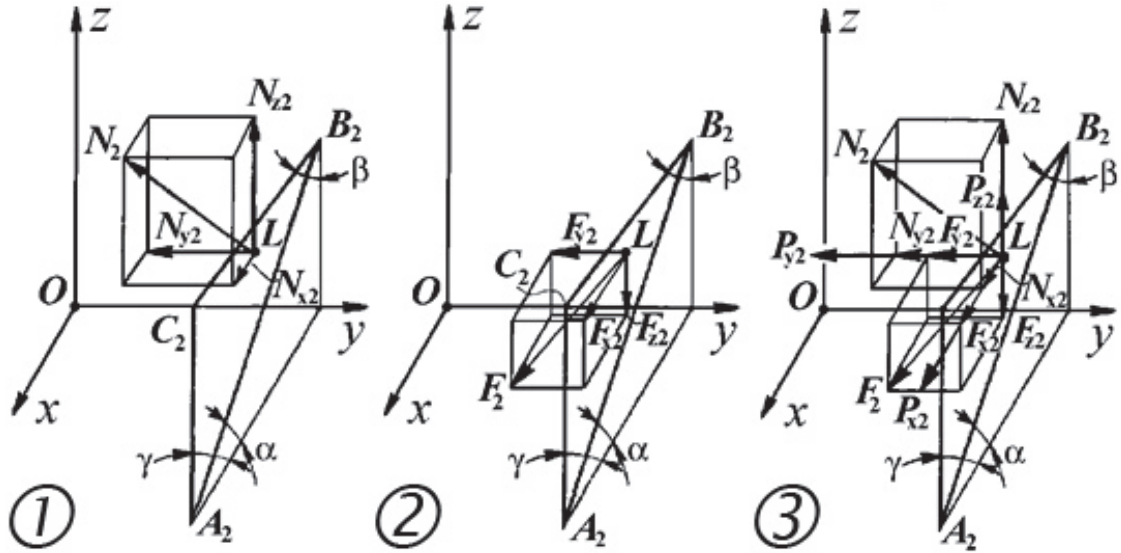
Figure 3.2. Diagram of forces acting on one of the wedges of share lifter: 1—normal component of $\overline{N}_2$ and its projections on the coordinate axes; 2—force of friction $\overline{F}_2$ and its projections on the coordinate axes; 3—total forces imparted by the wedge face: $\overline{P}_{x2}, \overline{P}_{y2}, \overline{P}_{z2}$.

3.2. Determination of Projections of Normal Reactions of Shares on Cartesian Coordinate Axes

It is necessary to find the magnitudes of forces $\overline{N}_{xi}, \overline{N}_{yi}, \overline{N}_{zi}$ vectored along the respective coordinate axes and depending on the direction of vector of force $\overline{N}_i$ ($i = 1, 2$) itself. In this process, the analytical expressions will be set up simultaneously for both the shares of the lifter. For face $A_1B_1C_1$, they are as follows:

$$
\begin{aligned}
N_{x1} &= N_1 \cos\left(x, \hat{\overline{N}}_1\right), \\
N_{y1} &= N_1 \cos\left(y, \hat{\overline{N}}_1\right), \\
N_{z1} &= N_1 \cos\left(z, \hat{\overline{N}}_1\right).
\end{aligned}
\tag{3.3}
$$

Respectively, for face $A_2B_2C_2$:

$$
\begin{aligned}
N_{x2} &= N_2 \cos\left(x, \hat{\overline{N}}_2\right), \\
N_{y2} &= N_2 \cos\left(y, \hat{\overline{N}}_2\right), \\
N_{z2} &= N_2 \cos\left(z, \hat{\overline{N}}_2\right),
\end{aligned}
\tag{3.4}
$$

where $\cos\left(x, \hat{\overline{N}}_i\right)$, $\cos\left(y, \hat{\overline{N}}_i\right)$, $\cos\left(z, \hat{\overline{N}}_i\right)$—direction cosines of the $\overline{N}_i$ ($i = 1, 2$) force vector.

Further, the relation between the mentioned direction cosines and the angles α, β and γ that define the design parameters of the share lifter is to be determined.

For this purpose, the intervals on the coordinate axes cut off by the working faces of the wedges will be denoted by a_i, b_i and c_i, ($i = 1, 2$)—i.e., in the case of face $A_1B_1C_1$ they will be intervals a_1, b_1, c_1, in the case of faces $A_2B_2C_2 - a_2, b_2, c_2$. Then, the coordinates of the three vertices of each wedge face ($A_1B_1C_1$ and $A_2B_2C_2$) in the assumed coordinate system $Oxyz$ are, respectively, equal to:

$$
\begin{aligned}
x_{A1} &= a_1; & y_{A1} &= -\tfrac{A_1A_2}{2}; & z_{A1} &= 0; \\
x_{B1} &= 0; & y_{B1} &= -\tfrac{A_1A_2}{2}; & z_{B1} &= c_1; \\
x_{C1} &= 0; & y_{C1} &= -\left[\left(\tfrac{A_1A_2}{2}\right) - b_1\right]; & z_{C1} &= 0; \\
x_{A2} &= a_2; & y_{A2} &= \tfrac{A_1A_2}{2}; & z_{A2} &= 0; \\
x_{B2} &= 0; & y_{B2} &= \tfrac{A_1A_2}{2}; & z_{B2} &= c_2; \\
x_{C2} &= 0; & y_{C2} &= \left(\tfrac{A_1A_2}{2}\right) - b_2; & z_{C2} &= 0.
\end{aligned}
\tag{3.5}
$$

Employing the analytical geometry principles [26] and based on (3.5), the equations of faces $A_1B_1C_1$ and $A_2B_2C_2$ can be set up in terms of the following determinants:

$$
A_1B_1C_1 : \begin{vmatrix} x_{A1} - a_1 & y_{A1} + \tfrac{A_1A_2}{2} & z_{A1} \\ -a_1 & b_1 \\ -a_1 & c_1 \end{vmatrix} = 0;
$$

$$
A_2B_2C_2 : \begin{vmatrix} x_{A2} - a_2 & y_{A2} - \tfrac{A_1A_2}{2} & z_{A2} \\ -a_2 & b_2 \\ -a_2 & c_2 \end{vmatrix} = 0.
\tag{3.6}
$$

It can be concluded from Figure 3.1 that the magnitudes of the respective intervals a_i, b_i, c_i, ($i = 1, 2$) on the respective coordinate axes are equal to:

$$
a_1 = \frac{b_1}{\tan\gamma}; a_2 = \frac{-b_2}{\tan\gamma}; c_1 = \frac{b_1}{\tan\beta}; c_2 = \frac{-b_2}{\tan\beta}; b_1 = b_2 = \frac{(A_1A_2 - C_1C_2)}{2}. \tag{3.7}
$$

Expanding the obtained determinants (2.6), the following equations of the faces of the share lifter's wedges are:

$$
\begin{aligned}
A_1B_1C_1 : \; & (x_{A1} - a_1)[b_1c_1 - 0 \cdot 0] + \left(y_{A1} + \tfrac{A_1A_2}{2}\right)[0 \cdot (-a_1) - (-a_1) \cdot c_1] \\
& + z_{A1}[(-a_1) \cdot 0 - b_1(-a_1)] = 0, \\
A_2B_2C_2 : \; & (x_{A2} - a_2)[(-b_2) \cdot c_2 - 0 \cdot 0] \\
& + \left(-y_{A2} - \tfrac{A_1A_2}{2}\right)[0 \cdot (-a_2) - (-a_2) \cdot c_2] \\
& + z_{A2}[(-a_2) \cdot 0 - (-b_2)(-a_2)] = 0.
\end{aligned}
\tag{3.8}
$$

After substituting (3.7) into (3.8) and performing the appropriate transformations, the equations of the working faces of the share lifter are obtained. They appear as follows:

$$A_1B_1C_1: \qquad x_{A1}\tan\gamma + y_{A1} + z_{A1}\tan\beta + \frac{C_1C_2}{2} = 0, \qquad (3.9)$$

$$A_2B_2C_2: \qquad x_{A2}\tan\gamma - y_{A2} + z_{A2}\tan\beta - \frac{C_1C_2}{2} = 0. \qquad (3.10)$$

It is known that the direction cosines for the vectors that are normal to the faces represented by (3.9) and (3.10) have the following values:

$$\begin{aligned}
\cos(x,\overline{N}_i) &= \frac{\tan\gamma}{\sqrt{\tan^2\gamma + 1 + \tan^2\beta}}, \\
\cos(y,\overline{N}_i) &= \frac{1}{\sqrt{\tan^2\gamma + 1 + \tan^2\beta}}, \\
\cos(z,\overline{N}_i) &= \frac{\tan\beta}{\sqrt{\tan^2\gamma + 1 + \tan^2\beta}}.
\end{aligned} \qquad (3.11)$$

Then, by substituting (3.11) into (3.3) and (3.4), the following values for the projections of the normal components of forces $\overline{N}_i$ ($i = 1, 2$) generated by the wedge faces on the respective coordinate axes are obtained.

For face $A_1B_1C_1$:

$$\begin{aligned}
N_{x1} &= \frac{N_1\tan\gamma}{\sqrt{\tan^2\gamma + 1 + \tan^2\beta}}; \\
N_{y1} &= \frac{N_1}{\sqrt{\tan^2\gamma + 1 + \tan^2\beta}}; \\
N_{z1} &= \frac{N_1\tan\beta}{\sqrt{\tan^2\gamma + 1 + \tan^2\beta}};
\end{aligned} \qquad (3.12)$$

For face $A_2B_2C_2$:

$$\begin{aligned}
N_{x2} &= \frac{N_2\tan\gamma}{\sqrt{\tan^2\gamma + 1 + \tan^2\beta}}; \\
N_{y2} &= \frac{-N_2}{\sqrt{\tan^2\gamma + 1 + \tan^2\beta}}; \\
N_{z2} &= \frac{N_2\tan\beta}{\sqrt{\tan^2\gamma + 1 + \tan^2\beta}}
\end{aligned} \qquad (3.13)$$

Since the values for the projections of the normal components of the forces generated by the working faces of the wedges have been found, it becomes possible to also determine some other forces imparted by them to the soil layer and directly to the root.

3.3. Analysis of Force Interaction with Working Faces of Shares during Approach of Lifting Tool to Root and Its Direct Contact with Root

Further, detailed analysis is to be made on the principal factors and forces arising in the process of operation of the share lifter have effect on the formation of the normal reactions $\overline{N}_1$ and $\overline{N}_2$ of the working faces of wedges $A_1B_1C_1$ and $A_2B_2C_2$, respectively, as well as the forces of friction $\overline{F}_1$ and $\overline{F}_2$ between the soil layer containing the root

and the faces of the mentioned wedges. In other words, it is necessary to establish the physical substance of the mentioned forces.

Firstly, the working faces of the wedges are under the action of the force of gravity $\overline{G}$ of the soil layer KL with the root in it. It is assumed that the force of gravity of the soil layer with the root is distributed equally between wedges $A_1B_1C_1$ and $A_2B_2C_2$ of the lifter—i.e., $G_1 = G_2 = \frac{1}{2}G$. Forces $\overline{G}_1$ and $\overline{G}_2$ generate the static parts of the normal reactions of the working faces of wedges $A_1B_1C_1$ and $A_2B_2C_2$. These parts of the reactions are denoted as $\overline{N}_{G1}$ and $\overline{N}_{G2}$, respectively. In addition to this, as a result of the motion of the soil layer on the mentioned surfaces, said weight forces give rise to the parts of the forces of friction $\overline{F}_{G1}$ and $\overline{F}_{G2}$.

Secondly, the working faces of wedges $A_1B_1C_1$ and $A_2B_2C_2$ are under the action of the forces of dynamic pressure of the incoming soil $\bar{I}_1$ and $\bar{I}_2$, respectively [27,28]. The action of said forces can be regarded as the continuous process of parts of the soil striking the faces of wedges $A_1B_1C_1$ and $A_2B_2C_2$. As a result of the continuous inflow of the soil mass on the faces of the wedges, an impact impulse is generated, which is equal to:

$$\bar{I}_1 dt = \bar{I}_2 dt = \left(\overline{V}_a - \overline{V}_o\right) dm \tag{3.14}$$

where $\overline{V}_a$—absolute velocity of the soil particles with masses of dm; $\overline{V}_o$—initial velocity of the soil particles prior to their collision with the wedge.

Since the initial velocity $\overline{V}_o = 0$, the following is derived from (3.14):

$$\bar{I}_1 = \bar{I}_2 = \frac{dm}{dt} V_a \tag{3.15}$$

The mass of the soil that falls on the wedges in a unit of time can be determined as follows:

$$\frac{dm}{dt} = ab\frac{\gamma_{ob.}}{g} V \tag{3.16}$$

where a and b are, respectively, the width and the thickness of the soil layer that is undercut by each wedge separately; $\gamma_{ob.}$—bulk specific gravity of the soil; g—free fall acceleration; V—velocity of translation of the lifter.

Hence, by substituting (3.16) into (3.15), the following is obtained:

$$I_1 = I_2 = ab\frac{\gamma_{ob.}}{g} V V_a \tag{3.17}$$

The forces of dynamic pressure act along the vector $\overline{V}_a$ of the absolute velocity of motion of the soil layer.

In order to find the trajectory and velocity of the motion of the layer on the wedge, an assumption is introduced that the length of the layer during its undercutting and its motion on the wedge do not change; therefore, the velocity V_r of the soil layer's

relative motion on the face of the wedge is equal to the velocity V of its translational motion—i.e., the velocity of translational motion of the lifter itself. When the layer moves in the area of the lifter's working channel, it is assumed that the trajectory of the motion on wedge $A_1B_1C_1$ of the point of the layer that was situated at point O_1 prior to the undercutting is represented by the right line A_1O_1'. The absolute trajectory is represented by the right line O_1O_1'. At the same time, $O_1'M_1 = O_1M_1$ and $\angle O_1'A_1M_1 = \angle O_1A_1M_1 = \gamma$ (Figure 3.1).

Similarly, when the soil layer moves on face $A_2B_2C_2$, $O_2'M_2 = O_2M_2$ and $\angle O_2'A_2M_2 = \angle O_2A_2M_2 = \gamma$. In this case, the relative and absolute trajectories of motion of the point of the soil layer are represented by the right lines A_2O_2' and O_2O_2' respectively.

According to the above, the trajectories of relative motion of any of the points of the soil layer that are in contact with the faces of wedges $A_1B_1C_1$ and $A_2B_2C_2$ are represented by right lines parallel to the right lines A_1O_1' and A_2O_2' respectively, their trajectories of absolute motion are represented by right lines parallel to O_1O_1' and O_2O_2' respectively.

Hence, the forces of friction $\overline{F}_1$ and $\overline{F}_2$ of the soil layer on the faces of wedges $A_1B_1C_1$ and $A_2B_2C_2$ are vectored parallel to lines A_1O_1' and A_2O_2' respectively, in the direction opposite to the relative motion of the soil layer on the wedges. The same can be said about the motion of the root and the direction of the forces of friction during the direct contact between the root and the working faces of the wedges, as the motion trajectory is defined by the geometric parameters of the lifter's wedges.

Forces $\overline{I}_1$ and $\overline{I}_2$ of the dynamic pressure of the incoming soil give rise to the dynamic parts of the normal reactions on wedges $\overline{N}_{I1}$ and $\overline{N}_{I2}$.

The normal components of the reactions of the working faces of the wedges that result from the action of the force of gravity G of the soil layer with the root are equal to:

$$N_{G1} = N_{G2} = \frac{G}{2(cos\delta - fsin\delta \cdot sin\gamma)} \tag{3.18}$$

where δ—dihedral angle ($\angle B_1M_1O_1$) between the lower face $A_1O_1C_1$ and the working face $A_1B_1C_1$ of the wedge; f—coefficient of sliding friction of the soil on the working faces of the wedges.

In the case of direct contact between the root and the working faces of the wedges, f_1—coefficient of sliding friction of the root on the faces of the wedges.

The part of the friction forces that arises during the movement of the soil layer with the root under the action of the weight forces G is equal to:

$$F_{G1} = F_{G2} = \frac{Gf}{2(cos\delta - fsin\delta \cdot sin\gamma)} \tag{3.19}$$

Since the absolute velocity V_a of the motion of the layer with the root is related to the translational velocity V of the lifter's motion under the following formula:

$$V_a = 2V sin\frac{\delta}{2} \cdot sin\gamma \tag{3.20}$$

and in accordance with (3.17), the following values of the incoming soil dynamic pressure forces are obtained:

$$I_1 = I_2 = \frac{2ab\gamma_{ob.}}{g}V^2 sin\frac{\delta}{2} \cdot sin\gamma \tag{3.21}$$

The normal components of the dynamic reactions of the wedge working faces $A_1B_1C_1$ and $A_2B_2C_2$ that arise under the action of forces $\bar{I}_1$ and $\bar{I}_2$ are equal to: $N_{I1} = N_{I2} = I_1\frac{cos\frac{\delta}{2}}{cos\delta - f sin\cdot\gamma sin\delta}$, or, taking into account (3.21):

$$N_{I1} = N_{I2} = \frac{ab\gamma_{ob.}}{g}V^2\frac{sin\delta \cdot sin\gamma}{(cos\delta - f sin\gamma \cdot sin\delta)} \tag{3.22}$$

The components of the forces of friction of the soil on the wedge faces $A_1B_1C_1$ and $A_2B_2C_2$ arising under the effect of the incoming soil dynamic pressure forces, are as follows:

$$F_{I1} = F_{I2} = f\frac{ab\gamma_{ob.}}{g}\frac{V^2 sin\delta sin\gamma}{(cos\delta - f sin\gamma sin\delta)} \tag{3.23}$$

The necessary condition for the operation of share lifters is the presence of the soil backup force $\bar{Q}$, which is vectored horizontally (along axis Ox) and opposite to the direction of the lifter's motion. The maximum magnitude of this backup force is equal to:

$$Qgr._{max.} \tag{3.24}$$

where $\sigma_{gr.}$—permissible soil compression stress; the multiplication factor 2 indicates that force $\bar{Q}$ is generated simultaneously on both wedges.

However, as the root together with the soil layer advances along the lifter's working channel, which gradually narrows, the backup force $\bar{Q}$ becomes considerably reduced as a result of the disintegration of the soil, and in the rear part of the tapering channel its action on the root becomes too small. In this case, it is necessary to determine the backup force $\bar{Q}$ using the following approximate expression: $Q = 2abk_{ud.}$ (where $k_{ud.}$—coefficient of specific resistance of loosened soil).

The resistance force $\bar{R}$, i.e., the force of bonding between the root and the soil, is assumed to be vectored opposite to the direction of action of the force extracting the root from the soil.

As noted above, the resistance force $\overline{R}$ can be decomposed into the force of resistance to the vertical displacement of the root $\overline{R}_z$ and the force of resistance to the horizontal displacement of the root $\overline{R}_x$. Moreover, the bending strains of the roots during their extraction from the soil are generated by the action of force $\overline{R}_x$ during the horizontal displacement of the roots in the lifter's channel. The bending strains cause damage to the root first of all in these cases when the bonding force between the root and the soil is rather strong. Generally, this happens in the rear part of the lifter's working channel during direct contact between the root and the working faces of the shares. Therefore, it is necessary to separately examine the interaction between the root and the wedge faces in the narrowed channel of the lifter and set up differential equations of motion of the root during its immediate extraction from the soil. In this case, the forces of interaction between the root and the working faces of the wedges are similar to those between the soil layer and the working faces of the wedges; therefore, these forces are assumed to be equal and, finally, the process of root extraction from the soil is assumed to be performed under the action of the forces shown in Figure 2.3.

3.4. Differential Equation of Motion of Root during Its Immediate Extraction from Soil by Share Lifter

The next step is to set up the differential equation of the motion of the root. In the vector notation, it appears as follows:

$$m\overline{a} \;=\; \overline{N}_{G1} + \overline{N}_{G2} + \overline{N}_{I1} + \overline{N}_{I2} + \overline{Q} + \overline{R}_x + \overline{R}_z + \overline{F}_1 + \overline{F}_2 + \overline{G}_k \qquad (3.25)$$

where m—mass of the root; a—acceleration of the root during its extraction from the soil; $\overline{R}_x$, $\overline{R}_z$—horizontal and vertical components, respectively, of the resistance force $\overline{R}$ exerted by the bonds between the root and the soil; $\overline{F}_1$, $\overline{F}_2$—total forces of friction that arise during the motion of the root on the working faces of the wedges $A_1B_1C_1$ and $A_2B_2C_2$, respectively; G_k—weight of the root.

It is evident that:

$$F_1 \;=\; f_1(N_{G1} + N_{I1}), F_2 \;=\; f_1(N_{G2} + N_{I2}), \qquad (3.26)$$

where f_1—coefficient of the friction of the side surface of the root on the wedge faces.

The differential Equation (3.25) has to be set down in the Cartesian coordinate system $Oxyz$. It ought to be noted that the projections of the normal reactions of the wedge working faces $A_1B_1C_1$ and $A_2B_2C_2$ on axis Oy have equal magnitudes and opposite directions. Hence, the extraction of the root from the soil, in effect, takes place in plane xOz and consequently the differential equation of the motion of the

root (3.25) in the vector notation is reduced to the system of two differential equations of the following form:

$$\left.\begin{array}{c} m\acute{x} = N_{G1x} + N_{G2x} + N_{I1x} + N_{I2x} - Q - R_x + F_{1x} + F_{2x}, \\ m\acute{z} = N_{G1z} + N_{G2z} + N_{I1z} + N_{I2z} - R_z - F_{1z} - F_{2z} - G_k. \end{array}\right\} \qquad (3.27)$$

It is necessary to determine the projections of the forces included in the system of differential equations under consideration. In accordance with (3.12) and (3.13), the projections of the normal reactions of the wedge faces $A_1B_1C_1$ and $A_2B_2C_2$ on the x and z axes can be found. These are equal to $N_{G1x} = N_{G2x} = \frac{N_{G1}tan\gamma}{\sqrt{tan^2\gamma+1+tan^2\beta}}$, respectively, or, taking into account (3.18):

$$N_{G1x} = N_{G2x} = \frac{Gtan\gamma}{2(cos\delta - fsin\delta \cdot sin\gamma)\sqrt{tan^2\gamma + 1 + tan^2\beta}} \qquad (3.28)$$

and $N_{G1z} = N_{G2z} = \frac{N_{G1}tan\beta}{\sqrt{tan^2\gamma+1+tan^2\beta}}$, or taking into account (3.18):

$$N_{G1z} = N_{G2z} = \frac{Gtan\beta}{2(cos\delta - fsin\delta \cdot sin\gamma)\sqrt{tan^2\gamma + 1 + tan^2\beta}} \qquad (3.29)$$

Similarly, the following is found from (3.12), (3.13) and (3.22):

$$N_{I1x} = N_{I2x} = \frac{ab\gamma_{ob.}}{g}V^2 \times \frac{sin\delta \cdot sin\gamma \cdot tan\gamma}{(cos\delta - fsin\delta \cdot sin\gamma)\sqrt{tan^2\gamma + 1 + tan^2\beta}}, \qquad (3.30)$$

$$N_{I1z} = N_{I2z} = \frac{ab\gamma_{ob.}}{g}V^2 \times \frac{sin\delta \cdot sin\gamma \cdot tan\beta}{(cos\delta - fsin\delta \cdot sin\gamma)\sqrt{tan^2\gamma + 1 + tan^2\beta}}. \qquad (3.31)$$

As the forces of friction are vectored oppositely to the directions of the relative motion of the soil layer and the root on the wedge faces $A_1B_1C_1$ and $A_2B_2C_2$ (parallel to the right lines $A_1O'_1$ and $A_2O'_2$), their projections on the coordinate axes Ox, Oy, Oz are equal to:

$$\begin{array}{c} F_{1x} = F_1(\cos^2\gamma + \sin^2\gamma\cos\delta), \\ F_{1y} = -F_1\cos\gamma\sin\gamma(1 - \cos\delta), \\ F_{1z} = -F_1\sin\gamma\sin\delta, \\ F_{2x} = F_2(\cos^2\gamma + \sin^2\gamma\cos\delta), \\ F_{2y} = F_2\cos\gamma\sin\gamma(1 - \cos\delta), \\ F_{2z} = -F_2\sin\gamma\sin\delta. \end{array} \qquad (3.32)$$

In (3.31) and (3.32) symbols are defined as follows:

$$
\begin{array}{ll}
\overline{N}_1 = \overline{N}_{G1} + \overline{N}_{I1} & \overline{N}_2 = \overline{N}_{G2} + \overline{N}_{I2} \\
\overline{F}_1 = \overline{F}_{G1} + \overline{F}_{I1} & \overline{F}_2 = \overline{F}_{G2} + \overline{F}_{I2} \\
N_{1x} = N_{G1x} + N_{I1x} & N_{2x} = N_{G2x} + N_{I2x} \\
F_{1x} = F_{G1x} + F_{I1x} & F_{2x} = F_{G2x} + F_{I2x} \\
N_{1z} = N_{G1z} + N_{I1z} & N_{2z} = N_{G2z} + N_{I2z} \\
F_{1z} = F_{G1z} + F_{I1z} & F_{2z} = F_{G2z} + F_{I2z}.
\end{array}
$$

Thus, after substituting all the obtained values, the system of Equation (3.27), a differential equation, assumes the following appearance:

$$
\left.
\begin{array}{l}
m\acute{x} = N_{1x} + N_{2x} - R_x + F_{1x} + F_{2x} - Q, \\
m\acute{z} = N_{1z} + N_{2z} - R_z - F_{1z} - F_{2z} - G_k.
\end{array}
\right\}
\tag{3.33}
$$

Obviously, the process of the root extraction from the soil becomes possible under the following condition:

$$
N_{1z} + N_{2z} - F_{1z} - F_{2z} - G_k > R_z
\tag{3.34}
$$

and, taking into account (3.29), (3.31) and (3.26), the following is obtained:

$$
\begin{aligned}
&\frac{\tan\beta}{\sqrt{\tan^2\gamma + 1 + \tan^2\beta}} \left[\frac{G}{\cos\delta - f\sin\delta\cdot\sin\gamma} + \frac{2ab\gamma_{ob.}V^2\sin\delta\cdot\sin\gamma}{g(\cos\delta - f\sin\delta\cdot\sin\gamma)} \right] \\
&- \frac{-Gf_1\sin\delta\cdot\sin\gamma}{\cos\delta - f\sin\delta\cdot\sin\gamma} - \frac{2ab\gamma_{ob.}V^2\sin^2\delta\cdot\sin^2\gamma\cdot f_1}{g(\cos\delta - f\sin\delta\cdot\sin\gamma)} - G_k \\
&> R_z.
\end{aligned}
\tag{3.35}
$$

When the condition of (3.35) is met, the extraction of the root from the soil takes place. The left-hand member of (3.35) represents the root extraction force acting along axis Oz subject to direct contact between the root and the shares.

After integrating the system of differential Equation (3.33) twice, the values of the projections of the velocity on axes Ox and Oz and the displacement of the root along the mentioned axes as functions of time t are obtained.

The first integrals appear as follows:

$$
\begin{aligned}
\acute{x} &= \tfrac{1}{m}(N_{1x} + N_{2x} - R_x + F_{1x} + F_{2x} - Q)t + C_1, \\
\acute{z} &= \tfrac{1}{m}(N_{1z} + N_{2z} - R_z - F_{1z} - F_{2z} - G_k)t + L_1,
\end{aligned}
\tag{3.36}
$$

the second integrals are equal to:

$$
\begin{aligned}
x &= \tfrac{1}{m}(N_{1x} + N_{2x} - R_x + F_{1x} + F_{2x} - Q)\tfrac{t^2}{2} + C_1 t + C_2, \\
z &= \tfrac{1}{m}(N_{1z} + N_{2z} - R_z - F_{1z} - F_{2z} - G_k)\tfrac{t^2}{2} + L_1 t + L_2,
\end{aligned}
\tag{3.37}
$$

where C_1, C_2, L_1, L_2—arbitrary constants.

In order to find the arbitrary constants, it is necessary to set the initial and boundary conditions:

$$\text{at } t_o = 0: \quad x = x_o, z = -h, \acute{x} = 0, \acute{z} = 0,$$
$$\text{at } t = t_1: \quad x = x_1, z = 0, \acute{x}_1 = V_1,$$

where t_o—starting moment of the root extraction; t_1—final moment of the root extraction process; x_o—distance from the root's vertical centreline to the origin of coordinates at the moment of time t_o; x_1—distance from the root's vertical centreline to the origin of coordinates at the final moment of extraction t_1; h—depth of the root's location in the soil; V_1—velocity of the root at the final moment of extraction.

Considering the initial conditions, the following values of the arbitrary constants are:

$$C_1 = 0, L_1 = 0, C_2 = x_o, L_2 = -h. \tag{3.38}$$

After substituting (3.38) into (3.36) and into (3.37), the following is obtained:

$$\acute{x} = \frac{1}{m}(N_{1x} + N_{2x} - R_x + F_{1x} + F_{2x} - Q)t, \tag{3.39}$$

$$\acute{z} = \frac{1}{m}(N_{1z} + N_{2z} - R_z - F_{1z} - F_{2z} - G_k)t, \tag{3.40}$$

$$x = \frac{1}{m}(N_{1x} + N_{2x} - R_x + F_{1x} + F_{2x} - Q)\frac{t^2}{2} + x_o, \tag{3.41}$$

$$z = \frac{1}{m}(N_{1z} + N_{2z} - R_z - F_{1z} - F_{2z} - G_k)\frac{t^2}{2} - h. \tag{3.42}$$

Then, the earlier obtained values of Forces (3.28)–(3.32) are substituted into (3.39)–(3.42). After performing the necessary transformations, the result is:

$$\acute{x} = \frac{1}{m}\left\{\frac{tan\gamma}{\sqrt{tan^2\gamma+1+tan^2\beta}} \times \left[\frac{G}{cos\delta-fsin\delta\cdot sin\gamma} + \frac{2ab\gamma_{ob.}V^2sin\delta\cdot sin\gamma}{g(cos\delta-fsin\delta\cdot sin\gamma)}\right]\right.$$
$$\left. +\frac{Gf_1(cos^2\gamma+sin^2\gamma\cdot cos\delta)}{cos\delta-fsin\delta\cdot sin\gamma} + \frac{2f_1ab\gamma_{ob.}V^2sin\delta\cdot sin\gamma(cos^2\gamma+sin^2\gamma\cdot cos\delta)}{g(cos\delta-fsin\delta\cdot sin\gamma)} - 2abk_{ud.} - R_x\right\}t, \tag{3.43}$$

$$\acute{z} = \frac{1}{m}\left\{\frac{tan\beta}{\sqrt{tan^2\gamma+1+tan^2\beta}} \times \left[\frac{G}{cos\delta-fsin\delta\cdot sin\gamma} + \frac{2ab\gamma_{ob.}V^2sin\delta\cdot sin\gamma}{g(cos\delta-fsin\delta\cdot sin\gamma)}\right]\right.$$
$$\left. -\frac{Gf_1sin\delta\cdot sin\gamma}{cos\delta-fsin\delta\cdot sin\gamma} - \frac{2f_1ab\gamma_{ob.}V^2sin^2\delta\cdot sin^2\gamma}{g(cos\delta-fsin\delta\cdot sin\gamma)} - G_k - R_z\right\}t, \tag{3.44}$$

$$x = \frac{1}{m}\left\{\frac{tan\gamma}{\sqrt{tan^2\gamma+1+tan^2\beta}} \times \left[\frac{G}{cos\delta-fsin\delta\cdot sin\gamma} + \frac{2ab\gamma_{ob.}V^2sin\delta\cdot sin\gamma}{g(cos\delta-fsin\delta\cdot sin\gamma)}\right]\right.$$
$$\left. +\frac{Gf_1(cos^2\gamma+sin^2\gamma\cdot cos\delta)}{cos\delta-fsin\delta\cdot sin\gamma} + \frac{2f_1ab\gamma_{ob.}V^2sin\delta\cdot sin\gamma(cos^2\gamma+sin^2\gamma\cdot cos\delta)}{g(cos\delta-fsin\delta\cdot sin\gamma)} - 2abk_{ud.} - R_x\right\}\frac{t^2}{2} + x_o, \tag{3.45}$$

$$z = \frac{1}{m}\left\{ \frac{\tan\beta}{\sqrt{\tan^2\gamma+1+\tan^2\beta}} \times \left[\frac{G}{\cos\delta-f\sin\delta\cdot\sin\gamma} + \frac{2ab\gamma_{ob.}V^2\sin\delta\cdot\sin\gamma}{g(\cos\delta-f\sin\delta\cdot\sin\gamma)} \right] \right.$$
$$\left. -\frac{Gf_1\sin\delta\cdot\sin\gamma}{\cos\delta-f\sin\delta\cdot\sin\gamma} \frac{2f_1ab\gamma_{ob.}V^2\sin^2\delta\cdot\sin^2\gamma}{g(\cos\delta-f\sin\delta\cdot\sin\gamma)} - G_k - R_z \right\}\frac{t^2}{2} - h. \tag{3.46}$$

(3.42) enables the time t_1 of the root extraction from the soil to be found. It will be equal to:

$$t_1 = \sqrt{\frac{2mh}{N_{1z} + N_{2z} - F_{1z} - F_{2z} - R_z - G_k}} \tag{3.47}$$

After this, the earlier obtained values of forces that are part of (3.47) are substituted into it. Proceeding with a number of transformations, the following value of the time t_1 is obtained:

$$t_1 = \sqrt{\frac{2mgh(\cos\delta-f\sin\delta\cdot\sin\gamma)\sqrt{\tan^2\gamma+1+\tan^2\beta}}{(2ab\gamma_{ob.}V^2\sin\delta\cdot\sin\gamma)(\tan\beta-\sin\gamma\cdot\sin\delta\cdot f_1)}}$$
$$\times \sqrt{\frac{1}{\sqrt{\tan^2\gamma+1+\tan^2\beta}-(R_z+G_k)q(\cos\delta-f\sin\delta\cdot\sin\gamma)}} \tag{3.48}$$
$$\times \sqrt{\frac{1}{\sqrt{\tan^2\gamma+1+\tan^2\beta}}}$$

As t_1 is the time spent for the root extraction from the soil by the share lifter, (3.48) can be used the determine the productivity of a root lifting unit.

In the situation where Condition (3.35) is not met, i.e., when the inequality of the opposite sense is true, the root remains bonded with the soil and its motion along axis Oz does not take place. Nevertheless, under the action of the forces entered in the first equation of system (2.33), the force is

$$P_x = N_{1x} + N_{2x} + F_{1x} + F_{2x} - Q \tag{3.49}$$

which overcomes the resistance force R_x bonding the root with the soil, and the bending of the root as a cantilever beam is observed, as the upper part of the root deflects along the line of action of the force P_x by some critical amount, after which the breaking of the root can take place.

Although, there is some permissible force $[P_x]$, which does not cause damage (breaking) to the root. Then, instead of force P_x in (3.49), its permissible value $[P_x]$ can be substituted:

$$[P_x] = N_{1x} + N_{2x} + F_{1x} + F_{2x} - Q \tag{3.50}$$

or, taking into account the already obtained values of the forces in the right-hand member of this expression, the following is obtained:

$$[P_x] = N_{G1x} + N_{G2x} + N_{I1x} + N_{I2x} + F_{G1x} + F_{G2x} + F_{I1x} + F_{I2x} - Q \tag{3.51}$$

Hence, considering the symmetric positions of the wedges, the result is:

$$[P_x] = 2N_{G1x} + 2N_{I1x} + 2F_{G1x} + 2F_{I1x} - Q \tag{3.52}$$

(3.52) can be rewritten as follows:

$$2N_{I1x} + 2F_{I1x} = [P_x] - 2N_{G1x} - 2F_{G1x} - Q \tag{3.53}$$

Then, the values of the forces in (3.53) are substituted into it.
We will then have:

$$
\begin{aligned}
&\frac{2ab\gamma_{ob.}}{g} \cdot \frac{V^2 sin\delta \cdot sin\gamma \cdot tan\gamma}{(cos\delta - f sin\delta \cdot sin\gamma)\sqrt{tan^2\gamma + 1 + tan^2\beta}} \\
&+ 2f_1 \frac{ab\gamma_{ob.} V^2 sin\delta \cdot sin\gamma (cos^2\gamma + sin^2\gamma \cdot cos\delta)}{g(cos\delta - f sin\delta \cdot sin\gamma)} \\
&= [P_x] - \frac{G tan\gamma}{(cos\delta - f sin\delta \cdot sin\gamma)\sqrt{tan^2\gamma + 1 + tan^2\beta}} \\
&- \frac{f_1 G(cos^2\gamma + sin^2\gamma \cdot cos\delta)}{(cos\delta - f sin\delta \cdot sin\gamma)} + 2abk_{ud}.
\end{aligned} \tag{3.54}
$$

From (3.54), the velocity V of the share lifter's translational motion, which does not result in damaging (breaking) the roots, can be found. It is equal to:

$$V = \sqrt{\frac{g([P_x] + 2abk_{ud})(cos\delta - f sin\delta \cdot sin\gamma)\sqrt{tan^2\gamma + 1 + tan^2\beta} - gG tan\gamma - f_1 gG(cos^2\gamma + sin^2\gamma \cdot cos\delta)\sqrt{tan^2\gamma + 1 + tan^2\beta}}{2ab\gamma_{ob.} sin\delta \cdot sin\gamma [tan\gamma + f_1(cos^2\gamma + sin^2\gamma \cdot cos\delta) \cdot \sqrt{tan^2\gamma + 1 + tan^2\beta}]}} \tag{3.55}$$

Thus, the kinematic parameters of the root extraction from the soil by the share lifter expressed in terms of its geometric parameters and taking into account the quality requirements of the performance of the work process under consideration have finally been found.

In order to enable the practical use of (3.55), it is necessary to establish the relation between the dihedral angle δ and the angles β and γ, which, in effect, define the angular parameters of the wedges, since the third angle α can be determined on the basis of the angles β and γ. It is evident from Figure 3.1 that:

$$tan\alpha = \frac{c_1}{a_1} \tag{3.56}$$

hence, taking into account (3.7), the result is:

$$tan\alpha = \frac{tan\gamma}{tan\beta} \tag{3.57}$$

Accordingly, the angle δ can be found with the use of the angles β and γ. The following relations can be derived from Figure 3.3:

$$\tan\delta = \frac{O_1 B_1}{O_1 M_1} \tag{3.58}$$

and

$$O_1 M_1 = O_1 A_1 \sin\gamma \tag{3.59}$$

Considering the fact that $O_1 B_1 = c_1$ and $O_1 A_1 = a_1$, it follows that:

$$\tan\delta = \frac{c_1}{a_1 \sin\gamma} \tag{3.60}$$

By substituting (3.7) into (3.60), the following is obtained:

$$\tan\delta = \frac{1}{\cos\gamma \cdot \tan\beta} \tag{3.61}$$

or:

$$\tan\delta = \frac{\cos\beta}{\sin\beta \cdot \cos\gamma} \tag{3.62}$$

and from this the final value of the angle δ is arrived at:

$$\delta = \arctan\frac{\cos\beta}{\sin\beta \cdot \cos\gamma} \tag{3.63}$$

Thus, adjusting the geometric parameters of the share lifter wedges, specifically the angles β and γ, on the basis of the analytical relationships arrived at in the previous considerations, it is possible to find the required kinematic parameters of the share-type lifting tool under the condition of not damaging the roots. For example, using (3.55), it is possible to find the relation between the permissible velocity of the lifter's translational motion V and its varying angles β and γ with all its other set design parameters entered in (3.55) staying invariable.

With the use of the PC programme developed for this purpose, the calculation of the permissible velocity of the share lifter's motion V under the condition of not damaging the sugar beet roots, for various values of the angle γ and several fixed values of the angle β, has been carried out. The initial data for the calculation are shown in Table 3.1.

Table 3.1. Parameters of share-type lifting tool for calculation.

Parameter	a	$[P_x]$	$\gamma_{ob.}$	f	f_1	g
Value	0.12 g	200 N	11,000 N·m^{-3}	0.60	0.50	9.81 m·s^{-2}

At the same time, some of the design parameters of the share lifter and the work process it performs depend on each other under the following relations:

Width of the strained soil layer:

$$b = a\tan\beta = 0.12\tan\beta, \tag{3.64}$$

Weight of the soil layer:

$$G = \gamma_{ob.}a^2(2a\tan\beta + 0.05)\frac{\tan\beta}{\sin\gamma} \tag{3.65}$$

On the basis of the results of the numerical calculations, graphs have been plotted that show the variation of the share lifter's translational motion velocity V in relation to the varying values of the angle γ (Figure 3.4).

As may be inferred from the shown graphs, the relations between the above-mentioned parameters follow patterns that are close to linear. At the same time, when the share lifter's angle of attack γ is increased, the value of its translational motion velocity V, which ensures the extraction of roots from the soil without damaging them, decreases. As regards the effect that the share lifter's angle of flare β has on its translational motion velocity V, it is evident from the graphs that the use of greater values of the angle also allows for higher levels of the translational motion velocity. Considering the fact that the statistical value of the angle of taper γ_k of sugar beet roots is equal to $20 \sim 28°$ the use of an angle of flare β of the share lifter close to 30^0 will also allow for a higher level of the translational motion velocity.
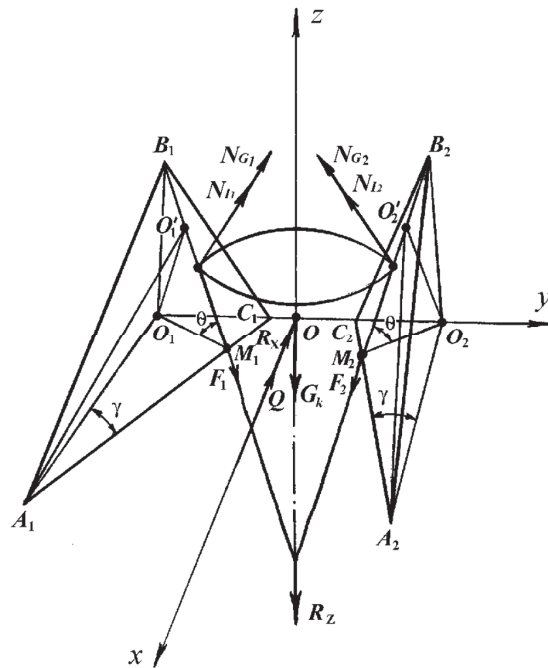
Figure 3.3. Force interaction between root and share lifter's wedges.
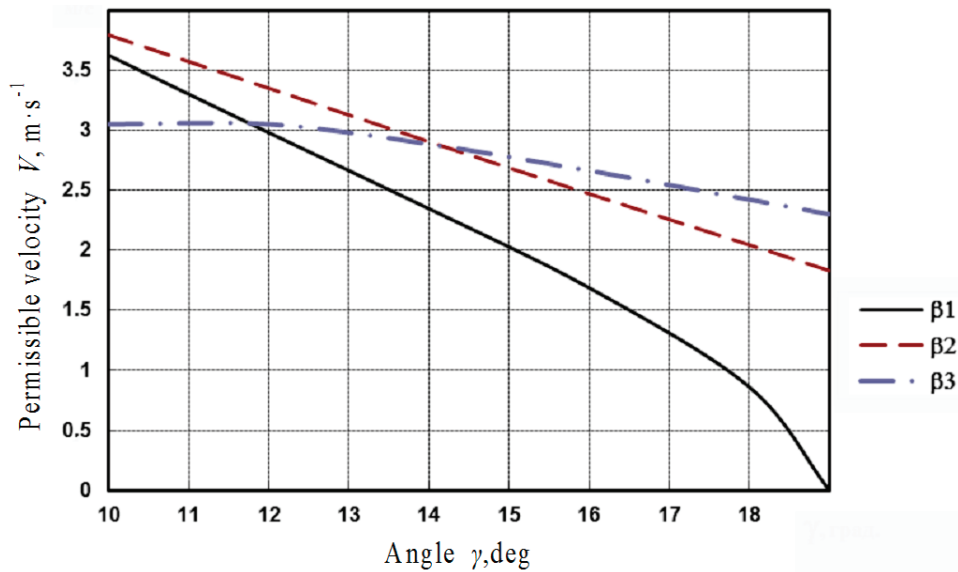
Figure 3.4. Relation between permissible velocity V of share lifter's translational motion and angle γ for: $\beta_1 = 15°, \beta_2 = 20°, \beta_3 = 30°$.

Thus, the results obtained by the calculations stipulate that values of $\gamma = 13 \sim 16°$, $\beta = 20 \sim 30°$ are to be considered the most rational values of the angles γ and β, which facilitate high velocities V of the share lifter's translational motion in the process of sugar beet root extraction from the soil without damaging the roots.

Thereby, the results of the PC-assisted numerical calculations with the use of the obtained analytical relationships prove the accuracy of the latter and provide ground for their practical use in the design and analysis of new, further developed lifting tools for beet harvesters.

3.5. Conclusions

1. The principal scientific result obtained in the second section is the development of the mathematical model of interaction between the working faces of wedges of the share-type lifting tool on the one hand and the soil around the root and directly the root itself on the other hand.

2. The system of differential equations of the motion of the root during its extraction from the soil by a standard share lifter has been set up. Its solution has allowed the establishment of the law of motion of the root on the working faces of the lifting shares up until its complete extraction as well the time spent for the extraction of the root from the soil to be determined.

3. The criterion of safety against the break-off of the tail parts of the roots during their digging by a standard share lifter has been established in terms of the permissible breaking side force. This criterion stipulates the permissible translational motion velocity of the lifter, which ensures keeping the roots free of break-off damage.

54

4. The relationship between the permissible translational motion velocity of the lifter that ensures extraction of the roots without their break-off damage and the angular parameters of the lifting tool has been determined. The calculations have revealed that the most rational values of the angles γ and β, which ensure the high velocity of the share lifter's translational motion and extraction of the sugar beet roots from the soil without their break-off, have to be assumed at rates of $\gamma = 13–16°$, $\beta = 20–30°$.

4. Theory of Oscillations of Root as Elastic Solid Fixed in Soil

4.1. Theory of Longitudinal Oscillations of Root as Elastic Solid Fixed in Soil

4.1.1. Main Methodological Principles

The theory of vibrational digging of sugar beet roots was established and published in the fundamental paper [6], in which the root was modelled as a solid with elastic properties and represented by a variable cross-section bar with one end fixed. In said paper, the analysed transverse oscillations of the root were described with the use of a fourth-order partial differential equation. After solving the mentioned equation, the results were used for determining the fundamental modes of the root's free oscillations. At the same time, the additionally set up equations of kinetostatics were used for finding the conditions of its extraction from the soil under the action of the perturbing force applied to it in the transverse horizontal plane.

The case where oscillatory motions of the vibration digging-up tool are applied to the beet root in the longitudinal vertical area will now be analytically analysed. It will be assumed that the root that is located in the soil is a complex solid elastic system with an infinite number of degrees of freedom, also modelled as the rod with a variable cross-section with the attached low end.

In order to fully define the deformations induced in such systems during oscillations, it is necessary to determine the displacements of all points of the system—i.e., it is necessary to find an infinite number of values (coordinates) defining these displacements at any instant of time. While the theoretical basis for a majority of the studies on the oscillations of holonomic systems with a finite number of degrees of freedom is provided by Lagrange equations of the second kind in generalised coordinates, the research into the oscillations of holonomic systems with an infinite number of degrees of freedom requires applying the Ostrogradsky–Hamilton principle of stationary action [20].

If the following two positions of a moving mechanical system are analysed: position (A) at the instant of time t_1 and position (B) at the instant of time $t_2(t_2 > t_1)$, then the actual displacement of the system in the time $t_2 - t_1$ is determined by the following equations:

$$q_k = q_k(t) \ldots (k = 1, 2, \ldots, n) \qquad (4.1)$$

where q_k—generalised coordinate of the system.

(4.1) represents the solution of the system of Euler–Lagrange differential equations, which will be given consideration later.

Together with the actual displacement of the system from position (A) to position (B), conceptional displacements from position (A) to position (B) in the same time $t_2 - t_1$, which are infinitely close to said actual one will be analysed for the comparison with it. These displacements are determined by the following altered equations:

$$\bar{q}_k(t) = q_k(t) + \delta q_k(t), \ (k = 1, 2, \ldots, n) \tag{4.2}$$

where δq_k—isochronal variations of the coordinates $q_1, q_2, \ldots, q_n$, i.e., the infinitely small quantities, by which the coordinates q_k in the actual displacement differ from the coordinates $\bar{q}_k$ in the displacements used for comparison at the same instant of time t.

The displacements $\bar{q}_k(t)$ are known as by-pass displacements. Since all the displacements, both the actual and conceptional ones, begin at position (A) and end simultaneously at position (B), it is obvious that at the mentioned positions the following is true:

$$\delta q_k(t_1) = \delta q_k(t_2) = 0 \tag{4.3}$$

Further, the following functional has to be investigated on the resulting set of displacements allowed by the restraints:

$$S = \int_{t_1}^{t_2} L \, dt \tag{4.4}$$

where $L = T - \Pi$—Lagrange function; T—kinetic energy of the system expressed in terms of the generalised coordinates; Π—potential energy of the system also expressed in terms of the generalised coordinates.

(4.4) is known as the "Ostrogradsky–Hamilton action". Subsequently, the Ostrogradsky–Hamilton principle of stationary action for a conservative system lies in the following: the action of (4.4) during the actual displacement has a stationary value as compared to its value during the by-pass displacements, which move the system from the set initial position to the same final position in the same time period $t_2 - t_1$.

The necessary condition of the stationary state of (4.4) is its first variation turning into zero—i.e.,

$$\delta S = 0 \tag{4.5}$$

In order to apply the Ostrogradsky–Hamilton principle in a theory of oscillations, (4.5) is fulfilled for the actual displacement. The Euler–Lagrange differential equations mentioned earlier are the necessary and sufficient conditions for the fulfilment of (4.5) and, consequently, for the stationary state of (4.4) during the actual displacement of the system.

If the integration function L of (4.4) depends only on first-order derivatives, the Euler–Lagrange equations are usual Lagrange equations of the second kind—i.e.,

$$\frac{d}{dt}\left(\frac{\partial L}{\partial \dot{q}_k}\right) - \frac{\partial L}{\partial q_k} = 0, \ (k = 1, 2, \ldots, n) \tag{4.6}$$

In case the integration function L depends not only on first-order derivatives but also on the second-order and higher derivatives, the necessary extremum conditions for such functionals are represented by fourth-order and higher partial differential equations.

In the theory of longitudinal, torsional and transverse oscillations of straight rods, the Hamilton–Ostrogradsky functionals are applied, which in the most generalised form look as follows:

$$S = \int_{t_1}^{t_2} \int_0^l L\left(t, x, y, \frac{\partial y}{\partial t}, \frac{\partial y}{\partial x}, \frac{\partial^2 y}{\partial t^2}, \frac{\partial^2 y}{\partial t \partial x}, \frac{\partial^2 y}{\partial x^2}\right) dx dt \tag{4.7}$$

Then, equations equal to the equation of Euler–Lagrange equations for (4.7) will look as follows:

$$\frac{\partial L}{\partial y} - \frac{\partial}{\partial t}\left(\frac{\partial L}{\partial p}\right) - \frac{\partial}{\partial x}\left(\frac{\partial L}{\partial q}\right) + \frac{\partial^2}{\partial t^2}\left(\frac{\partial L}{\partial r}\right) + \frac{\partial^2}{\partial t \partial x}\left(\frac{\partial L}{\partial s}\right) + \frac{\partial^2}{\partial x^2}\left(\frac{\partial L}{\partial u}\right) = 0 \tag{4.8}$$

where:

$$p = \frac{\partial y}{\partial t}, q = \frac{\partial y}{\partial x}, r = \frac{\partial^2 y}{\partial t^2}, s = \frac{\partial^2 y}{\partial t \partial x}, u = \frac{\partial^2 y}{\partial x^2} \tag{4.9}$$

4.1.2. Differential Equation of Longitudinal Oscillations of Root Body

It is assumed that the root that is located in the soil to be the rod with variable cross-section along its length with one end attached (Figure 4.1). The Hamilton–Ostrogradsky principle will now be applied for research of longitudinal oscillations of the root that occur under the action of the vertical disturbing force that changes according to the harmonic law of the following type:

$$Q_{zb.} = H\sin\omega t \tag{4.10}$$

where H is the amplitude of forced oscillations; ω is the frequency of forced oscillations.

As we can see from the scheme in Figure 4.1, the root having a cone-like body (the top angle of which equals 2γ and the top part of which is located above the level of the surface of the soil) is modelled as the rod with variable cross-section with the attached low end (point O). In the centre of gravity, designated as point C, force $\overline{G}$ is applied—the weight force of the root. h is its total length. Through the axis of symmetry of the root the vertical axis x is drawn, the beginning of which matches

59

point O. Connection of the root with the soil is determined by the general reaction of the soil $\overline{R}_x$, which is located along axis x.

The disturbing force $\overline{Q}_{zb.}$ stated above is simultaneously applied to the root from two digging-up plough shares from its two sides, and this is why it is presented in the scheme by two components: $\overline{Q}_{zb.1}$ and $\overline{Q}_{zb.2}$. The given forces are applied on distance x_1 from the origin of coordinates (point O) and they are the source of oscillations of the root in longitudinal vertical area that destroy connection of the root with the soil and form conditions for digging up of the latter from the soil. The Hamilton–Ostrogradsky functional S for the analysed vibrational process will created in the following. For this purpose, the necessary symbols will be applied:
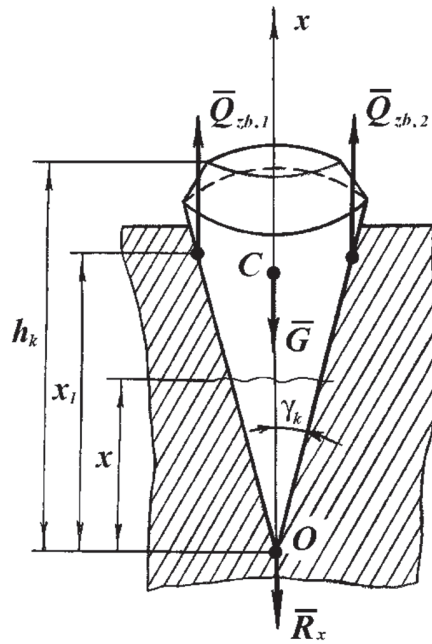
Figure 4.1. Scheme of the forces having an action on the root at the time of gripping by the vibration digging tool.

$F(x)$ is the area of cross-section of the root at a point located at the distance x from the low end m^2; E is the Young's modulus for material of the root N·m^{-2}; $y(x,t)$ is the longitudinal dislocation of a cross-section of the root at the time point t, m; $Q(x,t)$ is the intensity of longitudinal external load directed along the axis of the root N·m^{-1}; $\mu(x)$ is the mass per length of the root kg·m^{-1}.

Then, kinetic energy of the oscillatory motion of the root will be:

$$T = \frac{1}{2} \int_o^{h_k} \mu(x) \left(\frac{\partial y}{\partial t}\right)^2 dx \tag{4.11}$$

Potential energy of the elastic deformation is designated as follows:

$$\Pi_1 = \frac{1}{2} \int_0^{h_k} EF(x) \left(\frac{\partial y}{\partial x} \right)^2 dx \tag{4.12}$$

Potential stretching energy of the longitudinal load $Q(x, t)$ will look as follows:

$$\Pi_2 = \frac{1}{2} \int_0^{h_k} Q(x, t) y \, dx \tag{4.13}$$

Then, the Lagrange function L will be made.
Since:

$$L = T - \Pi_1 + \Pi_2 \tag{4.14}$$

then, considering (4.11), (4.12) and (4.13) into consideration, we obtain:

$$L = \frac{1}{2} \int_0^{h_k} \left[\mu(x) \left(\frac{\partial y}{\partial t} \right)^2 - EF(x) \left(\frac{\partial y}{\partial x} \right)^2 + Q(x, t) y \right] dx \tag{4.15}$$

By inserting (4.15) into (4.4), we will have:

$$S = \frac{1}{2} \int_{t_1}^{t_2} \int_0^{h_k} \left[\mu(x) \left(\frac{\partial y}{\partial t} \right)^2 - EF(x) \left(\frac{\partial y}{\partial x} \right)^2 + Q(x, t) y \right] dx \, dt \tag{4.16}$$

It is necessary to determine the necessary extremum conditions for (4.16) in accordance with (4.8) and (4.9). For this purpose, the required partial derivatives contained in (4.8) are determined as follows:

$$\frac{\partial L}{\partial y} = Q(x, t); \frac{\partial}{\partial t} \left(\frac{\partial L}{\partial p} \right) = \frac{\partial}{\partial t} \left(\frac{\partial L}{\partial \left(\frac{\partial y}{\partial t} \right)} \right) = \frac{\partial}{\partial t} \left(\frac{1}{2} \mu(x) \cdot 2 \frac{\partial y}{\partial t} \right) = \mu(x) \frac{\partial^2 y}{\partial t^2};$$

$$\frac{\partial}{\partial x} \left(\frac{\partial L}{\partial q} \right) = \frac{\partial}{\partial x} \left(\frac{\partial L}{\partial \left(\frac{\partial y}{\partial x} \right)} \right) = \frac{\partial}{\partial x} \left(\frac{-1}{2} EF(x) \cdot 2 \frac{\partial y}{\partial x} \right) = \frac{-\partial}{\partial x} \left[EF(x) \frac{\partial y}{\partial x} \right];$$

$$\frac{\partial^2}{\partial t^2} \left(\frac{\partial L}{\partial r} \right) = \frac{\partial^2}{\partial t^2} \left(\frac{\partial L}{\partial \left(\frac{\partial^2 y}{\partial t^2} \right)} \right) = 0; \tag{4.17}$$

$$\frac{\partial^2}{\partial t \partial x} \left(\frac{\partial L}{\partial S} \right) = \frac{\partial^2}{\partial t \partial x} \left(\frac{\partial L}{\partial \left(\frac{\partial^2 y}{\partial t \partial x} \right)} \right) = 0;$$

$$\frac{\partial^2}{\partial x^2} \left(\frac{\partial L}{\partial u} \right) = \frac{\partial^2}{\partial x^2} \left(\frac{\partial L}{\partial \left(\frac{\partial^2 y}{\partial x^2} \right)} \right) = 0.$$

By substituting the found values of the partial derivatives into (4.8), the following is obtained:

$$Q(x,t) - \mu(x)\frac{\partial^2 y}{\partial t^2} + \frac{\partial}{\partial x}\left[E \cdot F(x)\frac{\partial y}{\partial x}\right] = 0 \qquad (4.18)$$

or

$$\mu(x)\frac{\partial^2 y}{\partial t^2} - \frac{\partial}{\partial x}\left[EF(x)\frac{\partial y}{\partial x}\right] = Q(x,t) \qquad (4.19)$$

(4.19) is the equation of the longitudinal oscillations of the root under the action of the external longitudinal load $Q(x,t)$. Further, expressions of all values that are included in (4.8) will be found. Since the root has the shape of a cone, we find that its area of cross-section $F(x)$ at the point that is located at an arbitrary distance x from point O will be:

$$F(x) = \pi x^2 tan^2 \gamma_k \qquad (4.20)$$

It is obvious that the mass per length of the root can be determined using the following expression obtained using (4.18) too:

$$\mu(x) = \rho F(x) = \rho \pi x^2 tan^2 \gamma_k \qquad (4.21)$$

where ρ is the density of the root in kg·m^{-3}.

Since the value $Q(x,t)$ in (4.17), represents the intensity of the distributed load measured in N·m^{-1}, the perturbing force in the right-hand member of (4.19) in each specific case must be measured as the intensity of load. It is possible to determine the intensity of a concentrated load with the use of the first-order impulse function $\sigma_1(x)$ (m^{-1}) [20] (Dirac delta function) and to thereby include concentrated forces and moments of force in the contents of the load distributed over the length.

According to [20], $\sigma_1(x)$ is a function that is equal to zero at all values of x except $x = 0$, where it goes to infinity and is, at the same time equal to $\int_0^x \sigma_1(x)dx = \sigma_0(x)$, where $\sigma_0(x)$—a unit function defined as follows: $\sigma_0(x) = \begin{cases} 0 \text{ at } x < 0, \\ 1 \text{ at } x \geq 0. \end{cases}$

If $Q_{zb.}(t)$ is the concentrated disturbing force applied to point x_1 and measured in Newtons, then the function

$$Q_{zb.}(x,t) = Q_{zb.}(t)\sigma_1(x - x_1) \qquad (4.22)$$

has dimensions in N·m^{-1} and expresses intensity of the concentrated load in point x_1.

The function $\sigma_1(x - x_1)$ equals zero for all values of x, except for $x = x_1$, where it is transformed into infinity.

Let the disturbing force acting according to (4.10), be applied to the root at distance x_1 from the starting point (point O in Figure 4.1). Then, according to (4.22) we can write

$$Q_{zb.}(x,t) = Hsin\omega t \cdot \sigma_1(x - x_1) \tag{4.23}$$

Since the root is connected with the soil, which is an elastic environment, application of the disturbing force of (4.12) to the root leads to emergence of the force of resistance of the soil to movement of the root due to its oscillations. This force also has affects the process of own oscillations of the root in the soil, especially at the beginning of the oscillations process, until connections of the root with the soil are destroyed.

It is obvious that the force of resistance of the soil (for the entire body of the root) is the distributed load along the area of contact of the root with the soil, which is why we must determine its intensity as the force of resistance of the soil to movement of a length unit of the root.

Let c be the coefficient of the elastic deformation of the soil applied to the area of the contact measured in N·m^{-2}. It will now be assumed that the soil surrounding the root, under the action of the disturbing force $H \cdot sin\omega t$, performs forced oscillations according to the same harmonic law with the amplitude that is determined by elastic properties of the soil. Then, the intensity $P(x, t)$ in N·m^{-1} of resistance of the soil to movement of the root in point x will be:

$$P(x,t) = 2\pi cxtan\gamma_k \cdot y(x,t) \tag{4.24}$$

This allows to obtain the following relation for the longitudinal external load which, transformed using (4.23) and (4.24) becomes:

$$Q(x,t) = Q_{zb.}(x,t) - P(x,t) = Hsin\omega t \cdot \sigma_1(x-x_1) - 2\pi cxtan\gamma_k \cdot y(x,t), \tag{4.24'}$$

The total force of the bonding between the root and the soil R_x under the action of the perturbing force $Q_{zb.}(t)$ is equal to (prior and after integration):

$$R_x = \int_0^{h_1} 2\pi cxtan\gamma_k \cdot dx \Rightarrow R_x = c\pi h_1^2 tan\gamma_k. \tag{4.25}$$

where h_1—depth of the root's location (fixation) in the soil (m).

Then, considering (4.20), (4.21), (4.23) and (4.24), we obtain:

$$\rho\pi x^2 tan^2\gamma_k \frac{\partial^2 y}{\partial t^2} - \frac{\partial}{\partial x}\left[E\pi x^2 tan^2\gamma_k \frac{\partial y}{\partial x}\right] = Hsin\omega t\sigma_1(x-x_1) - 2\pi cxtan\gamma_k \cdot y(x,t)$$

$$\tag{4.26}$$

After transforming (4.26), i.e., differentiating the expression in square brackets with respect to x, the following equation of the oscillatory process is finally obtained:

$$\rho\pi x^2 tan^2\gamma_k \frac{\partial^2 y}{\partial t^2} - E\pi x^2 tan^2\gamma_k \frac{\partial^2 y}{\partial x^2} - 2E\pi x tan^2\gamma_k \frac{\partial y}{\partial x}$$
$$= Hsin\omega t\sigma_1(x-x_1) - 2\pi cx tan\gamma_k \cdot y(x,t). \tag{4.27}$$

Thus, the differential equation of the longitudinal oscillations of the root under the action of the perturbing force that varies following a harmonic law has been obtained. Since (4.27) is a linear partial differential equation with variable coefficients, it can be solved, the same as other equations of similar types, with the use of some special methods of the calculus of variations based on the application of the Ostrogradsky–Hamilton principle. They include the direct methods of the calculus of variations, the application of which is effective in the approximate analysis of the natural frequencies and mode shapes of the oscillations of a variable cross-section bar with the nonuniform distribution of stiffness and mass along the bar's centreline.

The root can be conventionally considered as a body that belongs to the mentioned type of bars. In the computing practices, the most extensively applied direct methods of the calculus of variations are the Ritz, Rayleigh and Galerkin methods.

4.1.3. Finding Mode Shapes and Natural Frequencies of Longitudinal Oscillations of Root Body

The Ritz method will be applied for finding the mode shapes and natural frequencies of the longitudinal oscillations of the root body [20].

Given (4.20), (4.21), (4.23) and (4.24), the Hamilton–Ostrogradsky function (4.8) will look as follows:

$$S = \frac{1}{2}\int_{t_1}^{t_2}\int_0^{h_k}\left\{\rho\pi x^2 tan^2\gamma_k\left(\frac{\partial y}{\partial t}\right)^2 - E\pi x^2 tan^2\gamma_k\left(\frac{\partial y}{\partial x}\right)^2\right.$$
$$\left. +Hsin\omega t\sigma_1(x-x_1)y(x,t) - -2\pi cx tan\gamma_k\, y^2(x,t)\right\}dxdt. \tag{4.28}$$

In order to find natural forms and frequencies of longitudinal oscillations of the root in the soil, the Ritz method can be applied [29]. According to the given method, we will need to find harmonic longitudinal oscillations of the root as follows:

$$y(x,t) = \phi(x)sin(pt+\alpha) \tag{4.29}$$

where $\phi(x)$ is the natural form of primary oscillations—i.e., the function that determines continuous population of amplitude longitudinal deviations of cross-section of the root from their equilibrium positions, m and p is the natural frequency of primary oscillations, s^{-1}.

Since natural forms and natural frequencies are related to free oscillations of the system, in (4.28) we must highlight the part that specifically describes free oscillations of the system. Obviously, the function will look as follows:

$$S_1 = \frac{1}{2} \int_{t_1}^{t_2} \int_0^{h_k} \left[\rho \pi x^2 tan^2 \gamma_k \left(\frac{\partial y}{\partial t} \right)^2 - E\pi x^2 tan^2 \gamma_k \left(\frac{\partial y}{\partial x} \right)^2 - 2\pi c x tan \gamma_k y^2(x,t) \right] dxdt \tag{4.30}$$

Inserting (4.29) into (4.30) so values of the partial derivatives from (4.29) are:

$$\begin{aligned} \frac{\partial y}{\partial t} &= \varphi(x) p cos(pt + \alpha) \\ \frac{\partial y}{\partial x} &= \varphi'(x) sin(pt + \alpha) \end{aligned} \tag{4.31}$$

Inserting (4.29) and (4.31) into (4.30), we will obtain:

$$\begin{aligned} S_1 = \frac{1}{2} \int_{t_1}^{t_2} \int_0^{h_k} &\left\{ \rho \pi x^2 tan^2 \gamma_k \cdot \varphi^2(x) p^2 cos^2(pt + \alpha) \right. \\ &- E\pi x^2 tan^2 \gamma_k \cdot [\varphi'(x)]^2 sin^2(pt + \alpha) \\ &\left. - 2\pi c x tan \gamma_k \varphi^2(x) sin^2(pt + \alpha) \right\} dxdt. \end{aligned} \tag{4.32}$$

The aim of the Ritz method is reduction in the variational problem and the problem of searching for extremum of function of any independent variables. Such a reduction is performed by means of selecting a special class of the functions that depend on a finite number of initially indefinite parameters $\alpha_1, \alpha_2, \ldots, \alpha_n$ from all possible admissible functions, on which the value of the functional is analysed. The substitution of such functions into the expression of the functional changes the latter into a function of the mentioned parameters, the extremum of which can be found with the use of known elementary methods.

According to the Ritz method, the value of (4.32) is analysed on population of linear combinations of functions—i.e., expressions that look as follows:

$$\varphi(x) = \sum_{i=1}^{n} \alpha_i \psi_i(x) \tag{4.33}$$

where α_i represents the parameters, variations of which enable us to obtain the required class of allowed functions; $\psi_i(x)$ represents the basic functions that are specifically chosen and are known functions that correspond to geometrical boundary conditions of the problem.

On the class of (4.33), we have:

$$S_2(\psi) = S_2(\alpha_1, \alpha_2, \ldots, \alpha_n) \tag{4.34}$$

65

The first variation of (4.32) is determined by the following expression:

$$\delta S_2(\psi) = \sum_{i=1}^{n} \frac{\partial S_2}{\partial \alpha_i} \delta \alpha_i \tag{4.35}$$

Proceeding from the necessary condition for the existence of an extremum of the functional—that is, $\delta S_2(\psi) = 0$—the following system of n equations with n unknown quantities α_i is obtained:

$$\frac{\partial S_2}{\partial \alpha_i} = 0, (i = 1, 2, \ldots, n) \tag{4.36}$$

By solving the system of Equation (4.36) and substituting the found quantities $\alpha_1, \alpha_2, \ldots, \alpha_n$ into (4.33), the formula for the fundamental modes of oscillations as a linear combination of the basic functions is obtained.

Inserting (4.33) into (4.32) produces:

$$\begin{aligned}
S_2 = \frac{\pi}{2p} \int_0^{h_k} \Bigg\{ & \rho \pi x^2 tan^2 \gamma_k \left[\sum_{i=1}^{n} \alpha_i \psi_i(x) \right]^2 p^2 \\
& - E\pi x^2 tan^2 \gamma_k \left[\left(\sum_{i=1}^{n} \alpha_i \psi_i(x) \right)' \right]^2 \\
& - 2\pi c x tan \gamma_k \left[\sum_{i=1}^{n} \alpha_i \psi_i(x) \right]^2 r \Bigg\} dx.
\end{aligned} \tag{4.37}$$

Since

$$\left[\sum_{i=1}^{n} \alpha_i \psi_i(x) \right]^2 = \sum_{i,k=1}^{n} \psi_i(x) \psi_k(x) \alpha_i \alpha_k \tag{4.38}$$

$$\left[\sum_{i=1}^{n} \alpha_i \psi_i'(x) \right]^2 = \sum_{i,k=1}^{n} \psi_i'(x) \psi_k'(x) \alpha_i \alpha_k \tag{4.39}$$

then, considering (4.38) and (4.39), (4.40) will look as follows:

$$S_2 = \frac{\pi}{2p} \int_0^{h_k} -E\pi x^2 tan^2 \gamma_k \sum_{i,k=1}^{n} \psi_i'(x) \psi_k'(x) \alpha_i \alpha_k - 2\pi c x tan \gamma_k \sum_{i,k=1}^{n} \psi_i(x) \psi_k(x) \alpha_i \alpha_k \Bigg] dx. \tag{4.40}$$

The following symbols will now be entered:

$$\int_0^{h_k} \rho \pi x^2 tan^2 \gamma_k \psi_i(x) \psi_k(x) dx = T_{ik},$$
$$\int_0^{h_k} E \pi x^2 tan^2 \gamma_k \psi_i'(x) \psi_k'(x) dx = U_{ik},$$
$$\int_0^{h_k} 2\pi c x tan\gamma_k \psi_i(x) \psi_k(x) dx = C_{ik}, \quad (4.41)$$
$$(i,k = 1,2,\ldots,n)$$

By inserting (4.41) into (4.40), we will acquire a functional as a function from the parameters $\alpha_1, \alpha_2, \ldots, \alpha_n$:

$$S_2(\alpha_1, \alpha_2, \ldots, \alpha_n) = \frac{\pi}{2p} p^2 \sum_{i,k=1}^n T_{ik}\alpha_i\alpha_k - \frac{\pi}{2p} \sum_{i,k=1}^n U_{ik}\alpha_i\alpha_k - \frac{\pi}{2p} \sum_{i,k=1}^n C_{ik}\alpha_i\alpha_k \quad (4.42)$$

The extremum analysis of (4.42) will now performed. For this purpose, we will differentiate (4.42) with respect to parameters of α_i, $(i = 1, 2, \ldots, n)$ and equate the obtained particular derivatives to zero. As a result of this, we will acquire a set of linear homogeneous equations with respect to the unknowns $a_1, a_2, \ldots, a_n$, from which, in turn, we can find the Ritz frequency equation for longitudinal oscillations of the root attached in the soil:

$$\frac{\partial S_2(\alpha_1, \alpha_2, \ldots, \alpha_n)}{\partial \alpha_1}$$
$$= \frac{\pi}{2p} p^2 (2T_{11}\alpha_1 + 2T_{12}\alpha_2 + \ldots + 2T_{1n}\alpha_n)$$
$$- \frac{-\pi}{2p} (2U_{11}\alpha_1 + 2U_{12}\alpha_2 + \ldots + 2U_{1n}\alpha_n)$$
$$- \frac{\pi}{2p} (2C_{11}\alpha_1 + 2C_{12}\alpha_2 + \ldots + 2C_{1n}\alpha_n);$$

$$\frac{\partial S_2(\alpha_1, \alpha_2, \ldots, \alpha_n)}{\partial \alpha_2}$$
$$= \frac{\pi}{2p} p^2 (2T_{21}\alpha_1 + 2T_{22}\alpha_2 + \ldots + 2T_{2n}\alpha_n)$$
$$- \frac{-\pi}{2p} (2U_{21}\alpha_1 + 2U_{22}\alpha_2 + \ldots + 2U_{2n}\alpha_n) \quad (4.43)$$
$$- \frac{\pi}{2p} (2C_{21}\alpha_1 + 2C_{22}\alpha_2 + \ldots + 2C_{2n}\alpha_n);$$

. . . .

$$\frac{\partial S_2(\alpha_1, \alpha_2, \ldots, \alpha_n)}{\partial \alpha_n}$$
$$= \frac{\pi}{2p} p^2 (2T_{n1}\alpha_1 + 2T_{n2}\alpha_2 + \ldots + 2T_{nn}\alpha_n)$$
$$- \frac{-\pi}{2p} (2U_{n1}\alpha_1 + 2U_{n2}\alpha_2 + \ldots + 2U_{nn}\alpha_n)$$
$$- \frac{\pi}{2p} (2C_{n1}\alpha_1 + 2C_{n2}\alpha_2 + \ldots + 2C_{nn}\alpha_n);$$

The obtained partial derivatives (4.43) have been equated to zero and certain transformations will be carried out. This results in obtaining the following system of linear homogeneous equations in the unknowns $\alpha_1, \alpha_2, \ldots, \alpha_n$ (as in (4.36)):

$$\left.\begin{array}{c} \left(p^2T_{11} - U_{11} - C_{11}\right)\alpha_1 + \left(p^2T_{12} - U_{12} - C_{12}\right)\alpha_2 + \ldots + \left(p^2T_{1n} - U_{1n} - C_{1n}\right)\alpha_n = 0, \\ \left(p^2T_{21} - U_{21} - C_{21}\right)\alpha_1 + \left(p^2T_{22} - U_{22} - C_{22}\right)\alpha_2 + \ldots + \left(p^2T_{2n} - U_{2n} - C_{2n}\right)\alpha_n = 0, \\ \ldots\ldots\ldots\ldots\ldots\ldots\ldots\ldots\ldots\ldots\ldots\ldots\ldots\ldots\ldots\ldots\ldots\ldots\ldots\ldots\ldots\ldots \\ \left(p^2T_{n1} - U_{n1} - C_{n1}\right)\alpha_1 + \left(p^2T_{n2} - U_{n2} - C_{n2}\right)\alpha_2 + \ldots + \left(p^2T_{nn} - U_{nn} - C_{nn}\right)\alpha_n = 0. \end{array}\right\} \quad (4.44)$$

According to [30], for the existence of a nonzero solution of a linear homogeneous system of equations it is necessary (and sufficient) for the determinant of the system to be equal to zero—i.e.,

$$\begin{vmatrix} p^2T_{11} - U_{11} - C_{11}\, p^2T_{12} - U_{12} - C_{12} \ldots p^2T_{1n} - U_{1n} - C_{1n} \\ p^2T_{21} - U_{21} - C_{21}\, p^2T_{22} - U_{22} - C_{22} \ldots p^2T_{2n} - U_{2n} - C_{2n} \\ \ldots\ldots\ldots\ldots\ldots\ldots\ldots\ldots\ldots\ldots\ldots\ldots\ldots\ldots\ldots\ldots \\ p^2T_{n1} - U_{n1} - C_{n1}\, p^2T_{n2} - U_{n2} - C_{n2} \ldots p^2T_{nn} - U_{nn} - C_{nn} \end{vmatrix} = 0 \quad (4.45)$$

Ritz equation of frequencies (4.45) for the longitudinal oscillations of the root fixed in the soil. Since (4.45) is an equation of the n-th degree in p^2, whose solution defines the sequence of natural frequencies $p_1^2 < p_2^2 < \ldots < p_n^2$.

It is known that with $n > 4$ the given equation cannot be solved in radicals, which is why it is necessary to apply numerical methods using a PC.

However, in reality, as a rule, only the lower frequencies are determined, most often the first and the second ones, which have the most significant actions on the technological process that is being analysed.

Therefore, the first and the second frequencies of natural oscillations of the root will now be determined.

For the purpose of determination of the first and the second frequencies, (4.45) will look as follows:

$$p_1^2 T_{11} - U_{11} - C_{11} = 0 \quad (4.46)$$

where:

$$p_1^2 = \frac{U_{11} + C_{11}}{T_{11}} \quad (4.47)$$

Next, the values T_{11}, U_{11} and C_{11} in (4.42) are to be calculated. The result of the calculations is:

$$T_{11} = \int_0^{h_k} \rho\pi x^2 tan^2\gamma_k \cdot \psi_1^2(x)dx \quad (4.48)$$

$$U_{11} = \int_0^{h_k} E\pi x^2 tan^2\gamma_k \cdot \left[\psi_1'(x)\right]^2 dx \quad (4.49)$$

$$C_{11} = \int_0^{h_k} 2\pi cx \tan\gamma_k \cdot \psi_1^2(x)dx. \tag{4.50}$$

For this purpose, it is necessary at this stage to select the basic functions contained in (4.33).

As is noted in [20], in many cases the mode shapes of oscillations of the homogeneous bar with a uniform cross-section and the same conditions of fixing as in the problem under consideration are assumed as the basic functions.

Such basic functions facilitate finding the shapes that meet not only the geometric boundary conditions required by the Ritz method, but also the dynamic boundary conditions of the problem.

Therefore, the mode shapes of longitudinal oscillations of a homogeneous bar with a uniform cross-section fixed at one end will be assumed as the basic functions in the problem under consideration. According to [20], such shapes appear as follows:

$$\psi_i(x) = sin\frac{(2i-1)\pi x}{2h_k}, (i = 1,2,3,\ldots) \tag{4.51}$$

Then,

$$\psi_i'(x) = \frac{(2i-1)\pi}{2h_k}cos\frac{(2i-1)\pi x}{2h_k}, (i = 1,2,3,\ldots) \tag{4.52}$$

The geometric boundary conditions for a bar with one fixed end appear, according to [20], as follows:

$$\text{at } x = 0 \text{ (at the fixed end)}: \quad \psi(0) = 0; \tag{4.53}$$

$$\text{at } x = h_k \text{ (at the free end)}: \quad \psi'(h_k) = 0. \tag{4.54}$$

The fulfilment of (4.53) and (4.54) has to be checked for (4.51) and (4.52), respectively: $\psi_i(0) = sin0 = 0, (i = 1,2,3,\ldots),$ $\psi_i'(h_k) = \frac{(2i-1)\pi}{2h_k}cos\frac{(2i-1)\pi}{2} = \frac{(2i-1)\pi}{2h_k}cos\left(\pi i - \frac{\pi}{2}\right) = \frac{(2i-1)\pi}{2h_k}\left(cos\pi icos\frac{\pi}{2} + sin\pi isin\frac{\pi}{2}\right) = 0, (i = 1,2,3,\ldots).$

Thereby, the requirements of the Ritz method with respect to the basic functions are satisfied.

Hence, the mode shape of the root's longitudinal oscillations for any n will appear, taking into account (4.33), as follows:

$$\phi(x) = \sum_{i=1}^{n} \alpha_i sin\frac{(2i-1)\pi x}{2h_k} \tag{4.55}$$

In particular, to find the first frequency of oscillations ($n = 1$) the following shape of longitudinal oscillations of the root is available:

$$\phi(x) = \alpha_1\psi_1(x) \text{ or } \phi(x) = \alpha_1 sin\frac{\pi x}{2h_k} \tag{4.56}$$

that is to say

$$\psi_1(x) = sin\frac{\pi x}{2h_k} \tag{4.57}$$

Then,

$$\psi_1'(x) = \frac{\pi}{2h_k}cos\frac{\pi x}{2h_k} \tag{4.58}$$

Taking into account (4.48) and (4.57), T_{11} is computed:

$$T_{11} = \rho\pi tan^2\gamma_k \int_0^{h_k} x^2 sin^2\frac{\pi x}{2h_k}dx \tag{4.59}$$

The integration of (4.59) is carried out with the use of the method of integrating by parts.

After applying said method twice, the following is obtained:

$$\int_0^{h_k} x^2 sin^2\frac{\pi x}{2h_k}dx = \frac{\left(\pi^2+6\right)}{6\pi^2}h_k^3 \tag{4.60}$$

Taking into account (4.60), (4.59) assumes the following form:

$$T_{11} = \rho\pi tan^2\gamma_k\frac{\left(\pi^2+6\right)}{6\pi^2}h_k^3 \tag{4.61}$$

Further, U_{11} is to be computed. For this purpose, (4.58) is substituted into (4.49), which results in:

$$U_{11} = \frac{E\pi^3 tan^2\gamma_k}{4h_k^2}\int_0^{h_k} x^2\left(1-sin^2\frac{\pi x}{2h_k}\right)dx, \text{ or}$$
$$U_{11} = E\pi tan^2\gamma_k\frac{\pi^2}{4h_k^2}\int_0^{h_k} x^2 cos^2\frac{\pi x}{2h_k}dx. \tag{4.62}$$

(4.62) is transformed as follows:

$$U_{11} = \frac{E\pi^3 tan^2\gamma_k}{4h_k^2}\int_0^{h_k} x^2 dx - \frac{E\pi^3 tan^2\gamma_k}{4h_k^2}\int_0^{h_k} x^2 sin^2\frac{\pi x}{2h_k}dx \tag{4.63}$$

(4.60) is substituted into (4.63); then, after a number of transformations, the following is obtained:

$$U_{11} = E\pi tan^2\gamma_k \frac{(\pi^2 - 6)}{24} h_k \qquad (4.64)$$

Taking into account (4.50) and (4.57), C_{11} is computed:

$$C_{11} = 2c\pi tan\gamma_k \int_0^{h_k} x\sin^2\frac{\pi x}{2h_k}dx \qquad (4.65)$$

Using the method of integrating by parts, the following is arrived at:

$$C_{11} = \frac{ch_k^2 tan\gamma_k}{2\pi}(\pi^2 + 4) \qquad (4.66)$$

From (4.45), taking into account (4.62), (4.64) and (4.66), after the necessary transformations, the square of the first frequency is found:

$$p_1^2 = \frac{0.505Etan\gamma_k + 2.207ch_k}{0.842\rho h_k^2 tan\gamma_k} \qquad (4.67)$$

from which the final expression defining the first frequency of the root's principal oscillations is obtained:

$$p_1 = \frac{\sqrt{0.505Etan\gamma_k + 2.207ch_k}}{0.917h_k\sqrt{\rho tan\gamma_k}} \qquad (4.68)$$

In order to calculate the first frequency of oscillation p_1 according to (4.68), the necessary values of the quantities contained in it have to be specified. According to [7], the following is applicable for sugar beet roots: $h_k = 250$ mm, $\gamma_k = 14°$, $E = 18.4 \cdot 10^6$ N·m^{-2}, $\rho = 750$ kg·m^{-3}. According to [6], the soil's elastic deformation coefficient c is assumed as $c = 2 \cdot 10^5$ N·m^{-3}.

After substituting the above-listed values into (4.69), the value of the first frequency is obtained: $p_1 = 496.4$ s^{-1}, or $p_1 = 79$ Hz.

The obtained calculated value of the first frequency is in high agreement with the experimental data presented in [7,31], where $p_1 = 75...120$ Hz.

The first frequency of the free oscillations of the root body of such a value provides a rather active input in the process of breaking the bonds between the root and the soil and facilitates the extraction of the root from the soil.

In order to determine the second frequency, (4.45) is used in the following form:

$$\begin{vmatrix} p^2T_{11} - U_{11} - C_{11}p^2T_{12} - U_{12} - C_{12} \\ p^2T_{21} - U_{21} - C_{21}p^2T_{22} - U_{22} - C_{22} \end{vmatrix} = 0 \qquad (4.69)$$

After expanding (4.67), the following second-degree equation in the unknown p^2 is arrived at:

$$
\begin{aligned}
&\left(T_{11}T_{22} - T_{12}^2\right)p^4 \\
&+(-T_{11}U_{22} - T_{11}C_{22} - U_{11}T_{22} - C_{11}T_{22} + 2T_{12}U_{12} + 2T_{12}C_{12})p^2 \\
&+U_{11}U_{22} + U_{11}C_{22} + C_{11}U_{22} + C_{11}C_{22} - U_{12}^2 - 2U_{12}C_{12} - C_{12}^2 = 0.
\end{aligned}
\tag{4.70}
$$

The multipliers in (4.70) (second-degree) have to be found: T_{11} is determined according to Expression (4.61), U_{11}—according to (4.64), C_{11}—according to (4.66).

It can be concluded from (4.41) that:

$$
T_{12} = \rho\pi tan^2\gamma_k \int_0^{h_k} x^2\psi_1(x)\psi_2(x)dx
\tag{4.71}
$$

Since $\psi_1(x)$ is determined from (4.57) and

$$
\psi_2(x) = sin\frac{3\pi x}{2h_k}
\tag{4.72}
$$

by inserting (4.57) and (4.72) into (4.71), we will have:

$$
T_{12} = \rho\pi tan^2\gamma_k \int_0^{h_k} x^2 sin\frac{\pi x}{2h_k} sin\frac{3\pi x}{2h_k}dx
\tag{4.73}
$$

The quantity U_{12} can be found. In accordance with (4.41), the following is obtained:

$$
U_{12} = E\pi tan^2\gamma_k \int_0^{h_k} x^2\psi_1'(x)\psi_2'(x)dx
\tag{4.74}
$$

where

$$
\psi_1'(x) = \frac{\pi}{2h_k}cos\frac{\pi x}{2h_k}, \quad \psi_2'(x) = \frac{3\pi}{2h_k}cos\frac{3\pi x}{2h_k}
\tag{4.75}
$$

Respectively, we will have:

$$
U_{12} = E\pi tan^2\gamma_k\frac{3\pi^2}{4h_k^2} \int_0^{h_k} x^2 cos\frac{\pi x}{2h_k}cos\frac{3\pi x}{2h_k}dx
\tag{4.76}
$$

Further, T_{22} is to be computed. According to (4.41) we will have:

$$
\begin{aligned}
T_{22} &= \rho\pi tan^2\gamma_k \int_0^{h_k} x^2\psi_2^2(x)dx \\
&\xrightarrow{\psi_2(x)\ from\ (4.72)} \\
T_{22} &= \rho\pi tan^2\gamma_k \int_0^{h_k} x^2 sin^2\frac{3\pi x}{2h_k}dx
\end{aligned}
\tag{4.77}
$$

Further, U_{22} is to be computed. According to (4.41) we will have:

$$U_{22} = E\pi\tan^2\gamma_k \int_0^{h_k} x^2 \left[\psi_2'(x)\right]^2 dx \xRightarrow{(4.75)} E\pi\tan^2\gamma_k \frac{9\pi^2}{4h_k^2} \int_0^{h_k} x^2\cos^2\frac{3\pi x}{2h_k} dx \quad (4.78)$$

Taking into account (4.41):

$$C_{12} = 2c\pi\tan\gamma_k \int_0^{h_k} x\sin\frac{\pi x}{2h_k}\sin\frac{3\pi x}{2h_k} dx \qquad (4.79)$$

$$C_{22} = 2c\pi\tan\gamma_k \int_0^{h_k} x\sin^2\frac{3\pi x}{2h_k} dx \qquad (4.80)$$

Thus, the analytic expressions for determining all the quantities included in the multiplying factors of p^4, p^2 and the free term of (4.68) (second-degree) have been obtained.

Using (4.61), (4.64), (4.70), (4.73), and (4.76)–(4.70) in the Mathcad environment, the values of the first and second frequencies of the free oscillations of the root body as a function of the value of the soil's elastic deformation coefficient c are computed. In accordance with [6], $c = 1{\cdot}10^5 \sim 20{\cdot}10^5$ N·m^{-3} is assumed. The results of the calculations are shown in Table 4.1.

Table 4.1. Values of first and second natural frequencies of longitudinal oscillations of root body.

Elastic Deformation Coefficient of Soil, c (N·m^{-3})	First Circular Frequency of Oscillation, p_1 (s^{-1})	First Frequency of Oscillation p_1 (Hz)	Second Circular Frequency of Oscillation p_2 (s^{-1})	Second Frequency of Oscillation p_2 (Hz)
0	480.173	76.422	3318	528.076
2×10^5	491.861	78.282	3321	528.554
4×10^5	503.276	80.099	3323	528.872
6×10^5	514.436	81.875	3326	529.346
8×10^5	525.356	83.613	3329	529.827
10×10^5	536.053	85.315	3331	530.145
12×10^5	546.538	86.984	3334	530.623
14×10^5	556.825	88.621	3337	531.100
16×10^5	566.923	90.229	3339	531.418
18×10^5	576.842	91.807	3342	531.896
20×10^5	586.592	93.359	3344	531.214

On the basis of the obtained computation results, the graphs of the first and second frequencies as functions of the soil's elastic deformation coefficient c have been plotted (Figures 4.2 and 4.3).
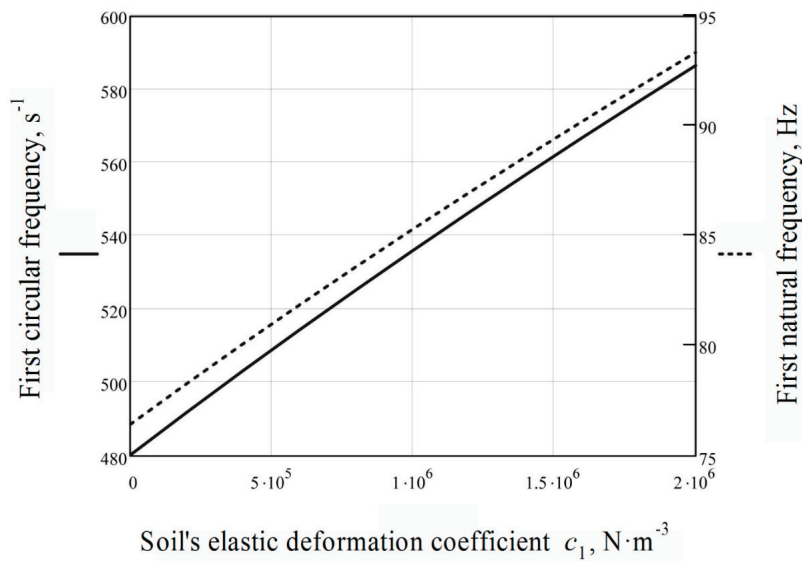
Figure 4.2. Relation between first natural frequency of longitudinal oscillations of root body and soil's elastic deformation coefficient c.
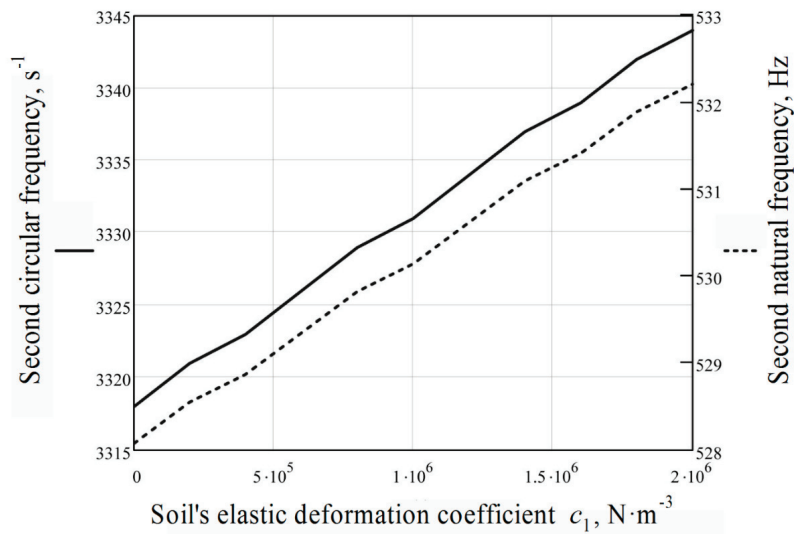
Figure 4.3. Relation between second natural frequency of longitudinal oscillations of root body and soil's elastic deformation coefficient c.

As can be seen in the presented graph (Figure 3.2), when the value of the soil's elastic deformation coefficient c changes within the range of $c = 0\,2 \cdot 10^6$ N·m^{-3}, the value of the first circular frequency monotonically increases within the range of $p_1 = 480 \sim 587$ s^{-1} and frequency changes within the range of 76.4–93.4 Hz.

It can be seen in the graph in Figure 3.3 that the second frequency of the free oscillations changes insignificantly, as the soil's elastic deformation coefficient c changes within the range of $c = 0.2 \cdot 10^6$ N·m^{-3}: the circular frequency varies, accordingly, within $p_2 = 3318 \sim 3344$ s^{-1} and the Hertz frequency varies within $528 \sim 532$ Hz.

The above-described method of computation of the first and second frequencies of the free oscillations of the root body fixed in the soil allows the values of the mentioned frequencies to be obtained within quite a wide spectrum of the parameters of the sugar beet root.

Moreover, on the basis of solving the Ritz equation of frequency (4.45) in the MathCad environment, it is possible to obtain the value of any frequency of the free longitudinal oscillations of the root as an elastic solid in an elastic medium.

4.1.4. Forced Longitudinal Oscillations of Root Body

Next, the analysis of the forced oscillations of the root will be discussed. The exclusively forced oscillations will happen according to the following law:

$$y(x,t) = \phi(x)\sin\omega t \tag{4.81}$$

where $\phi(x)$ is the form of the forced oscillations.

In order to determine the form of the forced oscillations of the root, (4.81) will be entered into (4.28) in advance to calculate needful derivates:

$$\frac{\partial y}{\partial t} = \omega\phi(x)\cos\omega t \tag{4.82}$$

$$\frac{\partial y}{\partial x} = \phi'(x)\sin\omega t \tag{4.83}$$

(4.82) and (4.83) will now be inserted into (4.28), and we will obtain:

$$S_3 = \frac{1}{2}\int_{t_1}^{t_2}\int_0^{h_k}\left\{\rho\pi x^2 tan^2\gamma_k \cdot \omega^2\varphi^2(x)\cos^2\omega t - E\pi x^2 tan^2\gamma_k[\varphi'(x)]^2\sin^2\omega t + H\sigma_1(x-x_1)\varphi(x)\sin^2\omega t - -2\pi cxtg\gamma_k\cdot\varphi^2(x)\sin^2\omega t\right\}dxdt. \tag{4.84}$$

By integrating (4.84) over t within the limits of one period $T = \frac{2\pi}{\omega}$, we will obtain:

$$S_4 = \frac{\pi}{2\omega}\int_0^{h_k}\left\{\rho\pi x^2 tan^2\gamma_k \cdot \varphi^2(x)\omega^2 - E\pi x^2 tan^2\gamma_k[\varphi'(x)]^2 + H\sigma_1(x-x_1)\varphi(x) - 2\pi xc \tan\gamma_k\cdot\varphi^2(x)\right\}dx. \tag{4.85}$$

According to the Ritz method, analysis of the value of (4.85) will be performed with respect to population of linear combinations of the following type:

$$\phi(x) = \alpha\psi(x) \tag{4.86}$$

where α is the parameter, variations of which let us obtain the class of the allowed functions; $\psi(x)$ is the basis function.

(4.86) will now be inserted into (4.85), and we will obtain:

$$S_4 = \frac{\pi}{2\omega} \int_0^{h_k} \Big\{ \rho\pi x^2 tan^2\gamma_k \cdot \alpha^2\psi^2(x)\omega^2$$
$$-E\pi x^2 \tan^2\gamma_k \cdot \alpha^2 [\psi'(x)]^2 + H\sigma_1(x - x_1)\alpha\psi(x) \tag{4.87}$$
$$-2\pi xc \tan\gamma_k \cdot \alpha^2\psi^2(x) \Big\} dx.$$

The following symbols will now be inserted:

$$\int_0^{h_k} \rho\pi x^2 tan^2\gamma_k \cdot \psi^2(x)dx = T \tag{4.88}$$

$$\int_0^{h_k} E\pi x^2 tan^2\gamma_k [\psi'(x)]^2 dx = U \tag{4.89}$$

$$\int_0^{h_k} 2\pi cx tan\gamma_k \cdot \psi^2(x)dx = M \tag{4.90}$$

$$\int_0^{h_k} H\sigma_1(x - x_1)\psi(x)dx = L \tag{4.91}$$

(4.86)–(4.89) will now be inserted into (4.85), and we will have:

$$S_4(\alpha) = \frac{\pi}{2\omega}\Big(\omega^2 T\alpha^2 - (U + M)\alpha^2 + L\alpha\Big) \tag{4.92}$$

So, in the population of functions (4.87), (4.88) is transformed into the function of the independent variable α—(4.92).

The first variation of (4.92) will be equal to:

$$\delta S_4(\alpha) = \frac{\partial S_4}{\partial\alpha}\delta\alpha \tag{4.93}$$

The necessary condition of the stationary (4.92) (i.e., existence of the extremum) is that its first variation equals zero (4.93):

$$\frac{\partial S_4}{\partial\alpha}\delta\alpha = 0 \tag{4.94}$$

from which we receive the following equation:

$$\frac{\partial S_4}{\partial \alpha} = 0 \tag{4.95}$$

Differentiating (4.92) over α will give

$$\frac{\partial S_4}{\partial \alpha} = \frac{\pi}{2\omega}\left(2\omega^2 T\alpha - 2(U+M)\alpha + L\right) \tag{4.96}$$

Taking (4.95) into consideration, the following equation is obtained:

$$2\omega^2 T\alpha - 2(U+M)\alpha + L = 0 \tag{4.97}$$

from which we find the required value of the parameter α. This will be:

$$\alpha = \frac{L}{2(U+M-\omega^2 T)}. \tag{4.98}$$

The form of the forced longitudinal oscillations of the rod with the constant cross-section with one end firmly attached, emerging under the action of the longitudinal harmonic force of frequency ω, applied at the point $x = x_1$ will now be assumed as the basis function $\psi(t)$.

According to [20], the form of the forced oscillations of the given rod looks as follows:

$$\psi(x) = D_1 sinax \text{ with } x \le x_1 \tag{4.99}$$

$$\psi(x) = D_2 cosa(h_k - x) \text{ with } x > x_1, \tag{4.100}$$

where:

$$D_1 = \frac{-1}{aEF}\frac{cosa(h_k - x_1)}{cosah_k} \tag{4.101}$$

$$D_2 = \frac{-1}{aEF}\frac{sinax_1}{cosah_k} \tag{4.102}$$

$$a = \omega\sqrt{\frac{\mu}{EF}} \tag{4.103}$$

μ is the mass per length of the rod; F is the area of the longitudinal section of the rod; E is the Young's module for material of the rod; h is the length of the rod; ω is the frequency of the forced oscillations of the rod.

Further, it is necessary to check the fulfilment of the boundary conditions for the basic functions (4.99) and (4.100). These are different for the fixed end of the bar ($x = 0 \Rightarrow \psi(0) = D_1 \cdot sin0 = 0$) and for the free end of the bar ($x = h_k \Rightarrow \psi'(h_k) = 0$).

The derivative of (4.100) is to be computed. It is equal to:

$$\psi'(x) = D_2 a \sin a (h_k - x) \tag{4.104}$$

Therefore, $\psi'(h_k) = D_2 a \sin a (h_k - h_k) = D_2 a \sin 0 = 0$.

Hence, the boundary conditions for the basic functions (4.99) and (4.100) are fulfilled; therefore, the assumed basic functions meet the requirements of the Ritz method.

Further, the values of the quantities T, U, M and L that enter into Expression (4.96) are to be computed.

In accordance with (4.99) and (4.100), the following can be written down:

$$T = \rho \pi \tan^2 \gamma_k \left[\int_0^{x_1} x^2 D_1^2 \sin^2 ax \, dx + \int_{x_1}^{h_k} x^2 D_2^2 \cos^2 a (h_k - x) \, dx \right] \tag{4.105}$$

By integrating the parts twice, the following values are obtained for the integrals contained in (4.105):

$$\int_0^{x_1} x^2 \sin^2 ax \, dx = \frac{x_1^3}{6} - \frac{x_1^2 \sin 2ax_1}{4a} - \frac{x_1 \cos 2ax_1}{4a^2} + \frac{\sin 2ax_1}{8a^3} \tag{4.106}$$

$$\int_{x_1}^{h_k} x^2 \cos^2 a (h_k - x) \, dx = \frac{h_k^3}{6} - \frac{x_1^3}{6} + \frac{1}{4a} x_1^2 \sin(2ah_k - 2ax_1) + \frac{1}{4a^2} h_k \\ - \frac{1}{4a^2} x_1 \cos(2ah_k - 2ax_1) - \frac{1}{8a^3} \sin(2ah_k - 2ax_1). \tag{4.107}$$

After substituting (4.106) and (4.107) into (4.105) and carrying out a number of algebraic transformations, it is found that:

$$T = \rho \pi \tan^2 \gamma_k \left\{ D_1^2 \left(\frac{x_1^3}{6} - \frac{x_1^2 \sin 2ax_1}{4a} - \frac{x_1 \cos 2ax_1}{4a^2} + \frac{\sin 2ax_1}{8a^3} \right) \right. \\ \left. + D_2^2 \frac{x_1 \cos(2ah_k - 2ax_1)}{4a^2} - \frac{\sin(2ah_k - 2ax_1)}{8a^3} \right]\right\}. \tag{4.108}$$

In order to determine the quantity U, the derivative of (4.99) is computed. This is as follows:

$$\psi'(x) = D_1 a \cos ax \tag{4.109}$$

By substituting (4.104) and (4.109) into (4.89), the following is arrived at:

$$U = E \pi \tan^2 \gamma_k \left[\int_0^{x_1} D_1^2 a^2 x^2 \cos^2 ax \, dx + \int_{x_1}^{h_k} D_2^2 a^2 x^2 \sin^2 a (h_k - x) \, dx \right] \tag{4.110}$$

(4.108) can be rearranged as follows:

$$U = E \pi \tan^2 \gamma_k \tag{4.111}$$

or

$$U = E\pi tan^2\gamma_k - D_2^2 a^2 \int_{x_1}^{h_k} x^2 cos^2 a(h_k - x)dx \Bigg].$$

(4.112)

Further, (4.106) and (4.107) are substituted into (4.112). After a number of transformations, the final result is:

$$U = E\pi tan^2\gamma_k \Bigg[\frac{D_1^2 a^2 x_1^3}{6} + \frac{D_2^2 a^2 \left(h_k^3 - x_1^3\right)}{6} + D_1^2 \left(\frac{x_1^2 \sin 2ax_1}{4} + \frac{x_1 \cos 2ax_1}{4} - \frac{\sin 2ax_1}{8a} \right)$$
$$- D_2^2 \left(\frac{x_1^2 a \sin(2ah_k - 2ax_1)}{4} + \frac{h_k}{4} - \frac{x_1 \cos(2ah_k - 2ax_1)}{4} - \frac{\sin(2ah_k - 2ax_1)}{8a} \right) \Bigg].$$

(4.113)

In order to determine the quantity M, the values of the basic functions (4.99) and (4.100) are substituted into (4.90):

$$M = 2\pi c D_1^2 tan\gamma_k \int_0^{x_1} x sin^2 ax dx + 2\pi c D_2^2 tan\gamma_k \int_{x_1}^{h_k} x cos^2 a(h_k - x)dx$$

(4.114)

Using the method of integration by parts, the following is found:

$$M = 2\pi c D_1^2 tan\gamma_k \left(\frac{x_1^2}{4} - \frac{x_1 sin2ax_1}{4a} + \frac{1 - cos2ax_1}{8a^2} \right)$$
$$+ 2\pi c D_2^2 tan\gamma_k \left[\frac{1 - cos2a(h_k - x_1)}{8a^2} - \frac{(h_k - x_1)^2}{4} + \frac{h_k(h_k - x_1)}{2} + \frac{x_1 sin2a(h_k - x_1)}{4a} \right].$$

(4.115)

In order to determine the quantity L, the values of the basic functions (4.99) and (4.100) are substituted into (4.91) and the following is obtained:

$$L = \int_0^{x_1} H\sigma_1(x - x_1)D_1 sinax dx + \int_{x_1}^{h_k} H\sigma_1(x - x_1)D_2 cosa(h_k - x)dx.$$

(4.116)

The integrals in (4.116) have to be computed.

Since (4.116) for determining the coefficient L contains the impulse function $\sigma_1(x - x_1)$, which does not belong to classical functions, it is to be noted that the computation of integrals containing such a function has to be carried out with the use of the method of integrating generalised functions.

The computation starts with finding the following integral and considering the definition and properties of the function $\sigma_1(x - x_1)$

$$
\begin{aligned}
HD_1 & \int_0^{x_1} \sigma_1(x - x_1)\sin ax\, dx \\
= HD_1 & \lim \int_0^{x_1-\varepsilon} \sigma_1(x - x_1)\sin ax\, dx \\
+HD_1 & \lim \int_{x_1-\varepsilon}^{x_1+\varepsilon} \sigma_1(x - x_1)\sin ax\, dx \\
= 0 + HD_1 & \sin ax_1 \lim \int_{x_1-\varepsilon}^{x_1+\varepsilon} \sigma_1(x - x_1)\, dx. \\
\text{When} & \lim \int_{x_1-\varepsilon}^{x_1+\varepsilon} \sigma_1(x - x_1)\, dx = 1 \implies \\
HD_1 & \int_0^{x_1} \sigma_1(x - x_1)\sin ax\, dx = HD_1\sin ax
\end{aligned}
\tag{4.117}
$$

Then, we can write:

$$
\begin{aligned}
HD_2 \int_{x_1}^{h_k} \sigma_1(x - x_1)\cos a(h_k - x)\, dx & = HD_2 \int_{x_1}^{h_k} \sigma_1(x - x_1)\cos a(h_k - x)\, dx \\
& = HD_2 \lim \int_{x_1+\varepsilon}^{h_k} \sigma_1(x - x_1)\cos a(h_k - x)\, dx = 0 \implies \\
HD_2 & \int_{x_1}^{h_k} \sigma_1(x - x_1)\cos a(h_k - x)\, dx = 0.
\end{aligned}
\tag{4.118}
$$

After substituting the values of (4.117) and (4.118) into (4.116), the value of L is found. This is equal to:

$$
L = HD_1\sin ax_1
\tag{4.119}
$$

By substituting (4.108), (4.113), (4.115) and (4.119) into (4.98), the necessary value of parameter α that allows for the stationary value of (4.85) is obtained.

Taking into consideration (4.86), (4.99) and (4.100), we can obtain the expression for the form of the forced oscillations of the root attached in the soil. They look as follows:

$$
\begin{aligned}
\phi(x) & = \alpha \cdot D_1\sin ax, \text{ with } x \le x_1, \\
\phi(x) & = \alpha \cdot D_2\cos a(h_k - x), \text{ with } x > x_1
\end{aligned}
\tag{4.120}
$$

where α is determined according to (4.98).

Having inserted (4.120) into (4.81), we can obtain the final law of the forced oscillations of the root attached in the soil. If we take into consideration the action of the disturbing force $H\sin\omega t$, the given law will be as follows:

$$
\begin{aligned}
y(x,t) & = D_1\alpha\sin ax\sin\omega t, \text{ with } x \le x_1 \\
y(x,t) & = D_2\alpha\cos a(h_k - x)\sin\omega t, \text{ with } x > x_1
\end{aligned}
\tag{4.121}
$$

For performing the numerical calculations of the forced oscillations of a root fixed in the soil, it is necessary to determine a number of the parameters present in (4.120) and (4.121). For example, the parameters D_1, D_2 and a are determined with the use of (4.101), (4.102) and (4.103), respectively.

As the above-mentioned expressions contain the earlier defined quantities E, F, μ and h_k, which are parameters of the uniform cross-section bar, the shapes of forced oscillations, which have been assumed as the basic functions, and said quantities have to be found. It is assumed that the mass of the bar with a uniform cross-section is equal to the mass of the root, which implies that the bar and the root have the same inertia properties.

It is also assumed that the specific gravity of the bar's material is equal to the root's density ρ. Hence, the bar and the root must have the same volume. One more assumption is that the bar and the root are of equal length h_k, which is essential in the case of longitudinal oscillations.

Hence, the root's volume is equal to:

$$V_k = \frac{1}{3}\pi r_k^2 h_k \tag{4.122}$$

where r_k—radius of the root (m) (that is, the radius of the cone base, as the root is in effect considered to be a cone-shaped solid).

The volume of the bar (cylinder of revolution) is equal to:

$$V_{cm.} = \pi r_{cm.}^2 h_k \tag{4.123}$$

where $r_{\text{CT.}}$—radius of the bar (m).

Equating (4.122) and (4.123), i.e., $V_k = V_{cm.}$, is also possible to obtain the bar's radius $r_{\text{CT.}} = \frac{r_k}{\sqrt{3}}$.

Hence, the bar's cross-section area F is equal to:

$$F = \frac{1}{3}\pi r_k^2 \tag{4.124}$$

while the bar's linear density μ is equal to:

$$\mu = \rho F = \frac{1}{3}\rho \pi r_k^2 \tag{4.125}$$

It is also assumed that the materials of the bar and the root have the same Young modulus, which is equal to E.

The results of the theoretical investigation of the forced oscillations of a root fixed in the soil can be used for setting up the algorithm of computation of said oscillations.

1. The parameters needed for computation have to be set.

The length (height) of the root h_k, its angle of taper γ_k, the Young modulus E for the root body, the specific gravity ρ of the root, force $P_{\text{OП.}}$ of resistance to the vertical extraction of a not undercut root from the soil are assumed, in accordance with [7],

to be equal to: $h_k = 250 \cdot 10^{-3}$ m; $\gamma_k = 14°$; $E = 18.4 \cdot 10^6$ N·m^{-2}; $\rho = 750$ kg·m^{-3}; $P_{O\Pi.} = 439 \sim 481$ N.

The other parameters that govern the process of vibrational digging of roots can be obtained with the use of the standard methods of computation as for root's radius $r_k = h_k tan\gamma_k = 250tan14° = 250 \cdot 0.2493 = 62$ mm. The amplitude H of the perturbing force is to be selected subject to the following condition: $H > P_{O\Pi.}$. Hence, taking into account the value of the resistance force $P_{O\Pi.}$, $H = 500$ N is assumed.

The frequency ω of the perturbing force is assumed, in accordance with [6], equal to $\omega = 125.6$ s^{-1}.

2. The parameter a is computed with the use of Expression (4.103), or, after a number of its transformations, the expression of the following form:

$$a = \omega \sqrt{\frac{\rho}{E}} \qquad (4.126)$$

The parameters D_1 and D_2 are computed with the use of Expressions (4.101) and (4.102), respectively, or, after a number of their transformations, the expressions of the following forms:

$$D_1 = \frac{-3}{aE\pi r_k^2} \frac{cosa(h_k - x_1)}{cosah_k} \qquad (4.127)$$

and

$$D_2 = \frac{-3}{aE\pi r_k^2} \frac{sinax_1}{cosah_k} \qquad (4.128)$$

(the latter two expressions are obtained from (4.101) and (4.102) by substituting the values found in (4.124) into them).

4. After this, parameter α is computed with the use of (4.98).

5. The expression for the shapes of the forced oscillations is generated in accordance with (4.120):

$$\varphi(x) = \alpha D_1 sinax, \text{ at } x \leq x_1$$
$$\varphi(x) = \alpha D_2 cosa(h_k - x), \text{ at } x > x_1 \qquad (4.129)$$

6. In accordance with (4.81), the law of the root's forced oscillations is established:

$$y(x,t) = \varphi(x) \sin \omega t \qquad (4.130)$$

where $\phi(x)$ is determined in accordance with (4.129).

7. Further, the maximum value of the amplitude of the forced oscillations is found:

$$max(D_1\alpha, D_2\alpha) \qquad (4.131)$$

8. It is necessary to carry out the comparative assessment of the obtained maximum value of the amplitude of the forced oscillations against the amplitude that is permissible with regard to the breaking of the root:

$$max(D_1\alpha, D_2\alpha) \leq [\phi] \tag{4.132}$$

where $[\phi]$—amplitude that is permissible for the root with regard to its tensile fracture (m).

9. In case the inequality of opposite sense is true, it is necessary to reduce the amplitude of the perturbing force and repeat the computation.

In what follows, an example of the PC-assisted computation of the amplitude of the longitudinal oscillations of the root body fixed in the soil is presented.

The calculation is performed using the Mathcad program in order to determine the relations between the amplitude of the forced longitudinal oscillations of the body of the root attached in the soil from the coefficient c of the elastic deformation of the soil surrounding the root, and the distance of the cross-section of the root from the conditional point of its attachment for the frequency of the disturbing force $v = 10\,\text{Hz}$ and $v = 20\,\text{Hz}$.

On the basis of the calculations, we obtained the following graphs (Figures 4.4 and 4.5).

As it is seen from the graphs stated above, in the case of an increase in the coefficient c of the elastic deformation of the surrounding soil, the amplitude of the forced oscillations of the root is reduced, and in the case of an increase in the distance x of the cross-section of the root from the point of conditional attachment with $x \leq x_1$ it is increased, and with $x \geq x_1$ it almost does not change.

Figure 4.5 shows the given relation for a number of specific cross-sections of the root, in particular: for $x = 0.07\,\text{m}$; $0.1\,\text{m}$; $0.12\,\text{m}$; $0.15\,\text{m}$ (point of gripping).

On the given graph we can quite clearly see the tendency of increase in the amplitude of the forced longitudinal oscillations in the case of an increase in the distance of the cross-section from the conditional point of attachment and the tendency of its reduction due to increase in the coefficient c of the elastic deformation of the surrounding soil.

For example, with $x = 0.07\,\text{m}$ and change in the coefficient c within the limits $c = 0\text{–}20 \cdot 10^5\,\text{N} \cdot \text{m}^{-3}$, the amplitude is changed within the limits of 0.7–0.47 mm; with $x = 0.1\,\text{m}$—within the limits of 0.67-0.99 mm; with $x = 0.12\,\text{m}$—within the limits of 0.81–1.19 mm; with $x = 0.15\,\text{m}$ (point of gripping)—within the limits of 1.01–1.49 mm.

However, as the graph in Figure 4.6 shows, for cross-section of the root above the point of gripping ($x \geq 0.15\,\text{m}$) the amplitude of forced oscillations of the body of the root with increasing distance of the cross-section from the conditional point of attachment almost does not change and remains the same as in the case of $x = 0.15\,\text{m}$.

However, the tendency of decrease in the amplitude from increase in the coefficient c is the same as for the sections below the point of gripping ($x \leq 0.15$).

(a) (b)
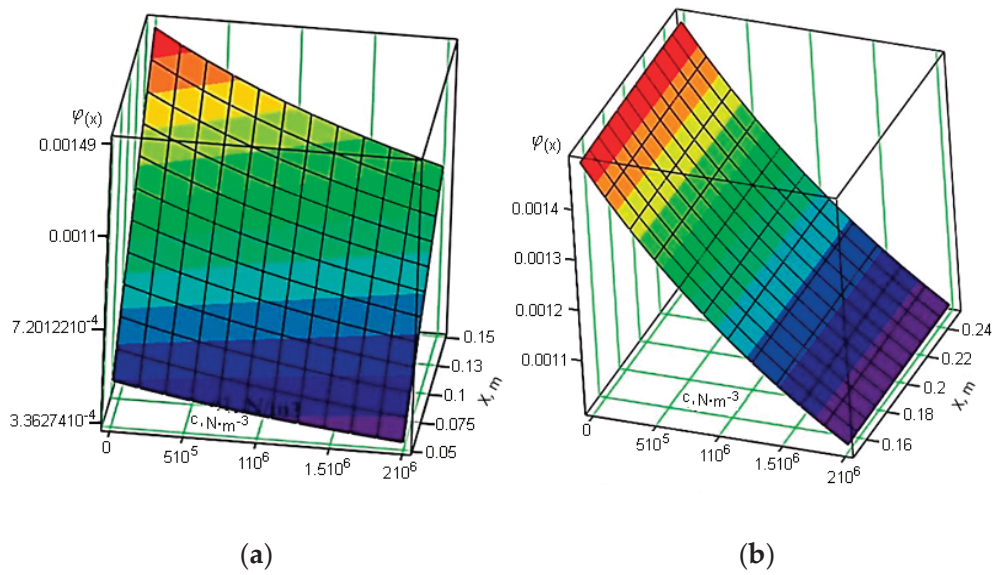
Figure 4.4.   Relation between the amplitude of the forced longitudinal oscillations of the root as an elastic body attached in the soil and the coefficient c of the elastic deformation of the surrounding soil, and between the distance x of the cross-section of the root and the conditional point of attachment: (**a**) $x \leq x_1$; (**b**) $x \geq x_1$, (x_1—point of gripping, $v = 20$ Hz).
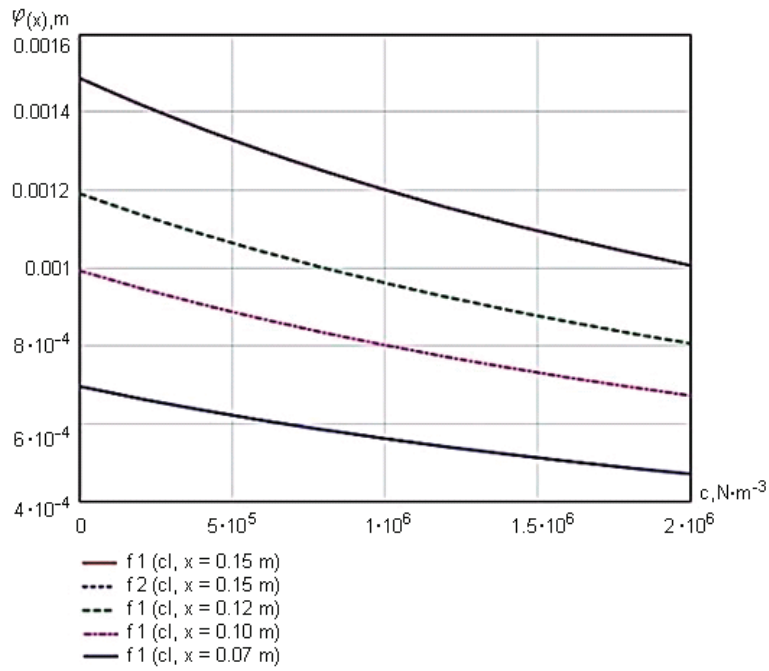
Figure 4.5. Relation between the amplitude of the forced longitudinal oscillations of the root as an elastic body and the distance x of the cross-section of the conditional point of attachment $x \leq x_1, v = 20$ Hz.
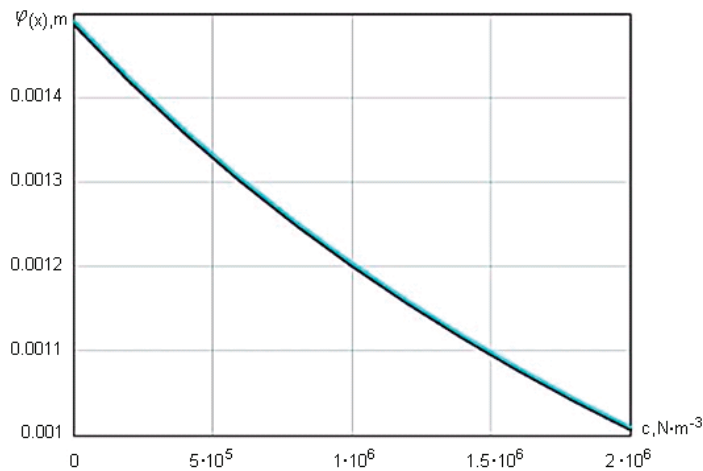
Figure 4.6. Relation between the amplitude of the forced longitudinal oscillations of the root as an elastic body and the distance x of the cross-section from the conditional point of attachment $(x \geq x_1), v = 20$ Hz.

In the case of the frequency of the disturbing force $v = 10$ Hz, values of the amplitude are slightly lower. For example, with $x = 0.07$ m the value of the amplitude remains within the limits of 0.45–0.66 mm; with $x = 0.1$—within the limits of 0.65–0.94 mm; with $x = 0.12$ m—within the limits of 1.13–0.78 mm; with $x = 0.15$ m (point of gripping)—within the limits of 0.97–1.41 mm.

Additionally, we have obtained the estimated relation between the amplitude of the forced longitudinal oscillations of the body of the root and the amplitude of the disturbing force for the frequency of the disturbing force $v = 20$ Hz (Figures 4.7 and 4.8).
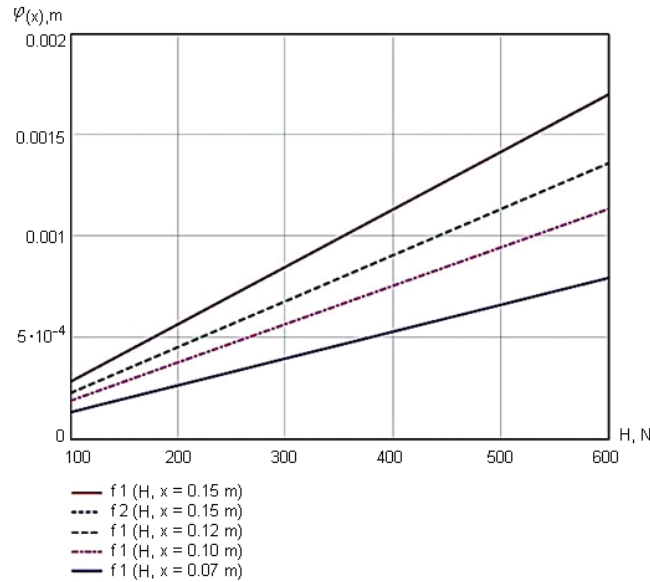
Figure 4.7. Relation between the amplitude of the forced longitudinal oscillations of the body of the root and the amplitude of the disturbing force ($x \leq x_1$, $v = 20$ Hz).
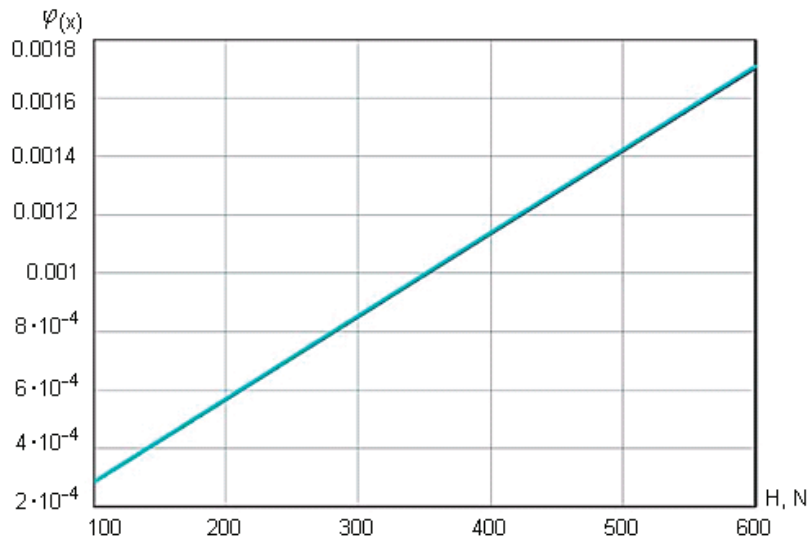
Figure 4.8. Relation between the amplitude of the forced longitudinal oscillations of the body of the root and the amplitude of the disturbing force ($x \geq x_1$, $v = 20$ Hz).

As it is seen from the presented graphs, an increase in the amplitude of the disturbing force leads to increase in the amplitude of longitudinal forced oscillations of the body of the root according to the linear law.

It should also be noted that below the point of gripping ($x \le 0.15$ m), with an increase in the distance of the cross-section of the root from the conditional point of attachment O, the amplitude also increases (Figure 4.7). For example, with $x = 0.07$ m the amplitude remains within the limits of 0.13~0.8 mm; with $x = 0.1$ m—within the limits of 0.19~1.14 mm; with $x = 1.12$ m—within the limits of 0.23~1.36 mm; with $x = 0.15$ m (point of gripping)—within the limits of 0.28~1.7 mm. However, above the point of gripping ($x \ge 0.15$ m), in the case of an increase in distance of the cross-section from the conditional point of attachment O, the amplitude almost does not change, as is shown on the graph in Figure 4.8.

In the case of the frequency of the disturbing force $v = 10$ Hz, the obtained values of amplitudes were a little bit lower; however, for $v = 10$ Hz they were the same. For example, with $x = 0.07$ m the amplitude remains within the limits of 0.12~0.76 mm; with $x = 0.1$ m—within the limits of 0.18~1.08 mm; with $x = 0.12$ m —within the limits of 0.21~1.3 mm; with $x = 0.15$ m (point of gripping)—within the limits of 0.27~1.62 mm.

Respectively, the obtained values of the frequencies of natural longitudinal oscillations and amplitudes of the forced longitudinal oscillations of the body of the root foster the process of intense knocking of the soil that adhered to the roots, and in the case of such amplitudes, tearing of the bodies of the roots is unlikely.

4.2. Theory of Transverse Oscillations of Root as Elastic Solid Fixed in Soil

4.2.1. Free Transverse Oscillations of Root as Elastic Solid Fixed in Soil

At the initial stage of the development of vibrational digging tools for beet harvesters, the forces were imparted on the root in the transverse horizontal plane, at a right angle to the line of translational motion of the lifter.

Nevertheless, despite the quite thorough analytical investigations of the process of vibrational digging of sugar beet roots by applying to them perturbing forces in the transverse horizontal plane as well as the full-scale engineering projects along this line of development, the industrial production of several pilot units and the performance of elaborate experimental studies and official tests, such vibrational digging tools have not gained ground.

The main reason for this was the conclusion that such vibrational lifting tools are unable to deliver a sufficiently high rate of travel (and, accordingly, a sufficiently high labour efficiency) subject to retaining the required harvesting quality indicators, which resulted from the fact that applying the perturbing forces to the beet roots in the plane that was perpendicular to the line of the lifter's translational motion would lead to the constant plugging of its working channel with root bodies and soil, break-off of the roots' tail parts and the complete loss of the self-cleaning ability. The power consumption rate of this process was also too high.

As was later established in experiments, the negative phenomenon could be completely avoided by switching the line of action of the perturbing forces from the transverse horizontal plane and the alignment perpendicular to the line of the lifter's translational motion into the longitudinal vertical plane. This changeover brought about a very good performance in the harvesting of sugar beet roots at high rates of travel. Virtually all universally known manufacturers of beet harvesting machinery launched the production of beet harvesters with vibrational lifting tools, which operated based on the principle of imparting perturbing forces to the roots in the longitudinal vertical plane.

In what follows, the case of transverse free and forced oscillations of the root body, where the directions of the perturbing forces and the translational motion of the vibrational lifting tool coincide, is analysed. Said case has not been investigated and is of considerable interest, both from the theoretic and practical points of view, as the alteration of the line of action of the perturbing force gives rise to substantial changes in the course of the process of vibrational lifting of roots. For example, with the mentioned line of action of the perturbing force the bonds between the root and the soil are broken more effectively (what is known as the loosening effect takes place); furthermore, the build-up of roots and soil in the working channel of the vibrational lifter is significantly reduced. In addition to this, the design of the vibrational lifter that operates on the described principle is less energy- and metal-intensive, etc. However, it will be proved theoretically that even with said line of action of the perturbing force certain deficiencies are observed, contrary to the longitudinal oscillations.

In the development of the theory of the transverse oscillations of the root body, assumptions similar to those stated in [20] are made. For example, in the first instance, it is assumed that the centreline of the root in the unstrained state is strictly rectilinear and coincides with the line of the centroids of the root's cross-sections; at the same time, the deflection of individual points on the root's centreline is vectored at a right angle to its rectilinear unstrained line. Further, it is assumed that the deflections of points on the root's centreline during transverse oscillations are contained in the same plane and are small deflections in the sense that the associated restoring forces remain within the range of proportionality.

First of all, it is necessary to set up the equivalent schematic model with a root that has its bottom point fixed (Figure 4.9).
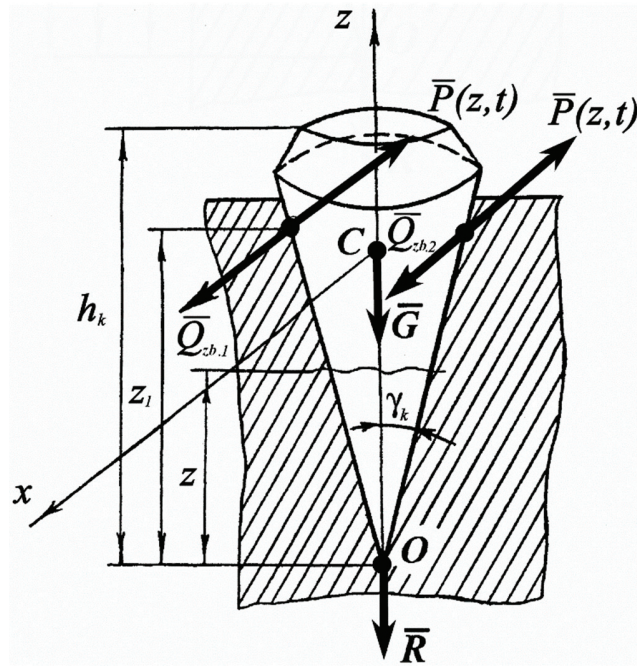
Figure 4.9. Equivalent schematic model of transverse oscillations of root body at the moment when vibrational digging tool grips it.

The root is a cone-shaped solid (its apex angle is equal to $2\gamma_k$, the upper part of it is positioned above the level of the soil surface) modelled as a variable cross-section bar with its lower end fixed (point O). At the same time, the cone is assumed to be cut off at point O. The force of the root's weight $\overline{G}$ is applied at the centre of mass designated as point C. The total length of the root is h_k. The vertical coordinate axis Oz, the origin of which coincides with the conventional point of fixation O, is drawn through the root's symmetry axis. The bonding between the root and the soil is defined by the soil's total reaction $\overline{R}$. The above-mentioned perturbing force is applied to the root simultaneously from the two digging shares on its two sides; therefore, in the schematic model it is represented by the two components $Q_{zb.1}$ and $Q_{zb.2}$. Said forces are applied at a distance of z_1 from the origin of coordinates (point O) and they give rise to the root's transverse oscillations, which break the bonds between the root and the soil and create the conditions for its extraction from the soil.

In the development of the theory of the transverse oscillations of the body of a root fixed in the soil, the Ostrogradsky–Hamilton variation principle will be applied. In this context, it is assumed that the transverse oscillations of the root are generated by the action of a horizontal perturbing force, which varies according to the harmonic law of the following form:

$$Q_{zb.} = H sin\omega t \tag{4.133}$$

where H—amplitude of the perturbing force (m); ω—frequency of the perturbing force (s^{-1}).

Further, it is necessary to set up the Ostrogradsky–Hamilton function that describes the transverse oscillations of the root.

Under the above-listed assumptions, the deflections of the points on the root's centreline during transverse oscillations are uniquely defined by the following function of two variables:

$$y = y(z, t) \tag{4.134}$$

where z—distance from the point on axis Oz, through which the root's cross-section passes, to the conventional point of the root fixation in the soil O (m); t—current time (s).

The following designations are necessary for further considerations:

$\mu(z)$—linear density (mass of a length unit) of the root (kg·m^{-1});

E_1—Young modulus of the material of the root (N·m^{-2});

$J(z)$—moment of inertia of a cross-section of the root about the neutral axis of the cross-section, which is at right angle to the oscillation plane (m^4);

$Q(z, t)$—intensity of the transverse external load vectored at a right angle to the axis of the root (axis Oz) along axis Ox (N·m^{-1}).

According to [20], the Ostrogradsky–Hamilton functional for a variable cross-section bar performing transverse oscillations under the action of an external transverse load is as follows:

$$S = \frac{1}{2} \int_{t_1}^{t_2} \int_0^{h_k} \left[\mu(z) \left(\frac{\partial y}{\partial t} \right)^2 - E_1 J(z) \left(\frac{\partial^2 y}{\partial z^2} \right)^2 + Q(z, t) y \right] dz dt \tag{4.135}$$

Taking into account the fact that the root is modelled by a conically shaped solid, the quantities that enter into (4.135) will be expressed in terms of the main parameters of the conic surface.

Obviously, the linear density of the root can be determined with the use of the following expression:

$$\mu(z) = \rho \pi z^2 tan^2 \gamma_k \tag{4.136}$$

where ρ—specific gravity of the root's material (kg·m^{-3}).

The moment of inertia $J(z)$ is determined as follows:

$$J(z) = \frac{\pi z^4 tan^4 \gamma_k}{4} \tag{4.137}$$

Since the quantity $Q(z, t)$ contained in (4.137) is an intensity of distributed load measured in N·m, the perturbing force $\overline{Q}_{zb.}$ that is a concentrated load measured in newtons (N) also has to have the unit of measurement N·m. For this purpose,

the impulse function of the first-order $\sigma_1(z)$ [20], determined as shown below, is introduced:

$$\sigma_1(z) = \begin{cases} \infty \text{ at} z = 0, \\ 0 \text{ at} z \neq 0, \end{cases}$$

$$\int\limits_0^z \sigma_1(z)dz = \sigma_o(z)$$

where $\sigma_o(z)$—unit function: $\sigma_o(z) = \begin{cases} 0 \text{ at} z < 0, \\ 1 \text{ at} z \geq 0. \end{cases}$

Thus, while $Q_{zb.}(t)$ is a concentrated perturbing force applied at point z_1 and measured in newtons, the function:

$$Q_{zb.}(z,t) = Q_{zb.}(t)\sigma_1(z - z_1) \tag{4.138}$$

has the unit of measurement N·m and expresses the intensity of concentrated load at point z_1. The function $\sigma_1(z - z_1)$ is equal to zero for all values of z except $z = z_1$, where it goes to infinity.

Hence, taking into consideration (4.133), the following can be written down:

$$Q_{zb.}(z,t) = Hsin\omega t\sigma_1(z - z_1) \tag{4.139}$$

As the root at the beginning of the oscillatory process is strongly bonded to the soil, which is an elastic medium, the force of the soil's resistance to the root's transverse oscillations arises, when the perturbing force (4.133) acts on the root. It is obvious that the soil's resistance force (for the whole root body) is a load distributed over the area of contact between the root and the soil. Moreover, it is an external force with respect to the root body and it acts as a perturbing force applied by the soil to the root.

Further, the designation c will denote the coefficient of the soil's elastic deformation (ratio between the first Winckler coefficient and the area of contact) (N/m^3). It is assumed that during transverse oscillations the root rests on the soil with half of its side surface throughout the whole depth of the root in the unbroken soil. The soil that contacts with that half of the side surface generates a distributed load vectored opposite to the perturbing force. Thus, during the transverse oscillations of the root and the digging tool itself, a distributed load arises on one side of the root after the other. Said load is applied to the root by the soil and is vectored opposite to the perturbing force.

Hence, considering the aforesaid information, it is possible to state that to a certain approximation the intensity of the distributed load of the soil's resistance $P(z,t)$ is equal to:

$$P(z,t) = \pi c z \tan\gamma_k \cdot y(z,t) \tag{4.140}$$

Since the perturbing forces applied by the vibrational digging tool and the resisting soil are vectored oppositely to each other, the resulting perturbing force acting on the root is equal to:

$$Q(z,t) = Q_{zb.}(z,t) - P(z,t),$$

or, taking into account (4.139) and (4.140), the following expression is obtained:

$$Q(z,t) = H\sin\omega t \sigma_1(z - z_1) - \pi c z \tan\gamma_k \cdot y(z,t) \tag{4.141}$$

Hence, taking into account (4.136), (4.137) and (4.141), (4.135) will be as follows:

$$S = \frac{1}{2}\int_{t_1}^{t_2}\int_o^{h_k}\left\{\rho\pi z^2\tan^2\gamma_k\left(\frac{\partial y}{\partial t}\right)^2 - E_1\frac{\pi z^4\tan^4\gamma_k}{4}\left(\frac{\partial^2 y}{\partial z^2}\right)^2 + H\sin\omega t\sigma_1(z-z_1)y(z,t) - \pi c z\tan\gamma_k y^2(z,t)\right\}dzdt. \tag{4.142}$$

It is necessary to first analyse the free transverse oscillations of the root fixed in the soil as an elastic solid in an elastic medium.

For this purpose, it is necessary to separate, in (4.142), the part that represents the free oscillations of the system.

Apparently, this functional has the following appearance:

$$S_1 = \frac{1}{2}\int_{t_1}^{t_2}\int_o^{h_k}\left[\rho\pi z^2\tan^2\gamma_k\left(\frac{\partial y}{\partial t}\right)^2\frac{-E_1\pi z^4\tan^4\gamma_k}{4}\left(\frac{\partial^2 y}{\partial z^2}\right)^2 - \pi c z\tan\gamma_k\cdot y^2(z,t)\right]dzdt \tag{4.143}$$

The basis for finding the mode shapes and natural frequencies of the free oscillations of the root in the soil is provided by the general principle of the linear theory of oscillations—i.e., the principle of superposition of small oscillations. Following the mentioned principle, the harmonic transverse oscillations of the following form have to be found:

$$y(z,t) = \phi(z)\sin(pt + \alpha) \tag{4.144}$$

where $\phi(z)$—fundamental mode of oscillations—i.e., the function that defines the continuous set of transverse amplitude (peak) deflections of the root's centreline from its equilibrium position (m); p —natural frequency of the transverse oscillations (s^{-1}).

Further, having initially computed all necessary derivatives of (4.144), (4.144) is substituted into (4.143):

$$\frac{\partial y}{\partial t} = \varphi(z)p\cos(pt + \alpha), \frac{\partial^2 y}{\partial z^2} = \varphi''(z)\sin(pt + \alpha). \tag{4.145}$$

By substituting (4.144) and (4.145) into (4.143), the following is obtained:

$$S_1 = \frac{1}{2}\int_{t_1}^{t_2}\int_0^{h_k}\left\{\rho\pi z^2 tan^2\gamma_k \cdot \varphi^2(z)p^2\cos^2(pt + \alpha) - \frac{E_1\pi z^4 tan^4\gamma_k}{4}\right. \\ \left.[\varphi''(z)]^2\sin^2(pt + \alpha) - \pi cz\tan\gamma_k \cdot \varphi^2(z)\sin^2(pt + \alpha)\right\}dzdt. \tag{4.146}$$

After integrating (4.146) with respect to t over one period $T = \frac{2\pi}{p}$, the result is:

$$S_1 = \frac{\pi}{2p}\int_0^{h_k}\left\{\rho\pi z^2 tan^2\gamma_k \cdot \varphi^2(z)p^2 - \frac{E_1\pi z^4 tan^4\gamma_k}{4}[\varphi''(z)]^2 - \pi cz\tan\gamma_k \cdot \varphi^2(z)\right\}dz \tag{4.147}$$

For finding the modes and frequencies of the free transverse oscillations of the root in the soil, the Ritz method can be applied.

Following the Ritz method, the values of (4.147) are analysed over the set of the linear combinations of functions of the following form:

$$\phi(z) = \sum_{i=1}^{n}\alpha_i\psi_i(z) \tag{4.148}$$

where α_i—parameters, the variation of which allows the obtention of the required class of admissible functions; $\psi_i(z)$—basic functions, which are the specially selected and known functions that meet the geometric conditions of the problem.

Hence, by substituting (4.148) into (4.147), the following is arrived at:

$$S_1 = \frac{\pi}{2p}\int_0^{h_k}\left\{\rho\pi z^2 tan^2\gamma_k\left[\sum_{i=1}^{n}\alpha_i\psi_i(z)\right]^2 p^2 - \frac{E_1\pi z^4 tan^4\gamma_k}{4}\right. \\ \left.\left[\sum_{i=1}^{n}\alpha_i\psi_i''(z)\right]^2 - \pi cz\tan\gamma_k\left[\sum_{i=1}^{n}\alpha_i\psi_i(z)\right]^2\right\}dz. \tag{4.149}$$

Since

$$\left[\sum_{i=1}^{n}\alpha_i\psi_i(z)\right]^2 = \sum_{i,k=1}^{n}\psi_i(z)\psi_k(z)\alpha_i\alpha_k, \tag{4.150}$$

$$\left[\sum_{i=1}^{n}\alpha_i\psi_i''(z)\right]^2 = \sum_{i,k=1}^{n}\psi_i''(z)\psi_k''(z)\alpha_i\alpha_k, \tag{4.151}$$

(4.150) and (4.151) are substituted into (4.149) and the following expression of the functional represented by a quadratic form is obtained:

$$S_1 = \frac{\pi}{2p} \int_0^{h_k} \left[\rho \pi z^2 tan^2 \gamma_k \cdot p^2 \sum_{i,k=1}^n \psi_i(z)\psi_k(z)\alpha_i\alpha_k - \frac{E_1 \pi z^4 tan^4 \gamma_k}{4} \times \right. $$
$$\left. \sum_{i,k=1}^n \psi_i''(z)\psi_k''(z)\alpha_i\alpha_k - \pi c z tan\gamma_k \sum_{i,k=1}^n \psi_i(z)\psi_k(z)\alpha_i\alpha_k \right] dz. \tag{4.152}$$

Further, the following designations are introduced:

$$\int_0^{h_k} \rho \pi z^2 tan^2 \gamma_k \cdot \psi_i(z)\psi_k(z)dz = T_{ik}, \int_0^{h_k} \frac{E_1 \pi z^4 tan^4 \gamma_k}{4} \psi_i''(z)\psi_k''(z)dz $$
$$= U_{ik}, \int_0^{h_k} \pi c z tan\gamma_k \cdot \psi_i(z)\psi_k(z)dz = C_{ik}, (i,k = 1,2,\ldots,n). \tag{4.153}$$

By substituting (4.153) into (4.152), the functional represented by a function of the parameters $\alpha_1, \alpha_2, \ldots, \alpha_n$ is obtained:

$$S_1(\alpha_1, \alpha_2, \ldots, \alpha_n) = \frac{\pi}{2p}p^2 \sum_{i,k=1}^n T_{ik}\alpha_i\alpha_k - \frac{\pi}{2p} \sum_{i,k=1}^n U_{ik}\alpha_i\alpha_k - \frac{\pi}{2p} \sum_{i,k=1}^n C_{ik}\alpha_i\alpha_k \tag{4.154}$$

It is necessary to determine the set of the parameters $\alpha_1, \alpha_2, \ldots, \alpha_n$, at which Functional (4.154) assumes a stationary value. For this purpose, (4.154) has to be differentiated with respect to the parameters $\alpha_i(i = 1,2,\ldots,n)$ and the obtained partial derivatives have to be equal to zero.

This will result in obtaining the following system of linear homogeneous equations in the unknown quantities $\alpha_1, \alpha_2, \ldots, \alpha_n$:

$$\left. \begin{array}{l} \left(p^2 T_{11} - U_{11} - C_{11}\right)\alpha_1 + \left(p^2 T_{12} - U_{12} - C_{12}\right)\alpha_2 + \ldots + \left(p^2 T_{1n} - U_{1n} - C_{1n}\right)\alpha_n = 0, \\ \left(p^2 T_{21} - U_{21} - C_{21}\right)\alpha_1 + \left(p^2 T_{22} - U_{22} - C_{22}\right)\alpha_2 + \ldots + \left(p^2 T_{2n} - U_{2n} - C_{2n}\right)\alpha_n = 0, \\ \ldots\ldots\ldots\ldots\ldots\ldots\ldots\ldots\ldots\ldots\ldots\ldots\ldots\ldots\ldots\ldots\ldots\ldots\ldots\ldots\ldots\ldots \\ \left(p^2 T_{n1} - U_{n1} - C_{n1}\right)\alpha_1 + \left(p^2 T_{n2} - U_{n2} - C_{n2}\right)\alpha_2 + \ldots + \left(p^2 T_{nn} - U_{nn} - C_{nn}\right)\alpha_n = 0. \end{array} \right\} \tag{4.155}$$

where the coefficients $U_{ik}, T_{ik}C_{ik}(i,k = 1,2,\ldots,n)$ are determined in accordance with (4.153).

In order for a nonzero solution of a system of linear homogeneous equations to exist, it is necessary for the determinant of the system to be equal to zero—i.e.,

$$\begin{vmatrix} p^2 T_{11} - U_{11} - C_{11} & p^2 T_{12} - U_{12} - C_{12} & \ldots & p^2 T_{1n} - U_{1n} - C_{1n} \\ p^2 T_{21} - U_{21} - C_{21} & p^2 T_{22} - U_{22} - C_{22} & \ldots & p^2 T_{2n} - U_{2n} - C_{2n} \\ \ldots\ldots\ldots\ldots\ldots\ldots\ldots\ldots\ldots\ldots\ldots\ldots\ldots\ldots\ldots\ldots \\ p^2 T_{n1} - U_{n1} - C_{n1} & p^2 T_{n2} - U_{n2} - C_{n2} & \ldots & p^2 T_{nn} - U_{nn} - C_{nn} \end{vmatrix} = 0 \tag{4.156}$$

(4.156), in which the coefficients $U_{ik}, T_{ik}C_{ik}(i,k = 1,2,\ldots,n)$ are determined in accordance with (4.153), is the Ritz equation of frequencies for the transverse oscillations of the root fixed in the soil. Since (4.153) is an equation of the n-th degree

in p^2, its solution specifies a sequence of natural frequencies: $p_1^2 < p_2^2 < \ldots < p_n^2$, where $p_1, p_2, \ldots, p_n$—first, second, ... n-th natural frequency, respectively.

In practice, only the lowest frequencies, which have the most substantial effect on the work process under consideration, are generally determined. Therefore, the first two frequencies of the free transverse oscillations of the root body will be analysed.

For this purpose, it is necessary to select the basic functions contained in (4.148).

As has been pointed out in [20], in many cases the required results are obtained by taking the mode shapes of transverse oscillations of a homogeneous bar with a uniform stiffness of $E_1 J$ under the same fixation conditions as in the problem under consideration as the basic functions. Such basic functions make it possible to find the shapes that not only meet the geometric conditions as required by the Ritz method, but the dynamic boundary conditions of the problem as well.

Therefore, the mode shapes of transverse oscillations of a homogeneous bar with uniform stiffness of $E_1 J$ and linear density μ are taken as the basic functions.

In accordance with [20], such shapes appear as follows:

$$\psi_i(z) = \left[U(k_i z) - \frac{S(k_i h_k)}{T(k_i h_k)} V(k_i z) \right] \tag{4.157}$$

where $U(z), S(z), T(z), V(z)$—Krylov functions, while:

$$U(z) = \tfrac{1}{2}(chkz - coskz), S(z) = \tfrac{1}{2}(chkz + coskz), T(z) = \tfrac{1}{2}(shkz + sinkz), V(z) = \tfrac{1}{2}(shkz - sinkz), \tag{4.158}$$

$k_i h_k$—roots of the following equation:

$$chkh_k coskh_k + 1 = 0 \text{First two roots } [20] = k_1 h_k = 1875; k_2 h_k = 4694 \tag{4.159}$$

It ought to be noted that the basic functions selected in this way meet the geometric and dynamic boundary conditions of the problem:

$$y(0) = y'(0) = 0, y''(h_k) = y'''(h_k) = 0. \tag{4.160}$$

Further, by substituting (4.157) into (4.153), the following is obtained:

$$T_{ik} = \rho \pi tan^2 \gamma_k \int_0^{h_k} \left[U(k_i z) - \frac{S(k_i h_k)}{T(k_i h_k)} V(k_i z) \right] \left[U(k_k z) - \frac{S(k_k h_k)}{T(k_k h_k)} V(k_k z) \right] z^2 dz \tag{4.161}$$
$$i, k = 1, 2, \ldots, n$$

$$U_{ik} = \frac{\pi E_1 tan^4 \gamma_k}{4} \int_0^{h_k} k_i^2 k_k^2 \left[S(k_i z) - \frac{S(k_i h_k)}{T(k_i h_k)} T(k_i z) \right] \left[S(k_k z) - \frac{S(k_k h_k)}{T(k_k h_k)} T(k_k z) \right] z^4 dz \tag{4.162}$$
$$i, k = 1, 2, \ldots, n$$

$$C_{ik} = c\pi tan\gamma_k \int_0^{h_k} \left[U(k_iz) - \frac{S(k_ih_k)}{T(k_ih_k)} V(k_iz) \right] \left[U(k_kz) - \frac{S(k_kh_k)}{T(k_kh_k)} V(k_kz) \right] zdz \quad (4.163)$$

As can be concluded from (4.161), (4.162) and (4.163), $T_{ik} = T_{ki}, U_{ik} = U_{ki}, C_{ik} = C_{ki}$.

Hence, for determining the first two frequencies it is necessary to compute the values of the coefficients $T_{11}, T_{12}, T_{22}. , U_{11}, U_{12}, U_{22}, C_{11}, C_{12}, C_{22}$ in accordance with (4.161)–(4.163), where the Krylov functions $S(k_ih_k), T(k_ih_k)$ are to be computed at the above-stated values of k_ih_k,. Obviously, the computation of the coefficients T_{ik}, U_{ik}, C_{ik} has to be carried out with the use of a PC. The obtained values of the coefficients T_{ik}, U_{ik}, C_{ik} are substituted into the Ritz equation of frequencies (4.156) at $n = 2$ (determinant of second order), which is used for determining the natural frequencies p_1, p_2 of the transverse oscillations of the root.

On the basis of the developed theory, the algorithm of computation of the natural frequencies of the transverse oscillations of the root as an elastic solid fixed in the soil can be developed.

1. The data needed for the calculation are set in accordance with [7]: length of the root $h_k = 0.25$ m; elastic modulus of the root body $E_1 = 18.4 \cdot 10^6$ N·m^{-2}; specific gravity of the root's material $\rho = 750$ kg·m^{-3}; angle of taper of the root $\gamma_k = 14°$; parameters for the calculation of frequencies (for the first two frequencies: $k_1 = 7.50$ m^{-1}, $k_2 = 18.78$ m^{-1}, [20]).

2. The Krylov functions $U(z), S(z), T(z), V(z)$ are set in accordance with (4.158).

3. The coefficients T_{ik}, U_{ik}, C_{ik} are calculated in accordance with (4.161), (4.162), (4.163), respectively; $i, k = 1, 2, \ldots, n, T_{ik} = T_{ki}, U_{ik} = U_{ki}, C_{ik} = C_{ki}$. (For the first two frequencies: $i, k = 1, 2$.)

4. The Ritz equation of frequencies is generated in accordance with (4.156). (For the first two frequencies, it is a determinant of second order, $n = 2$).

5. The Ritz equation of frequencies is solved in the MathCad environment. Implementing the described algorithm for the above-stated data, the values of the first and second frequencies of the natural transverse oscillations of the root body fixed in the soil are computed as a function of the soil's elastic deformation coefficient c. The following range is assumed: $c = 0\ 20 \cdot 10^5$ N·m^{-3}.

The results of the calculations are presented in Table 4.2.

On the basis of the obtained computation results, the graphs of the first and second frequencies as functions of the soil's elastic deformation coefficient c have been plotted (Figures 4.10 and 4.11).

As can be seen in the presented graph (Figure 4.10), when the value of the soil's elastic deformation coefficient c changes within the range of $c = 0 \sim 2 \cdot 10^6$ N·m^{-3}, the value of the first circular frequency monotonically increases within the range of $p_1 = 35.6 \sim 226.5$ s^{-1}, or 5.7–36.0 Hz. Hence, the first frequency of the

free transverse oscillations of the root body increases significantly together with the increase in the coefficient of elastic deformation of the soil c.

Table 4.2. Values of first and second natural frequencies of transverse oscillations of root body.

Elastic Deformation Coefficient of Soil, c (N·m^{-3})	First Circular Frequency of Oscillation, p_1 (s^{-1})	First Frequency of Oscillation p_1 (Hz)	Second Circular Frequency of Oscillation p_2 (s^{-1})	Second Frequency of Oscillation p_2 (Hz)
0	35.644	5.673	1744	277.566
2×10^5	79.217	12.608	1746	277.885
4×10^5	106.205	16.903	1748	278.203
6×10^5	127.605	20.309	1750	278.521
8×10^5	145.897	23.22	1752	278.839
10×10^5	162.136	25.805	1754	279.158
12×10^5	176.889	28.153	1756	279.476
14×10^5	190.501	30.319	1758	279.794
16×10^5	203.202	32.341	1760	280.113
18×10^5	215.152	34.243	1762	280.431
20×10^5	226.472	36.044	1764	280.749
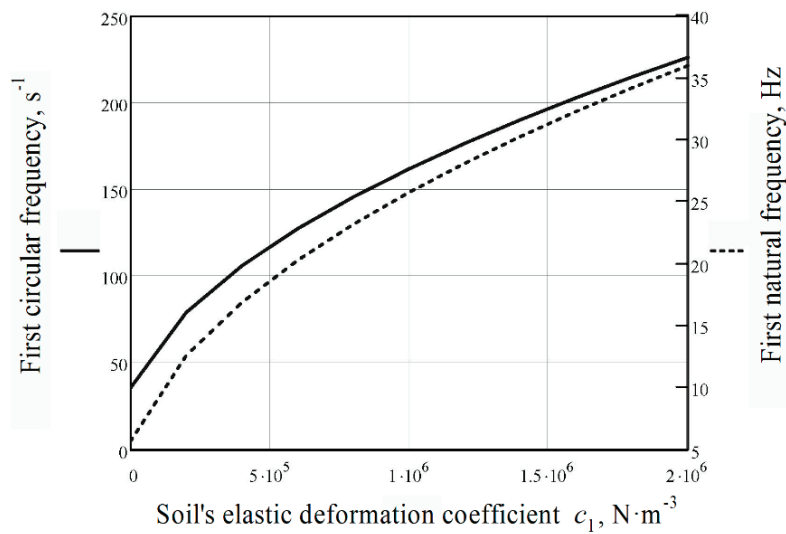
Figure 4.10. Relation between first natural frequency of transverse oscillations of root body and soil's elastic deformation coefficient c.
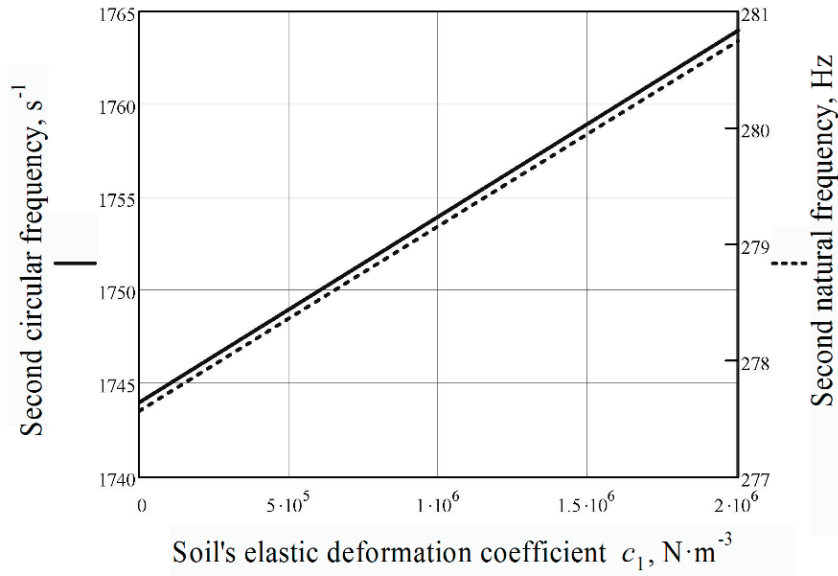
Figure 4.11. Relation between second natural frequency of transverse oscillations of root body and soil's elastic deformation coefficient c.

It can be seen in the graph (Figure 4.11) that the second frequency of the free transverse oscillations changes insignificantly, when the soil's elastic deformation coefficient c changes within the range of $c = 0 \sim 2 \cdot 10^6$ N·m^{-3}: respectively, the circular frequency varies within $p_2 = 1744 \sim 1764$ s^{-1}, or 277.6–280.7 Hz.

The obtained calculated value of the first frequency is in agreement with the experimental data presented in [20]. Such a frequency allows for the intensive breaking of the bonds between the root and the soil and the active shaking off of the soil from the surface of the root.

The method that has been worked out facilitates finding any frequencies of the free transverse oscillations of the root as an elastic solid in an elastic medium.

4.2.2. Forced Transverse Oscillations of the Root as Elastic Solid Fixed in Soil

The next step is to investigate the forced transverse oscillations of the root body fixed in the soil. Since the perturbing force acts on the root at a frequency of ω, the purely forced oscillations take place under the following law [20]:

$$y(z,t) = \varphi(z)\sin\omega t \tag{4.164}$$

where $\phi(z)$—shape of the forced oscillations.

The necessary partial derivatives of (4.164) are computed as follows:

$$\frac{\partial y}{\partial t} = \omega\phi(z)\cos\omega t, \quad \frac{\partial^2 y}{\partial z^2} = \phi''(z)\sin\omega t. \tag{4.165}$$

By substituting (4.164) and (4.165) into (4.142), the following is obtained:

$$S = \frac{1}{2} \int_{t_1}^{t_2} \int_0^{h_k} \Big\{ \rho \pi z^2 tan^2 \gamma_k \cdot \omega^2 \varphi^2(z) cos^2 \omega t - \frac{E_1 \pi z^4 tan^4 \gamma_k}{4} \Big.$$
$$\Big. [\varphi''(z)]^2 sin^2 \omega t + H\sigma_1(z - z_1)\varphi(z) sin^2 \omega t - \pi cz tan \gamma_k \cdot \varphi^2(z) sin^2 \omega t \Big\} dz dt. \tag{4.166}$$

After integrating (4.166) with respect to z over one period $T = \frac{2\pi}{\omega}$, the result is:

$$S = \frac{\pi}{2\omega} \int_0^{h_k} \Big\{ \rho \pi z^2 tan^2 \gamma_k \cdot \varphi^2(z) \omega^2 - \frac{E_1 \pi z^4 tan^4 \gamma_k}{4} \Big.$$
$$\Big. [\varphi''(z)]^2 + H\sigma_1(z - z_1)\varphi(z) - \pi cz tan \gamma_k \cdot \varphi^2(z) \Big\} dz. \tag{4.167}$$

In accordance with the Ritz method, the values of (4.166) are analysed over the set of linear combinations of the following form:

$$\phi(z) = \alpha \psi(z) \tag{4.168}$$

where α—parameter to be found, the variation of which allows the obtention of the class of admissible functions; $\psi(z)$—basic function.

(4.168) will be inserted into (4.167) and we will obtain:

$$S = \frac{\pi}{2\omega} \int_0^{h_k} \Big\{ \rho \pi z^2 tan^2 \gamma_k \cdot \alpha^2 \psi^2(z) \omega^2 \Big.$$
$$\Big. - \frac{E_1 \pi z^4 tan^4 \gamma_k}{4} \alpha^2 [\psi''(z)]^2 + H\sigma_1(z - z_1)\alpha\psi(z) - \pi cz tan \gamma_k \cdot \alpha^2 \psi^2(z) \Big\} dz. \tag{4.169}$$

The following symbols will now be entered:

$$\int_0^{h_k} \rho \pi z^2 tan^2 \gamma_k \cdot \psi^2(z) dz = M \tag{4.170}$$

$$\int_0^{h_k} \frac{E_1 \pi z^4 tan^4 \gamma_k}{4} [\psi''(z)]^2 dz = N \tag{4.171}$$

$$\int_0^{h_k} \pi cz tan \gamma_k \psi^2(z) dz = R \tag{4.172}$$

$$\int_0^{h_k} H\sigma_1(z - z_1)\psi(z) dz = L \tag{4.173}$$

(4.170)–(4.173) will now be inserted into (4.169), and we will have:

$$S = \frac{\pi}{2\omega} \Big(\omega^2 M \alpha^2 - (N + R)\alpha^2 + L\alpha \Big) \tag{4.174}$$

Hence, over the set of functions (4.168), (4.169) becomes a function of the independent variable α.

The necessary condition of existence of an extremum of (4.174) is its first-order derivative with respect to α being equal to zero.

Differentiating (4.174) with respect to α and equating the obtained derivative to zero, the following equation is arrived at:

$$2\omega^2 M\alpha - 2(N+R)\alpha + L = 0 \qquad (4.175)$$

from which parameter α can be determined; the result is:

$$\alpha = \frac{L}{2(N+R-\omega^2 M)} \qquad (4.176)$$

Further, the shape of the forced transverse oscillations of a homogeneous bar with a uniform stiffness of $E_1 J$ and one end rigidly fixed that are generated by the action of a transverse harmonic unit force at a frequency of ω, with said force being applied at the point $z = z_1$, is taken as the basic function $\psi(z)$. In accordance with [20], said shape appears as follows:

$$\psi(z) = CU(kz) + DV(kz), \qquad 0 \le z < z_1 \qquad (4.177)$$

$$\psi(z) = CU(kz) + DV(kz) + \frac{1}{k^3 E_1 J} V[k(z-z_1)], \qquad z_1 \le z \le h_k, \qquad (4.178)$$

where $U(kz), V(kz)$—Krylov functions; $k = \sqrt[4]{\frac{\mu\omega^2}{E_1 J}}$; μ—linear density of the bar; C, D—arbitrary constants determined on the basis of the boundary conditions (4.160).

It ought to be noted that the values of the function $\psi(z)$ at the point $z = z_1$ computed with the use of (4.177) and (4.178) are identical and equal to: $\psi(z_1) = CU(kz_1) + DV(kz_1)$.

As the following boundary conditions are observed at the free end of the bar $z = h_k$: $y''(h_k) = 0, y'''(h_k) = 0$, the second and third derivatives of (4.178) with respect to z can be obtained as follows:

$$\begin{aligned}
\psi''(z) &= Ck^2 S(kz) + Dk^2 T(kz) + \frac{1}{k^3 E_1 J}k^2 T[k(z-z_1)], z_1 \le z \le h_k, \\
\psi'''(z) &= Ck^3 V(kz) + Dk^3 S(kz) + \frac{1}{k^3 E_1 J}k^3 S[k(z-z_1)], z_1 \le z \le h_k.
\end{aligned} \qquad (4.178')$$

Taking into account the boundary conditions at the free end of the bar $(z = h_k)$, the following system of equations with respect to the unknowns $\psi(z), C, D$ is arrived at:

$$\left.\begin{aligned}
-\psi(z) + CU(kz) + DV(kz) &= \begin{cases} 0, 0 \le z \le z_1, \\ -\frac{1}{k^3 E_1 J}V[k(z-z_1)], z_1 \le z \le h_k, \end{cases} \\
CS(kh_k) + DT(kh_k) &= \frac{-1}{k^3 E_1 J}T[k(h_k-z_1)], \\
CV(kh_k) + DS(kh_k) &= \frac{-1}{k^3 E_1 J}S[k(h_k-z_1)].
\end{aligned}\right\} \qquad (4.179)$$

The determinant of the system appears as follows:

$$\Delta = \begin{vmatrix} -1 & U(kz) & V(kz) \\ 0 & S(kh_k) & T(kh_k) \\ 0 & V(kh_k) & S(kh_k) \end{vmatrix}.$$ (4.179')

Expanding said determinant along the first column, the following is obtained:

$$\Delta = T(kh_k)V(kh_k) - S^2(kh_k) = \frac{-1}{2}(1 + chkh_k coskh_k)$$ (4.180)

From (4.179), $\psi(z)$ can be found:

$$\psi(z) = \frac{-1}{\Delta k^3 E_1 J} \begin{vmatrix} 0 & U(kz) & V(kz) \\ T[k(h_k - z_1)] & S(kh_k) & T(kh_k) \\ S[k(h_k - z_1)] & V(kh_k) & S(kh_k) \end{vmatrix}, 0 \le z \le z_1,$$

$$\psi(z) = \frac{-1}{\Delta k^3 E_1 J} \begin{vmatrix} V[k(z - z_1)] & U(kz) & V(kz) \\ T[k(h_k - z_1)] & S(kh_k) & T(kh_k) \\ S[k(h_k - z_1)] & V(kh_k) & S(kh_k) \end{vmatrix}, z_1 \le z \le h_k.$$ (4.181)

Opening the determinant found above, we obtain:

$$\psi(z) = \frac{U(kz)}{\Delta k^3 E_1 J}\{T[k(h_k - z_1)]S(kh_k) - T(kh_k)S[k(h_k - z_1)]\}$$
$$-\frac{V(kz)}{\Delta k^3 E_1 J}\{T[k(h_k - z_1)]V(kh_k) - S[k(h_k - z_1)]S(kh_k)\}, 0 \le z \le z_1,$$ (4.181')

$$\psi(z) = -\frac{V[k(z - z_1)]}{\Delta k^3 E_1 J}\{S^2(kh_k) - T(kh_k)V(kh_k)\}$$
$$+\frac{U(kz)}{\Delta k^3 E_1 J}\{T[k(h_k - z_1)]S(kh_k) - T(kh_k)S[k(h_k - z_1)]\}$$ (4.182)
$$-\frac{V(kz)}{\Delta k^3 E_1 J}\{T[k(h_k - z_1)]V(kh_k) - S[k(h_k - z_1)]S(kh_k)\}, z_1 \le z \le h_k$$

The following symbols will now be entered:

$$\frac{T[k(h_k - z_1)]S(kh_k) - T(kh_k)S[k(h_k - z_1)]}{\Delta k^3 E_1 J} = B$$ (4.183)

$$\frac{T[k(h_k - z_1)]V(kh_k) - S[k(h_k - z_1)]S(kh_k)}{\Delta k^3 E_1 J} = G$$ (4.184)

$$\frac{S^2(kh_k) - T(kh_k)V(kh_k)}{\Delta k^3 E_1 J} = K$$ (4.185)

(4.183), (4.184), and (4.185) will now be inserted into (4.181) and (4.182), and we will have:

$$\psi(z) = BU(kz) - GV(kz), 0 \le z \le z_1$$ (4.186)

$$\psi(z) \;=\; -KV[k(z-z_1)] + BU(kz) - GV(kz), z_1 \le z \le h_k \tag{4.187}$$

Further, the coefficients M, N, R, L that enter into (4.174) are determined.

By substituting (4.186) and (4.187) into (4.170), the value of the coefficient M can be found:

$$
\begin{aligned}
M \;=\; & \rho\pi \tan^2 \gamma_K \int_0^{Z_1} \left[BU(kz) - GV(kz)^2 \right] z^2 dz \\
& + \rho\pi \tan^2 \gamma_K \int_{Z_1}^{h_k} \{ -KV[k(z-z_1)] + BU(kz) - GV(kz) \}^2 z^2 dz.
\end{aligned}
\tag{4.188}
$$

In order to determine the coefficient N, the second derivatives of (4.186) and (4.187) have to be found.

$$\psi''(z) \;=\; Bk^2 S(kz) - Gk^2 T(kz), 0 \le z \le z_1 \tag{4.189}$$

$$\psi''(z) \;=\; -Kk^2 T[k(z-z_1)] + Bk^2 S(kz) - Gk^2 T(kz), z_1 < z \le h_k \tag{4.190}$$

By substituting (4.189) and (4.190) into (4.171), the value of the coefficient N is found:

$$
\begin{aligned}
N \;=\; & \frac{E_1 \pi \tan^4 \gamma_K}{4} \int_0^{Z_1} k^4 [BS(kz) - GT(kz)]^2 z^4 dz \\
& + \frac{E_1 \pi \tan^4 \gamma_K}{4} \int_{Z_1}^{h_k} k^4 \{ -KT[k(z-z_1)] + BS(kz) - GT(kz) \}^2 z^4 dz.
\end{aligned}
\tag{4.191}
$$

By substituting (4.186) and (4.187) into (4.172), the value of the coefficient R is obtained:

$$
\begin{aligned}
R \;=\; & c\pi \tan \gamma_K \int_0^{Z_1} \left[BU(kz) - GV(kz)^2 \right] z dz \\
& + c\pi \tan \gamma_K \int_{Z_1}^{h_k} \{ -KV[k(z-z_1)] + BU(kz) - GV(kz) \}^2 z dz.
\end{aligned}
\tag{4.192}
$$

The value of the coefficient L will be obtained by substituting (4.184) and (4.185) into (4.173):

$$
\begin{aligned}
L \;=\; & \int_0^{Z_1} H\sigma_1 (z - z_1) [BU(kz) - GV(kz)] dz \\
& + \int_{Z_1}^{h_k} H\sigma_1 (z - z_1) \{ -KV[k(z-z_1)] + BU(kz) - GV(kz) \} dz.
\end{aligned}
\tag{4.193}
$$

The computation of the coefficients M, N and R can be performed with the use of a PC or by direct integration with the Krylov functions, or, after the conversion into elementary functions, with the use of (4.158).

Since (4.193) for finding the coefficient L contains the impulse function $\sigma_1(z - z_1)$, which does not belong to classical functions, the integrals contained in said expression and containing the impulse function will be computed analytically.

First, the following integral is analysed: $\int_0^{z_1} H\sigma_1(z - z_1)[BU(kz) - GV(kz)]dz$.

Considering the definition and properties of the function $\sigma_1(z - z_1)$, the following can be written:

$$\int_0^{z_1} H\sigma_1(z - z_1)[BU(kz) - GV(kz)]dz$$

$$= \lim_{\substack{\varepsilon \to 0 \\ \varepsilon > 0}} \int_0^{z_1-\varepsilon} H\sigma_1(z - z_1)[BU(kz) - GV(kz)]dz$$

$$+ \lim_{\substack{\varepsilon \to 0 \\ \varepsilon > 0}} \int_{z_1-\varepsilon}^{z_1+\varepsilon} H\sigma_1(z - z_1)[BU(kz) - GV(kz)]dz \qquad (4.194)$$

$$= 0 + H[BU(kz_1) - GV(kz_1)] \lim_{\substack{\varepsilon \to 0 \\ \varepsilon > 0}} \int_{z_1-\varepsilon}^{z_1+\varepsilon} \sigma_1(z - z_1)dz.$$

$$\lim_{\substack{\varepsilon \to 0 \\ \varepsilon > 0}} \int_{z_1-\varepsilon}^{z_1+\varepsilon} \sigma_1(z - z_1)dz = 1$$

$$\int_0^{z_1} H\sigma_1(z - z_1)[BU(kz) - GV(kz)]dz = H[BU(kz_1) - GV(kz_1)]$$

It ought to be noted that over the intervals, the function $\psi(z)$ has different analytic expressions ((4.186) and (4.187), respectively); nevertheless, in the case of $\varepsilon \to 0$ the limits of said expressions are identical and equal to $\psi(z_1) = BU(kz_1) - GV(kz_1)$ so, when the limit in (4.194) is integrated, any of the mentioned expressions can be selected for the function $\psi(z)$—for example, (4.186)

Further, the next integral of (4.193) is computed:

$$\int_{z_1}^{h_k} H\sigma_1(z - z_1)\{-KV[k(z - z_1)] + BU(kz) - GV(kz)\}dz$$

$$\lim_{\substack{\varepsilon \to 0 \\ \varepsilon > 0}} \int_{z_1+\varepsilon}^{h_k} H\sigma_1(z-z_1)\{-KV[k(z-z_1)] + BU(kz) - GV(kz)\}dz = 0, \quad (4.195)$$

since the following is true over the interval $\sigma_1(z-z_1) = 0$.

By substituting the values of (4.193) and (4.195) into (4.193), the following is obtained:

$$L = H[BU(kz_1) - GV(kz_1)] \quad (4.196)$$

By substituting (4.188), (4.191), (4.192) and (4.196) into (4.176), the necessary value of the parameter α, at which (4.167) has a stationary value, is found. Hence, taking into account (4.168), (4.186) and (4.187), the expressions for the shape of the forced transverse oscillations of a root body fixed in the soil are obtained.

Said expressions appear as follows:

$$\begin{aligned} \phi(z) &= \alpha[BU(kz) - GV(kz)], \ 0 \le z \le z_1, \\ \phi(z) &= \alpha\{-KV[k(z-z_1)] + BU(kz) - GV(kz)\}, z_1 \le z \le h_k \end{aligned} \quad (4.197)$$

where α is determined in accordance with (4.174).

By substituting (4.197) into (4.164), the law of the forced transverse oscillations of a root body fixed in the soil is finally arrived at:

$$\begin{aligned} \phi(z) &= \alpha[BU(kz) - GV(kz)]sin\omega t, \ 0 \le z \le z_1, \\ \phi(z) &= \alpha\{-KV[k(z-z_1)] + BU(kz) - GV(kz)\}sin\omega t, z_1 \le z \le h_k \end{aligned} \quad (4.198)$$

Further, some of the quantities contained in the expressions obtained above need to be determined and will be given detailed consideration.

Since the shapes of the forced transverse oscillations of the bar with a uniform stiffness of $E_1 J$ have been taken as the basic functions, it is necessary to determine the mentioned quantity. Apparently, the cylinder-shaped bar is an example of the bar with a uniform stiffness in the case of $E_1 = const$. Therefore, it is assumed that the mentioned bar has a shape of the cylinder of revolution, which has an axial moment of inertia of cross-section equal to:

$$J = \frac{\pi r_{cm.}^4}{4} \quad (4.199)$$

where $r_{cm.}$—radius of the bar (m).

It is also assumed that the mass of the bar is equal to that of the root. Additionally, assuming that the specific gravity of the bar's material is equal to the density of the root ρ, the bar and the root with the same mass must have the same volume. Another assumption is that the bar and the root have the same length equal to h_k.

Since the root can be represented by a right circular cone and the bar—by a cylinder of revolution—the following relation between their volumes can be observed:

$$\frac{1}{3}\pi r_k^2 h_k = \pi r_{cm.}^2 h_k, \tag{4.200}$$

where r_k—radius of the root (of the cone base) (m).

It can be found from the latter relation that: $r_{cm.} = \frac{r_k}{\sqrt{3}}$.

Then, given the (4.199), the following is obtained: $J = \frac{\pi r_k^4}{36}$.

Further, it is assumed that the Young modulus of the bar's material is the same as the Young modulus of the root and is equal to E.

Hence, the stiffness of the bar is equal to:

$$E_1 J = \frac{\pi r_k^4 E}{36} \tag{4.201}$$

or, given the $r_k = h_k tan\gamma_k$, we will finally have:

$$E_1 J = \frac{\pi h_k^4 tan^4 \gamma_k E}{36} \tag{4.202}$$

The linear density μ of the bar is determined as follows. By reason of the assumption that the masses of the bar and the root are equal, the mass m of the bar is found: $m = \frac{1}{3}\pi r_k^2 h_k \rho$; in this case, $\mu = \frac{m}{h_k} = \frac{1}{3}\pi r_k^2 \rho$, or $\mu = \frac{1}{3}\pi h_k^2 tan^2 \gamma_k \cdot \rho$.

After it becomes possible to determine the quantity k, which is equal to:

$$k = \sqrt[4]{\frac{\mu \omega^2}{E_1 J}} \tag{4.203}$$

Based on the results of the above-stated theoretical investigation of the forced transverse oscillations of the root body, an algorithm of PC-assisted computation of said oscillations can be generated.

The algorithm comprises the following stages:

Reference data required for the computation—specifically, the length of root h_k, its angle of taper γ_k, Young modulus E_1, specific gravity ρ, amplitude of perturbing force H, frequency of perturbing force ω, soil's elastic deformation coefficient c, and coordinate of point of gripping z_1—are set.

Quantity $E_1 J$ is computed in accordance with (4.202).

Quantity k is computed in accordance with (4.203).

Determinant Δ is found to be in accordance with (4.180).

Coefficients B, G, K are computed in accordance with (4.183), (4.184), and (4.185), respectively.

Coefficients M, N, R, L are determined in accordance with Expressions (4.188), (4.191), (4.192), and (4.197), respectively.

Parameter α is computed in accordance with (4.176).

Shape (amplitude) of forced transverse oscillations is in accordance with (4.197) for a number of root body cross-sections (for a number of values of z).

An example of the PC-assisted computation of the amplitude of forced transverse oscillations of a root body fixed in the soil as a function of the surrounding soil's elastic deformation coefficient c and the distance of the root's cross-section from the conventional point of fixation is presented below.

The assumed reference data have been the same as in the computation of free transverse oscillations of a root body fixed in the soil.

The computation has been carried out in the Mathcad environment on the basis of the algorithm developed above. As a result, the following graphs have been obtained (Figure 4.12).

(a) (b)
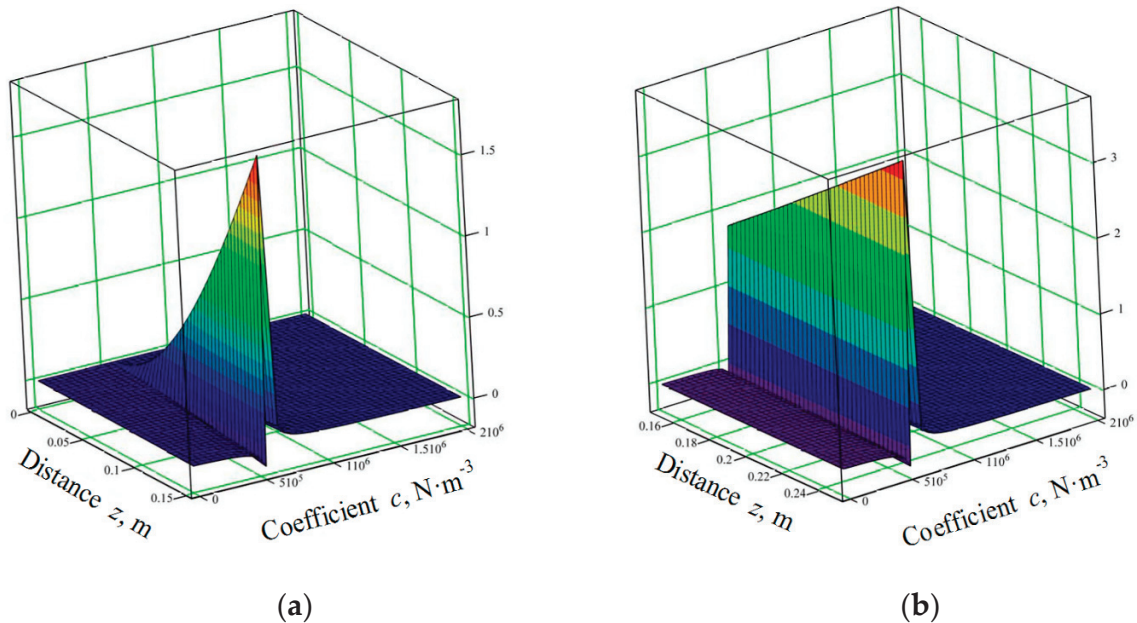
Figure 4.12. Relation between amplitude of forced transverse oscillations of root body and elastic deformation coefficient of soil c and distance from root's cross-section to conventional point of fixation z: (a) $z = 0 \sim 0.15$ m; (b) $z = 0.15 \sim 0.25$ m; (amplitude of perturbing force $N = 500$ N, frequency of perturbing force $\nu = 20$ Hz).

As is seen from the presented graphs (Figure 4.12), the amplitude of the forced transverse oscillation of the root body sharply rises at $c = 5.5 \cdot 10^5 \sim 6.0 \cdot 10^5$ N·m^{-3}. These are the values of the soil's elastic deformation coefficient c, at which the first frequency of the root's free oscillations is in the neighbourhood of $p_1 = 20$ Hz (Figure 4.10).

Hence, the resonance is observed within the mentioned range of values of the soil's elastic deformation coefficient c and at the frequency of forced oscillations $v = 20$ Hz; therefore, the amplitude in this case can reach values in excess of 0.3 m. This, certainly, will result in the breaking of the root; moreover, as is seen from the graphs (Figure 4.12), within the resonance state limits the amplitude sharply rises as the cross-section is removed farther from the conventional point of fixation, especially in the case of the cross-sections located below the point of gripping (Figure 4.12a). At all other values of the soil's elastic deformation coefficient c, the amplitude depends little on the distance from root's cross-section to the conventional point of the root's fixation in the soil.

In Figure 4.13, the graphs depicting the relations between the amplitude of forced transverse oscillations of the root body and the soil's elastic deformation coefficient c at various frequencies of the perturbing force v are shown.

As is seen from the presented graphs, when the frequency of the perturbing force rises, the resonance range shifts to the right:

at $v = 10$ Hz, resonance is observed at $c = 1.5 \cdot 10^5 – 1.7 \cdot 10^5$ N·m^{-3};
at $v = 15$ Hz, resonance is observed at $c = 3.0 \cdot 10^5 – 3.5 \cdot 10^5$ N·m^{-3};
at $v = 20$ Hz, resonance is observed at $c = 5.5 \cdot 10^5 – 6.0 \cdot 10^5$ N·m^{-3}.

According to the obtained results, the amplitude of forced oscillations of the root body exceeds 20 mm at the following values of the soil's elastic deformation coefficient c:

at $v = 10$ Hz—$c = 0 – 4.5 \cdot 10^5$ N·m^{-3};
at $v = 15$ Hz—$c = 0.5 \cdot 10^5 – 6.0 \cdot 10^5$ N·m^{-3};
at $v = 20$ Hz—$c = 3.0 \cdot 10^5 – 8.5 \cdot 10^5$ N·m^{-3}.

Thus, in the instances when the perturbing force acts at right angle to the root's centreline, the breaking of the root can take place at certain frequencies of the perturbing force and value of elastic deformation coefficient of the soil c, which is different in the case of the vertical perturbing force, under the action of which the root can be stretched by no more than 1.7 mm (Figures 4.4–4.8). The natural frequencies of longitudinal oscillations of a root body fall within the range of 76.4–93.4 Hz, while the frequency of the perturbing force does not exceed 20 Hz; hence, the resonance is impossible. The final conclusion is that the designs of vibrational digging tools have to allow the generation of a vertical perturbing force and not a horizontal one.

(**a**)

(**b**)
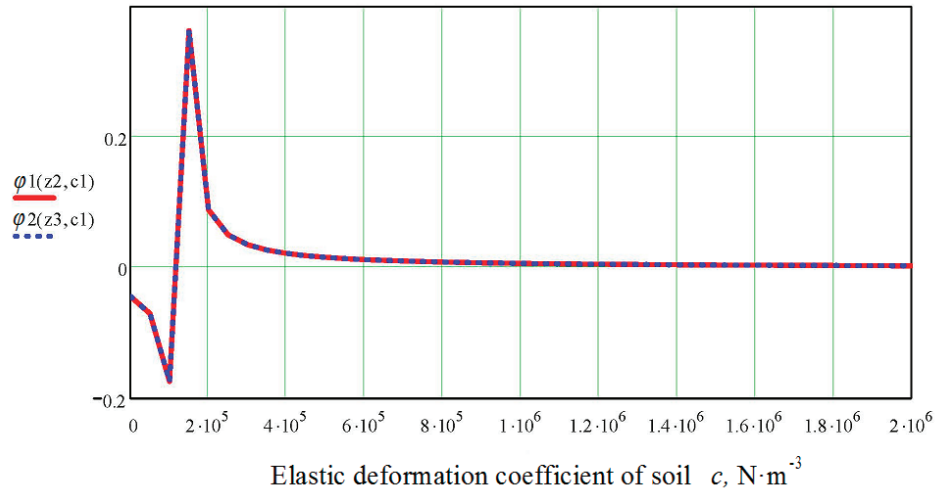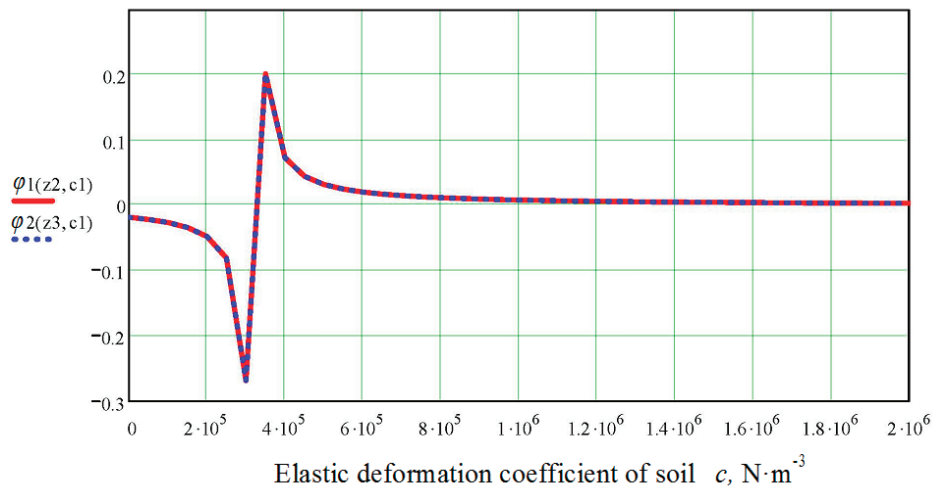
Figure 4.13. *Cont.*
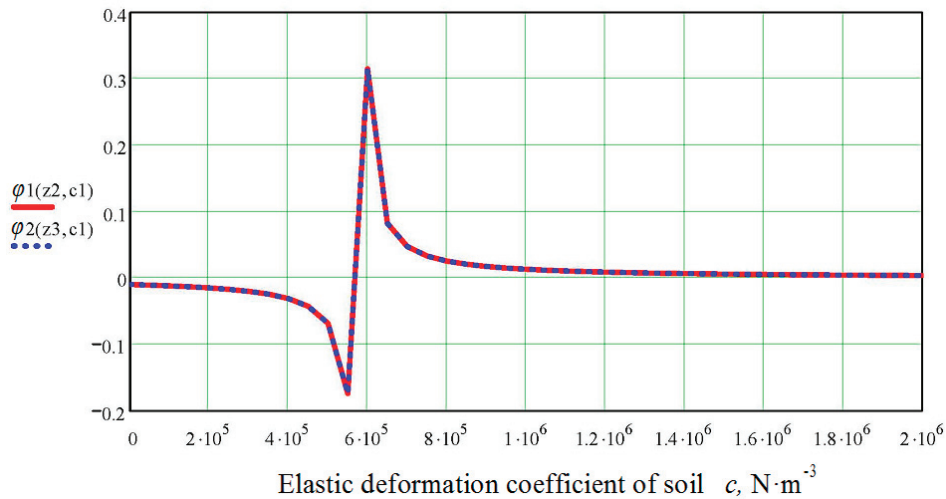
Figure 4.13. Relation between amplitude of forced transverse oscillations of root body and elastic deformation coefficient of soil c and perturbing force frequency v for root's cross-section at point of gripping ($z = z_1 = 0.15$ m): (a) $v = 10$ Hz; (b) $v = 15$ Hz; (c) $v = 20$ Hz (perturbing force amplitude $N = 500$ N).

4.3. Conclusions

1. The presented theory has been developed with regard to longitudinal oscillations of the root of sugar beet as a body attached in the soil as an elastic body in an elastic environment that emerges under the action of the vertical disturbing force that changes according to the harmonic law. The Hamilton–Ostrogradsky variational principle of stationary action is used for longitudinal oscillations of the root taking into account the physical and mechanical properties of the root of sugar beet as an elastic body and the surrounding soil. Using the Ritz direct variational method, the Ritz frequencies equation has been obtained, from which different frequencies of free longitudinal oscillations of the root as an elastic body are determined. This, for example, allowed the obtention of the analytical expression for calculation of the first natural frequency depending on the physical and mechanical properties of the root and elasticity of the soil surrounding it, which plays the main role in destruction of the tights of the root with the soil. According to the calculations performed, when the coefficient c of the elastic deformation of the soil is changed, the first frequency of natural oscillations of the body of the root monotonously increases within the limits of 76.4–93.4 Hz, which sufficiently and precisely corresponds to the experimental data in [7,31]. At the same time, the second frequency is changed within the limits of 528–532 Hz—i.e., it has little dependency on the coefficient c of the elastic deformation of the soil.

2. The Hamilton–Ostrogradsky functional for forced longitudinal oscillations of the root as an elastic body was constructed, on the basis of which the theory of forced oscillations of the beet root in the soil was created. The results of theoretical research of the forced oscillations of beet root attached in the soil were the basis for finding the algorithm for calculation on a PC of the specified oscillations—in particular, finding the law of the forced longitudinal oscillations and amplitude under the condition of prevention of damage (tearing) of the beet root depending on the coefficient c of the elastic deformation of the soil and the amplitude of the disturbing force.

It was analytically established that the amplitude of the forced oscillations of the body of the root decreases in the case of an increase in the coefficient c of elastic deformation of the soil and increases in the case of an increase in distance of the cross-section of the beet root from the conditional point of its attachment in the soil. For example, with x = 0.07 m and the change in the coefficient c within the limits of $c = 0$–$20\ 105\ \text{N·m}^{-3}$, the amplitude is measured within the limits of 0.47–0.7 mm; with x = 0.1 m—within the limits of 0.67–0.99 mm; with x = 0.12 m—within the limits of 0.81–1.19 mm; with x = 0.15 m (point of gripping)—within the limits of 1.01–1.49 mm.

However, for the cross-sections of the root above the point of gripping (x ≥ 0.15 m), the amplitude of the forced oscillations of the body of the root almost does not change in the case of an increase in the distance of the cross-section from the conditional point of attachment and remains the same as in the case of x = 0.15 m. However, the tendency for the amplitude to decrease from an increase in the coefficient c is the same as for sections below the point of gripping (x ≤ 0.15 m).

The paper also presents the calculations performed for the amplitude of forced longitudinal oscillations in the case of change in the amplitude of the disturbing force within the limits of 100–600 N. As the calculations demonstrated, the increase in the amplitude of the disturbing force leads to an increase in the longitudinal forced oscillations of the body of the beet root according to the linear law and an increase in the distance of the area of cross-section of the root from the conditional point of its attachment in the soil also leads to increase in the amplitude.

For example, with x = 0.07 m, the amplitude remains within the limits of 0.13–0.8 mm, with x = 0.1 m—within the limits of 0.19–1.14 mm, with x = 0.12 m—within the limits of 0.23–1.36 mm, with x = 0.15 m (point of gripping)—within the limits of 0.28–1.7 mm. However, above the point of gripping in the case of an increase in the distance of the cross-section from the conditional point of attachment, the amplitude almost does not change.

3. The theory of free transverse oscillations of the root in the soil as an elastic solid in an elastic medium has been developed. On the basis of the Ostrogradsky–Hamilton variation principle of stationary action and with the use

of the Ritz method, the Ritz equation of frequencies for free transverse oscillations has been generated. By solving said equation, the first two frequencies of free transverse oscillations of the root body, which play a leading part in the destruction of the bonds between the root and the soil, have been determined.

A relation has been established between the first and second frequencies of the free transverse oscillations of the root body on the one hand and the coefficient of elastic deformation of the soil c on the other hand. For example, when the coefficient c varies within the range of 0–2·106 N·m^{-3}, the first frequency varies within the range of 5.7–36 Hz and the second one varies within the range of 277.6–280.7 Hz—i.e., the first frequency depends on the coefficient c to a great extent, and its influence on the second frequency is insignificant.

4. On the basis of the above-mentioned principle, the theory of the forced transverse oscillations of the root body generated by the action of a horizontal perturbing force that varies following a harmonic law and is vectored along the line of the lifter's translational motion has been worked out. The algorithm of computation of transverse oscillations has been devised—in particular, for finding the amplitude of transverse oscillations under the condition of not breaking the root in relation to the soil's elastic deformation coefficient c and the amplitude of the perturbing force.

It has been proved that at certain values of the soil's elastic deformation coefficient c, resonance takes place, and the amplitude of transverse oscillations can reach values in excess of 0.3 m.

Thus, in the instances when the perturbing force is at a right angle to the root's centreline, the breaking of the root can take place at certain frequencies of the perturbing force and value of elastic deformation coefficient of the soil c, which is different in the case of the vertical perturbing force, under the action of which the root can be stretched not more than 1.7 mm. The natural frequencies of longitudinal oscillations of a root body fall within the range of 76.4–93.4 Hz, while the frequency of the perturbing force does not exceed 20 Hz; hence, the resonance is impossible.

The final conclusion is that the designs of vibrational digging tools have to aim at the generation of a vertical perturbing force and not a horizontal one.

5. Theory of Extraction of Root from Soil during Vibrational Lifting

5.1. Differential Equations of Oscillations of Root in Soil Based on Kinematic

The theory of the free and forced longitudinal and transverse oscillations of a root body fixed in the soil generated by the action of a vibrational digging tool on the root, presented in the previous sections, facilitates the analysis of the effect that the mentioned oscillations have on the process of disrupting the bonds between the root and the soil, as well as the evaluation of the kinematic parameters of vibrational lifting subject to not damaging the roots. Nevertheless, said study is not sufficient for the complete analysis of the extraction of roots from the soil. It is also necessary to give separate consideration to the dynamic system "root—digging tool" in order to analyse the process of oscillations in the soil and extraction of the root from it as a rigid body, which takes place under the effect of the vibration of the digging tool in the longitudinal and vertical planes and the tool's translational motion.

As can be concluded from the above, the analysis of the process of the root extraction from the soil with the use of a vibrational digging tool requires considering the direct contact between the root and the working faces of the shares during its gripping by the tool. Said contact can occur directly between the lifter's working faces and the root body, or such a contact can take place through a sufficiently thin layer of soil. In order to analyse the mentioned process in detail, it is necessary to distinguish three modes of the root extraction from the soil—i.e., the three essential stages of the interaction between the root and the working faces of the vibrational digging tool. This need results from the fact that at each stage of its extraction the root performs various kinds of mechanical motions in consequence of the breaking of the bonds between the root and the soil; therefore, the differential equations representing said motions also differ from each other.

Further, the possible modes of the interaction between the vibrational digging tool and the root are described. The first stage is as follows. The vibrational digging tool performs the gripping of the root; however, the root is still strongly bonded with the soil. In this case, the root starts performing oscillatory motions in the soil as a rigid body in an elastic medium, as at this stage the soil surrounding the root can be considered as an elastic medium.

In the second stage, the bonds between the root and the soil in the area of the motion of the vibrational digging tool's working faces are almost broken and the soil surrounding the root in its upper part (at the running depth of the lifter in the soil) is already sufficiently loosened; nevertheless, the process of direct extraction has not

yet started. At this stage of extraction, the root performs motion in the soil as a rigid body with one point fixed or as a rigid body rotating about a fixed axis. It ought to be noted that during the root extraction, the soil surrounding the root maintains resistance over its whole conical surface (the root firmly embeds in the soil in the process of its growth). As a consequence, when the working faces of the vibrating digging tool that moves at a certain depth in the soil break the upper layer of the soil and disrupt the bonds, the lower part of the root still resides in the unstrained compact layer of the soil and it can be assumed that in this part there is a point on the root's symmetry axis, which can be considered as the point of fixation of the root in the soil. The motion of the root at the second stage can be described with the use of kinematic and dynamic Euler equations as the motion of a symmetrical rigid body with one point fixed or a rigid body rotating about a fixed axis (in the longitudinal and vertical plane).

In the third stage, the bonds between the root and the soil are completely broken (in its upper and lower parts) and the process of directly extracting the root from the soil begins. At this stage, the root's motion can be seen as the motion of a free rigid body under the action of a certain system of forces. Such a motion can be described with the use of the differential equations of the motion of the root's centre of mass and the differential equations of the rotation of the root as a rigid body about its centre of mass.

In what follows, the first stage of the root extraction from the soil is analysed in detail. Since it is possible that some roots are offset from the centreline of the row, the cases where the root is in direct contact with only one of the wedges of the vibrating digging tool are not to be ruled out. In such cases, the root performs three-dimensional oscillations about the conventional point of fixation in the soil as a solid body in an elastic medium. The root is gripped by the vibrating digging tool asymmetrically.

Further, we have to show, in the equivalent schematic model, the adopted coordinate systems. First, we relate to the vibrating digging tool the orthogonal Cartesian coordinate system $O_1 x_1 y_1 z_1$ with the centre O_1 in the middle of its necked-in passage. In this system, axis $O_1 x_1$ is in line with the direction of the tool's translational motion, axis $O_1 z_1$ points vertically up, and axis $O_1 y_1$ points to the right (Figure 5.1). The vibrating digging tool's oscillatory movements in the longitudinal vertical plane should be examined in reference to the coordinate system $O_1 x_1 y_1 z_1$.
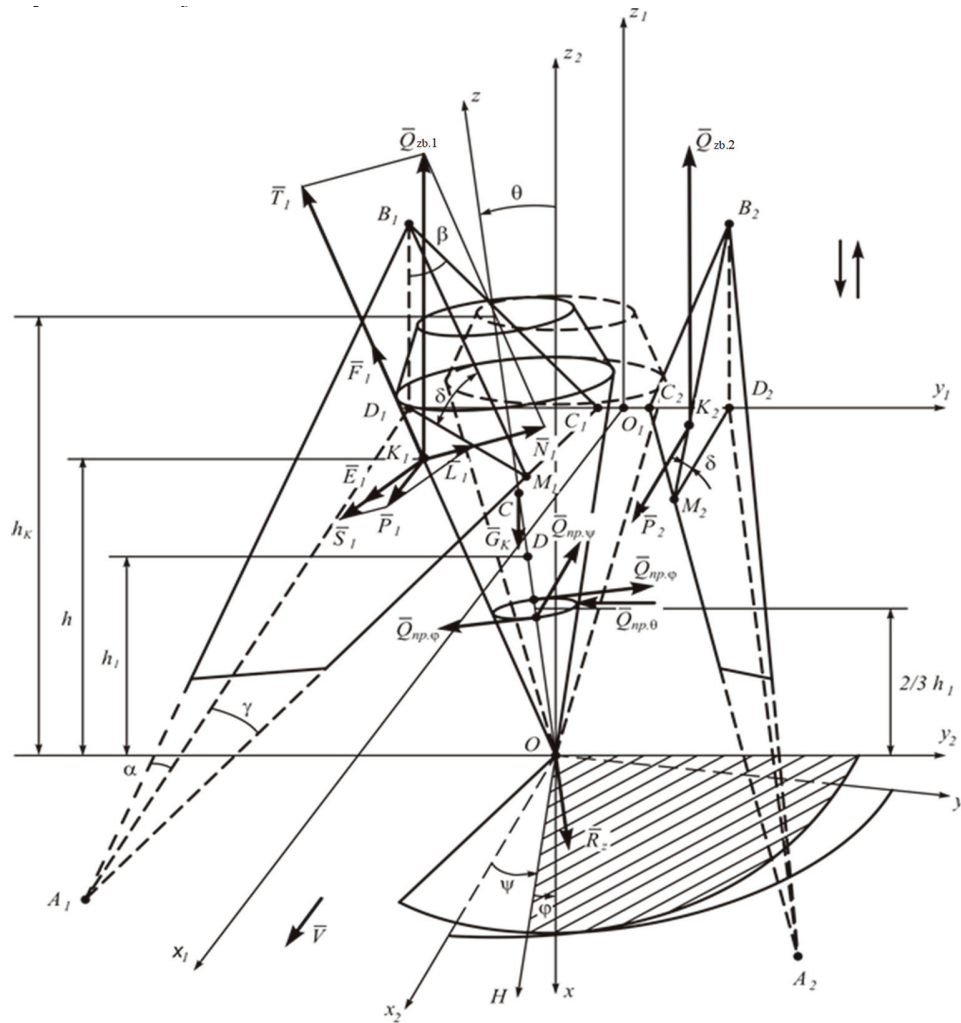
Figure 5.1. Equivalent schematic model of the force interaction between the vibrating digging tool and the beet root during the latter's gyration about the conventional point of fixation in the ground.

We also introduce the moving coordinate system $Oxyz$ rigidly connected with the beet root and having an origin at point O, which is the point of fixation of the beet root in the ground, its axis Oz being aligned with the root's symmetry axis and pointing upwards, axes Ox and Oy placed in the plane that is perpendicular to axis Oz.

Additionally, to characterise the gyration of the root about the fixation point O it is necessary to introduce one more orthogonal Cartesian coordinate system $O_2 x_2 y_2 z_2$, which is shown in Figure 5.1.

Since the vibrating digging tool at the moment it contacts the beet root advances linearly along axis $O_1 x_1$ $(O_1 x_2)$, the root deflects from its vertical position (effectively from axis Oz_2) through angle ψ unidirectionally with the motion of the tool. In the most general case, the initial contact between the beet root and the tool is asymmetric, meaning that one of the digging shares moves into direct contact with the root body,

while the other one makes contact through a certain thickness of the broken soil. This results in the beet root's deflection from its vertical position transversely through angle θ following the deformation of soil (of the aforementioned thickness). Moreover, the difference in the torques produced by the direct contact of the root with one of the shares and its contact with the other share through the thickness of soil can result in the rotation of the root through angle φ about axis Oz. Overall, summing up the above-mentioned physical conditions, we have good reason to believe that the beet root in its interaction with the vibrating digging tool, during its lifting, immediately simultaneously performs the rotation about a line OH (nodal line) through the angle θ, the rotation about axis Oz_2 through the angle ψ and the rotation about axis Oz through the angle φ. Hence, the introduced angular displacements in the space of the root during its lifting from the ground are Euler angles, with the angle θ being a nutation angle, the angle ψ a precession angle, the angle φ an intrinsic rotation angle.

We also have to take into account that, since the root body has a conical shape, the direct contact between the digging shares and the root body is lost in the case of the vibrating digging tool going down. As a result, the perturbing force stops acting on the beet root, and therefore the root, due to the elasticity of the soil surrounding it, and the root body's own elastic properties tend to return to the vertical equilibrium position. With the following upward motion, the digging shares resume their contact with the root body, take hold of the root, and impart the perturbing force on it and the mentioned process of root rotations recurs.

Thus, the beet root performs oscillations about the line of nodes *OH* about axis Oz_2 and about axis Oz. Actually, the root's oscillations at the first stage of its lifting from the ground comprise the longitudinal linear oscillations of the point of the root's fixation in the ground O and the angular oscillations of the root relative to point O, characterised by the variation of the Euler angles θ, ψ and φ.

The equivalent schematic model of the interaction between the root and the working faces of the vibrating digging tool at the first stage of extraction has to be set up. For this purpose, the vibrating digging tool is represented as the two wedges $A_1B_1C_1$ and $A_2B_2C_2$, each of them having three-dimensional inclination at angles of α, β, γ and both of them positioned with respect to each other in such a way that the working channel necking rearwards is created (Figure 5.1). The mentioned wedges perform oscillatory motions in the longitudinal and vertical plane (the mechanism that drives the oscillatory motion of the shares is not shown); the line of the translational motion of the vibrating digging tool is shown by an arrow. The projections of points B_1 and B_2 on axis O_1y_1 are designated as points D_1 and D_2, respectively.

It is assumed that the faces of wedges $A_1B_1C_1$ and $A_2B_2C_2$ interact at the corresponding points with the root that is approximated as a cone-shaped body; that said, in the general case the gripping of the root by the tool can be asymmetrical.

This asymmetry results from the fact that the root's symmetry axis (axis Oz) can be somewhat offset from the row centreline. It is assumed that before the direct contact between the root and the tool starts, axis Oz is parallel to axis O_1z_1.

We have assumed that the beet root is in direct contact with only one of the work faces of the vibrating digging tool—specifically, $A_1B_1C_1$ at point K_1—while face $A_2B_2C_2$ acts on the root body surface via soil of a certain thickness and this contact can occur at point K_2 (Figure 5.1). Certainly, the contact between the vibrating digging tool and the root body at point K_2 is made throughout an area surrounding point K_2, but in our further considerations we are going to assume that point K_2 is the point of application of the forces imparted on the beet root.

Additionally, the asymmetry of the contact with the beet root is also due to the fact that its symmetry axis (axis Oz) can be offset relative to the centreline of the sowing rows (due to the requirements of the agricultural sowing and plant handling technologies). We assume that prior to the commencement of the direct contact between the beet root and the digging tool, axis Oz is parallel to axis O_1z_1.

Additionally, we have to designate some representative points in the equivalent schematic model. Thus, the right lines drawn via points B_1 and B_2, perpendicular to the wedge sides A_1C_1 and A_2C_2, respectively, generate at their intersections with said wedge sides the respective points M_1 and M_2. Hence, δ is the dihedral angle ($\angle B_1M_1D_1$) between the first wedge's lower base $A_1D_1C_1$ and the work face $A_1B_1C_1$ and also the dihedral angle ($\angle B_2M_2D_2$) between the second wedge's lower base $A_2D_2C_2$ and the work face wedge $A_2D_2C_2$. Angle $2\gamma_k$ is the apical angle of the cone used as a model of the beet root. The meaning of other dimensions can be understood from the equivalent schematic model (Figure 5.1).

Now, let us consider the forces originating from the interaction between the vibrating digging tool and the beet root.

Since the digging tool, as has been stated, is a vibrational tool, it imparts the vertical perturbing force $\overline{Q}_{zb.}$, which varies under the following harmonic law:

$$Q_{zb.} = Hsin\omega t \qquad (5.1)$$

where H—amplitude of the perturbing force; ω—frequency of the perturbing force.

This force plays the primary role in the process of soil breaking in the zone of the digging tool's work passage and the direct lifting of the beet root out of the ground. The perturbing force $\overline{Q}_{zb.}$ is applied to the beet root or the soil surrounding it on two sides; therefore, it is represented in the equivalent schematic model by two components $\overline{Q}_{zb.1}$ and $\overline{Q}_{zb.2}$, which apparently have the following values:

$$Q_{zb.1} = Q_{zb.2} = 0.5Nsin\omega t \qquad (5.2)$$

Further considerations require careful analysis of the relation between the oscillations of the vibrating digging tool and the concurrent action of the perturbing force $\overline{Q}_{zb.}$ on the root. It is sufficient to carry out the analysis for only one oscillation period, from $\omega t = 0$ to $\omega t = 2\pi$. In all other oscillation periods, the process is repeated. As mentioned above, the perturbing force $\overline{Q}_{zb.}$ acts on the beet root only when the digging shares of the tool move up from their lowermost position to their uppermost position, making contact with the conical root body. Further, the assumption is that on the interval $[0, \pi]$, the digging tool moves upwards from its lowest position $-a$ to its highest position a, where a is the amplitude of oscillations of the tool, and on the interval $[\pi, 2\pi]$ the digging tool moves downwards from position a to position $-a$. Hence, the oscillations of the tool have to take place in accordance with the following harmonic law:

$$z_K = -a cos\omega t \qquad (5.3)$$

where z_K—displacement of the tool from the horizontal axis, about which the oscillations take place (m); ω—frequency of oscillations of the tool (s^{-1}).

For this reason, during the movement of the digging shares of the tool up on the interval $[0, \pi]$, the perturbing force $\overline{Q}_{zb.}$ acts on the beet root following the sinusoidal law (5.1). In this process, on the interval $\left[0, \frac{\pi}{2}\right]$ it increases from the zero value $Q_{zb.} = 0$ at point $\omega t = 0$ to the maximum value $Q_{zb.} = H$ at point $\omega t = \frac{\pi}{2}$.

On the interval $\left[\frac{\pi}{2}, \pi\right]$ it decreases from its maximum value $Q_{zb.} = H$ to the minimum one $Q_{zb.} = 0$. On the interval $[\pi, 2\pi]$, the digging shares of the tool move down, and therefore the perturbing force $\overline{Q}_{zb.}$ does not act on the root on this leg. On the interval $[2\pi, 4\pi]$, everything recurs. Thus, in general, on the intervals $[2k\pi, (2k + 1)\pi]$, $k = 0, 1, 2, \ldots$, the perturbing force $\overline{Q}_{zb.}$ acts on the beet root following the sinusoidal law (5.1), and on the intervals $[(2k - 1)\pi, 2k\pi]$, $k = 0, 1, 2, \ldots$, it has no effect on the beet root, since it is equal to zero.

As the cutting edges, A_1C_1 and A_2C_2 of the digging shares are located below the contact points K_1 and K_2, the soil in the area of the contact between the beet root and the vibrating digging tool is already sufficiently broken, but the soil breaking occurs primarily in the front part of the tool's passage, while the direct contact between the beet root and the tool occurs in the middle and rear parts of the work passage. Therefore, in the case of asymmetric contact with the beet root at point K_1, the root is under the direct effect of the perturbing force $\overline{Q}_{zb1}$, while at the contact point K_2 the perturbing force $\overline{Q}_{zb.2}$ acts only on the thickness of broken soil, which makes us assume that this latter force is virtually not imparted directly on the root body. Hence, at the first contact between the root body and the vibrating digging tool, the effect of perturbing force $\overline{Q}_{zb.2}$ on the beet root can be ignored and it can be assumed that the root is under the effect of only the perturbing force $\overline{Q}_{zb.1}$ acting from the side of face $A_1B_1C_1$—i.e., only one digging share.

Certainly, due to the necking shape of the working channel and the lifter's translational motion, at the second or third stages of the gripping of the root by the tool, the direct contact between the root and the tool will occur on both the shares; in extreme cases, this will happen through a thin layer of soil. It can be assumed that through a thin layer of soil the perturbing force is transferred in full and the (probable) difference can be observed only in the forces of friction arising on the working faces of the shares as a consequence of the different coefficients of friction.

In addition, it should be pointed out that an interesting aspect of the asymmetric contact with the beet root is that it makes the rotation of the root about its axis possible, promoting the intensive breaking of the bonds between the root and the soil (phenomenon of the root's spinning in the ground during it being dug out). Therefore, in the case of asymmetric contact between the beet root and the vibrating digging tool, we are going to only use the force action of work face $A_1B_1C_1$ of one digging share in the differential equations for the root's motion. For this purpose, we decomposed force $\overline{Q}_{zb.1}$ into two components: $\overline{N}_1$, normal to face $A_1B_1C_1$, and $\overline{T}_1$, tangential to the same face, as shown in the equivalent schematic model in Figure 5.1. This force is equal to:

$$\overline{Q}_{zb.1} = \overline{N}_1 + \overline{T}_1 \tag{5.4}$$

Apparently, the $\overline{T}_1$ force vector is parallel to the right line B_1M_1.

As the vibrating digging tool advances linearly along axis O_1x_1 relative to the beet root fixed in the ground, driving force $\overline{P}_1$ acts along the course of the translational movement (along axis O_1x_1) and also acts on the root along that axis at the moment when contact is made between the beet root and digging tool. Now, let us also decompose force $\overline{P}_1$ into two components: $\overline{L}_1$, normal to wedge face $A_1B_1C_1$ and $\overline{S}_1$, tangential to the same face—i.e.,

$$\overline{P}_1 = \overline{L}_1 + \overline{S}_1 \tag{5.5}$$

Thus, at the contact point K_1 the beet root is under the effect of the force applied by wedge $A_1B_1C_1$, which is equal to:

$$\overline{N}_{K_1} = \overline{N}_1 + \overline{L}_1 \tag{5.6}$$

and points along the normal to the surface of wedge $A_1B_1C_1$.

Apparently, the magnitude of this force is:

$$N_{K_1} = N_1 + L_1 \tag{5.7}$$

Additionally, at the contact point K_1, the force of friction $\overline{F}_{K_1}$ is applied, which counteracts the slipping of the beet root on the work face of the wedge $A_1B_1C_1$ during its contact with the vibrating digging tool. The vector of this force is in opposition

to the vector of the relative velocity of the wedge's slipping on the surface of the beet root. The root weight force $\overline{G}_k$ is applied vertically at the centre of mass (point C) of the beet root. Additionally, during the contact between the beet root and the vibrating digging tool, when the latter's shares move upwards, the root is under the effect of the soil's elastic deformation force acting along axis Oz, designated as $\overline{R}_z$ in the equivalent schematic model (Figure 5.1).

Further, it is necessary to determine the values of the above-mentioned forces acting on the root during its contact with the vibrating digging tool. The tangential component $\overline{T}_1$ of the perturbing force $\overline{Q}_{zb.1}$ and the tangential component $\overline{S}_1$ of the driving force $\overline{P}_1$ do not act directly on the beet root—they only cause the breaking of the soil around the beet root, and therefore they are not included in the differential equations of the movement of the root as a solid body. Using the schematic model in Figure 5.1, the following expressions that define the normal $\overline{N}_1$ and tangential $\overline{T}_1$ components of the perturbing force $\overline{Q}_{zb.1}$ are obtained:

$$N_1 = Q_{zb.1}cos\delta, \tag{5.8}$$

$$T_1 = Q_{zb.1}sin\delta. \tag{5.9}$$

With the use of the same schematic model, the following expressions for finding the normal $\overline{L}_1$ and tangential $\overline{S}_1$ components of the driving force $\overline{P}_1$ are obtained:

$$L_1 = P_1 sin\gamma, \tag{5.10}$$

$$S_1 = P_1 cos\gamma. \tag{5.11}$$

The magnitude of force $\overline{N}_{K_1}$, taking into account (5.7), (5.8) and (5.10), is equal to:

$$N_{K_1} = Q_{zb.1}cos\delta + P_1 sin\gamma \tag{5.12}$$

or, taking into account (5.2), the following is arrived at:

$$N_{K_1} = 0.5Hcos\delta \cdot sin\omega t + P_1 sin\gamma \tag{5.13}$$

Subsequently, the value of the force of friction $\overline{F}_{K_1}$ is equal to:

$$F_{K_1} = fN_{K_1} = f(Q_{zb.1}cos\delta + P_1 sin\gamma) \tag{5.14}$$

or, taking into account (5.2), the following is arrived at:

$$F_{K_1} = 0.5fHcos\delta \cdot sin\omega t + fP_1 sin\gamma \tag{5.15}$$

It is obvious that during the direct contact between wedge $A_1B_1C_1$ and the surface of the root, the vector of the force of friction $\overline{F}_{K_1}$ will always lie in the wedge's plane $A_1B_1C_1$. Since at the start of the gripping the root is still strongly bonded with the soil, it is possible that the root slips on the face of the wedge in the direction that is opposite to the line of action of force $\overline{T}_1$ (parallel to the line B_1M_1) and in the direction that is opposite to the line of action of force $\overline{S}_1$.

The mentioned slips can occur under the action of forces $\overline{Q}_{zb.1}$ and $\overline{P}_1$, respectively. Therefore, the vector of the relative velocity of the wedge slipping on the surface of the root can be resolved into the components in the above-mentioned directions. Hence, the force of friction $\overline{F}_{K_1}$ can also be decomposed into the two components $\overline{F}_1$ and $\overline{E}_1$ in the directions of the vectors $\overline{T}_1$ and $\overline{S}_1$, respectively—that is:

$$\overline{F}_{K1} = \overline{F}_1 + \overline{E}_1 \qquad (5.16)$$

The magnitudes of components $\overline{F}_1$ and $\overline{E}_1$ have to be determined. On account of the above considerations, it is possible to conclude that on the intervals $[2k\pi, (2k+1)\pi], k = 0, 1, 2, \ldots$—in particular, on the interval $[0, \pi]$, the magnitude of the force of friction $\overline{F}_{K_1}$ is determined in accordance with (5.15); moreover, on the interval $\left[0, \frac{\pi}{2}\right]$, it increases from the minimum value:

$$F1 sin\gamma_{K_1 min} \qquad (5.17)$$

to the maximum value:

$$F\frac{1}{2}cos\delta_1 sin\gamma_{K_1 max} \qquad (5.18)$$

while on the interval $\left[\frac{\pi}{2}, \pi\right]$, it decreases from $F_{K_1 max}$ to $F_{K_1 min}$. That said, the direction of the vector on the interval $\left[0, \frac{\pi}{2}\right]$ also changes. Vector $\overline{F}_{K_1 min}$ has the same direction as the friction force vector for a traditional lifter (in the absence of a perturbing force)—i.e., parallel to the right line A_1O_1', while $\angle O_1'A_1M_1 = \gamma$ (Figure 3.3). Vector $\overline{F}_{K_1 max}$ deflects from vector $\overline{F}_{K_1 min}$ through a certain angle of $\alpha_{K_1 max}$.

Thus, on the interval $\left[0, \frac{\pi}{2}\right]$, vector $\overline{F}_{K_1}$ strokes from vector $\overline{F}_{K_1 min}$ to vector $\overline{F}_{K_1 max}$, on the interval $\left[\frac{\pi}{2}, \pi\right]$—from vector $\overline{F}_{K_1 max}$ to vector $\overline{F}_{K_1 min}$. Thereby, the angle of deflection α_{k1} of vector $\overline{F}_{K_1}$ from vector $\overline{F}_{K_1 min}$ on the interval $[0, \pi]$ varies under the following law:

$$\alpha_{K_1} = \alpha_{K_1 max} sin\omega t \qquad (5.19)$$

Apparently, the value $\alpha_{K_1 max}$ depends first of all on the ratio $\frac{H}{P_1}$ and the greater said ratio is, the greater the value is. Hence, on the interval $[0, \pi]$, the magnitude of the friction force vector $\overline{F}_{K_1}$ varies in accordance with (5.15); its direction is in accordance with (5.19).

Thus, on the interval $[0, \pi]$, the following values of components $\bar{F}_1$ and $\bar{E}_1$ are arrived at:

$$F_1 = F_{K_1} sin(\alpha_{K_1} - \gamma) \tag{5.20}$$

$$E_1 = F_{K_1} cos(\alpha_{K_1} - \gamma) \tag{5.21}$$

or, taking into account (5.15) and (5.19), the following is arrived at:

$$F_1 = (0.5fHcos\delta \cdot sin\omega t + fP_1 sin\gamma)sin(\alpha sin\omega_{K_1 max}) \tag{5.22}$$

$$E_1 = (0.5fHcos\delta \cdot sin\omega t + fP_1 sin\gamma)cos(\alpha_{k_{1max}} sin\omega t - \gamma) \tag{5.23}$$

(5.22) and (5.23) are applicable on any of the intervals $[2k\pi, (2k+1)\pi], k = 0, 1, 2, \ldots$

It is obvious that on the intervals $[(2k-1)\pi, 2k\pi], k = 1, 2, \ldots$, the force of friction $\bar{F}_{K_1}$ is equal to:

$$F_{K_1} = F1 sin\gamma_{K_1 min} \tag{5.24}$$

Hence, on the mentioned intervals, the following is true:

$$F_1 = F sin\gamma_1 sin\gamma sin\gamma_1 sin^2\gamma_{K_1 min} \tag{5.25}$$

$$E_1 = F cos\gamma_1 sin\gamma cos\gamma \frac{1}{2} sin2_{K_1 min} \tag{5.26}$$

Further, the forces that arise as a consequence of the deformation of the soil as an elastic medium during the motion of the root in it have to be computed. When the root rotates about its centreline (axis Oz) through the angle of φ, a distributed load appears on the surface of contact between the root and the soil in the area of the latter's unbroken layer or, to be more accurate, a couple of distributed loads, as the intensity vectors of said load are directed tangentially to the root's surface and distributed over the circumference in the planes of the root's cross-sections. The action of the couple is specified by its moment about the Oz axis vectored along the Oz axis.

Said moment can be calculated as follows.

It is assumed that c_1—coefficient of elastic deformation of the soil, which shows by how much the force on the surface of contact increases when the surface of contact is displaced over a unit of contact area (N·m^{-2}).

Consider an element of surface dF of the contact between the root and the soil in its unbroken area located at a distance of z from the point of fixation O, $0 \leq z \leq h_1$, where h_1—depth of the root's position in the unbroken area of the soil. The radius of the root's cross-section situated at said distance of z from point O is equal to $ztan\gamma_k$, where $2\gamma_k$—angle of apex of the cone (the root is modelled as a cone-shaped solid).

Further, it is assumed that $d\alpha$—angle at the centre intercepted by the element of surface dF in the plane of the cross-section under consideration.

Apparently, the height of the element of surface is equal to $\frac{dz}{cos\gamma_k}$.

Subsequently, the area of the element of surface dF is equal to:

$$dS = ztan\gamma_k d\alpha \frac{dz}{cos\gamma_k} \qquad (5.27)$$

As the element of surface dF rotates through an angle of φ, the soil surrounding the root is subjected to a shear strain of dS_ϕ, which is equal to: $dS_\varphi = \frac{dS}{2\pi}\varphi$, or, considering (5.27), the following is arrived at:

$$dS_\varphi = \frac{zsin\gamma_k d\alpha dz}{2\pi cos^2\gamma_k}\varphi. \qquad (5.28)$$

where the angle φ is measured in radians.

Hence, the elementary elastic force exerted by the soil, when the element of surface dF rotates through an angle of φ, is equal to:

$$dF_{np.} = \frac{c_1 zsin\gamma_k d\alpha dz}{2\pi cos^2\gamma_k}\varphi \qquad (5.29)$$

The elementary moment of said elementary force about axis Oz is equal to:

$$dM_{np.\varphi} = \frac{-c_1 zsin\gamma_k d\alpha dz}{2\pi cos^2\gamma_k}\varphi ztan\gamma_k \qquad (5.30)$$

The moment of the elastic soil deformation force due to the angular displacement of the beet root through the angle φ is equal to:

$$M_{\Pi p.\varphi} = -\int_0^{h_1}\int_0^{2\pi} \frac{c_1 z^2 dz\varphi sin^2\gamma_k d\alpha}{2\pi cos^3\gamma_k} \qquad (5.31)$$

where c_1—elastic stiffness of the soil that determines the increase in the force acting on the contact surface in the case of displacement of the contact surface for a contact area unit (N·m^{-2}).

By integrating (5.31), the following is obtained:

$$M_{\Pi p.\varphi} = \frac{-c_1 h_1^3\varphi sin^2\gamma_k}{3cos^3\gamma_k} \qquad (5.32)$$

Further, the values of the elastic forces exerted by the soil, when the root fixed in the soil rotates about the Oz_2 axis through an angle of $\psi\overline{Q}_{np.\psi}$, and about the nodal

line OH through an angle of $\theta \overline{Q}_{np.\theta}$ have to be computed. Obviously, the mentioned forces are also loads distributed over the surface of contact between the root and the unbroken layer of soil. It is assumed that, during the rotation of the root through angles of ψ and θ, deformation is observed in that part of the soil, which is in contact with half of the side surface of the cone (i.e., part of the root that sits in the unbroken layer of soil). The designation c will further denote the coefficient of the soil's elastic deformation (ratio between the first Winckler coefficient and the area of contact) (N·m^{-3}).

Subsequently, the moment of force $Q_{np.\psi}$ about axis Oz_2 is equal to:

$$M_\psi\left(\overline{Q}_{np.\psi}\right) = - \int_0^{h_1} \int_0^\pi \frac{c sin\gamma_k \cdot \psi d\alpha z^3 dz\theta \cdot cos(\gamma_k + \psi)}{cos^3\gamma_k} \tag{5.71}$$

By integrating (5.71), the following is obtained:

$$M_\psi\left(\overline{Q}_{np.\psi}\right) = \frac{-c\pi h_1^4 sin\gamma_k \cdot \psi\theta \cdot cos(\gamma_k + \psi)}{4cos^3\gamma_k} \tag{5.72}$$

$$M_\psi\left(\overline{G}_k\right) = 0 \tag{5.73}$$

as the force vector $\overline{G}_k$ is parallel to axis Oz_2.

$$M_\psi\left(\overline{R}_z\right) = 0 \tag{5.74}$$

as the force vector $\overline{R}_z$ intersects axis Oz_2.

Thus, taking into account the obtained expressions of the moments (5.60), (5.61), (5.62), (5.64) or (5.65), (5.69) and (5.72) and (5.74), the magnitude of the resultant moment of all external forces about axis Oz_2 that causes the root's rotation about axis Oz_2 through an angle of ψ is found:

$$M_\psi^e = P_1(htan\gamma_k - h\theta) + f\left(\tfrac{H}{2}cos\delta \cdot sin\omega t + P_1 sin\gamma\right)cos\left(\alpha sin\omega_{K_1 max}()\right)$$
$$\times(htan\gamma_k - h\theta) - \frac{c\pi h_1^4 sin\gamma_k \cdot \psi\theta cos(\gamma_k - \theta)}{4cos^3\gamma_k} - \frac{c\pi h_1^4 sin\gamma_k \cdot \psi\theta cos(\gamma_k + \psi)}{4cos^3\gamma_k}, \tag{5.75}$$
$$\omega t \in [2k\pi, (2k+1)\pi], k = 0, 1, 2, \cdots,$$

or

$$M_\psi^e = P_1(htan\gamma_k - h\theta) + 0.5fP_1 sin2\gamma (htan\gamma_k - h\theta)$$
$$- \frac{c\pi h_1^4 sin\gamma_k \cdot \theta\psi cos(\gamma_k - \theta)}{4cos^3\gamma_k} - \frac{c\pi h_1^4 sin\gamma_k \cdot \psi\theta \cdot cos(\gamma_k + \psi)}{4cos^3\gamma_k}, \tag{5.76}$$
$$\omega t \in [(2k-1)\pi, 2k\pi], k = 1, 2, \cdots$$

Further, it is necessary to find the moments of all external forces that cause the root's rotation about the nodal line OH. As plane zOz_2 is at right angle to the nodal

line *OH*, in order to find the moments of all forces about axis *OH* it is necessary to project each of the forces on plane zOz_2. With this aim in mind, it ought to be noted that plane zOz_2 is angularly displaced about axis Oz_2 with respect to plane y_2Oz_2 through an angle of ψ, as the angle between the axes that uniquely set the positions of these planes, i.e., between axes Ox_2 and *OH*, is equal to ψ. Hence, the following values of the mentioned moments are obtained:

$$M_\theta(\overline{Q}_{zb.1}) = -Q_{zb.1}h \cdot tan\gamma_k \tag{5.77}$$

since the vector of force $\overline{Q}_{zb.1}$ is parallel to plane zOz_2.

$$M_\theta(\overline{P}_1) = P_1 sin\psi \cdot h \tag{5.78}$$

since the vector of force $\overline{P}_1$ deflects from the perpendicular to plane zOz_2 (nodal line *OH*) through an angle of ψ.

$$M_\theta(\overline{E}_1) = E_1 sin\psi \cdot h \tag{5.79}$$

or, taking into account (5.23) or (5.26), (5.79) finally obtains the following appearance:

$$M_\theta(\overline{E}_1) = f\left(\tfrac{H}{2}cos\delta \cdot sin\omega t + P_1 sin\gamma\right)cos\left(\alpha sin\omega_{K_1max}()sin\psi\right)$$
$$\omega t \in [2k\pi, (2k+1)\pi], k = 0,1,2,\cdots, \tag{5.80}$$

or

$$M_\theta(\overline{E}_1) = \frac{1}{2}fP_1 sin2\gamma \cdot sin\psi \cdot h, \omega t \in [(2k-1)\pi, 2k\pi], k = 1,2,\cdots \tag{5.81}$$

$$M_\theta(\overline{F}_1) = 0 \tag{5.82}$$

since the vector of force $\overline{F}_1$ intersects axis *OH* at point *O*.

$$M_\theta(\overline{Q}_{np.\psi}) = 0 \tag{5.83}$$

since the vector of force $\overline{Q}_{np.\psi}$, which is the resultant force of the distributed load, intersects axis *OH*.

The moment created by the distributed load, which is represented by the resultant force $\overline{Q}_{np.\theta}$, can be determined as follows.

It is obvious that said moment for an elementary force $d\overline{Q}_{np.\theta}$ about the nodal line *OH* is equal to:

$$M_\theta(d\overline{Q}_{np.\theta}) = -dQ_{np.\theta}cos\psi \cdot z \tag{5.84}$$

or, taking into account (5.37), the result is:

$$M_\theta\left(d\overline{Q}_{np.\theta}\right) = \frac{-csin\gamma_k\theta d\alpha z^3 dz cos\psi}{cos^3\gamma_k} \tag{5.85}$$

Subsequently, the moment of force $\overline{Q}_{np.\theta}$ about the nodal line OH is equal to:

$$M_\theta\left(\overline{Q}_{np.\theta}\right) = -\int_0^{h_1}\int_0^\pi \frac{csin\gamma_k\theta d\alpha z^3 dz cos\psi}{cos^3\gamma_k} \tag{5.86}$$

After the integration of (5.86), the following is arrived at:

$$M_\theta\left(\overline{Q}_{np.\theta}\right) = \frac{-c\pi h_1^4 sin\gamma_k\theta cos\psi}{4cos^3\gamma_k}. \tag{5.87}$$

$$M_\theta\left(\overline{G}_k\right) = G_k\frac{2}{3}h_k\theta \tag{5.88}$$

$$M_\theta\left(\overline{R}_z\right) = 0 \tag{5.89}$$

as the vector of force $\overline{R}_z$ intersects axis OH.

Thus, taking into account (5.77), (5.78), (5.80) or (5.81), (5.87), (5.88) and (5.89) of the moments, the magnitude of the resultant moment of all external forces about axis OH is found:

$$M_\theta^e = -Q_{zb.1}htan\gamma_k + P_1 sin\psi \cdot h + f\left(\frac{H}{2}cos\delta \cdot sin\omega t + P_1 sin\gamma\right)\times$$
$$cos\left(\alpha sin\omega_{K_1 max}()sin\psi \frac{2}{3}_{kk}\frac{c\pi h_1^4 sin\gamma_k\cdot\theta\cdot cos\psi}{4cos^3\gamma_k}\right) \tag{5.90}$$
$$\omega t \in [2k\pi, (2k+1)\pi], k = 0, 1, 2, \cdots,$$

As the rotations of the root through angles of ϕ, ψ and θ are caused by the action of the moments M_ϕ^e, M_ψ^e and M_θ^e, respectively, and these rotations constitute the complete motion of the root as a rigid body, then, evidently, the resultant moment $\overline{M}_O^e$ of all external forces about point O, which is the very cause of the root's motion about point O, is equal to the vector sum of the moments M_ϕ^e, M_ψ^e and M_θ^e—i.e., it can be decomposed on axes Oz, Oz_2 and OH—that is:

$$\overline{M}_O^e = M_\varphi^e\overline{k} + M_\psi^e\overline{k}_2 + M_\theta^e\vec{i}' \tag{5.91}$$

where $\overline{k}, \overline{k}_2, \vec{i}'$—unit vectors of axes Oz, Oz_2 and OH, respectively.

In order to determine the resultant moments of all external forces about axes Ox, Oy and Oz, it is necessary to project (5.91) on axes Ox, Oy and Oz, respectively. For this purpose, the table of direction cosines of the unit vectors $\overline{k}_2, \vec{i}'$ in the system of

moving axes $Oxyz$, which is presented in [32] to generate kinematic Euler equations, has to be used. After substituting angle θ with $-\theta$ in the table, the following relations are obtained:

	x	y	z
$\bar{k}_2$	$-sin\theta \cdot sin\varphi$	$-sin\theta \cdot cos\varphi$	$cos\theta$
$\bar{i}'$	$cos\phi$	$-sin\phi$	0
$\bar{k}$	0	0	1

After projecting (5.91) on axis Ox, the result is:

$$M_x^e = -M_\psi^e sin\theta \cdot sin\varphi + M_\theta^e cos\varphi \tag{5.92}$$

By substituting the obtained values of moments (5.75) or (5.76) and (5.90) or (5.91) into (5.92), the following is obtained:

$$\begin{aligned}
M_x^e = & \left[-P_1(h \cdot tan\gamma_k - h\theta) - f\left(\tfrac{H}{2}cos\delta \cdot sin\omega t + P_1 sin\gamma\right)cos\left(\alpha_{K_1 max} sin\omega t - \gamma\right) \right. \\
& \left. \times(h \cdot tan\gamma_k - h\theta) + \tfrac{c\pi h_1^4 sin\gamma_k \cdot \theta\psi}{4cos^3\gamma_k}\left(cos(\gamma_k - \theta) + cos(\gamma_k + \psi)\right) \right] sin\theta \cdot sin\varphi \\
& + \left[-Q_{zb.1}h \cdot tan\gamma_k + P_1 sin\psi \cdot h + f\left(\tfrac{H}{2}cos\delta \cdot sin\omega t + P_1 sin\gamma\right) \right. \\
& \left. \times cos\left(\alpha sin\omega_{K_1 max}()sin\psi\tfrac{2}{3}_{kk}\tfrac{c\pi h_1^4 sin\gamma_k \cdot \theta cos\psi}{4cos^3\gamma_k}\right)\|cos\varphi \right] \\
& \omega t \in [2k\pi, (2k+1)\pi], k = 0, 1, 2, \cdots,
\end{aligned} \tag{5.93}$$

or:

$$\begin{aligned}
M_x^e = & \left[-P_1(h \cdot tan\gamma_k - h\theta) - \tfrac{1}{2}fP_1 sin\gamma(h \cdot tan\gamma_k - h\theta) \right. \\
& \left. + \tfrac{s\pi h_1^4 sin\gamma_k \cdot \theta\psi}{4cos^3\gamma_k}\left(cos(\gamma_k - \theta) + cos(\gamma_k + \psi)\right) \right] sin\theta \cdot sin\varphi \\
& + \left[P_1 sin\psi \cdot h + \tfrac{1}{2}fP_1 sin2\gamma \cdot sin\psi \cdot h - \tfrac{2}{3}G_k h_k\theta\tfrac{-s\pi h_1^4 sin\gamma_k \cdot \theta \cdot cos\psi}{4cos^3\gamma_k} \right] cos\varphi, \\
& \omega t \in [(2k-1)\pi, 2k\pi], k = 1, 2, \cdots
\end{aligned} \tag{5.94}$$

127

The projection of (5.91) on axis Oy provides the following result:

$$M_y^e = -M_\psi^e \sin\theta \cdot \cos\varphi - M_\theta^e \sin\varphi \tag{5.95}$$

After the substitution of (5.75) or (5.76) and (5.90) or (5.91) into (5.95), the following is obtained:

$$
\begin{aligned}
M_y^e = &\left[-P_1(htan\gamma_k - h\theta) - f\left(\tfrac{H}{2}\cos\delta \cdot \sin\omega t + P_1\sin\gamma\right)\cos\left(\alpha_{K_1 max}\sin\omega t - \gamma\right)\right.\\
&\left.\times(htan\gamma_k - h\theta) + \tfrac{s\pi h_1^4 sin\gamma_k \cdot \theta\psi}{4\cos^3\gamma_k}\big(\cos(\gamma_k - \theta) + \cos(\gamma_k + \psi)\big)\right] \times \sin\theta\cos\varphi \\
&-\left[-Q_{zb.1}h \cdot tan\gamma_k + P_1\sin\psi h + f\left(\tfrac{H}{2}\cos\delta \cdot \sin\omega t + P_1\sin\gamma\right)\right.\\
&\left.\times\cos\left(\alpha\sin\omega_{K_1 max}()\sin\psi \tfrac{2}{3}kk\tfrac{c\pi h_1^4 sin\gamma_k \cdot \theta\cos\psi}{4\cos^3\gamma_k}\right)\right|\Big|\sin\varphi\Big] \\
&\omega t \in [2k\pi, (2k+1)\pi], k = 0, 1, 2, \cdots,
\end{aligned}
\tag{5.96}
$$

or:

$$
\begin{aligned}
M_y^e = &\left[-P_1(htan\gamma_k - h\theta) - \tfrac{1}{2}fP_1\sin 2\gamma(htan\gamma_k - h\theta)\right.\\
&\left.+\tfrac{c\pi h_1^4 sin\gamma_k \theta\psi}{4\cos^3\gamma_k}\big(\cos(\gamma_k - \theta) + \cos(\gamma_k + \psi)\big)\right]\sin\theta \cdot \cos\varphi- \\
&\omega t \in [(2k-1)\pi, 2k\pi], k = 1, 2, \cdots
\end{aligned}
\tag{5.97}
$$

The projection of (5.91) on axis Oz results in the following:

$$M_z^e = M_\varphi^e + M_\psi^e \cos\theta \tag{5.98}$$

By substituting the values of the moments (5.58) or (5.59), (5.75) or (5.76) into (5.98), the following is obtained:

$$
\begin{aligned}
M_z^e = &\left[P_1\cos\theta \cdot htan\gamma_k + f\left(\tfrac{H}{2}\cos\delta \cdot \sin\omega t + P_1\sin\gamma\right)\cos\left(\alpha_{K_1 max}\sin\omega t - \gamma\right)\right.\\
&\left.\times \cos\theta \cdot htan\gamma_k - \tfrac{c_1 h_1^3 \varphi sin^2\gamma_k}{3\cos^3\gamma_k}\right] + \left[P_1(htan\gamma_k - h\theta) + f\left(\tfrac{H}{2}\cos\delta \cdot \sin\omega t + P_1\sin\gamma\right)\right.\\
&\left.\cos\left(\alpha\sin\omega_{K_1 max}()r(htan\gamma_k - h\theta)\tfrac{c\pi h_1^4 \cdot sin\gamma_k \cdot \theta\psi}{4\cos^3\gamma_k}\right) \times \big(\cos(\gamma_k - \theta) + \cos(\gamma_k + \psi)\big)\right]\cos\theta, \\
&\omega t \in [2k\pi, (2k+1)\pi], k = 0, 1, 2, \cdots,
\end{aligned}
\tag{5.99}
$$

or:

$$
\begin{aligned}
M_z^e = &\left[P_1\cos\theta \cdot h \cdot tan\gamma_k + \tfrac{1}{2}fP_1\sin 2\gamma \cdot \cos\theta \cdot h \cdot tan\gamma_k - \tfrac{c_1 h_1^3 \cdot \varphi \cdot sin^2\gamma_k}{3\cos^3\gamma_k}\right] \\
&\omega t \in [(2k-1)\pi, 2k\pi], k = 1, 2, \cdots
\end{aligned}
\tag{5.100}
$$

Thereby, the resultant moments M_x^e, M_y^e and M_z^e, which are terms of the system of equations (5.54), have been determined.

Further, it is necessary to determine the axial moments of inertia I_x, I_y and I_z, which are also terms of the mentioned system of equations. It is assumed that

the root's mass is m_k and its height is h_k. Subsequently, the radius of the root as a cone-shaped solid is equal to:

$$r_k = h_k \cdot tan\gamma_k \tag{5.101}$$

Further, the system of coordinates $Cx_cy_cz_c$ with its origin at the centre of mass of the root (point C) is defined, where axis Cx_c is parallel to axis Ox, axis Cy_c is parallel to axis Oy and axis Cz_c lies in axis Oz. Subsequently, in accordance with [32]:

$$I_{z_C} = \frac{3}{10}m_k r_k^2 \tag{5.102}$$

$$I_{x_C} = I_{y_C} = \frac{3}{20}m_k\left(\frac{1}{4}h_k^2 + r_k^2\right) \tag{5.103}$$

Additionally, it is obvious that:

$$I_z = I_{z_C} = \frac{3}{10}m_k r_k^2 \tag{5.104}$$

The following is obtained by the Huygens–Steiner theorem:

$$I_x = I_{x_C} + m_k\left(\frac{2}{3}h_k\right)^2 \tag{5.105}$$

or:

$$I_x = \left(\frac{347}{720} + \frac{3}{20}tan^2\gamma_k\right)m_k \cdot h_k^2 \tag{5.106}$$

Since $I_{y_C} = I_{x_C}$, the following is finally arrived at:

$$I_y = I_x = \left(\frac{347}{720} + \frac{3}{20}tan^2\gamma_k\right)m_k \cdot h_k^2 \tag{5.107}$$

Thus, the root's moments of inertia about axes Ox, Oy and Oz have been determined. Thereafter, by substituting (5.93) or (5.94), (5.96) or (5.97), (5.99) or (5.100), (5.104), (5.107) into the system of Equations (5.45) and taking into account (5.2) and (5.47), after some transformations, the system of differential equations that describe the root's motion in the case of asymmetric gripping by the vibrating digging

tool at the first stage of extraction is obtained. This system of equations appears as follows:

$$\left(0.48 + 0.15 \tan^2 y_k\right) m_k h_k^2 \frac{d\omega_x}{dt} + \left(0.15 \tan^2 \gamma_k + 0.52\right) m_k h_k^2 \omega_y \omega_z$$
$$= \left[-P_1(h \tan \gamma_k - h\theta)\right.$$
$$-f(0.5H \cos \delta \cdot \sin \omega t + P_1 \sin \gamma) \cos\left(\alpha_{K_1 max} \sin \omega t - \gamma\right)(h \tan \gamma_k - h\theta)$$
$$\left.+ \frac{c\pi h_1^4 \sin \gamma_k \cdot \theta \psi (\cos(\gamma_k - \theta) - \cos(\gamma_k + \psi))}{4 \cos^3 \gamma_k}\right] \sin \theta \cdot \sin \varphi$$
$$+ \left[-0.5Hh \tan \gamma_k \cdot \sin \omega t + hP_1 \sin \psi\right.$$
$$+ f(0.5H \cos \delta \cdot \sin \omega t + P_1 \sin \gamma) \cos\left(\alpha_{K_1 max} \sin \omega t - \gamma\right) \sin \psi \cdot h + \tfrac{2}{3} G_k$$
$$\left.\cdot h_k \cdot \theta - \frac{c\pi h_1^4 \cdot \sin \gamma_k \cdot \theta \cdot \cos \psi}{4 \cos^3 \gamma_k}\right] \cos \varphi,$$

$$\left(0.48 + 0.15 \tan^2 y_k\right) m_k h_k^2 \frac{d\omega_y}{dt} + \left(0.48 - 0.15 \tan^2 \gamma_k\right) m_k h_k^2 \omega_z \omega_x$$
$$= \left[-P_1(h \tan \gamma_k - h\theta)\right.$$
$$-f(0.5H \cos \delta \cdot \sin \omega t + P_1 \sin \gamma) cos\left(\alpha_{K_1 max} \sin \omega t - \gamma\right)(h \tan \gamma_k - h\theta)$$
$$\left.+ \frac{c\pi h_1^4 \sin \gamma_k \cdot \theta \psi (\cos(\gamma_k - \theta) - \cos(\gamma_k + \psi))}{4 \cos^3 \gamma_k}\right] \sin \theta \cdot \cos \varphi$$
$$- \left[-0.5Hh \tan \gamma_k \cdot \sin \omega t + hP_1 \sin \psi\right. \tag{5.108}$$
$$+ f(0.5H \cos \delta \cdot \sin \omega t + P_1 \sin \gamma) cos\left(\alpha_{K_1 max} \sin \omega t - \gamma\right) \sin \psi \cdot h + \tfrac{2}{3} G_k$$
$$\left.\cdot h_k \cdot \theta - \frac{c\pi h_1^4 \cdot \sin \gamma_k \cdot \theta \cdot \cos \psi}{4 \cos^3 \gamma_k}\right] \sin \varphi,$$

$$0.3 m_k h_k^2 \tan^2 \gamma_k \frac{d\omega_z}{dt}$$
$$= hP_1 \cos \theta \cdot \tan \gamma_k + f(0.5H \cos \delta \cdot \sin \omega t + P_1 \sin \gamma)$$
$$\cdot \cos\left(\alpha_{K_1 max} \cdot \sin \omega t - \gamma\right) \cos \theta \cdot \tan \gamma_k h - \frac{c_1 h_1^3 \cdot \varphi \cdot \sin^2 \gamma_k}{3 \cos^3 \gamma_k}$$
$$+ \left[P_1(h \tan \gamma_k - h\theta)\right.$$
$$+ f(0.5H \cos \delta \cdot \sin \omega t + P_1 \sin \gamma) cos\left(\alpha_{K_1 max} \sin \omega t - \gamma\right)(h \tan \gamma_k - h\theta)$$
$$\left.+ \frac{c\pi h_1^4 \cdot \theta \cdot \psi \cdot \sin \gamma_k (\cos(\gamma_k - \theta) - \cos(\gamma_k + \psi))}{4 \cos^3 \gamma_k}\right] \cos \theta,$$

$$\omega_1 = -\dot{\psi} \sin \theta \cdot \sin \varphi - \dot{\theta} \cos \varphi,$$
$$\omega_2 = -\dot{\psi} \sin \theta \cdot \cos \varphi - \dot{\theta} \sin \varphi,$$
$$\omega_3 = -\dot{\psi} \cos \theta - \dot{\varphi},$$
$$\omega t \in \left[2k\pi, (2k+1)\pi\right] \qquad k = 0, 1, 2, \ldots\ldots$$

or

$$
\left.\begin{aligned}
&\left(0.48 + 0.15\tan^2\gamma_k\right)m_k h_k^2\frac{d\omega_x}{dt} + \left(0.15\tan^2\gamma_k + 0.52\right)m_k\cdot h_k^2\cdot\omega_y\cdot\omega_z \\
&= \left[-P_1(h\tan\gamma_k - h\cdot\theta) - \tfrac{1}{2}fP_1\sin 2\gamma\,(h\cdot\tan\gamma_k - h\cdot\theta)\right. \\
&\quad \left. + \frac{c\pi h_1^4\sin\gamma_k\cdot\theta\cdot\psi}{4\cos^3\gamma_k}\left(\cos(\gamma_k - \theta) + \cos(\gamma_k + \psi)\right)\right]\sin\theta\cdot\sin\varphi \\
&\quad + \left[hP_1\sin\psi + \tfrac{1}{2}fhP_1\sin 2\gamma\cdot\sin\psi + \tfrac{2}{3}G_k h_k\theta - \frac{c\pi h_1^4\sin\gamma_k\cdot\theta\cdot\cos\psi}{4\cos^3\gamma_k}\right]\cos\varphi, \\
&\left(0.48 + 0.15\tan^2\gamma_k\right)m_k h_k^2\frac{d\omega_y}{dt} + \left(0.48 - 0.15\tan^2\gamma_k\right)m_k h_k^2\omega_z\omega_x \\
&= \left[-P_1(h\tan\gamma_k - h\theta) - 0.5fP_1\sin 2\gamma\,(h\tan\gamma_k - h\cdot\theta)\right. \\
&\quad \left. + \frac{c\pi h_1^4\sin\gamma_k\cdot\theta\cdot\psi}{4\cos^3\gamma_k}\left(\cos(\gamma_k - \theta) + \cos(\gamma_k + \psi)\right)\right]\sin\theta\cdot\cos\varphi \\
&\quad - \left[hP_1\sin\psi + 0.5fhP_1\sin 2\gamma\cdot\sin\psi + \tfrac{2}{3}G_k h_k\theta - \frac{c\pi h_1^4\sin\gamma_k\cdot\theta\cdot\cos\psi}{4\cos^3\gamma_k}\right]\sin\varphi, \\
&0.3m_k h_k^2\tan^2\gamma_k\frac{d\omega_z}{dt} = hP_1\cos\theta\cdot\tan\gamma_k + 0.5fhP_1\sin 2\gamma\cdot\cos\theta\cdot\tan\gamma_k \\
&\quad - \frac{c_1 h_1^3\varphi\cdot\sin^2\gamma_k}{3\cos^3\gamma_k} + \left[P_1(h\tan\gamma_k - h\theta) + 0.5fP_1\sin 2\gamma\,(h\tan\gamma_k - h\theta)\right. \\
&\quad \left. - \frac{c\pi h_1^4\theta\cdot\sin\gamma_k\cdot\psi}{4\cos^3\gamma_k}\left(\cos(\gamma_k - \theta) + \cos(\gamma_k + \psi)\right)\right]\cos\theta, \\
&\omega_x = -\dot\psi\sin\theta\cdot\sin\varphi - \dot\theta\cos\varphi, \\
&\omega_y = -\dot\psi\sin\theta\cdot\cos\varphi + \dot\theta\sin\varphi, \\
&\omega_z = \dot\psi\cos\theta + \dot\varphi, \\
&\omega t \in \left[(2k-1)\pi, 2k\pi\right], \quad k = 1, 2, \cdots
\end{aligned}\right\} \quad (5.109)
$$

It is obvious that the above systems of differential equations must meet the following initial conditions: at $t = 0$:

$$
\varphi(0) = 0, \psi(0) = 0, \theta(0) = 0, \acute{\varphi}(0) = 0, \acute{\psi}(0) = 0, \acute{\theta}(0) = 0. \quad (5.110)
$$

Since (5.108) contains the moments of the restoring forces (the soil's resistance forces), the system describes the three-dimensional process of the root's oscillations in the soil as an elastic medium. The integration of systems of differential equations such as (5.108) or (5.109) poses considerable mathematical difficulties. Obtaining an analytical solution is impossible. This system of equations can be solved only with the use of numerical techniques with the assistance of modern PCs.

If (5.109) is considered by itself, it describes the motion of the root in case the digging tool grips it asymmetrically in the absence of the action of perturbing forces—i.e., when $\overline{Q}_{zb.} = 0$.

Thus, by applying the original kinematic and dynamic Euler equations, the system of differential equations of the root's oscillations during its vibrational digging for the case when the root interacts with one wedge of the vibrating digging tool at one of its points has been set up. In the next part of the study, the case when the root interacts with both wedges of the vibrating digging tool is investigated.

5.2. Differential Equations of a Root's Angular Oscillations in Soil During Symmetric Gripping by a Vibrating Digging Tool

As was noted above, the gripping of the root by the vibrating digging tool on only one side lasts for a short while. As a result of the lifter's translational motion and the necking of the working channel, at the next stage the digging tool proceeds to gripping the root on both sides. At the same time, if the root has no offset from the row's centreline (i.e., it is situated strictly on the centreline of the row) and is on the axis of symmetry of the vibrating digging tool, the root will be gripped on both sides from the beginning (known as symmetric gripping).

This is the kind of gripping of the root by the digging shares that enables the process of complete extraction of the root from the soil. Therefore, the following investigation deals with the process of the root extraction in the case of symmetric gripping by the tool at the first stage of extraction (when the root is still fast bonded with the soil).

It is necessary to set up the equivalent schematic model of the interaction between the root and the working faces of the vibrating digging tool in the case of symmetric gripping (Figure 5.2).

Distinct from asymmetric gripping, in the case of symmetric gripping the interaction forces appear on the working faces of both shares, as is shown in Figure 5.2. At the points of contact K_1 and K_2 between the root and the respective wedge faces $A_1B_1C_1$ and $A_2B_2C_2$, the root is under the action of the perturbing forces $\overline{Q}_{zb.1}$ and $\overline{Q}_{zb.2}$, respectively.

We resolved these perturbing forces into the normal components $\overline{N}_1$ and $\overline{N}_2$ and tangential components $\overline{T}_1$ and $\overline{T}_2$, as shown in Figure 5.2. The compositions of the forces will be as follows:

$$\overline{Q}_{zb.1} = \overline{N}_1 + \overline{T}_1 \tag{5.111}$$

$$\overline{Q}_{zb.2} = \overline{N}_2 + \overline{T}_2 \tag{5.112}$$

Apparently, the lines of the force vectors $\overline{T}_1$ and $\overline{T}_2$ will be parallel to the right lines B_1M_1 and B_2M_2, respectively.

As the vibrational lifting tool advances linearly along axis O_1x_1 with respect to the beet root fixed in the soil, at the moment when the tool grips the root, there are also moving forces $\overline{P}_1$ and $\overline{P}_2$ acting along axis O_1x_1. We resolved the moving forces $\overline{P}_1$ and $\overline{P}_2$ into the normal components $\overline{L}_1$ and $\overline{L}_2$ and tangential components $\overline{S}_1$ and $\overline{S}_2$ with reference to planes $A_1B_1C_1$ and $A_2B_2C_2$, respectively—i.e.,

$$\overline{P}_1 = \overline{L}_1 + \overline{S}_1 \tag{5.113}$$

$$\overline{P}_2 = \overline{L}_2 + \overline{S}_2 \tag{5.114}$$

The force vectors $\bar{S}_1$ and $\bar{S}_2$ act along the vector lines of speed of the shares relative to the root surface during the translational motion of the vibrational lifting tool.
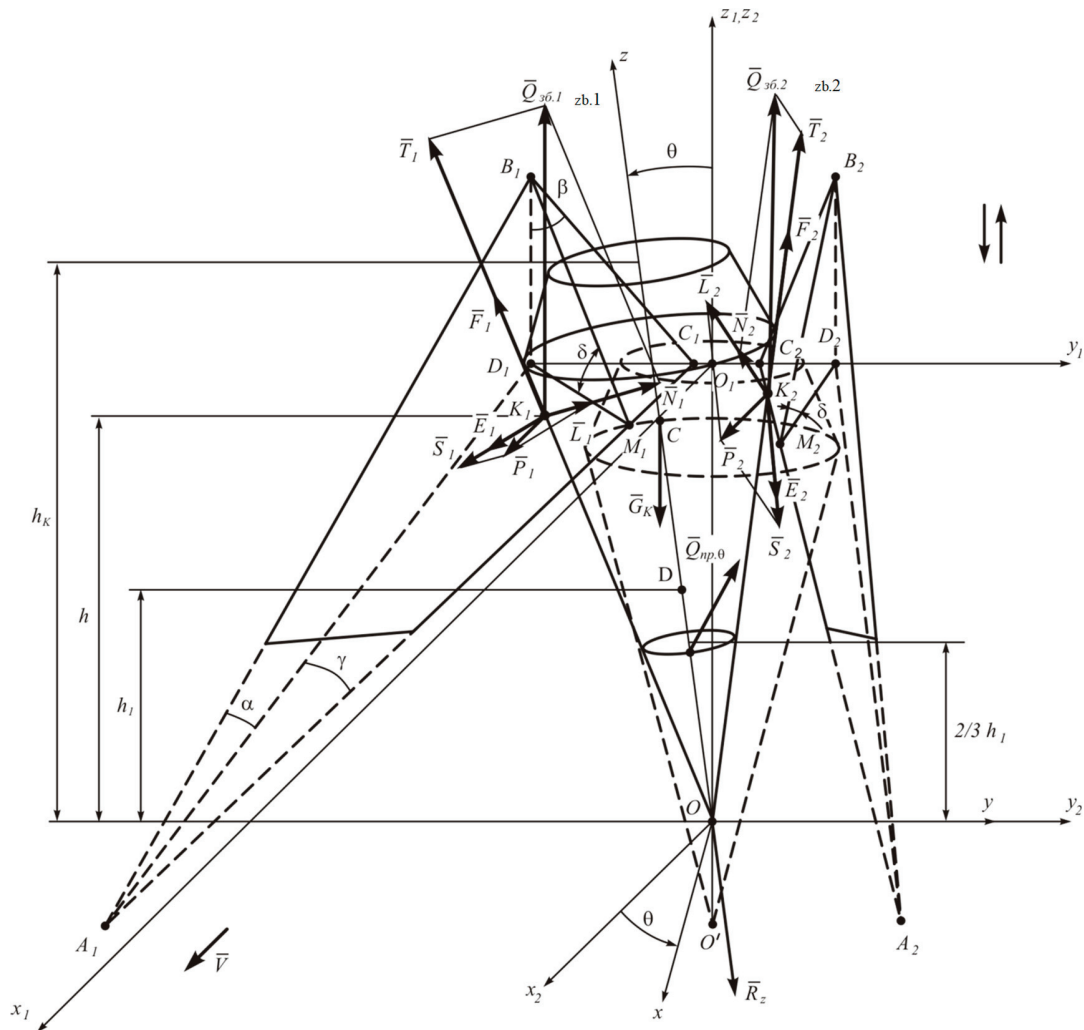
Figure 5.2. Force interaction between root and wedges of vibrating digging tool in the case of symmetric gripping of root.

Thus, the lifting wedges $A_1B_1C_1$ and $A_2B_2C_2$ exert the following forces on the sugar beet root at the contact points K_1 and K_2:

$$\bar{N}_{K1} = \bar{N}_1 + \bar{L}_1, \tag{5.115}$$

$$\bar{N}_{K_2} = \bar{N}_2 + \bar{L}_2, \tag{5.116}$$

which act along the normal to planes $A_1B_1C_1$ and $A_2B_2C_2$, respectively.

Obviously, the magnitudes of these forces are as follows:

$$N_{K_1} = N_1 + L_1 \tag{5.117}$$

$$N_{K_2} = N_2 + L_2 \qquad (5.118)$$

In addition to this, at the contact points K_1 and K_2 the friction forces $\overline{F}_{K1}$ and $\overline{F}_{K2}$, respectively, are applied, which counteract the slipping of the beet root body on the working surfaces of wedges $A_1B_1C_1$ and $A_2B_2C_2$ when the lifting tool grips the root. The vectors of these forces have opposite directions that those of the vectors of the relative speed of the beet root slipping on the surfaces of said wedges.

At the root's centre of gravity (point C), the root weight force $\overline{G}_k$ is applied. The forces of resistance exerted by the loosened soil during the beet root's movement in the working passage of the vibrational lifting tool along axis O_1z_1 are designated as $\overline{R}_{z1}$.

In contrast to asymmetric gripping, symmetric gripping does not cause the root to rotate about its centreline Oz ($\phi = 0$) or to rotate about axis Oz_2 ($\psi = 0$). The only rotation of the root that takes place is its rotation about axis Oy_2 through an angle of θ along the line of translational motion of the vibrational lifter (i.e., along axis Ox_2).

At the same time, it ought to be noted that the rotation of a solid about one of the axes is not always a special case of a solid's motion around a fixed point. This becomes evident from the analysis of the kinematic Euler equations. For example, it is impossible to derive the kinematic relations for the rotation of the solid about axis Oy_2 from these equations, which is what occurs in the case under consideration. Therefore, this case has to be investigated separately as the rotation of a solid about a fixed axis.

Moreover, in the case of symmetric gripping the point of fixation in the soil, O oscillates in the longitudinal and vertical plane.

Thereby, in this case the soil's elastic forces $\overline{Q}_{np.\varphi}$ and $\overline{Q}_{np.\psi}$ are absent. The only restoring force that acts during the oscillations of the root about point O is force $\overline{Q}_{np.\theta}$, and during the oscillations of the point of fixation O—forces $\acute{R}_{z1}$ and $\acute{R}_{x1}$.

Now, we are going to find the magnitudes of the forces shown in Figure 5.2. The tangential components $\acute{T}_1$ and $\acute{T}_2$ of the perturbing forces $\overline{Q}_{zb.1}$, and $\overline{Q}_{zb.2}$, respectively, and the tangential components $\acute{S}_1$ and $\acute{S}_2$ of the moving forces $\acute{P}_1$ and $\acute{P}_1$, respectively, do not have any direct effect on the beet root—they only produce loosening of the soil around the root.

It should be noted, taking into account the symmetry of the beet root gripping by the vibrational lifting tool, that the same forces generated on the two share working surfaces during their interaction with the beet root will have equal magnitudes and symmetrical lines of action with respect to the symmetry plane $x_1O_1z_1$ (Figure 4.2). Accordingly, from the schematic model of forces we derive the formulae for finding

the normal components $\acute{N}_1$ and $\acute{N}_2$ and the tangential components $\acute{T}_1$ and $\acute{T}_2$ of the perturbing forces $\overline{Q}_{zb.1}$, and $\overline{Q}_{zb.2}$. They have the following values:

$$N_1 \ = \ N_2 \ = \ Q_{zb.1} \tag{5.119}$$

$$T_1 \ = \ T_2 \ = \ Q_{zb.1}sin\delta \tag{5.120}$$

From the same schematic force model the formulae for finding the normal components $\acute{L}_1$ and $\acute{L}_1$ and tangential components $\acute{S}_1$ and $\acute{S}_2$ of the moving forces $\acute{P}_1$ and $\acute{P}_2$, respectively, can be derived:

$$L_1 \ = \ L_2 \ = \ P_1 sin\gamma \tag{5.121}$$

$$S_1 \ = \ S_2 \ = \ P_1 cos\gamma \tag{5.122}$$

The magnitudes of forces $\acute{N}_{K1}$ and $\acute{N}_{K2}$ are as follows, taking into account (5.117), (5.119) and (5.121):

$$N_{K1} \ = \ N_{K2} \ = \ Q_{zb.1}cos\delta + P_1 sin\gamma \tag{5.123}$$

or, considering (5.2), we come to the following:

$$N_{K1} \ = \ N_{K2} \ = \ 0.5Hcos\delta sin\omega t + P_1 sin\gamma \tag{5.124}$$

Hence, the magnitudes of the friction forces $\acute{F}_{K1}$ and $\acute{F}_{K2}$ are:

$$F_{K1} \ = \ F_{K2} \ = \ fN_{K1} \ = \ f(Q_{zb.1}cos\delta + P_1 sin\gamma) \tag{5.125}$$

or, considering (5.2), we come to:

$$F_{K1} \ = \ F_{K2} \ = \ 0.5fHcos\delta sin\omega t + fP_1 sin\gamma \tag{5.126}$$

where f—coefficient of friction.

Apparently, during the immediate contact between wedges $A_1B_1C_1$ and $A_2B_2C_2$ and the beet root surface, the friction force vectors $\acute{F}_{K1}$ and $\acute{F}_{K2}$ always lie in wedge planes $A_1B_1C_1$ and $A_2B_2C_2$, respectively. In addition to this, due to the soil resistance forces, the slipping of the beet root on the surfaces of the wedges along the lines of action of forces $\acute{T}_1$, $\acute{T}_2$ (parallel to the lines B_1M_1 and B_2M_2) and in the direction opposite to forces $\acute{S}_1$ and $\acute{S}_2$ is possible.

The above-mentioned slipping can result from the action of forces $\overline{Q}_{zb.1}$, $\overline{Q}_{zb.2}$ and $\acute{P}_1$, $\acute{P}_2$, respectively. Therefore, the vector of the relative speed of the beet root slipping on the surfaces of the wedges can be resolved into components in the above-said directions. Thus, the friction force $\acute{F}_{K1}$ can also be resolved into two

components: $\acute{F}_1$—in the direction opposite to the vector $\acute{T}_1$, and $\acute{E}_1$—in the direction of the vector $\acute{S}_1$—i.e.,

$$\acute{F}_{K1} = \acute{F}_1 + \acute{E}_1 \tag{5.127}$$

Similarly, the friction force $\acute{F}_{K2}$ can be resolved into two components as well: $\acute{F}_2$—in the direction opposite to the vector $\acute{T}_2$, and $\acute{E}_2$—in the direction of the vector $\acute{S}_2$—i.e.,

$$\acute{F}_{K2} = \acute{F}_2 + \acute{E}_2 \tag{5.128}$$

Obviously, $F_1 = F_2$, $E_1 = E_2$.

Now, let us find the magnitudes of the components of forces $\acute{F}_1$ and $\acute{E}_1$, and consequently $\acute{F}_2$ and $\acute{E}_2$. Based on the above considerations, a deduction can be made that in the intervals $[2k\pi, (2k + 1)\pi]$, $k = 0, 1, 2, \ldots$, particularly in the interval $[0, \pi]$, the magnitude of the friction force $\acute{F}_{K1}$ ($\acute{F}_{K2}$) shall be determined in accordance with (5.18); moreover, in the interval $[0, \pi/2]$ $\left[0, \frac{\pi}{2}\right]$, it rises from its minimum value:

$$\acute{F}_{K1min} = \acute{F}_{K2min} = fP_1 sin\gamma \tag{5.129}$$

to the maximum value:

$$\acute{F}_{K1max} = \acute{F}_{K2max} = \frac{1}{2}fHcos\delta + fP_1 sin\gamma \tag{5.130}$$

While in the interval $[\pi/2, \pi]$. $\left[\frac{\pi}{2}, \pi\right]$ it decreases from $\acute{F}_{K1max}$ ($\acute{F}_{K2max}$) to $\acute{F}_{K1max}$ ($\acute{F}_{K2max}$). Besides that, the direction of the friction force vector in the interval $\left[0, \frac{\pi}{2}\right]$. also changes. The vector $\acute{F}_{K1min}$ ($\acute{F}_{K2min}$) has the same direction as the friction force vector of a usual share lifter (in the absence of any perturbing force), i.e., parallel to the right lines A_1O_1' (A_2O_2'), while $\angle O_1'A_1M_1 = \angle O_2'A_2M_2 = \gamma$ (Section 2). The vector $\acute{F}_{K1max}$ ($\acute{F}_{K2max}$) deflects from the vector $\acute{F}_{K1min}$ ($\acute{F}_{K2min}$) through a certain angle α_{K1max} (α_{K2max}), while $\alpha_{K1max} = \alpha_{K2max}$

Therefore, in the interval $\left[0, \frac{\pi}{2}\right]$ the force vector $\acute{F}_{K1}$ ($\acute{F}_{K2}$) changes from the vector $\acute{F}_{K1min}$ ($\acute{F}_{K2min}$) to the vector $\acute{F}_{K1max}$ ($\acute{F}_{K2max}$), and in the interval $\left[\frac{\pi}{2}, \pi\right]$—from the vector $\acute{F}_{K1max}$ ($\acute{F}_{K2max}$) to the vector $\acute{F}_{K1min}$ ($\acute{F}_{K2min}$). Hence, the angle α_{K1} (α_{K2}) of the deflection of the vector $\acute{F}_{K1}$ ($\acute{F}_{K2}$) from the vector $\acute{F}_{K1min}$ ($\acute{F}_{K2min}$) changes in the interval $[0, \pi]$ under the following law:

$$\alpha_{K2} = \alpha_{K1} = \alpha_{K1max} sin\omega t \tag{5.131}$$

Apparently, the value α_{K1max} (α_{K2max}) depends first of all on the ratio $\frac{H}{P_1}\left(\frac{H}{P_2}\right)$ $\frac{H}{P_1}\left(\frac{H}{P_2}\right)$ and the greater the ratio is, the greater the value grows. Therefore, in the interval $[0, \pi]$ the magnitude of the friction force vector $\acute{F}_{K1}$ ($\acute{F}_{K2}$) changes according to (5.126), while its direction—according to (5.131).

Therefore, in the interval $[0, \pi]$ we have the following values of the component forces $\acute{F}_1$ ($\acute{F}_2$) and $\acute{E}_1$ ($\acute{E}_2$):

$$F_1 = F_2 = F_{K1}\sin(\alpha_{K1} - \gamma) \tag{5.132}$$

$$E_1 = E_2 = F_{K1}\cos(\alpha_{K1} - \gamma) \tag{5.133}$$

then, taking into account (5.126) and (5.131), we obtain:

$$F_1 = F_2 = \left(\frac{1}{2}fH\cos\delta\cdot\sin\omega t + fP_1\sin\gamma\right)\sin(\alpha_{K1max}\sin\omega t - \gamma) \tag{5.134}$$

$$E_1 = E_2 = \left(\frac{1}{2}fH\cos\delta\cdot\sin\omega t + fP_1\sin\gamma\right)\cos(\alpha_{K1max}\sin\omega t - \gamma) \tag{5.135}$$

(5.134) and (5.135) are effective in any of the intervals $[2k\pi, (2k + 1)\pi]$, $k = 0, 1, 2,$ ...

Obviously, within the intervals $[(2k + 1)\pi, 2k\pi]$, $k = 0, 1, 2, \ldots$, the friction forces $\acute{F}_{K1}$ ($\acute{F}_{K2}$) are as follows:

$$F_{K1} = F_{K2} = F_{K1min} = fP_1\sin\gamma \tag{5.136}$$

Hence, the following is observed in the denoted intervals:

$$F_1 = F_2 = F_{K1min}\sin\gamma = fP_1\sin\gamma\cdot\sin\gamma = fP_1\sin^2\gamma \tag{5.137}$$

$$E_1 = E_2 = F_{K1min}\cos\gamma = fP_1\sin\gamma\cdot\cos\gamma = \frac{1}{2}fP_1\sin2\gamma \tag{5.138}$$

The soil's elastic force $\overline{Q}_{np.\theta}$ is determined in accordance with (5.39).

The bonding force $\overline{R}_{z1}$ between the root and the soil is also determined with (5.44).

Further, the differential equation of the root's rotational motion about axis O_{y1} has to be set up. In accordance with [32], the required equation appears as follows:

$$I_{y2}\frac{d^2\theta}{dt^2} = M^e_{y2} \tag{5.139}$$

where θ—angular displacement of the root about axis O_{y2}; I_{y2}—moment of inertia of the root about axis O_{y2}; M^e_{y2}—moment of force about axis O_{y2} (sum of the moments of all external forces acting on the root about axis O_{y2}).

The moments of all external forces about axis O_{y2} are determined in accordance with the schematic model of forces shown in Figure 5.2. These moments are equal to:

$$M_{y2}\left(\overline{Q}_{zb.1}\right) = M_{y2}\left(\overline{Q}_{zb.2}\right) = -Q_{zb.1}h\theta \tag{5.140}$$

since the vectors of forces $\overline{Q}_{zb.1}$ and $\overline{Q}_{zb.2}$ are parallel to plane $x_2 O z_2$.

$$M_{y_2}\left(\overline{P}_1\right) = M_{y_2}\left(\overline{P}_2\right) = P_1 \cos \theta h \tag{5.141}$$

since the vectors of forces $\overline{P}_1$ and $\overline{P}_2$ are parallel to plane $x_2 O z_2$.

$$M_{y_2}\left(\overline{F}_1\right) = M_{y_2}\left(\overline{F}_2\right) = 0 \tag{5.142}$$

since the vectors of forces $\overline{F}_1$ and $\overline{F}_2$ intersect axis $O y_2$.

$$M_{y_2}\left(\overline{E}_1\right) = M_{y_2}\left(\overline{E}_2\right) = E_1 \cos \gamma \cdot h \cos \theta \tag{5.143}$$

Taking into account (5.135), the following is obtained:

$$\begin{aligned} M_{y_2}\left(\overline{E}_1\right) &= M_{y_2}\left(\overline{E}_2\right) \\ &= (0.5 f H \cos \delta \cdot \sin \omega t + f P_1 \sin \gamma) \\ &\cdot \cos(\alpha_{K1max} \sin \omega t - \gamma) \cos \gamma \cdot h \cos \theta, \\ \omega t &\in [2k\pi, (2k+1)\pi], \quad k = 0, 1, 2, \dots . \end{aligned} \tag{5.144}$$

or, taking into account (5.138), the result is:

$$\begin{aligned} M_{y_2}\left(\overline{E}_1\right) = M_{y_2}\left(\overline{E}_2\right) &= 0.5 f P_1 \sin 2\gamma \cdot \cos \gamma \cdot h \cos \theta, \\ \omega t &\in [(2k-1)\pi, 2k\pi], \quad k = 1, 2, \dots . \end{aligned} \tag{5.145}$$

$$M_{y_2}\left(\overline{G}_k\right) = \frac{2}{3} G_k h_k \theta \tag{5.146}$$

$$M_{y_2}\left(\overline{R}_{z_1}\right) = 0 \tag{5.147}$$

since the vector of force $\overline{R}_{z_1}$ intersects axis $O y_2$.

$$M_{y_2}\left(\overline{Q}_{np.\theta}\right) = -\frac{2}{3} Q_{np.\theta} h_1 \cos(\gamma_k + \theta) \tag{5.148}$$

or, taking into account (5.39), the following is arrived at:

$$M_{y_2}\left(\overline{Q}_{np.\theta}\right) = -\frac{2 c \pi h_1^4 \theta \sin \gamma_k \cdot \cos(\gamma_k + \theta)}{9 \cos^3 \gamma_k} \tag{5.149}$$

Hence, taking into account (5.140), (5.141), (5.144) or (5.145), (5.146), (5.147) and (5.149) of the moments, the magnitude of the rotary moment $M^e_{y_2}$ of all external forces about axis Oy_2 is obtained as follows:

$$
\begin{aligned}
M^e_{y_2} &= -2Q_{zb.1}h\theta + 2P_1\cos\theta h + (fH\cos\delta\cdot\sin\omega t + 2fP_1\sin\gamma) \\
&\cdot\cos\!\left(\alpha_{K_1,max}\sin\omega t - \gamma\right)\cos\gamma\cdot\cos\theta + \tfrac{2}{3}G_kh_k\theta - \frac{2c\pi h_1^4\theta\sin\gamma_k\cdot\cos(\gamma_k+\theta)}{9\cos^3\gamma_k} \\
&\omega t\in[2k\pi,(2k+1)\pi],\quad k = 0,1,2,\dots
\end{aligned}
\tag{5.150}
$$

or

$$
\begin{aligned}
M_{\gamma_2} &= -2P_1\cos\theta h + fP_1\sin2\gamma\cdot\cos\gamma\cdot h\cos\theta + \tfrac{2}{3}G_kh_k\theta \\
&-\frac{2c\pi h_1^4\theta\sin\gamma_k\cdot\cos(\gamma_k+\theta)}{9\cos^3\gamma_k} \\
&\omega t\in[(2k-1)\pi,2k\pi],\quad k = 1,2,\dots
\end{aligned}
\tag{5.151}
$$

The moment of the root's inertia I_{y2} about axis O_{y2} is determined with (5.107).

By substituting (5.2), (5.107) and (5.150) or (5.151) into the differential Equation (5.139) and carrying out certain transformations, the differential equation of the root's rotational motion about axis O_{y2} is obtained, which appears as follows:

$$
\begin{aligned}
&\left(0.48 + 0.15\tan^2 y_k\right)m_k h_k^2\frac{d^2\theta}{dt^2} \\
&= -Hh\theta\sin\omega t + 2P_1\cos\theta h \\
&+(fH\cos\delta\cdot\sin\omega t + 2fP_1\sin\gamma)\cos\!\left(\alpha_{K_1max}\sin\omega t - \gamma\right)\cdot\cos\gamma\cdot h\cos\theta \\
&+\tfrac{2}{3}G_kh_k\theta\frac{2c\pi h_1^4\sin\gamma_k\cdot\cos(\gamma_k-\theta)}{9\cos^3\gamma_k} \\
&\omega t\in[2k\pi,(2k+1)\pi],\quad k = 0,1,2,\dots
\end{aligned}
\tag{5.152}
$$

or

$$
\begin{aligned}
&\left(0.48 + 0.15\tan^2 y_k\right)m_k h_k^2\frac{d^2\theta}{dt^2} \\
&= 2P_1\cos\theta h + fP_1\sin2\gamma \\
&+ \cos\gamma\cdot h\cos\theta + \tfrac{2}{3}G_kh_k\theta\frac{2c\pi h_1^4\sin\gamma_k\cdot\cos(\gamma_k-\theta)}{9\cos^3\gamma_k} \\
&\omega t\in[(2k-1)\pi,2k\pi],\quad k = 1,2,\dots
\end{aligned}
\tag{5.153}
$$

The initial conditions for the above differential equation can be written as follows:

$$
\text{at } t = 0: \theta = 0,\ \dot\theta = 0.
\tag{5.154}
$$

By virtue of the fact that the (5.152) and (5.153) contain the moment of restoring force, specifically $M_{y2}\!\left(\overline{Q}_{np.\theta}\right)$, they describe the oscillations of the root about axis O_{y2} in plane $x_2\,O_{z2}$.

The obtained differential equation can only be solved with the use of numerical methods and the PC.

Thus, the differential equations describing the angular oscillations of the root about its fixation point that arise under the action of the vertical perturbing force

imparted on the root by the vibrating digging tool and the tractive force generated by the translational motion of the lifter have been set up.

5.3. Analysis of Translational Oscillations of Root Together with Its Point of Fixation in the Longitudinal and Vertical Plane

Further, it is necessary to analyse the oscillations of the root in the soil together with its point of fixation O in the longitudinal and vertical plane at the first stage of extraction. As noted above, the oscillations under consideration are translational motions; therefore, it is sufficient to analyse the oscillations of a single point of the root—for example, its point of fixation. As the root still remains strongly bonded with the soil, it will oscillate together with the surrounding soil, which remains unbroken in the layer below the cutting edges of the shares. The mass of said soil can be designated as $m_{gr.}$; then, its weight $\overline{G}_{gr.}$ is equal to $G_{gr.} = m_{gr.}g$, where g—acceleration of gravity. As the analysed process is considered for the case of the symmetric gripping of the root by the tool, the schematic model of the forces of interaction between the root and the tool shown in Figure 5.3 will be used for setting up the differential equation that describes the mentioned oscillatory process.
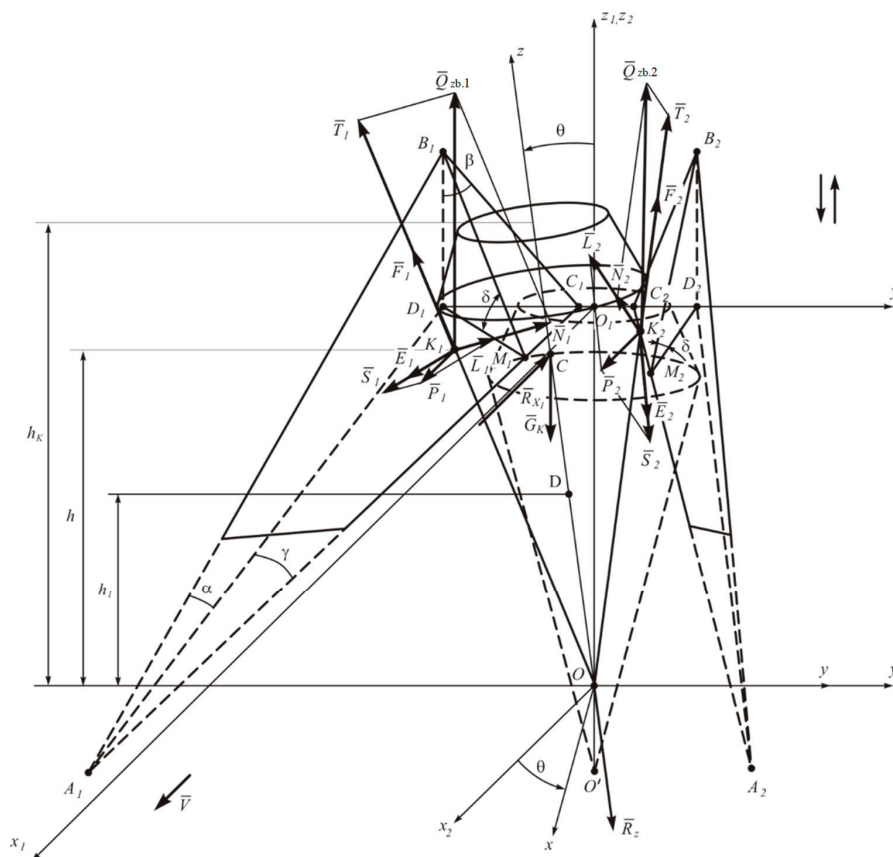
Figure 5.3. Force interaction between root and shares of vibrating digging tool during its translational oscillations together with its conventional point of fixation in soil.

The required differential equation in the vector notation appears as follows:

$$\left(m_k + m_{gr.}\right)\bar{a} = \bar{N}_1 + \bar{N}_2 + \bar{L}_1 + \bar{L}_2 + \bar{F}_1 + \bar{F}_2 + \bar{E}_1 + \bar{E}_2 + \bar{G}_k + \bar{G}_{gr.} + \bar{R}_{z_1} + \bar{R}_{x_1}, \qquad (5.155)$$

where $\bar{a}$—acceleration of the root (i.e., of point O).

In order to analyse the oscillatory process under consideration in detail, (5.155) can be written in its projections on the axes of the Cartesian coordinate system $O_1x_1y_1z_1$. It ought to be noted that in view of the fact that the projections of the normal reactions N_i, L_i ($i = 1, 2$) of the working faces $A_1B_1C_1$ and $A_2B_2C_2$ on axis O_1y have equal magnitudes and opposite senses, the analysed oscillatory process takes place in effect in plane $x_1O_1z_1$ (in the case of symmetric gripping); hence, (5.155) is reduced to the following system of two equations:

$$\left.\begin{array}{l} \left(m_k + m_{gr.}\right)\ddot{x}_1 = N_{1x_1} + L_{1x_1} + N_{2x_1} + L_{2x_1} - F_{1x_1} + E_{1x_1} - F_{2x_1} + E_{2x_1} - R_{x_1}, \\ \left(m_k + m_{gr.}\right)\ddot{z}_1 = N_{1z_1} + L_{1z_1} + N_{2z_1} + L_{2z_1} + F_{1z_1} + E_{1z_1} + E_{2z_1} + E_{2z_1} - G_k - \bar{G}_{gr.} - R_{x_1} \end{array}\right\} \qquad (5.156)$$

Let us determine the values of the force projections on axes Ox_1 and Oz_1 used in the (5.156). As was shown in Section 3, the projections of the normal components $\acute{N}_1$ and $\acute{N}_2$ on axis O_{1x1}, are as follows:

$$N_{1x_1} = N_{2x_1} = \frac{N_1 \tan \gamma}{\sqrt{\tan^2 \gamma + 1 + \tan^2 \beta}}, \qquad (5.157)$$

or, taking into account (5.119), we obtain:

$$N_{1x_1} = N_{2x_1} = \frac{Q_{zb1} \cos \delta \cdot \tan \gamma}{\sqrt{\tan^2 \gamma + 1 + \tan^2 \beta}}. \qquad (5.158)$$

The projections of the normal components $\bar{L}_1$ and $\bar{L}_2$ on axis O_{1x1} have the following values:

$$L_{1x_1} = L_{2x_1} = \frac{L_1 \tan \gamma}{\sqrt{\tan^2 \gamma + 1 + \tan^2 \beta}}. \qquad (5.159)$$

or, taking into account (5.121), we obtain:

$$L_{1x_1} = L_{2x_1} = \frac{P_1 \sin \gamma \cdot \tan \gamma}{\sqrt{\tan^2 \gamma + 1 + \tan^2 \beta}}. \qquad (5.160)$$

For the projections of the friction force components $\bar{F}_1$ and $\bar{F}_2$, the following expressions are obtained:

$$F_{1x_1} = F_{2x_1} = F_1 \cos \delta \cdot \sin \gamma, \tag{5.161}$$

or, taking into account (5.134), we have:

$$F_{1x_1} = F_{2x_1} = (0.5fH \cos \delta \cdot \sin \omega t + fP_1 \sin \gamma) \sin\left(\alpha_{k_1 max} \sin \omega t - \gamma\right) \cos \delta \cdot \sin \gamma,$$
$$\omega t \in [2k\pi, (2k+1)\pi], \ k = 0, 1, 2, \ldots \tag{5.162}$$

Taking into consideration (5.137), we come to:

$$F_{1x_1} = F_{2x_1} = fP_1 \sin^3 \gamma \cdot \cos \delta \ , \omega t \in [(2k-1)\pi, 2k\pi], \ k = 1, 2, \ldots \tag{5.163}$$

The projections of the friction force components $\bar{E}_1$ and $\bar{E}_2$ on axis $O_1 x_1$ will be as follows:

$$E_{1x_1} = E_{2x_1} = E_1 \cos \gamma, \tag{5.164}$$

or, taking into account (5.135), the following expression can be obtained:

$$E_{1x_1} = E_{2x_1} = (0.5fH \cos \delta \cdot \sin \omega t + fP_1 \sin \gamma) \cos\left(\alpha_{k_1 max} \sin \omega t - \gamma\right) \cos \gamma,$$
$$\omega t \in [2k\pi, (2k+1)\pi], \ k = 0, 1, 2, \ldots \tag{5.165}$$

Taking into account (5.138), we obtain:

$$E_{1x_1} = E_{2x_1} = 0.5fP_1 \sin 2\gamma \cdot \cos \gamma, \ \omega t \in [(2k-1)\pi, 2k\pi], \quad k = 1, 2, \ldots \tag{5.166}$$

Force $\bar{R}_{x1}$ is projected on axis Ox_1 at full size. It is determined according to the following expression:

$$R_{x1} = \frac{c\pi h_1^2 \sin \gamma_k}{2 \cos^2 \gamma_k} x_1. \tag{5.167}$$

(5.167) is obtained in the similar way as (5.44).

As was shown in Section 3, the projections of the normal components $\bar{N}_1$ and $\acute{N}$ on axis $O_1 z_1$ are as follows:

$$N_{1z_1} = N_{2z_1} = \frac{N_1 \tan \beta}{\sqrt{\tan^2 \gamma + 1 + \tan^2 \beta}}, \tag{5.168}$$

or, taking into account (5.119), we come to:

$$N_{1z_1} = N_{2z_1} = \frac{Q_{zb1} \cos \delta \cdot \tan \beta}{\sqrt{\tan^2 \gamma + 1 + \tan^2 \beta}} \tag{5.169}$$

The projections of the normal components $\bar{L}_1$ and $\bar{L}_2$ on axis O_1z_1 will be equal to:

$$L_{1z_1} = L_{2z_1} = \frac{L_1 \tan\beta}{\sqrt{\tan^2\gamma + 1 + \tan^2\beta}} \tag{5.170}$$

or, taking into account (5.121), we have:

$$L_{1z_1} = L_{2z_1} = \frac{P_1 \sin\gamma \cdot \tan\beta}{\sqrt{\tan^2\gamma + 1 + \tan^2\beta}} \tag{5.171}$$

The projections of the friction force components $\bar{F}_1$ and $\bar{F}_2$ on axis O_1z_1 will be equal to:

$$F_{1z_1} = F_{2z_1} = F_1 \sin\delta, \tag{5.172}$$

or, taking into account (5.134), we have:

$$F_{1z_1} = F_{2z_1} = (0.5fH\cos\delta\cdot\sin\omega t + fP_1\sin\gamma)\sin\left(\alpha_{k_1 max}\sin\omega t - \gamma\right)\sin\delta,$$
$$\omega t \in [2k\pi, (2k+1)\pi], \ k = 0,1,2,\ldots \tag{5.173}$$

Taking into consideration (5.137), we obtain:

$$F_{1z_1} = F_{2z_1} = fP_1\sin^2\gamma\sin\delta, \quad \omega t \in [(2k-1)\pi, 2k\pi], \quad k = 1,2,\ldots \tag{5.174}$$

The projections of the friction force components $\bar{E}_1$ and $\bar{E}_2$ on axis O_1z_1 are equal to zero in any interval—i.e., $E_{1z1} = E_{2z1} = 0$.

Force $\bar{R}_{z_1}$ is projected on axis O_1z_1 at full size. It is determined according to Expression (4.44) and is the principal restoring force in the oscillatory process under consideration.

By substituting (5.158), (5.160), (5.162) or (5.163), (5.165) or (5.166), (5.167), (5.169), (5.171), (5.173) or (5.174), (5.44) into (5.156), we obtain the following system of differential equations:

$$\left.\begin{array}{l}
\left(m_k + m_{gr.}\right)\ddot{x}_1 = \dfrac{2Q_{zb1}\cdot\cos\delta\cdot\tan\gamma}{\sqrt{\tan^2\gamma+1+\tan^2\beta}} + \dfrac{2P_1\cdot\sin\gamma\cdot\tan\gamma}{\sqrt{\tan^2\gamma+1+\tan^2\beta}} \\[3mm]
-(fH\cos\delta\cdot\sin\omega t + 2P_1\cdot\sin\gamma)\cdot\sin\left(\alpha_{k_1 max}\sin\omega t - \gamma\right)\cdot\cos\delta\cdot\sin\gamma \\[3mm]
+(fH\cos\delta\cdot\sin\omega t + 2P_1\cdot\sin\gamma)\cdot\cos\left(\alpha_{k_1 max}\sin\omega t - \gamma\right)\cos\gamma - \dfrac{c\pi h_1^2 \sin\gamma_k}{2\cos^2\gamma_k}x_1, \\[3mm]
\left(m_k + m_{gr.}\right)\ddot{z}_1 = \dfrac{2Q_{zb1}\cdot\cos\delta\cdot\tan\beta}{\sqrt{\tan^2\gamma+1+\tan^2\beta}} + \dfrac{2P_1\cdot\sin\gamma\cdot\tan\beta}{\sqrt{\tan^2\gamma+1+\tan^2\beta}} + \\[3mm]
(fH\cos\delta\cdot\sin\omega t + 2P_1\cdot\sin\gamma)\cdot\sin\left(\alpha_{k_1 max}\sin\omega t - \gamma\right)\cdot\sin\delta - G_k - G_{gr.} - \dfrac{c_1\pi h_1\sin\gamma_k z_1}{\cos^2\gamma_k} \\[3mm]
\omega t \in [2k\pi, (2k+1)\pi], \quad k = 0,1,2,\ldots
\end{array}\right\} \tag{5.175}$$

143

or:

$$\left(m_k + m_{gr.}\right)\ddot{x}_1 = \frac{2P_1 \cdot \sin\gamma \cdot \tan\gamma}{\sqrt{tan^2\gamma + 1 + tan^2\beta}} - 2fP_1\sin^3\gamma \cdot \cos\delta + 2fP_1\sin 2\gamma \cdot \cos\gamma - \frac{c\pi h_1^2 \sin\gamma_k}{2\cos^2\gamma_k}x_1,$$

$$\left(m_k + m_{gr.}\right)\ddot{z}_1 = \frac{2P_1 \cdot \sin\gamma \cdot \tan\beta}{\sqrt{tan^2\gamma + 1 + tan^2\beta}} + 2fP_1\sin^2\gamma \cdot \sin\delta - G_k - G_{gr.} - \frac{c_1\pi h_1 \sin\gamma_k z_1}{\cos^2\gamma_k},$$

$$\omega t \in \left[(2k-1)\pi, 2k\pi\right], \quad k = 1,2,\dots \tag{5.176}$$

In view of the fact that on the interval $\omega t \in \left[(2k-1)\pi, 2k\pi\right], \quad k = 1,2,\dots$ forces $Q_{zb._1}$ and $Q_{zb._2}$ do not act on the root (the tool moves downwards), they in (5.176).

Thus, the obtained systems of differential equations describe the process of the root extraction from the soil at its first stage in two cases: when the tool moves upwards symmetrically and directly gripping the root (5.176) and when the tool moves downwards and the root is not under the action of the perturbing force (4.177).

It is obvious that (4.177) describes the process of the root extraction from the soil by a standard share lifter as a result of the translational motion of the lifter under the action of the driving forces $\overline{P}_1$ and $\overline{P}_2$ during the direct contact between the root and the working faces of the shares.

As the system of differential Equation (5.175) is nonlinear, it can only be solved with the use of approximate numerical techniques and the assistance of the PC under preset initial conditions.

The initial conditions for (5.175) and (5.176) are written as follows at $t = 0$:

$$\dot{x}_1 = 0, \quad \dot{z}_1 = 0, x_1 = 0, \quad z_1 = 0, \tag{5.177}$$

However, if certain assumptions are made, (5.175) can be reduced to a system of linear differential equations, which will considerably simplify the solving of the system of differential equations under consideration.

At a first approximation, it is assumed that, within a short time interval, the vectors of forces of friction $\overline{F}_{K_1}$ and $\overline{F}_{K_2}$ retain the same directions, i.e., the angle between the vectors $\overline{F}_{K_1 min}$ and $\overline{F}_{K_1}$, is constant and equal to $\frac{\alpha_{K_1 max}}{2}$; similarly, the angle between vectors $\overline{F}_{K_2 min}$ and $\overline{F}_{K_2}$ is constant and equal to $\frac{\alpha_{K_2 max}}{2}$ at the same time, $\frac{\alpha_{K_1 max}}{2} = \frac{\alpha_{K_2 max}}{2}$.

By substituting (5.2) into (5.175), we obtain the following system of differential equations:

$$\left(m_k + m_{gr.}\right)\ddot{x}_1 + \frac{c\pi h_1^2 \sin\gamma_k}{2\cos^2\gamma_k}x_1 = \left[\frac{\cos\delta \cdot \tan\gamma}{\sqrt{tan^2\gamma + 1 + tan^2\beta}} - f\cos^2\delta \cdot \sin\gamma \cdot \sin\left(\frac{\alpha_{k_1 max}}{2} - \gamma\right) + f\cos\delta \cdot \cos\gamma \cdot \cos\left(\frac{\alpha_{k_1 max}}{2} - \gamma\right)\right] \cdot H\sin\omega t$$

$$+ \frac{2P_1 \cdot \sin\gamma \cdot \tan\beta}{\sqrt{tan^2\gamma + 1 + tan^2\beta}} - 2fP_1\cos\delta \sin\left(\frac{\alpha_{k_1 max}}{2} - \gamma\right)\sin^2\gamma + 2fP_1\cos\left(\frac{\alpha_{k_1 max}}{2} - \gamma\right)\sin 2\gamma,$$

$$\left(m_k + m_{gr.}\right)\ddot{z}_1 + \frac{c_1\pi h_1 \sin\gamma_k}{\cos^2\gamma_k}z_1 = \left[\frac{\cos\delta \cdot \tan\beta}{\sqrt{tan^2\gamma + 1 + tan^2\beta}} + \frac{f}{2}\sin 2\delta \cdot \sin\left(\frac{\alpha_{k_1 max}}{2} - \gamma\right)\right] \cdot H\sin\omega t$$

$$+ \frac{2P_1 \cdot \sin\gamma \cdot \tan\beta}{\sqrt{tan^2\gamma + 1 + tan^2\beta}} + 2fP_1\sin\gamma \sin\delta \sin\left(\frac{\alpha_{k_1 max}}{2} - \gamma\right) - \left(m_k + m_{gr.}\right)g,$$

$$\omega t \in \left[2k\pi, (2k+1)\pi\right], \quad k = 0,1,2,\dots \tag{5.178}$$

144

or:

$$
\left.
\begin{aligned}
\left(m_k + m_{gr.}\right)\ddot{x}_1 + \frac{c\pi h_1^2 \sin\gamma_k}{2\cos^2\gamma_k}x_1 &= \frac{2P_1\cdot\sin\gamma\cdot\tan\beta}{\sqrt{\tan^2\gamma + 1 + \tan^2\beta}} - 2fP\sin^3\gamma\cdot\cos\delta + 2fP_1\sin 2\gamma\cdot\cos\gamma, \\
\left(m_k + m_{gr.}\right)\ddot{z}_1 + \frac{c_1\pi h_1 \sin\gamma_k}{\cos^2\gamma_k}z_1 &= \frac{2P_1\cdot\sin\gamma\cdot\tan\beta}{\sqrt{\tan^2\gamma + 1 + \tan^2\beta}} + 2fP\sin^2\gamma\cdot\sin\delta - \left(m_k + m_{gr.}\right)g, \\
\omega t &\in \left[\,(2k-1)\pi, 2k\pi\right], \quad k = 1,2,\ldots
\end{aligned}
\right\}
\tag{5.179}
$$

(5.178) and (5.179) are systems of second-order linear differential equations with constant coefficients with right-hand sides. (5.178) describes the free and forced oscillations of the root (its point of fixation O) along axes O_1x_1 and O_1z_1 together with the soil surrounding the root at the first stage of extraction; (5.179) describes the displacement of the root along axes O_1x_1 and O_1z_1 in the absence of the perturbing force—i.e., when the tool moves downwards. Thereby, the systems of nonlinear differential equations (5.175) and (5.176), which can be solved only approximately with the use of numerical techniques, have been changed to systems of linear differential equations (5.178) and (5.179), which are approximate equations, but nonetheless can be solved by quadrature. Hence, the analytic relations that describe the root's oscillatory process at the first stage of extraction have been obtained.

In order to simplify the notation of (5.178) and (5.179), the following designations are introduced:

$$
\frac{c\pi h_1^2 \sin\gamma_k}{2\cos^2\gamma_k\left(m_k + m_{gr.}\right)} = k_1^2,
\tag{5.180}
$$

$$
\left[\frac{\cos\delta\cdot\tan\gamma}{\sqrt{\tan^2\gamma + 1 + \tan^2\beta}} - 2f\cos^2\delta + \sin\gamma\cdot\sin\left(\frac{\alpha_{k_1 max}}{2} - \gamma\right) + f\cos\delta\cdot\cos\gamma\cdot\cos\left(\frac{\alpha_{k_1 max}}{2} - \gamma\right)\right]
$$
$$
\cdot\frac{1}{\left(m_k + m_{gr.}\right)} = A_1,
\tag{5.181}
$$

$$
\left[\frac{2\sin\gamma\cdot\tan\gamma}{\sqrt{\tan^2\gamma + 1 + \tan^2\beta}} - 2f\cos\delta v\sin\left(\frac{\alpha_{k_1 max}}{2} - \gamma\right)\sin^2\gamma + f\cos\left(\frac{\alpha_{k_1 max}}{2} - \gamma\right)\sin 2\gamma\right]
$$
$$
\cdot\frac{1}{\left(m_k + m_{gr.}\right)} = B_1,
\tag{5.182}
$$

$$
\frac{c_1\pi h_1 \sin\gamma_k}{\cos^2\gamma_k\left(m_k + m_{gr.}\right)} = k_2^2,
\tag{5.183}
$$

$$
\left[\frac{\cos\delta\cdot\tan\beta}{\sqrt{\tan^2\gamma + 1 + \tan^2\beta}} + \frac{f}{2}\sin 2\delta\cdot\sin\left(\frac{\alpha_{k_1 max}}{2} - \gamma\right)\right]\frac{1}{\left(m_k + m_{gr.}\right)} = A_2,
\tag{5.184}
$$

$$
\left[\frac{2\sin\gamma\cdot\tan\beta}{\sqrt{\tan^2\gamma + 1 + \tan^2\beta}} + 2f\sin\gamma\cdot\sin\delta\cdot\sin\left(\frac{\alpha_{k_1 max}}{2} - \gamma\right)\right]\frac{1}{\left(m_k + m_{gr.}\right)} = B_2,
\tag{5.185}
$$

$$\left[\frac{2\sin\gamma\cdot\tan\gamma}{\sqrt{\tan^2\gamma+1+\tan^2\beta}}-2f\sin^3\gamma\cdot\cos\delta\cdot\sin 2\gamma\cdot\cos\gamma\right]\frac{1}{\left(m_k+m_{gr.}\right)}=B_1',\quad(5.186)$$

$$\left[\frac{2\sin\gamma\cdot\tan\beta}{\sqrt{\tan^2\gamma+1+\tan^2\beta}}-2f\sin^2\gamma\cdot\sin\delta\right]\frac{1}{\left(m_k+m_{gr.}\right)}=B_2'\quad(5.187)$$

After substituting (5.180)–(5.187) into the systems of equations, said systems of equations will be as follows:

$$\left.\begin{array}{l}\ddot{x}_1+k_1^2x_1=A_1H\sin\omega t+B_1P_1,\\[4pt]\ddot{z}_1+k_2^2z_1=A_2H\sin\omega t+B_2P_1-g,\end{array}\right\}$$
$$\omega t\in[\,2k\pi,(2k+1)\pi],\quad k=0,1,2,\ldots.\qquad(5.188)$$

or:

$$\left.\begin{array}{l}\ddot{x}_1+k_1^2x_1=B_1'P_1,\\[4pt]\ddot{z}_1+k_2^2z_1=B_2'P_1-g,\end{array}\right\}$$
$$\omega t\in[(2k-1)\pi,\,2k\pi],\quad k=1,2,\ldots.\qquad(5.189)$$

The first step is to integrate the (5.188). The first and second differential equations in (4.189) have the following characteristic equations, respectively:

$$r^2+k_1^2=0,\qquad(5.190)$$

$$r^2+k_2^2=0.\qquad(5.191)$$

Since the roots of these equations are purely imaginary and are equal, respectively, to $\pm k_1 i$ and $\pm k_2 i$ where i—imaginary unit, the general solutions of the homogeneous differential equations appear as follows:

$$x_{1oH.}=C_1\cos k_1 t+C_2\sin k_1 t,\qquad(5.192)$$

$$z_{1oH.}=C_3\cos k_2 t+C_4\sin k_2 t,\qquad(5.193)$$

where C_1, C_2, C_3, C_4—arbitrary constants determined in accordance with the initial conditions. As ω is not a root of the characteristic Equation (5.190) and (5.191), the partial solutions of (5.188) are sought in the following form:

$$x_{1part.}=L_1\sin\omega t+M_1\cos\omega t+Q_1,\qquad(5.194)$$

$$z_{1part.}=L_2\sin\omega t+M_2\cos\omega t+Q_2,\qquad(5.195)$$

where $L_1, M_1, Q_1, L_2, M_2, Q_2$—unknown coefficients, which are, in this case, the constant quantities that can be determined with the use of the method of indefinite

coefficients. After the implementation of said method, the following values of the required coefficients are obtained:

$$L_1 = \frac{A_1 H}{k_1^2 - \omega^2}, \qquad M_1 = 0, \qquad Q_1 = \frac{B_1 P_1}{k_1^2}, \qquad (5.196)$$

$$L_2 = \frac{A_2 H}{k_2^2 - \omega^2}, \qquad M_2 = 0, \qquad Q_2 = \frac{B_2 P_1 - g}{k_2^2}. \qquad (5.197)$$

Having substituted (5.196) and (5.197) into (5.194) and (5.195), respectively, the following result is obtained:

$$x_{1part.} = \frac{A_1 H}{k_1^2 - \omega^2} \sin \omega t + \frac{B_1 P_1}{k_1^2}, \qquad (5.198)$$

$$z_{1part.} = \frac{A_2 H}{k_2^2 - \omega^2} \sin \omega t + \frac{B_2 P_1 - g}{k_2^2} \qquad (5.199)$$

The general solutions of the first and second differential equations in (5.188) taking into account (5.192), (5.193), (5.198) and (5.199), are equal to, respectively:

$$\left.\begin{array}{l} x_1 = C_1 \cos k_1 + C_2 \cos k_1 t + \frac{A_1 H}{k_1^2 - \omega^2} \sin \omega t + \frac{B_1 P_1}{k_1^2} \\[2mm] z_1 = C_3 \cos k_2 t + C_4 \sin k_2 t + \frac{A_2 H}{k_2^2 - \omega^2} \sin \omega t + \frac{B_2 P_1 - g}{k_2^2} \end{array}\right\} \qquad (5.200)$$

The arbitrary constants C_1, C_2, C_3 and C_4 can be determined on the basis of the initial conditions (5.177). For this purpose, each expression in (5.200) is differentiated:

$$\left.\begin{array}{l} \dot{x}_1 = -C_1 k_1 \sin k_1 t + C_2 k_1 \cos k_1 t + \frac{A_1 H \omega}{k_1^2 - \omega^2} \cos \omega t, \\[2mm] \dot{z}_1 = -C_3 k_2 \sin k_2 t + C_4 k_2 \cos k_2 t + \frac{A_2 H \omega}{k_2^2 - \omega^2} \cos \omega t. \end{array}\right\} \qquad (5.201)$$

By substituting the initial conditions (5.177) into (5.200) and (5.201), the following two systems of linear equations are obtained:

$$\left.\begin{array}{l} 0 = C_1 + \frac{B_1 P_1}{k_1^2} \\[2mm] 0 = C_2 k_1 + \frac{A_1 H \omega}{k_1^2 - \omega^2} \end{array}\right\} \qquad (5.202)$$

$$\left.\begin{array}{l} 0 = C_3 + \frac{B_2 P_1 - g}{k_2^2}, \\[2mm] 0 = C_4 k_2 + \frac{A_2 H \omega}{k_2^2 - \omega^2}. \end{array}\right\} \qquad (5.203)$$

By solving the systems of (5.202) and (5.203), the following values of the arbitrary constants are obtained:

$$C_1 = -\frac{B_1 P_1}{k_1^2}, \qquad C_2 = -\frac{A_1 H\omega}{k_1\left(k_1^2-\omega^2\right)},$$
$$C_3 = -\frac{B_2 P_1 - g}{k_2^2}, \qquad C_4 = -\frac{A_2 H\omega}{k_2\left(k_2^2-\omega^2\right)}. \tag{5.204}$$

By substituting the values of the arbitrary constants (5.204) into (5.200), the law of the translational oscillatory motion of the root (point of fixation O) along axes $O_1 x_1$ and $O_1 z_1$, respectively, is obtained:

$$\left.\begin{array}{l} x_1 = -\frac{B_1 P_1}{k_1^2}\cos k_1 t - \frac{A_1 H\omega}{k_1\left(k_1^2-\omega^2\right)}\sin k_1 t + \frac{A_1 H}{k_1^2-\omega^2}\sin \omega t + \frac{B_1 P_1}{k_1^2}, \\[2mm] z_1 = -\frac{B_2 P_1 - g}{k_2^2}\cos k_2 t - \frac{A_2 H\omega}{k_2\left(k_2^2-\omega^2\right)}\sin k_2 t + \frac{A_2 H\omega}{k_2^2-\omega^2}\sin \omega t + \frac{B_2 P_1 - g}{k_2^2} \\[2mm] \left[\omega t \in 2k\pi, (2k+1)\pi\right], \quad k = 0, 1, 2, \ldots . \end{array}\right\} \tag{5.205}$$

The first two terms in the right side of each of the equations in (5.205) describe the free oscillations of the root (its point of fixation O) in the soil along axes $O_1 x_1$ and $O_1 z_1$, where the first of said terms corresponds to the free oscillations that the root performs in the absence of the perturbing force, and the second one also corresponds to the free oscillations, but with an amplitude depending on the present perturbing force. The latter are known as free accompanying oscillations [20]. The third terms in the right-hand sides of the equations in (5.205) correspond to purely forced oscillations of the root. The frequency of the free and free accompanying oscillations of the root (point of fixation O) in the soil along axis $O_1 x_1$ is equal to k_1 and determined from (5.180):

$$k_1 = \frac{h_1}{\cos \gamma_k}\sqrt{\frac{c\pi \sin \gamma_k}{2\left(m_k + m_{gr.}\right)}}. \tag{5.206}$$

The frequency of said oscillations along axis Oz_1 is equal to k_2 and determined from (5.183):

$$k_2 = \frac{1}{\cos \gamma_k}\sqrt{\frac{c_1 \pi h_1 \sin \gamma_k}{m_k + m_{gr.}}}. \tag{5.207}$$

As can be concluded from (5.205), the amplitudes of the free and free accompanying oscillations along axes $O_1 x_1$ and $O_1 z_1$ are equal to, respectively:

$$\frac{B_1 P_1}{k_1^2}, \qquad \frac{A_1 H\omega}{k_1\left(k_1^2 - \omega^2\right)}, \qquad \frac{B_2 P_1 - g}{k_2^2}, \qquad \frac{A_2 H\omega}{k_2\left(k_2^2 - \omega^2\right)}. \tag{5.208}$$

The frequency of the forced oscillations is equal to the frequency of the perturbing force, i.e., to ω. The amplitudes of the forced oscillations of the root along axes O_1x_1 and O_1z_1 are, as can be concluded from (5.205), equal to, respectively:

$$\frac{A_1 H}{k_1^2 - \omega^2}, \qquad \frac{A_2 H \omega}{k_2^2 - \omega^2}. \tag{5.209}$$

By substituting the values of the arbitrary constants (5.204) into the system of Equation (5.201), the law of variation of the velocity of the root's oscillatory motion as a function of time t along axes O_1x_1 and O_1z_1, respectively, is obtained:

$$\left.\begin{array}{l} \dot{x}_1 = \frac{B_1 P_1}{k_1} \sin k_1 t - \frac{A_1 H \omega}{k_1^2 - \omega^2} \cos k_1 t + \frac{A_1 H \omega}{k_1^2 - \omega^2} \cos \omega t \\[2mm] \dot{z}_1 = \frac{B_2 P_1 - g}{k_2} \sin k_2 t - \frac{A_2 H \omega}{k_2^2 - \omega^2} \cos k_2 t + \frac{A_2 H \omega}{k_2^2 - \omega^2} \cos \omega t, \end{array}\right\} \tag{5.210}$$
$$[\omega t \in 2k\pi, (2k+1)\pi], \quad k = 0, 1, 2, \ldots.$$

Further, the system of differential Equations (5.189) is subjected to integration. Since the characteristic equations of (4.190) are the same as in the case of (5.188), the general solutions of the homogeneous equations of the differential equations under consideration appear the same as (5.192) and (5.193). Taking into consideration the terms in the right-hand sides of the differential equations in (5.189), the partial solutions of said equations are:

$$x_{1part.} = Q_1, \tag{5.211}$$

$$z_{1part.} = Q_2, \tag{5.212}$$

where Q_1, Q_2—indefinite constants. After applying the method of indefinite coefficients, the following values of the constants Q_1, Q_2 are obtained:

$$Q_1 = \frac{B_1' P_1}{k_1^2} \tag{5.213}$$

$$Q_2 = \frac{B_2' P_1 - g}{k_2^2} \tag{5.214}$$

Having substituted (5.213) and (5.214) into (5.211) and (5.212), the following result is obtained:

$$x_{1part.} = \frac{B_1' P_1}{k_1^2}, \tag{5.215}$$

$$z_{1part.} = \frac{B_2' P_1 - g}{k_2^2}. \tag{5.216}$$

Thereby, the general solutions of the first and second differential equations in (5.189) are equal to, respectively:

$$\left.\begin{aligned} x_1 &= C_1 \cos k_2 t + C_2 \sin k_1 t + \frac{B_1' P_1}{k_1^2}, \\ z_1 &= C_3 \cos k_2 t + C_4 \sin k_2 t \frac{B_2' P_1 - g}{k_2^2}. \end{aligned}\right\} \tag{5.217}$$

The arbitrary constants C_1, C_2, C_3, C_4 can be determined from the initial conditions (5.177). For this purpose, each of the expressions in (5.217) is subjected to differentiation:

$$\left.\begin{aligned} \dot{x}_1 &= -C_1 k_1 \sin k_1 t + C_2 k_1 \cos k_1 t, \\ \dot{z}_1 &= -C_3 k_2 \sin k_2 t + C_4 k_2 \cos k_2 t. \end{aligned}\right\} \tag{5.218}$$

By substituting the initial conditions (5.177) into (5.217) and (5.218), the following two systems of linear equations are obtained:

$$\left.\begin{aligned} 0 &= C_1 + \frac{B_1' P_1}{k_1^2} \\ 0 &= C_2 k_1, \end{aligned}\right\} \tag{5.219}$$

$$\left.\begin{aligned} 0 &= C_3 + \frac{B_2' P_1 - g}{k_2^2} \\ 0 &= C_4 k_2, \end{aligned}\right\} \tag{5.220}$$

Solving (5.219) and (5.220), the following is arrived at:

$$C_1 = -\frac{B_1' P_1}{k_1^2}, \qquad C_2 = 0 \qquad C_3 = -\frac{B_2' P_1 - g}{k_2^2}, \qquad C_4 = 0 \tag{5.221}$$

By substituting the values of the arbitrary constants (5.221) into (5.217), the law of the root's oscillatory motion in the soil along axes $O_1 x_1$ and $O_1 z_1$, respectively, on the intervals $[(2k-1)\pi, \ 2k\pi]$, $k = 1, 2, \dots n$ is obtained:

$$\left.\begin{aligned} x_1 &= -\frac{B_1' P_1}{k_1^2} \cos k_1 t + \frac{B_1' P_1}{k_1^2}, \\ z_1 &= -\frac{B_2' P_1 - g}{k_2^2} \cos k_2 t + \frac{B_2' P_1 - g}{k_2^2}. \end{aligned}\right\} \tag{5.222}$$

The first terms in (5.222) describe the free oscillations performed by the root along axes $O_1 x_1$ and $O_1 z_1$ in the absence of the perturbing force. The frequencies of the root's free oscillations in the soil along axes $O_1 x_1$ and $O_1 z_1$ are determined in accordance with (5.206) and (5.207), respectively. The amplitudes of the root's

free oscillations in the soil on the intervals $[(2k-1)\pi,\ 2k\pi]$, $k = 1, 2, \ldots n$ (in the absence of the perturbing force) along axes O_1x_1 and O_1z_1 are equal to, respectively:

$$\frac{B_1' P_1}{k_1^2},\quad \frac{B_2' P_1 - g}{k_2^2} \tag{5.223}$$

By substituting the values of the arbitrary constants (5.221) into (5.218), the law of variation of the velocity of the root's oscillatory motion in the soil as a function of time t along axes O_1x_1 and O_1z_1, respectively, is obtained:

$$\left.\begin{array}{l} \dot{x}_1 = \frac{\frac{B_1' P_1}{k_1}}{k_1}\sin k_1 t \\ \dot{z}_1 = \frac{B_2' P_1 - g}{k_2}\sin k_2 t \end{array}\right\}\omega t \in [\,(2k-1)\pi, 2k\pi\,],\quad k = 1, 2, \ldots. \tag{5.224}$$

Thus, the translational oscillations of the root (meaning its fixation point O) in the soil in the longitudinal and vertical plane at the first stage of extraction have been analysed.

Using the results of the developed theory of the oscillatory process performed by the root as a rigid body fixed in the soil, the algorithm of computation of the kinematic parameters of said process can be set up as follows.

1. The initial data required for the computation are set.
2. The quantities A_1, B_1, A_2, B_2, B_1', B_2' are computed in accordance with (5.181), (5.182), (5.184), (5.185), (5.186), and (5.187), respectively.
3. Frequencies k_1 and k_2 of the free and free accompanying oscillations are computed in accordance with Expressions (5.206) and (5.207), respectively.
4. The amplitudes of the free and free accompanying oscillations are computed in accordance with (5.208).
5. The amplitudes of the forced oscillations of the root are computed in accordance with (5.209).
6. The law of the root's oscillatory motion is established in accordance with (5.205).
7. The graphs for various values of the kinematic parameters of the oscillatory process and the condition of the soil, in which the root is fixed, are plotted.

The values of the initial data required for the computation are selected in accordance with [7,31].

Mass of the root is $m_k = 0.9$ kg; mass of the soil surrounding the root is m_g $m_{gr.} = 0.4$ kg; length of the root is $h_k = 0.25$ m; angles of the trihedral wedges of the vibrational lifting tool are $\gamma = 14°$, $\beta = 52°$; coefficient of friction of steel on the surface of the root is $f = 0.45$; amplitude of the perturbing force is $H = 500$ N; magnitude of the lateral moving force is $P_1 = 400$ N; maximum angle of deflection of the friction force vector from the vector of the minimum value of this force is $\alpha_{k_1 max} = 30°$; elastic

deformation coefficients of the soil are $c_1 = 2 \cdot 10^5$ N·m^{-2}, $c = 3 \cdot 10^5$ N·m^{-3}; frequency of oscillation of the lifting shares is $v = 10$ Hz; angle of taper of the root is $\gamma_k = 15°$; dihedral angle δ between the working face of the share and the bottom side of the trihedral wedge is determined in accordance with Expression (3.63).

The computation is carried out in the MathCAD environment.

The relation between the frequencies and amplitudes of the oscillations of the root in the soil as a rigid body in an elastic medium on the one hand and the varying elastic deformation coefficient of the soil on the other hand is a research topic of considerable interest.

According to [20], the soil's elastic deformation coefficient c can vary within the range of $0.2 \cdot 10^5$–$30 \cdot 10^5$ N·m^{-3}.

The figures below (Figures 5.4 and 5.5) show the graphs of relation between the angular frequencies and Hertz frequencies of the free and free accompanying oscillations of the root as a rigid body fixed in the soil on the one hand and the soil's elastic deformation coefficients c_1 and c on the other hand, plotted with the use of the above-stated algorithm and initial data for computation. The frequencies of the free and free accompanying oscillations significantly rise with the increase in the soil's elastic deformation coefficients. Moreover, when the coefficient c varies within the range of $0.3 \cdot 10^5$–$30 \cdot 10^5$ N·m^{-3}, the frequency of the free and free accompanying oscillations varies within the range of 2.1–20.9 Hz on axis Ox_1; when the coefficient c_1 varies within the range of $0.2 \cdot 10^5$–$20 \cdot 10^5$ N·m^{-2}, said frequency varies within the range of 6.6–66.8 Hz on axis Oz_1.
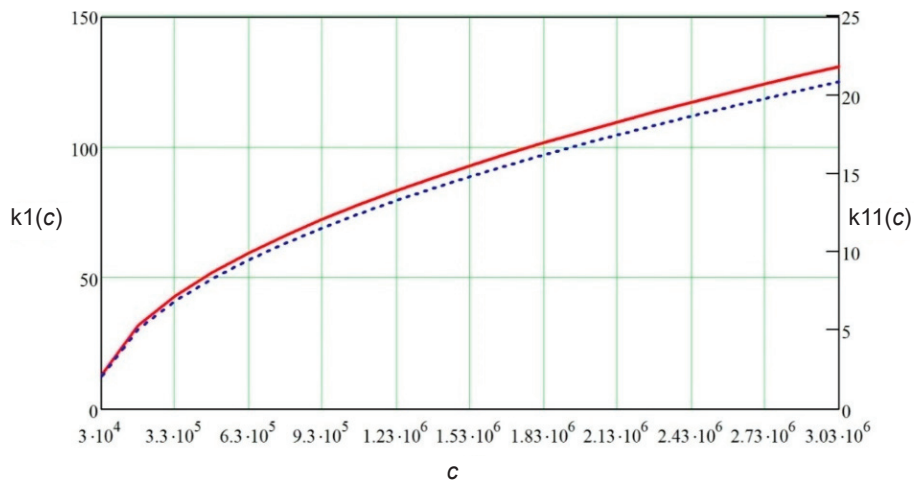
Figure 5.4. Graphs of relation between angular frequencies k_1 and frequencies k_{11} of free and free accompanying oscillations along axis Ox_1 and soil's elastic deformation coefficient c ($H = 500$ N; $P_1 = 400$ N; $v = 10$ Hz).
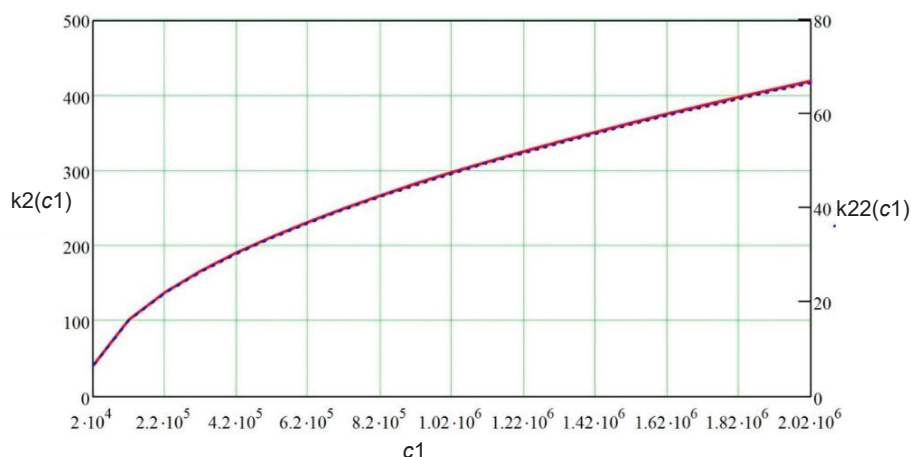
Figure 5.5. Graphs of relation between angular frequencies k_2 and frequencies k_{22} of free and free accompanying oscillations along axis Oz_1 and soil's elastic deformation coefficient c_1 ($H = 500$ N; $P_1 = 400$ N; $v = 10$ Hz).

As can be concluded from Expressions (5.208) and (5.209), the values of the frequencies in their turn have an effect on the values of the amplitudes of the free, free accompanying and forced oscillations of the root as a rigid body fixed in the soil.

This is evident from the graphs below that show the final result of the analysis of the relation between the above-mentioned amplitudes and the elastic deformation coefficients of the soil.

At greater values of the soil's elastic deformation coefficients, the amplitude of the free and free accompanying oscillations of the root as a rigid body fixed in the soil asymptotically approaches zero. For example, when the soil's elastic deformation coefficient approaches a value of $20 \cdot 10^5$ N·m^{-3}, the amplitudes are equal to:

Free oscillations: along axis Ox_1—5.3 mm; along axis Oz_1—0.6 mm;

Free accompanying oscillations: along axis Ox_1—6 mm; along axis Oz_1—0.3 mm.

However, in the most frequently used soils the amplitude of the free oscillations of the root as a rigid body in the elastic soil (Figures 5.6 and 5.7) is equal to:

along axis Ox_1: at $c = 2 \cdot 10^5$ N·m^{-3}—89 mm;

at $c = 3 \cdot 10^5$ N·m^{-3}—49 mm;
at $c = 4 \cdot 10^5$ N·m^{-3}—33 mm;

along axis Oz_1: at $c = 2 \cdot 10^5$ N·m^{-3} – 5.8 mm;

at $c = 3 \cdot 10^5$ N·m^{-3}—4.0 mm;
at $c = 4 \cdot 10^5$ N·m^{-3}—3.0 mm.
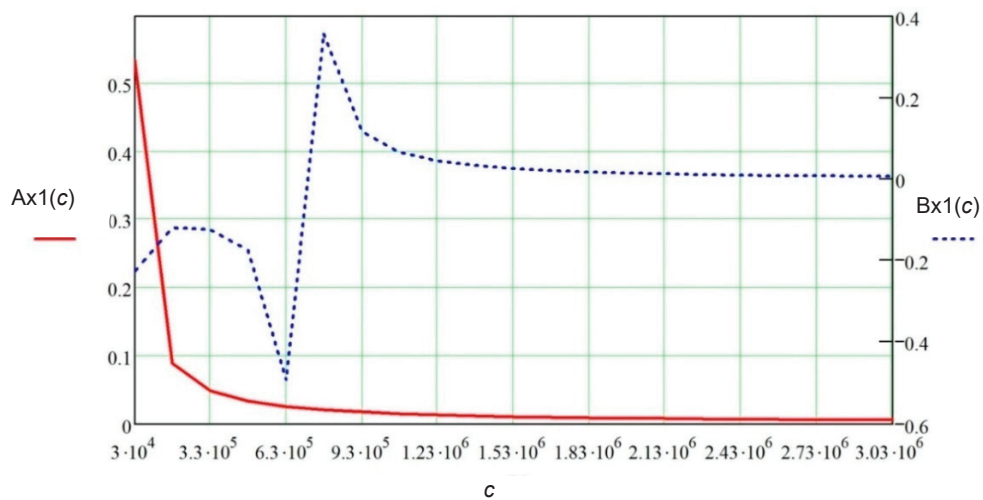
The amplitude of the free accompanying oscillations is equal to:

along axis Ox_1: at $c = 2 \cdot 10^5$ N·m^{-3}—67 mm;

153

at $c = 3 \cdot 10^5$ N·m^{-3}—55 mm;

at $c = 4 \cdot 10^5$ N·m^{-3}—52 mm;

along axis Oz_1: at $c = 2 \cdot 10^5$ N·m^{-3}—16 mm;

at $c = 3 \cdot 10^5$ N·m^{-3}—7 mm;

at $c = 4 \cdot 10^5$ N·m^{-3}—4.2 mm.

The amplitude of the forced oscillations (Figure 5.8) is equal to:

along axis Ox_1: at $c = 2 \cdot 10^5$ N·m^{-3}—145 mm;

at $c = 3 \cdot 10^5$ N·m^{-3}—86 mm;

at $c = 4 \cdot 10^5$ N·m^{-3}—61 mm;

along axis Oz_1: at $c = 2 \cdot 10^5$ N·m^{-3}—16 mm;

at $c = 3 \cdot 10^5$ N·m^{-3}—10 mm;

at $c = 4 \cdot 10^5$ N·m^{-3}—7.3 mm

Figure 5.6. Graphs of relation between amplitudes of free A_{x^1} and free accompanying oscillations B_{x^1} along axis Ox_1 and soil's elastic deformation coefficient c ($H = 500$ N; $P_1 = 400$ N; $v = 10$ Hz).
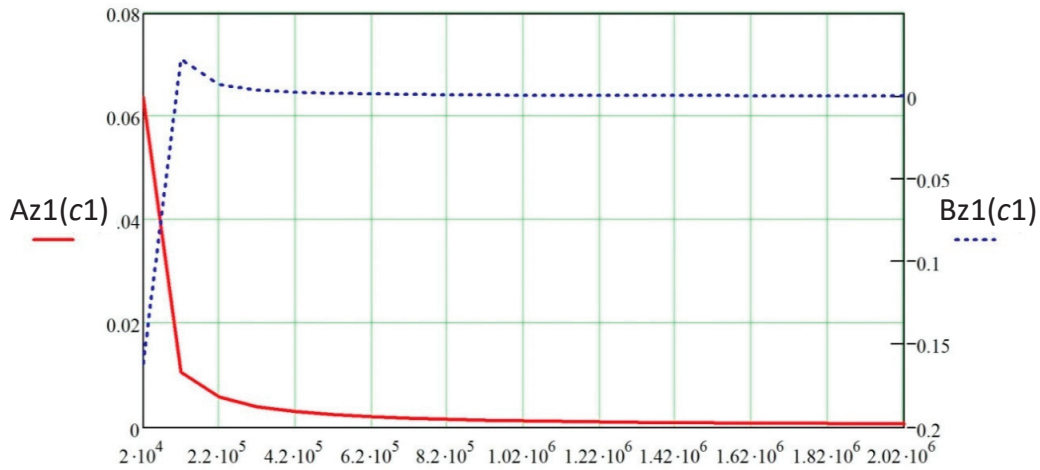
Figure 5.7. Graphs of relation between amplitudes of free A_{z1} and free accompanying oscillations B_{z1} along axis Oz_1 and soil's elastic deformation coefficient c (($H = 500$ N; $P_1 = 400$ N; $v = 10$ Hz).

As is seen in the graphs in Figure 5.8, at sufficiently high values of the soil's elastic deformation coefficients, the amplitude of the forced oscillations of the root as a rigid body fixed in the soil also asymptotically approaches zero. For example, at $c = 20 \cdot 10^5$ N·m^{-3} the amplitude of the forced oscillations along axis Ox_1 is equal to 13 mm; at $c_1 = 20 \cdot 10^5$ N·m^{-3} and along axis Oz_1 it is equal to 1.4 mm.

As can be seen from the graphs in Figures 5.6–5.8, at some values of the soil's elastic deformation coefficients, abrupt changes of the amplitudes are observed due to the frequencies of free and free accompanying oscillations drawing near the frequencies of forced oscillations.

The graphic representations of the law of the translational oscillations of the root as a rigid body fixed in the soil obtained with the use of the analytic relations (5.205) for several values of the soil's elastic deformation coefficients c_1 and c and the frequencies of oscillations of the digging tool are shown below (Figures 5.9–5.11).

As can be seen in the presented graphs (Figures 5.9–5.11), the root's centre of mass in 0.025 s performs a translation along axis Ox_1 for a distance of 50 mm at a perturbing force frequency of $v = 10$, 15 and 20 Hz and along axis Oz_1 at a perturbing force frequency of $v = 10$ Hz—for a distance of 33 mm ($c_1 = 2 \cdot 10^5$ N·m^{-2}), for a distance of 21 mm ($c_1 = 3 \cdot 10^5$ N·m^{-2}) or for a distance of 13 mm ($c_1 = 4 \cdot 10^5$ N·m^{-2}); at $v = 15$ Hz—for a distance of 35 mm ($c_1 = 2 \cdot 10^5$ N/m^2), for a distance of 25 mm ($c_1 = 3 \cdot 10^5$ N·m^{-2}) or for a distance of 15 mm ($c_1 = 4 \cdot 10^5$ N·m^{-2}); at $v = 20$ Hz—for a distance of 40 mm ($c_1 = 2 \cdot 10^5$ N·m^{-2}), for a distance of 30 mm ($c_1 = 3 \cdot 10^5$ N·m^{-2}) or for a distance of 20 mm ($c_1 = 4 \cdot 10^5$ N·m^{-2}).

As is noted in [31], in order to destruct the bonds between the large size roots and the soil partially, it is necessary to lift them by up to 6–8 mm, in the case of small size roots—up to 4 mm, while the complete breaking of the bonds needs a displacement

of 12–25 mm. Hence, the obtained values of the amplitudes of oscillations at the above-stated initial data fully allow, as can be seen from the graphs (Figures 5.9–5.11), the disruption of all bonds between the roots and the soil and establish the conditions for their direct lifting.

The next phase of investigation is the analysis of the root's motion in the soil during direct lifting, where the bonds with the soil are destroyed to such an extent that the motion of the root up along the lifter's working channel begins.
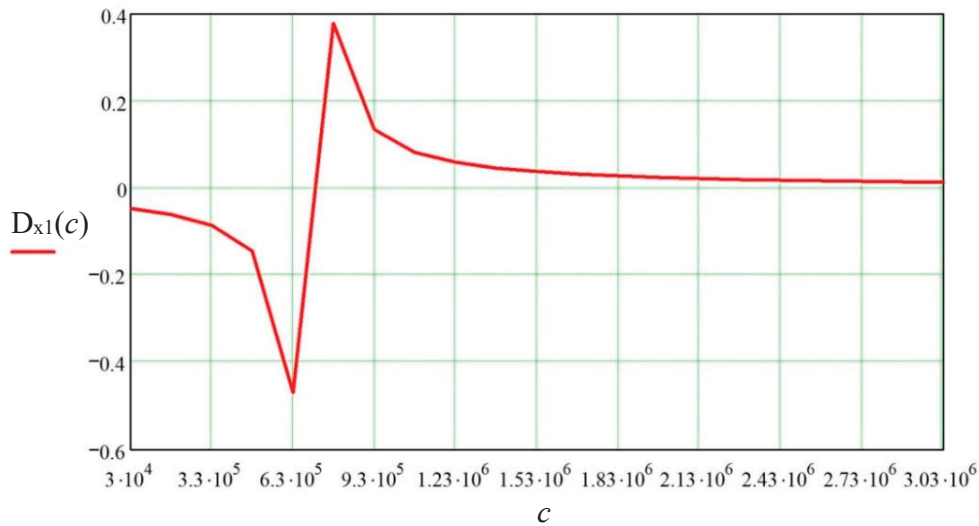
(a)
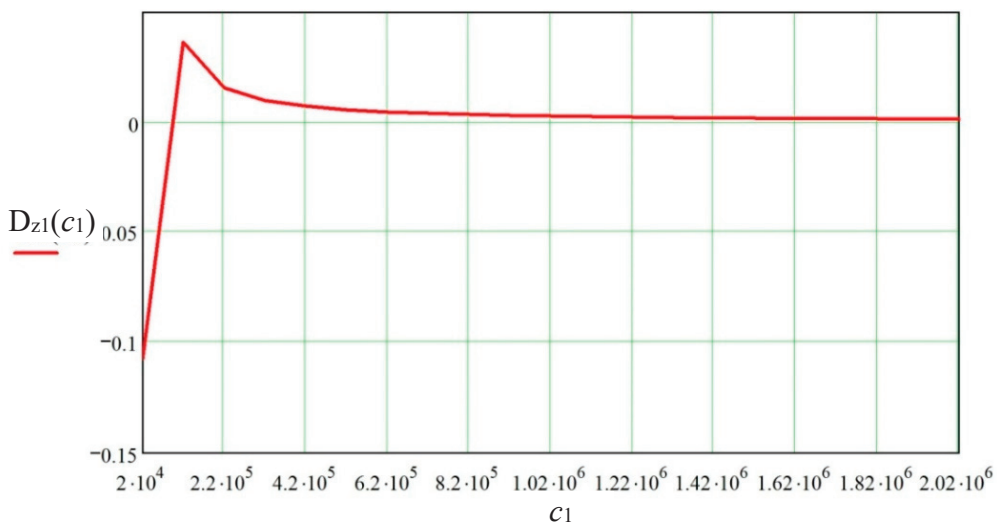
(b)

Figure 5.8. Graph of relation between amplitude of forced oscillations D_{xz1} along axis Ox_1 and soil's elastic deformation coefficient c (a) and graph of relation between amplitude of forced oscillations D_{z1} along axis Oz_1 and soil's elastic deformation coefficient c_1 (b) ($H = 500$ N; $P_1 = 400$ N; $v = 10$ Hz).
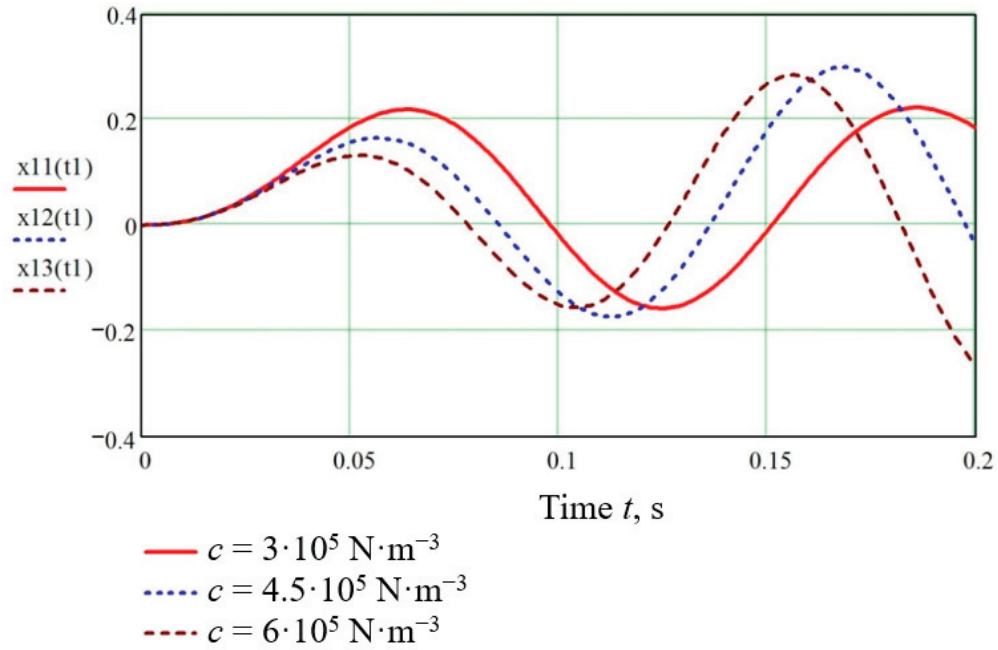
(a)
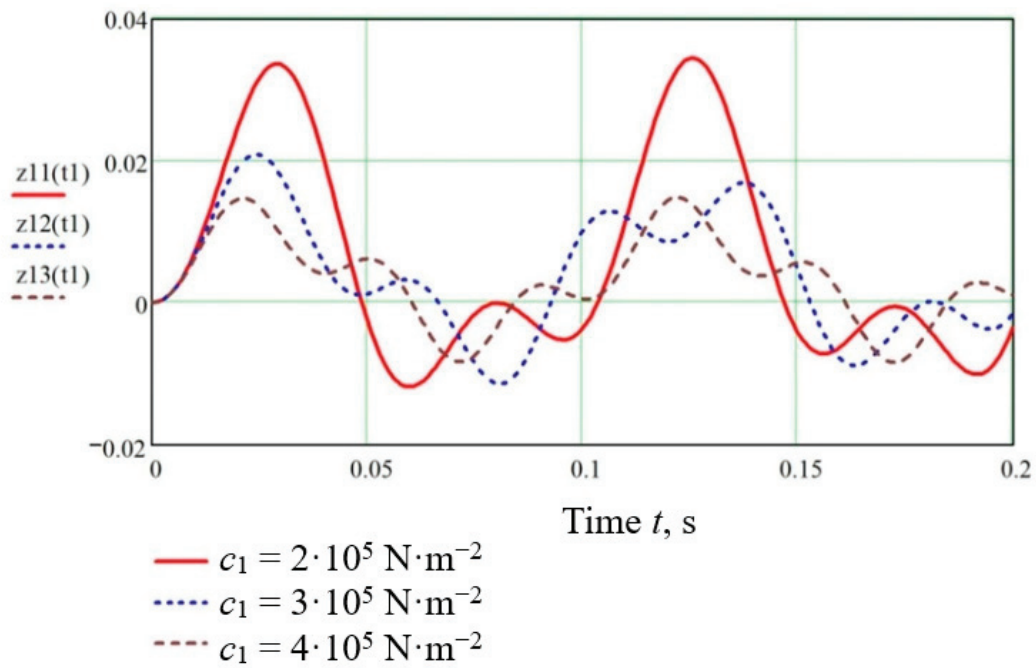
(b)

Figure 5.9. Graphs of functions (law of oscillatory process) $x_1(t)$ **(a)** and $z_1(t)$ **(b)** that describe oscillations of root as rigid body fixed in soil at respective values of soil's elastic deformation coefficients c_1 and c ($H = 500$ N; $P_1 = 400$ N; $\nu = 10$ Hz).
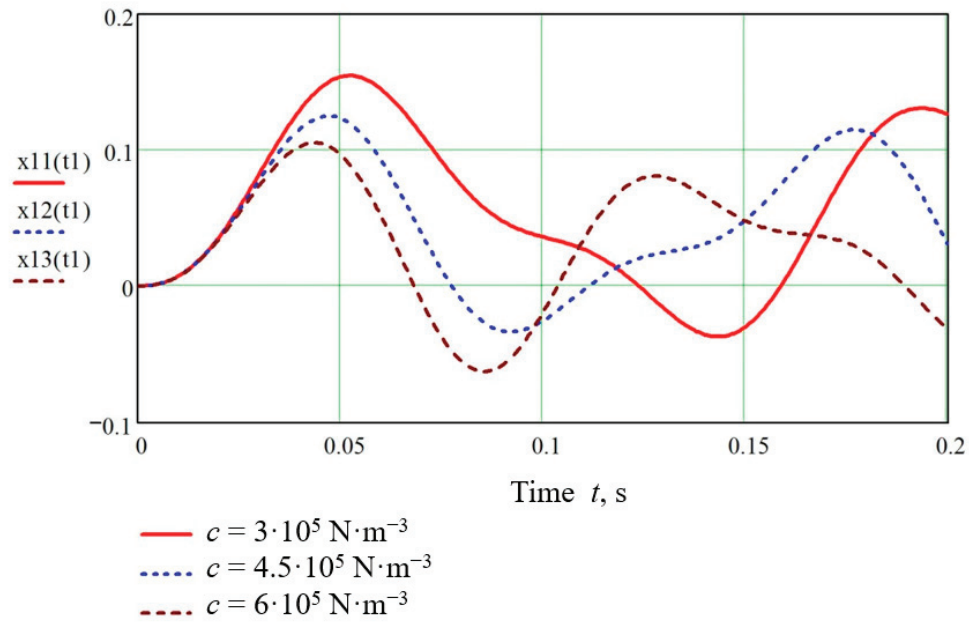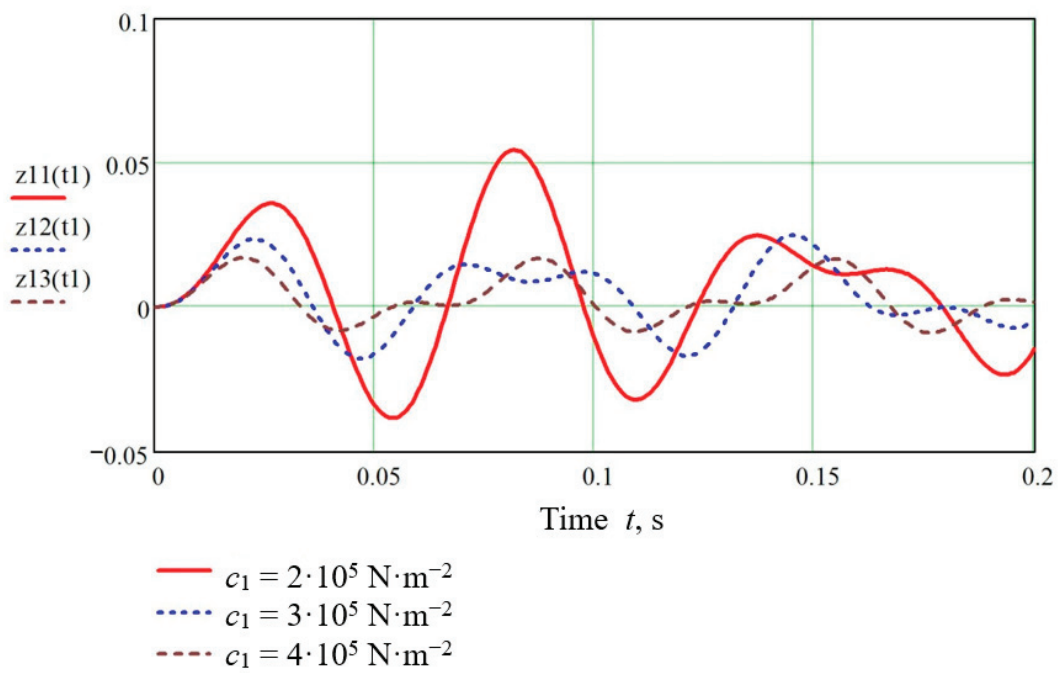
Figure 5.10. Graphs of functions (law of oscillatory process) $x_1(t)$ **(a)** and $z_1(t)$ **(b)** that describe oscillations of root as rigid body fixed in soil at respective values of soil's elastic deformation coefficients c_1 and c ($H = 500$ N; $P_1 = 400$ N; $v = 15$ Hz).

(a)
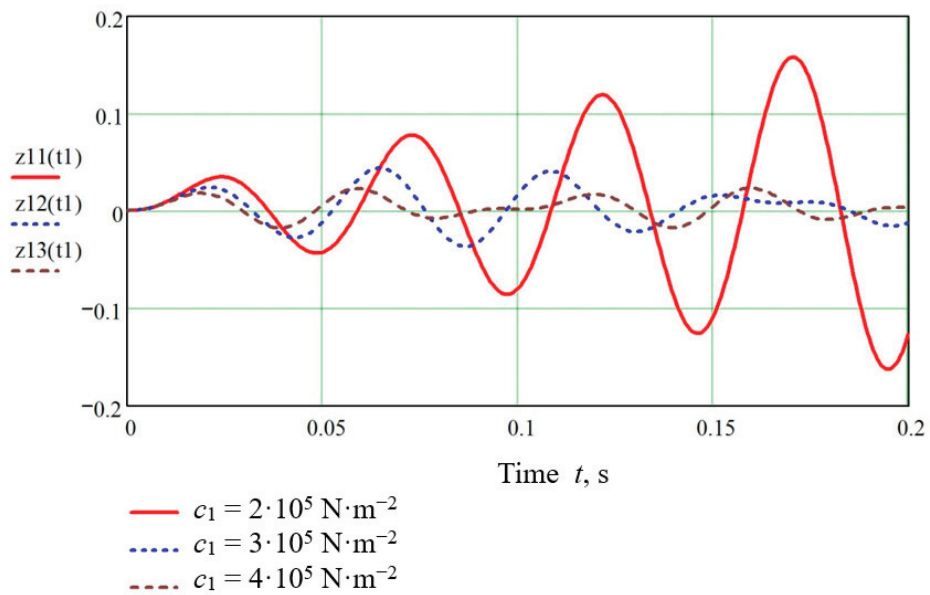
(b)

Figure 5.11. Graphs of functions (law of oscillatory process) $x_1(t)$ (**a**) and $z_1(t)$ (**b**) that describe oscillations of root as rigid body fixed in soil at respective values of soil's elastic deformation coefficients c_1 and c ($H = 500$ N; $P_1 = 400$ N; $v = 20$ Hz).

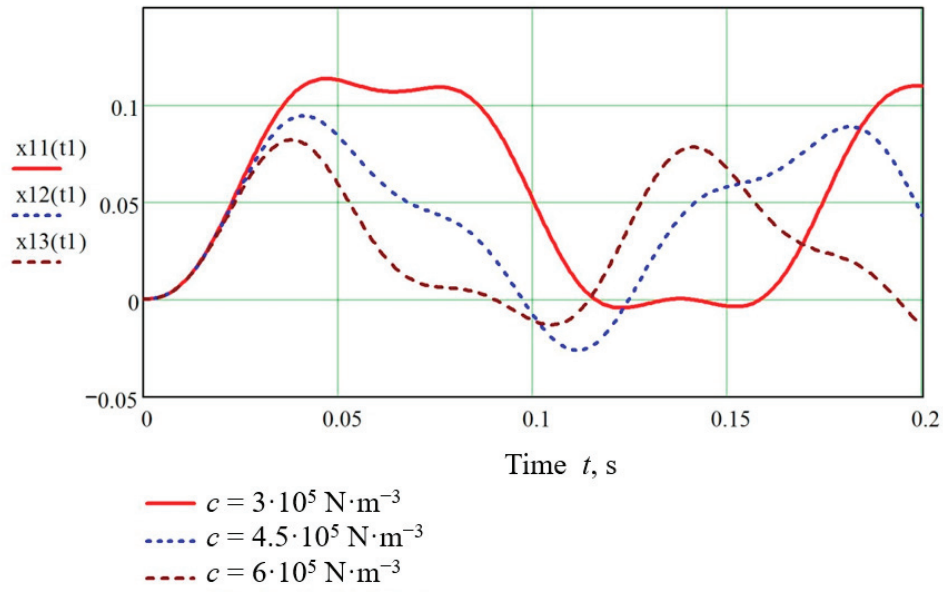## 5.4. Direct Lifting of Root from Soil during Vibrational Digging

As a consequence of the above oscillatory processes, where the root oscillates in the soil as in an elastic medium, the bonds between the root and the soil are actively

159

broken and, therefore, forces $\overline{Q}_{np.\theta}, \overline{R}_x, \overline{R}_z$ (Figure 4.3), which act as restoring forces, start sharply diminishing; consequently, the oscillatory processes change into the processes of continuous translation of the root along axes O_1x_1 and O_1z_1 as well as continuous turn of the root about its centre of mass (point C) through a certain angle of θ without the root returning to the previous position.

Thus, the stage of direct lifting of the root from the soil starts. The transient process from the root's oscillatory motion to its continuous translation in the soil can be described in detail as follows. Under the action of the vertical perturbing force $\overline{Q}_{zb.}$, the root performs translational oscillations together with the soil surrounding it in accordance with Equations (5.205) and (5.222); at the same time, the closer the soil is to the root, the more the soil's oscillations are synchronised with the oscillations of the root. Additionally, vice versa, the farther the soil is from the root, the less its oscillations copy the oscillations of the root, due to the elastoplastic properties of the soil. Ultimately, there is a distance from the root where no oscillation happens at all, but the boundary of the area of soil that oscillates together with the root is rather indistinct. Smooth transition from the area of soil that oscillates to the area that does not oscillate is observed; therefore, the discontinuity of the soil at the boundary between said areas is unlikely.

The more probable place for the discontinuity of the soil is in close proximity to the root's surface or on the very surface of it. That explains why significantly less caked soil is left on the roots during vibrational lifting as compared to the traditional share lifting.

As mentioned above, the extraction is possible only when the root is gripped by the digging tool symmetrically; therefore, simultaneously with the translational oscillations of the root in accordance with Equations (5.205) and (5.222), the oscillation of the root about axis Oy_2 (Figure 5.3) through a certain angle of θ takes place in accordance with Equations (5.152) and (5.153).

At the first stage of extraction, especially during the first oscillations, the restoring force $\overline{Q}_{np.\theta}$ and consequently its moment about axis Oy_2 are at their maximum. Therefore, the angle of deflection θ is rather insignificant and the complete or partial restoration of the root's vertical position is possible in view of the translational motion of the lifter. Nevertheless, owing to the action of the translational oscillations of the root together with the soil surrounding it, the compactness of said soil decreases and, accordingly, force $\overline{Q}_{np.\theta}$ also becomes smaller. Thus, with each oscillation of the root its angle of deflection θ increases, while the restoration of the previous position declines. The root rocks about axis Oy_2 with the gradual increase in angle θ—i.e., the tilt of the root forward along the lifter's line of travel. This results in the breaking of the bonds between the root and the soil along axis O_1x_1, starting from the upper part of the conical surface of the root sitting in unbroken soil and gradually drawing near the point of fixation O. Hence, it can be concluded from the

above-stated information that the disruption of the bonds between the root and the soil takes place simultaneously in two directions—along axes O_1x_1 and O_1z_1. At the same time, the bonding forces between the root and the soil $\overline{R}_z, \overline{R}_x$ and the soil's elastic forces $\overline{Q}_{np.\theta}$ gradually decrease to the minimum value, where the oscillatory processes change into the processes of continuous translation of the root upward along axis O_1z_1 and forward along axis O_1x_1 and continuous turn of the root about its centre of mass (point C) through an angle of θ up to the complete extraction of the root from the soil. As regards forces $\overline{R}_x, \overline{R}_z$ and $\overline{Q}_{np.\theta}$, they just change into the resistance forces exerted by the broken soil when the root moves in the working channel of the lifter. It can be assumed that they depend on the velocity of the root's motion in the broken soil or are, with small inaccuracy, just constant quantities.

The displacement of the root during its direct lifting from the soil has to be analysed with respect to the fixed system of coordinates $O_1x_1y_1z_1$. Additionally, it is necessary to set up the moving system of coordinates $Cx_cy_cz_c$ rigidly bound to the root, its origin being situated at the root's centre of mass (point C), axis Cz_c being directed along the axis of symmetry of the root, and axes Cx_c and Cy_c lying in the plane that is at right angle to axis Cz_c (Figure 5.12).

First, it is necessary to set up the differential equations of the motion of the root's centre of mass (point C)—i.e., the translational motion of the root along axes O_1x_1 and O_1z_1.

Obviously, the schematic model of the forces that act on the root during its motion along the working channel of the lifter in the process of its direct lifting from the soil to some extent differs from the schematic model of forces shown in Figure 4.3. In particular, the couple of the forces of resistance of the broken soil that affects the turning of the root about its centre of mass (point C) is applied here instead of force $\overline{Q}_{np.\theta}$.

For a first approximation, it is assumed that the moment of said couple is constant and equal to M. Similarly, the forces of resistance to the translational motion of the root in the broken soil along axes O_1x_1 and O_1y_1, i.e., forces $\overline{R}_{x_1}$ and $\overline{R}_{z_1}$, respectively, are also assumed to be constant.

Moreover, in view of the fact that the root moves upwards, the directions of the friction force vectors $\overline{F}_{K1}$ and $\overline{F}_{K2}$ partially change; therefore, the components $\overline{F}_1, \overline{F}_2$, $\overline{E}_1$ and $\overline{E}_2$ of said forces of friction will be determined by the expressions that are to some extent different from (5.134) and (5.135), respectively—that is:

$$F_1 \;=\; F_2 \;=\; (0.5fH\cos\delta\cdot\sin\omega t + fP_1\sin\gamma)\sin\!\left(\gamma + \alpha_{K_1max}\sin\omega t\right), \qquad (5.225)$$

$$E_1 \;=\; E_2 \;=\; (0.5fH\cos\delta\cdot\sin\omega t + fP_1\sin\gamma)\cos\!\left(\gamma + \alpha_{K_1max}\sin\omega t\right). \qquad (5.226)$$

In this case, the vectors $\overline{F}_1$ and $\overline{F}_2$ are opposite to the vectors $\overline{T}_1$ and $\overline{T}_2$, which is contrary to the schematic model of forces shown in Figure 5.3, where their senses coincide.
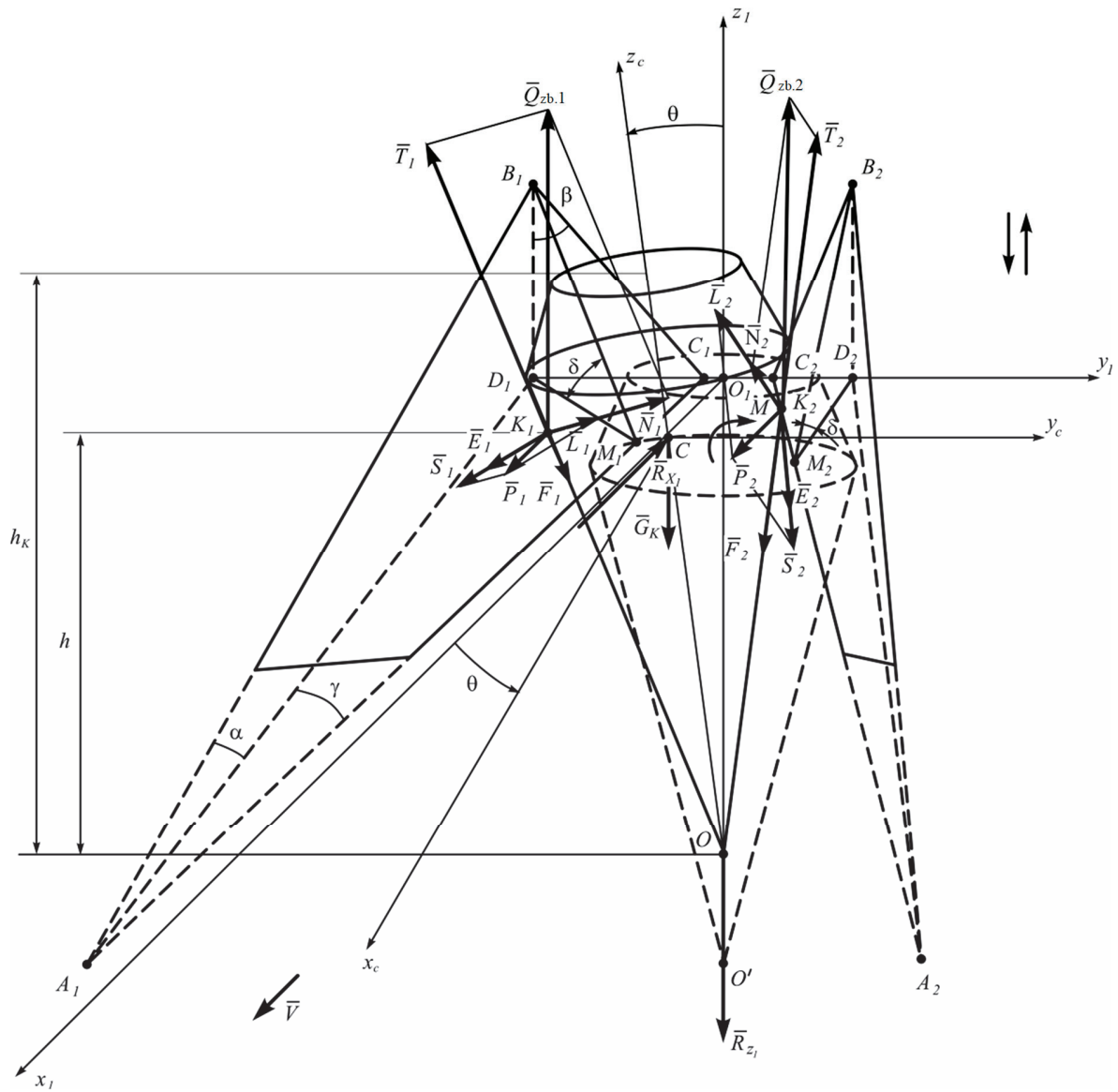
Figure 5.12. Force interaction between root and wedges of vibrating digging tool during its direct extraction from soil.

The described schematic model of forces is shown in Figure 5.12. Moreover, at this stage of extraction the mass of the soil stuck to the root is quite small and can be ignored.

Taking into account the above-stated information, the differential equation of the motion of the root's centre of mass during its direct lifting from the soil in the vector notation appears as follows:

$$m_k \bar{a} = \bar{N}_1 + \bar{N}_2 + \bar{L}_1 + \bar{L}_2 + \bar{F}_1 + \bar{F}_2 + \bar{E}_1 + \bar{E}_2 + \bar{G}_k + \bar{R}_{z_1} + \bar{R}_{x_1}, \quad (5.227)$$

where $\bar{a}$—acceleration of the root's centre of mass.

Since the process of extraction occurs, as stated above, at the time when the root is gripped by the digging tool symmetrically, the motion of the root along the working channel of the lifter effectively takes place in the longitudinal and vertical plane (plane $x_1 O_1 z_1$); hence, (5.227) can be resolved into the system of two equations in the projections on axes $O_1 x_1$ and $O_1 z_1$ in the following form:

$$\left. \begin{array}{l} m_k \ddot{x}_1 = N_{1x_1} + N_{2x_1} + L_{1x_1} + L_{2x_1} + F_{1x_1} + F_{2x_1} + E_{1x_1} + E_{2x_1} - R_{x_1}, \\ m_k \ddot{z}_1 = N_{1z_1} + N_{2z_1} + L_{1z_1} + L_{2z_1} - F_{1z_1} - F_{2z_1} - G_k - R_{z_1}. \end{array} \right\} \quad (5.228)$$

The projections of the forces in (5.228) have to be determined. The projections of the forces $\bar{N}_1, \bar{N}_2, \bar{L}_1, \bar{L}_2$ on axes $O_1 x_1$ and $O_1 z_1$ are determined in accordance with (5.158), (5.160) and (5.169), (5.171), respectively.

Taking into account (5.161) and (5.225), the projections of the components $\bar{F}_1$ and $\bar{F}_2$ of the forces of friction on axis $O_1 x_1$ are equal to:

$$F_{1x_1} = F_{2x_1} = (0.5 fH \cos \delta \cdot \sin \omega t + f P_1 \sin \gamma) \sin(\gamma + \alpha_{K_{1max}} \sin \omega t) \cos \delta \cdot \sin \gamma,$$
$$\omega t \in [2k\pi, (2k+1)\pi], \quad k = 0, 1, 2, \dots$$
$$(5.229)$$

Taking into account (5.164) and (5.226), the projections of components $\bar{E}_1$ and $\bar{E}_2$ of the forces of friction on axis $O_1 x_1$ are equal to:

$$E_{1x_1} = E_{2x_1} = (0.5 fH \cos \delta \cdot \sin \omega t + f P_1 \sin \gamma) \cos(\gamma + \alpha_{K_{1max}} \sin \omega t) \cos \gamma,$$
$$\omega t \in [2k\pi, (2k+1)\pi] \quad k = 0, 1, 2, \dots$$
$$(5.230)$$

The projections of the components $\bar{F}_1$ and $\bar{F}_2$ on axis $O_1 z_1$ are determined in a similar way.

Taking into account (5.172) and (5.225), the following is obtained:

$$F_{1z_1} = F_{2z_1} = (0.5 fH \cos \delta \cdot \sin \omega t + f P_1 \sin \gamma) \sin(\gamma + \alpha_{K_{1max}} \sin \omega t) \sin \delta,$$
$$\omega t \in [2k\pi, (2k+1)\pi] \quad k = 0, 1, 2, \dots$$
$$(5.231)$$

The projections of components $\bar{E}_1$ and $\bar{E}_2$ of the forces of friction on axis $O_1 z_1$ are equal to zero—i.e., $\bar{E}_{1z1} = \bar{E}_{2z1} = 0$.

The projections of the components $\bar{F}_1, \bar{F}_2, \bar{E}_1, \bar{E}_2$ on axes $O_1 x_1$ and $O_1 z_1$ on the intervals $[(2k-1)\pi, 2k\pi]$ $k = 1, 2, \ldots$ are determined in accordance with Expressions (5.163), (5.166) and (5.174), respectively.

By substituting (5.158), (5.160), (5.229) or (5.163) or (5.166), (5.169), (5.170), or (5.174) into (5.228), the following systems of differential equations are obtained:

$$
\left.
\begin{aligned}
m_k \ddot{x}_1 &= \frac{2Q_{zb_1} \cos\delta \cdot \tan\gamma}{\sqrt{\tan^2\gamma + 1 + \tan^2\beta}} + \frac{2fP_1 \sin\gamma \cdot \tan\gamma}{\sqrt{\tan^2\gamma + 1 + \tan^2\beta}} + (fH \cdot \cos\delta \cdot \sin\omega t + 2fP_1 \sin\gamma) \\
&\quad \cdot \sin\left(\gamma + \alpha_{K_1 max} \sin\omega t\right) \cos\delta \cdot \sin\gamma \\
&\quad + (fHH \cdot \cos\delta \cdot \sin\omega t + 2fP_1 \sin\gamma) \cdot \cos\left(\gamma + \alpha_{K_1 max} \sin\omega t\right) \cos\gamma - R_{x_1,} \\
m_k \ddot{z}_1 &= \frac{2Q_{zb_1} \cos\delta \cdot \tan\beta}{\sqrt{\tan^2\gamma + 1 + \tan^2\beta}} + \frac{2fP_1 \sin\gamma \cdot \tan\beta}{\sqrt{\tan^2\gamma + 1 + \tan^2\beta}} \\
&\quad - (fH \cdot \cos\delta \cdot \sin\omega t + 2fP_1 \sin\gamma) \cdot \sin\left(\gamma + \alpha_{K_1 max} \sin\omega t\right) \sin\delta - G_k - R_{z_1}, \\
&\qquad \omega t \in [2k\pi, (2k+1)\pi], \quad k = 0, 1, 2, \ldots
\end{aligned}
\right\}
\tag{5.232}
$$

$$
\left.
\begin{aligned}
m_k \ddot{x}_1 &= \frac{2P_1 \sin\gamma \cdot \tan\gamma}{\sqrt{\tan^2\gamma + 1 + \tan^2\beta}} + 2fP_1 \sin^3\gamma v \cos\delta + fP_1 \sin 2\gamma \cdot \cos\gamma - R_{x_1} \\
m_k \ddot{z}_1 &= \frac{2P_1 \sin\gamma \cdot \tan\beta}{\sqrt{\tan^2\gamma + 1 + \tan^2\beta}} + 2fP_1 \sin^2\gamma \sin\delta - G_k - R_{z_1}, \\
&\qquad \omega t \in [(2k-1)\pi, 2k\pi], \quad k = 1, 2
\end{aligned}
\right\}
\tag{5.233}
$$

In (5.232) and (5.233) the magnitudes of the loosened soil resistance forces $\bar{R}_{x1}$ and $\bar{R}_{z1}$ acting during the beet root's movement in the working passage of the vibrational lifting tool are regarded as constant.

Now, we are going to establish the initial conditions for (5.232) and (5.233) Since the beet root prior to the start of its direct lifting from the soil performs oscillations around the equilibrium position, the initial conditions for the coordinates of the root's centre of mass (point C) can be at the initial instant of time $x_1 = x_{10}, z_1 = -h_k/3$ where x_{10} is the distance from the vertical centreline of the beet root to the origin of coordinates (point O_1)

An error can arise only within the limits of the beet root oscillation amplitude, which is very insignificant as compared with the length of the lifting tool working passage and the running depth in soil where the root lifting is carried out. Further, considering that during each oscillation within the whole period the instants exist, when the beet root displacement velocity is equal to zero, we take, as the initial time point, such an instance during the last oscillation followed further by direct beet root lifting from the soil. Thus, the initial conditions for (5.50) and (5.51) will be as follows: at $t = 0$:

$$
\dot{x}_1 = 0, \quad \dot{z}_1 = 0, \quad x_1 = x_{10}, \quad z_1 = -\frac{1}{3}h_k.
\tag{5.234}
$$

After substituting (5.2) into (5.232) and making certain transformations, we obtain the following system of differential equations:

$$
\begin{aligned}
\ddot{x}_1 &= \frac{1}{m_k}\Big[\frac{\cos\delta\cdot\tan\gamma}{\sqrt{tan^2\gamma+1+tan^2\beta}} + f\cos^2\delta\cdot\sin\big(\gamma+\alpha_{K_1max}\sin\omega t\big)\sin\gamma + f\cos\delta\cos\big(\gamma+\alpha_{K_1max}\sin\omega t\big)\cdot\cos\gamma\Big]\cdot H\sin\omega t \\
&\quad +\frac{2}{m_k}\Big[\frac{\cos\delta\cdot\tan\gamma\beta}{\sqrt{tan^2\gamma+1+tan^2\beta}} - f\cos^2\delta\cdot\sin\big(\gamma+\alpha_{K_1max}\sin\omega t\big)\cos\delta + f\sin\gamma\cdot\cos\gamma\cdot\cos\big(\gamma+\alpha_{K_1max}\sin\omega t\big)\Big]P_1 - \frac{R_{x_1}}{m_k}, \\
\ddot{z}_1 &= \Big[\frac{\cos\delta\cdot\tan\beta}{\sqrt{tan^2\gamma+1+tan^2\beta}} - f\cos\delta\cdot\sin\big(\gamma+\alpha_{K_1max}\sin\omega t\big)\sin\delta\Big]\cdot H\sin\omega t \\
&\quad +\frac{2}{m_k}\Big[\frac{\sin\gamma\cdot\tan\gamma\beta}{\sqrt{tan^2\gamma+1+tan^2\beta}} - f\sin\gamma\cdot\sin\big(\gamma+\alpha_{K_1max}\sin\omega t\big)\Big]P_1 - \frac{G_k}{m_k} - \frac{R_{z_1}}{m_k} \\
&\qquad \omega t\in[2k\pi,(2k+1)\pi],\quad k=0,1,2,\dots
\end{aligned}
\tag{5.235}
$$

(5.235) is nonlinear. It can be integrated only with the use of approximate numerical methods on a PC. First, we are going to make certain assumptions. As a first approximation, we assume that the friction force vectors $\overline{F}_{K_1}$ and $\overline{F}_{K_2}$ maintain a constant direction—i.e., the angle between vectors $\overline{F}_{K_1min}$ and $\overline{F}_{K_1}$ is constant and equal to $\frac{\alpha_{K_1max}}{2}$; similarly, the angle between vectors $\overline{F}_{K_2min}$ and $\overline{F}_{K_2}$ is also constant and equal to $\frac{\alpha_{K_2max}}{2}$, while $\frac{\alpha_{K_2max}}{2} = \frac{\alpha_{K_1max}}{2}$.

Taking into account these assumptions, (5.235) acquires the following form:

$$
\begin{aligned}
\ddot{x}_1 &= \frac{1}{m_k}\Big[\frac{\cos\delta\cdot\tan\gamma}{\sqrt{\tan^2\gamma+1+\tan^2\beta}} - f\cos^2\delta\cdot\sin\big(\gamma+\tfrac{\alpha_{K_1max}}{2}\big)\sin\gamma + f\cos\delta\cdot\cos\big(\gamma+\tfrac{\alpha_{K_1max}}{2}\big)\cos\gamma\Big]\cdot H\sin\omega t \\
&\quad +\frac{2}{m_k}\Big[\frac{\sin\gamma\cdot\tan\gamma}{\sqrt{\tan^2\gamma+1+\tan^2\beta}} + f\sin^2\gamma\cdot\sin\big(\gamma+\tfrac{\alpha_{K_1max}}{2}\big)\cos\delta + f\sin\gamma\cdot\cos\gamma\cdot\cos\big(\gamma+\tfrac{\alpha_{K_1max}}{2}\big)\Big]P_1 - \frac{R_{x_1}}{m_k}, \\
\ddot{x}_1 &= \frac{1}{m_k}\Big[\frac{\cos\delta\cdot\tan\beta}{\sqrt{\tan^2\gamma+1+\tan^2\beta}} - f\cos\delta\cdot\sin\big(\gamma+\tfrac{\alpha_{K_1max}}{2}\big)\sin\delta\Big]\cdot H\sin\omega t \\
&\quad +\frac{2}{m_k}\Big[\frac{\sin\gamma\cdot\tan\gamma\beta}{\sqrt{\tan^2\gamma+1+\tan^2\beta}} - f\sin\gamma\cdot\sin\big(\gamma+\alpha_{K_1max}\sin\omega t\big)\cdot\sin\delta\Big]P_1 - \frac{R_{z_1}}{m_k} - g, \\
&\qquad \omega t\in[2k\pi,(2k+1)\pi],\quad k=0,1,2,\dots
\end{aligned}
\tag{5.236}
$$

where g—gravitational acceleration.

The system of differential Equation (5.236) is a system of linear second-order differential equations. It can be solved by using the integration method.

To reduce the expression of (5.236), we introduce the following designations.

$$
\frac{1}{m_k}\Big[\frac{\cos\delta\cdot\tan\gamma}{\sqrt{\tan^2\gamma+1+\tan^2\beta}} + f\cos^2\delta\cdot\sin\big(\gamma+\tfrac{\alpha_{K_1max}}{2}\big)\sin\gamma + f\cos\delta\cdot\cos\big(\gamma+\tfrac{\alpha_{K_1max}}{2}\big)\cos\gamma\Big] = \varphi_1,
\tag{5.237}
$$

$$
\frac{2}{m_k}\Big[\frac{\sin\gamma\cdot\tan\gamma}{\sqrt{\tan^2\gamma+1+\tan^2\beta}} + f\sin^2\gamma\cdot\sin\big(\gamma+\tfrac{\alpha_{K_1max}}{2}\big)\cos\delta + f\sin\gamma\cdot\cos\gamma\cdot\cos\big(\gamma+\tfrac{\alpha_{K_1max}}{2}\big)\Big] = \psi_1,
\tag{5.238}
$$

$$
\frac{1}{m_k}\Big[\frac{\cos\delta\cdot\tan\beta}{\sqrt{\tan^2\gamma+1+\tan^2\beta}} - f\cos\delta\cdot\sin\big(\gamma+\tfrac{\alpha_{K_1max}}{2}\big)\sin\delta\Big] = \varphi_2,
\tag{5.239}
$$

$$
\frac{2}{m_k}\Big[\frac{\sin\gamma\cdot\tan\beta}{\sqrt{\tan^2\gamma+1+\tan^2\beta}} - f\sin\gamma\cdot\sin\big(\gamma+\tfrac{\alpha_{K_1max}}{2}\big)\sin\delta\Big] = \psi_2.
\tag{5.240}
$$

Taking into consideration (5.237)–(5.250), (5.54) assumes the following form:

$$\left.\begin{array}{rcl}\ddot{x}_1 &=& \varphi_1 H \sin \omega t + \psi_1 P_1 - \dfrac{R_{x_1}}{m_k}, \\[2mm] \ddot{z}_1 &=& \varphi_2 H \sin \omega t + \psi_2 P_1 - \dfrac{R_{z_1}}{m_k} - g. \end{array}\right\} \qquad (5.241)$$

Now, we are going to integrate (5.241). The first integral will be as follows:

$$\left.\begin{array}{rcl}\dot{x}_1 &=& -\dfrac{\varphi_1 H}{\omega} \cos \omega t + \psi_1 P_1 t - \dfrac{R_{x_1}}{m_k} t + \dfrac{\varphi_1 H}{\omega} + C_1, \\[2mm] \dot{z}_1 &=& -\dfrac{\varphi_2 H}{\omega} \cos \omega t + \psi_2 P_1 t - \dfrac{R_{z_1}}{m_k} t - g t + L_1. \end{array}\right\} \qquad (5.242)$$

where C_1 and L_1 are arbitrary constants.

The second integral of (5.242) will be as follows:

$$\left.\begin{array}{rcl}x_1 &=& -\dfrac{\varphi_1 H}{\omega^2} \sin \omega t + \dfrac{\psi_1 P_1 t^2}{2} - \dfrac{R_{x_1} t^2}{2m_k} + C_1 t + C_2, \\[2mm] z_1 &=& -\dfrac{\varphi_2 H}{\omega^2} \sin \omega t + \dfrac{\psi_2 P_1 t^2}{2} - \dfrac{R_{z_1} t^2}{2m_k} - \dfrac{g t^2}{2} + L_1 t + L_2, \end{array}\right\} \qquad (5.243)$$

where C_2 and L_2 are arbitrary constants.

The arbitrary constants C_1, L_1, C_2 and L_2 are determined by the initial conditions of (4.235). These arbitrary constants are equal to:

$$C_1 = \dfrac{\varphi_1 H}{\omega}, \qquad L_1 = \dfrac{\varphi_2 H}{\omega}, \qquad C_2 = x_{10}, \qquad L_2 = -\dfrac{1}{3} h_k. \qquad (5.244)$$

By substituting the values of the arbitrary constants C_1 and L_1 into the system of differential Equations (5.242), we obtain:

$$\left.\begin{array}{rcl}\dot{x}_1 &=& -\dfrac{\varphi_1 H}{\omega^2} \cos \omega t + \psi_1 P_1 t - \dfrac{R_{x_1} t}{m_k} + \dfrac{\varphi_1 H}{\omega}, \\[2mm] \dot{z}_1 &=& -\dfrac{\varphi_2 H}{\omega^2} \cos \omega t + \psi_2 P_1 t - \dfrac{R_{z_1} t}{m_k} - g t + \dfrac{\varphi_2 H}{\omega}. \end{array}\right\} \qquad (5.245)$$

By substituting the values of the derived arbitrary constants C_1, C_2, L_1 and L_2 into (5.243), we obtain:

$$\left.\begin{array}{rcl}x_1 &=& -\dfrac{\varphi_1 H}{\omega^2} \sin \omega t + \dfrac{\psi_1 P_1 t^2}{2} - \dfrac{R_{x_1} t^2}{2m_k} + \dfrac{\varphi_1 H t}{\omega} + x_{10}, \\[2mm] z_1 &=& -\dfrac{\varphi_2 H}{\omega^2} \sin \omega t + \dfrac{\psi_2 P_1 t^2}{2} - \dfrac{R_{z_1} t^2}{2m_k} - \dfrac{g t^2}{2} + \dfrac{\varphi_2 H t}{\omega} - \dfrac{1}{3} h_k. \end{array}\right\} \qquad (5.246)$$

(5.245) and (5.246), respectively, characterise the laws of variation of the speed and displacement of the beet root's centre of mass in the process of its direct lifting from the soil. From the second equation of (5.264), the time t_1 of the direct beet root lifting from the soil can be found. For this purpose, we have to substitute the value $z_1 = 0$ into the left member of said equation and solve the resulting equation

for t_1. Since the equation is transcendental, it is impossible to derive any analytic expression to find t_1. However, it can be solved with the use of a PC applying the known methods. The computed value of t_1 can be subsequently used for determining the productivity of the sugar beet root harvesting machine equipped with vibrational lifting tools.

Next, we are going to give consideration to (5.233). To reduce the expression of this system of equations, we again introduce the following designations:

$$\frac{1}{m_k}\left(\frac{2\sin\gamma\cdot\tan\gamma}{\sqrt{\tan^2\gamma+1+\tan^2\beta}}+2f\sin^3\gamma\cdot\cos\delta+f\sin2\gamma\cdot\cos\gamma\right)=\psi_1'. \qquad (5.247)$$

$$\frac{1}{m_k}\left(\frac{2\sin\gamma\cdot\tan\beta}{\sqrt{\tan^2\gamma+1+\tan^2\beta}}-2f\sin^2\gamma\cdot\sin\delta\right)=\psi_2'. \qquad (5.248)$$

Taking into account (5.247) and (5.248), (5.233) will take the following form:

$$\left.\begin{array}{l}\ddot{x}_1=\psi_1'P_1-\frac{R_{x_1}}{m_k},\\[2mm]\ddot{z}_1=\psi_2'P_1-\frac{G_k}{m_k}-\frac{R_{z_1}}{m_k},\end{array}\right\}\omega t\in[(2k-1)\pi,\quad2k\pi],\quad k=1,2,\dots \qquad (5.249)$$

After the first integration of (5.249), we obtain:

$$\left.\begin{array}{l}\dot{x}_1=\psi_1'P_1t-\frac{R_{x_1}}{m_k}t+C_1,\\[2mm]\dot{z}_1=\psi_2'P_1t-\frac{G_k}{m_k}t-\frac{R_{z_1}}{m_k}t+L_1,\end{array}\right\}\omega t\in[(2k-1)\pi,\quad2k\pi],\quad k=1,2,\dots \qquad (5.250)$$

where C_1 and L_1—are arbitrary constants,

After the second integration of (4.250), we obtain:

$$\left.\begin{array}{l}x_1=\psi_1'P_1\frac{t^2}{2}-\frac{R_{x_1}t^2}{2m_k}+C_1t+C_2,\\[2mm]z_1=\psi_2'P_1\frac{t^2}{2}-\frac{G_kt^2}{2m_k}-\frac{R_{z_1}t^2}{2m_k}+L_1t+L_2,\\[2mm]\omega t\in[(2k-1)\pi,\quad2k\pi],\quad k=1,2,\dots\end{array}\right\} \qquad (5.251)$$

where C_2 and L_2—are arbitrary constants.

The arbitrary constants C_1, L_1, C_2 and L_2 are determined by the initial conditions of (5.234). These arbitrary constants are equal to:

$$C_1=0,\qquad L_1=0,\qquad \widetilde{N}_2=x_{10},\qquad L_2=-\frac{1}{3}h_k \qquad (5.252)$$

By substituting the values of the arbitrary constants C_1 and L_1 into (5.250), we obtain:

$$\left.\begin{aligned}
\dot{x}_1 &= \psi_1' P_1 t - \frac{R_{x_1}}{m_k} t, \\
\dot{z}_1 &= \psi_2' P_1 t - \frac{G_k}{m_k} t - \frac{R_{z_1}}{m_k} t, \\
\omega t &\in [(2k-1)\pi, \ 2k\pi], \qquad k = 1, 2, \dots
\end{aligned}\right\}$$

(5.253)

By substituting the values of the arbitrary constants C_1, L_1, C_2 and L_2 into (5.251), we obtain:

$$\left.\begin{aligned}
x_1 &= \psi_1' P_1 \frac{t^2}{2} - \frac{R_{x_1} t^2}{2m_k} + x_{10}, \\
z_1 &= \psi_2' P_1 \frac{t^2}{2} - \frac{G_k t^2}{2m_k} - \frac{R_{z_1} t^2}{2m_k} - \frac{1}{3} h_k, \\
\omega t &\in [(2k-1)\pi, \ 2k\pi], \qquad k = 1, 2, \dots
\end{aligned}\right\}$$

(5.254)

(5.253) and (5.254), respectively, characterise the laws of variation of the speed and displacement of the beet root's centre of mass in the process of its direct lifting from the soil in the absence of the perturbing force action.

Now, we are going to derive the differential equation of the beet root's rotation around its centre of mass (around axis Cy, which passes through the beet root's centre of mass (point C) parallel to axis $O_1 y_1$). According to [32], said equation will have the following form:

$$I_{\gamma_c} = \frac{d^2 \theta}{dt^2} = M_{\gamma_c}^e,$$

(5.255)

where θ is the angular displacement of the beet root around axis Cy_c; I_{yc} is the root's moment of inertia with reference to axis Cy_c; M_{yc}^e is the moment of rotation around axis Cy_c (total moment of all external forces applied to the beet root with reference to axis Cy_c).

Further, let us find the moments of all external forces with reference to axis Cy_c in accordance with the schematic model of forces presented in Figure 5.12. As the movement of the beet root's centre of mass is considered with reference to the coordinate system $x_1 O_1 y_1 z_1$, we will determine the positions of K_1 and K_2—the points of contact between the root and the digging shares' working surfaces $A_1 B_1 C_1$ and $A_2 B_2 C_2$ with reference to the same coordinate system. As we can see in the schematic model in Figure 5.12, the ordinate of the contact points K_1 and K_2 in the assumed coordinate system will be equal to $z_{K1} = z_{K2} = -h_k + h$ where h is the distance from the conditional fixation point O to the plane that extends through the contact points and is perpendicular to the beet root symmetry axis.

Since the movement of the vibrational lifting tool shares takes place at a certain depth, the value of h for the specific beet root can vary only within the share oscillation amplitude, which is considerably smaller in comparison with the value of h. Therefore, the value of h for any specific beet root can be regarded constant. The ordinate of the

beet root's centre of mass (point C) at a random instant will be $z_c = z_1$ where z_1 is determined by the second equation of (5.246).

Thus, the ordinate of points K_1 and K_2 varies from the ordinate of point C by the value $-h_k + h - z_1$ and, therefore, for example, from the very beginning of the direct lifting $\left(z_1 = -\frac{h_k}{3}\right)$ we have $-h_k + h + \frac{h_k}{3} = h - \frac{2h_k}{3}$.

Then, the moments of all external forces applied to the beet root at a random instant will be equal to:

$$M_{\gamma_c}\left(\overline{Q}_{zb.1}\right) = M_{\gamma_c}\left(\overline{Q}_{zb.2}\right) = -Q_{zb1}(-h_k + h - z_1)\sin\theta, \qquad (5.256)$$

since the force vectors $\overline{Q}_{p1}$ and $\overline{Q}_{p2}$ are parallel to plane $x_1 O_1 z_1$.

$$M_{\gamma_c}\left(\overline{P}_1\right) = M_{\gamma_c}\left(\overline{P}_2\right) = P_1\cos\theta(-h_k + h - z_1), \qquad (5.257)$$

since the force vectors $\overline{P}_1$ and $\overline{P}_2$ are parallel to plane $x_1 O_1 z_1$

$$M_{\gamma_c}\left(\overline{F}_1\right) = M_{\gamma_c}\left(\overline{F}_2\right) = F_1\cos\gamma_k(-h_k + h - z_1)\sin\theta. \qquad (5.258)$$

or, taking into account (5.225), we have:

$$\begin{aligned}
M_{\gamma_c}\left(\overline{F}_1\right) &= M_{\gamma_c}\left(\overline{F}_2\right) \\
&= (0.5fH\cos\delta\cdot\sin\omega t + fP_1\sin\gamma) \\
&\cdot \sin(\gamma + \alpha_{K1max}\sin\omega t)\cos\gamma_k(-h_k + h - z_1)\sin\theta, \\
&\omega t \in [2k\pi, (2k+1)\pi], \quad k = 0,1,2,\ldots
\end{aligned} \qquad (5.259)$$

Then, taking into consideration (5.137), we obtain:

$$\begin{aligned}
M_{\gamma_c}\left(\overline{F}_1\right) = M_{\gamma_c}\left(\overline{F}_2\right) &= fP_1\sin^2\gamma\cdot\cos\gamma_k(-h_k + h - z_1)\sin\theta, \\
&\omega t \in [(2k-1)\pi,\ 2k\pi], \quad k = 1,2,\ldots.
\end{aligned} \qquad (5.260)$$

$$M_{\gamma_c}\left(\overline{E}_1\right) = M_{\gamma_c}\left(\overline{E}_2\right) = E_1\cos\gamma(-h_k + h - z_1)\cos\theta. \qquad (5.261)$$

Considering (5.226), we obtain:

$$\begin{aligned}
M_{\gamma_c}\left(\overline{E}_1\right) &= M_{\gamma_c}\left(\overline{E}_2\right) \\
&= (0.5fH\cos\delta\cdot\sin\omega t + fP_1\sin\gamma) \\
&\cdot \cos(\gamma + \alpha_{K1max}\sin\omega t)\cos\gamma(-h_k + h - z_1)\cos\theta, \\
&\omega t \in [2k\pi, (2k+1)\pi], \quad k = 0,1,2,\ldots
\end{aligned} \qquad (5.262)$$

Additionally, after using (5.138), we will come to:

$$M_{\gamma_c}\left(\overline{E}_1\right) = M_{\gamma_c}\left(\overline{E}_2\right) = 0.5 f P_1 \sin 2\gamma / \cos \gamma (-h_k + h - z_1) \cos \theta,$$
$$\omega t \in [(2k-1)\pi, \ 2k\pi], \qquad k = 1,2,\ldots. \tag{5.263}$$

$$M_{\gamma_c} = \left(\overline{G}_k\right) = 0, \tag{5.264}$$

$$M_{\gamma_c} = \left(\overline{R}_{x_1}\right) = 0, \tag{5.265}$$

$$M_{\gamma_c} = \left(\overline{R}_{z_1}\right) = 0, \tag{5.266}$$

since vectors $\overline{G}_k$, $\overline{R}_{x_1}$ and $\overline{R}_{z_1}$ intersect axis Cy_c.

Hence, based on (5.256), (5.257), (5.259) or (5.260), (5.262) or (5.263), (5.264), (5.265), (5.266) and the moment M of the couple of forces of the loosened soil's resistance to the rotation of the beet root, we find the value of the rotation moment $M^e_{y_c}$ of all external forces with reference to axis Cy_c is as follows:

$$M^e_{y_c} = 2Q_{zb.1}(-h_k + h - z_1) \sin \theta + 2P_1 \cos \theta (-h_k + h - z_1)$$
$$+ (fH \cos \delta \cdot \sin \omega t + 2fP_1 \sin \gamma) \sin(\gamma + \alpha_{K1max} \sin \omega t) \cdot \cos \gamma_k (-h_k + h - z_1) \sin \theta$$
$$+ (fH \cos \delta \cdot \sin \omega t + 2fP_1 \sin \gamma) \cdot \cos(\gamma + \alpha_{K1max} \sin \omega t) \cos \gamma (-h_k + h - z_1) \cos \theta - M,$$
$$\omega t \in [2k\pi, (2k+1)\pi], \qquad k = 0,1,2,\ldots. \tag{5.267}$$

or, after some transformations:

$$M^e_{y_c} = 2P_1(-h_k + h - z_1) \cos \theta + 2fP_1(-h_k + h - z_1) \sin^2 \gamma \cdot$$
$$\cos \gamma_k \cdot \sin \theta + fP_1(-h_k + h - z_1) \sin 2\gamma \cdot \cos \gamma \cdot \cos \theta - M,$$
$$\omega t \in [(2k-1)\pi, \ 2k\pi], \qquad k = 0,1,2,\ldots. \tag{5.268}$$

The moment of inertia I_{yc} of the beet root with reference to axis Cy_c is determined with the use of Expression (5.103). By substituting (5.2), (5.103), (5.267) or (5.268) into (5.255), we obtain the differential equation of the beet root's rotation around axis Cy_c during its direct lifting from the soil, which has the following form:

$$\left(0.038 + 0.15 \tan^2 \gamma_k\right) m_k h_k^2 \frac{d^2\theta}{dt^2} = -H(-h_k + h - z_1) \sin \theta \sin \omega t$$
$$+ 2P_1 \cos \theta (-h_k + h - z_1) + (fH \cos \delta \cdot \sin \omega t + 2fP_1 \sin \gamma) \sin(\gamma + \alpha_{K1max} \sin \omega t)$$
$$\cdot \cos \gamma_k (-h_k + h - z_1) \sin \theta + (fH \cos \delta \cdot \sin \omega t + 2fP_1 \sin \gamma)$$
$$\cdot \cos(\gamma + \alpha_{K1max} \sin \omega t) \cos \gamma (-h_k + h - z_1) \cos \theta - M,$$
$$\omega t \in [2k\pi, (2k+1)\pi], \qquad k = 0,1,2,\ldots. \tag{5.269}$$

or

$$\left(0.038 + 0.15 \tan^2 \gamma_k\right) m_k h_k^2 \frac{d^2\theta}{dt^2} = 2P_1 \cos \theta (-h_k + h - z_1)$$
$$+ 2fP_1 \sin^2 \gamma \cdot \cos \gamma_k (-h_k + h - z_1) \sin \theta$$
$$+ 2fP_1 \sin 2\gamma \cos \gamma (-h_k + h - z_1) \cos \theta - M,$$
$$\omega t \in [(2k-1)\pi, \ 2k\pi], \qquad k = 1,2,\ldots. \tag{5.270}$$

The initial conditions for the obtained differential equation are established based on the same considerations as for (5.234) and they will have the following form:

$$\text{at} \quad t = 0 : \theta = 0, \quad \dot{\theta} = 0. \tag{5.271}$$

(5.269) is nonlinear. It can only be solved with the use of numerical techniques and a PC. With this approach, the value z_1 for each cycle of using the numerical algorithm has to be obtained from the second equation in (5.246) for the respective instant t_k.

(5.270) is also nonlinear, since it includes the value z_1, which is a variable, and for any instant t_k this value z_1 has to be obtained from the second equation in (5.254).

Thus, the obtained analytic expressions, essentially, constitute the theory of direct sugar beet root lifting from the soil with the use of vibrational lifting tools. The reached analytic expressions make it possible to define the kinematic modes of vibration-assisted beet root lifting based on the requirement of keeping the roots intact and the design parameters of the vibrational lifting tool.

Now, let us apply the achieved results of the developed theory and construct an algorithm for computing the kinematic parameters of the work process under consideration. Here are its main provisions:

1. First, specify the required initial data for the calculation.
2. Then, find the values φ1, ψ1, φ2, ψ2 in accordance with (5.237), (5.238), (5.239) and (5.240), respectively.
3. Next, find the sugar beet root motion law during its direct lifting from the soil, according to (5.246).
4. Now, move to drawing the diagrams for various values of the initial parameters; from these diagrams, the time of duration of the direct beet root lifting from the soil can be found.
5. In order to carry out the numerical calculations, we have to specify the required parameters. Thus, according to [7,31], the specified parameters have the following values:

- (Average) mass of a sugar beet root: mk = 0.9 kg;
- (Average) length of a sugar beet root: hk = 0.25 m;
- Angles of the vibrational lifting tool's trihedral wedges: $\gamma = 14°$, $\beta = 52°$;
- Friction coefficient of steel on the sugar beet root surface: f = 0.45;
- Resistance force exerted by the soil when a sugar beet root moves in it: Rx = 100 N, Rz = 100 N;
- Amplitude of perturbing force: H = 500 N;
- Transverse moving force: P1 = 400 N;

- Angle of deflection of the friction force vector from the vector of its minimal value: $\alpha_{K1max} = 30°$;
- Initial position of the sugar beet root's centre of mass on axis O_1x_1: $x_{10} = 0.2$ m.

The dihedral angle δ between the wedge's working surface and the lower base of the lifting tool can be derived from: $\delta = \arctan\dfrac{\cos\beta}{\sin\delta\cdot\cos\gamma}$.

Calculations have been carried out for several values of the vibrational lifting tool oscillation frequency.

Based on the obtained law of motion of the beet root's centre of mass (5.63) in the system of coordinates $x_1O_1z_1$, we draw the graphs $x_1 = x_1(t)$, $z_1 = z_1(t)$ in the MathCAD environment (Figure 5.13) in order to determine the lifting time.

As may be inferred from the graphs, the duration of the beet root lifting from the soil ($z_1 = 0$) reaches only 0.032 s.
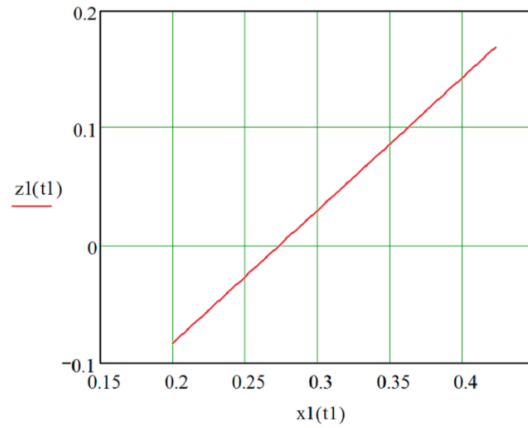
In Figure 5.14, the motion trajectory of the beet root's centre of mass during the direct beet root lifting from the soil is shown.

It becomes evident from the presented graph that within the interval of lifting the beet root from the soil ($-0.083 \le z_1 \le 0$), its centre of mass moves effectively on a straight line.

Obviously, this motion trajectory represents the actual trajectory of motion of the beet root's centre of mass only as a certain approximation since the soil resistance forces during the beet root displacement R_{x1} and R_{z1} are assumed to have constant magnitudes.

(a)   (b)
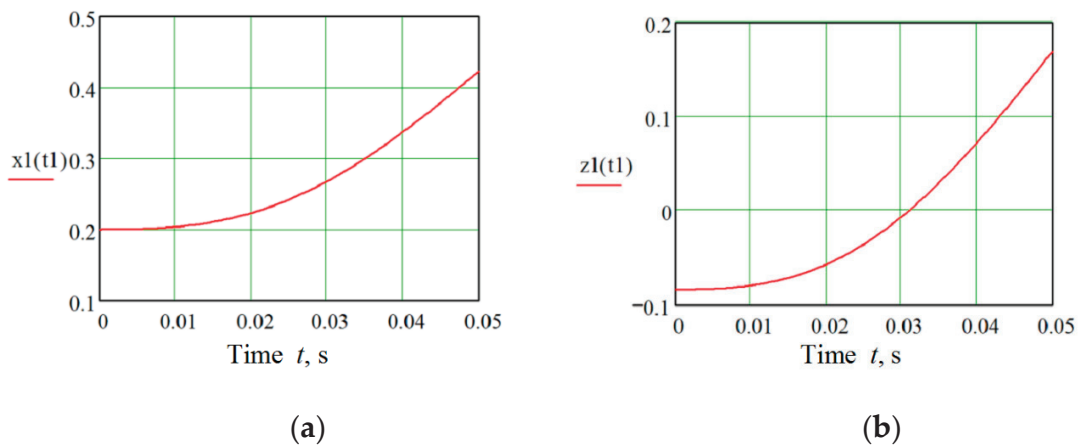
Figure 5.13. Graphs of the root's centre of mass displacement along axes O_1x_1 (a) and O_1z_1 (b) as a function of time during the direct beet root lifting from the soil ($H = 500$ N; $P_1 = 400$ N; $R_x = 100$ N; $R_z = 100$ N; $v = 10$ Hz).

Figure 5.14. Beet root motion trajectory in the coordinate system $x_1 O_1 z_1$ during the direct lifting of the root from the soil: ($H = 500$ N, $P_1 = 400$ N, $R_x = 100$ N, $R_z = 100$ N, $v = 10$ Hz).

Additionally, calculations have been carried out for the displacement of the beet root's centre of mass along axis $O_1 z_1$ until its complete lifting from the soil as a function of the changing perturbing force amplitude and $z_1 = z_1(H, t)$ at $P_1 = $ const and $z_1 = z_1(P, t)$ at $P = $ const have been obtained.
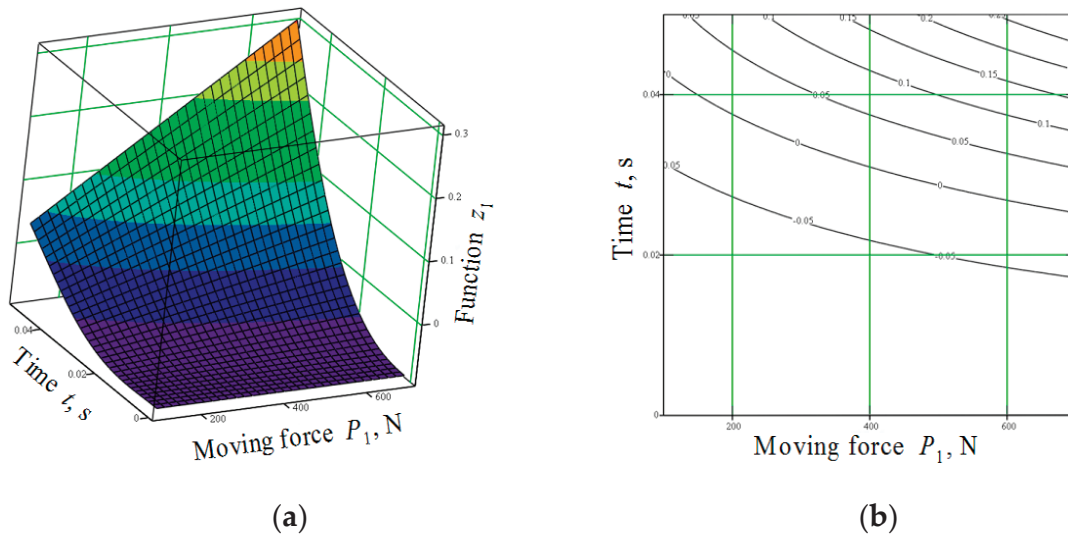
In Figure 5.15, the surface and profile graphs of $z_1 = z_1(H, t)$ subject to the perturbing force amplitude variation within a range of $H = 100$–700 N (for a transverse moving force value of $P_1 = 400$ N and an oscillation frequency value of $v = 10$ Hz) are presented.

(a)   (b)
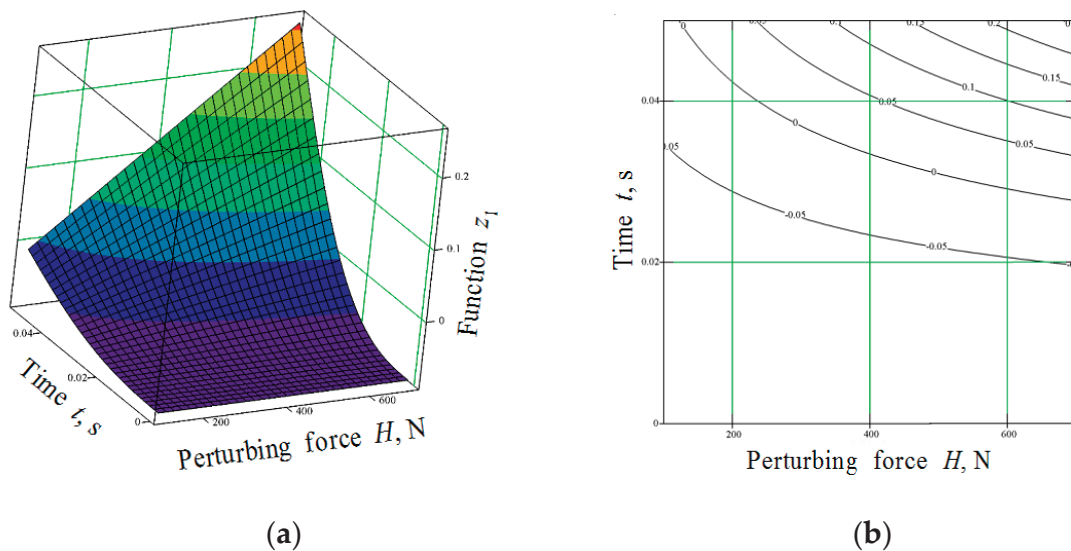
Figure 5.15. Surface (**a**) and profile graphs (**b**) of function $z_1 = z_1(H, t)$ for the perturbing force amplitude's variation within a range of $H = 100$–700 N ($P_1 = 400$ N, $v = 10$ Hz).

As one may see in the shown graph, when the perturbing force amplitude changes within a range of 100–700 N, the time of beet root lifting from the soil changes within an interval of 0.053–0.028 s.

In Figure 5.16, the surface and profile graphs of the function $z_1 = z_1(P_1, t)$, subject to the transverse moving force variation within a range of $P_1 = 100$–700 N (for a perturbing force amplitude value of $H = 500$ N and an oscillation frequency value of $v = 10$ Hz), are presented.

| (a) | (b) |

Figure 5.16. Surface (**a**) and profile graphs (**b**) of function $z_1 = z_1(P_1, t)$ for the transverse moving force variation within a range of $P_1 = 100$–700 N ($H = 500$ N, $v = 10$ Hz).

As may be inferred from the shown graph, when the transverse moving force changes within a range of 100–700 N, the time of beet root lifting from the soil changes within a range of 0.043–0.026 s.

Based on the developed technique, a similar computation can be carried out for any values of the oscillation frequency of the vibrating digging tool.

5.5. Conclusions

1. A theory of lifting sugar beet roots from the soil with vibrational lifting tools has been worked out. This includes the analytic description of the work process at all stages of lifting, starting from the instant when the vibrational lifting tool grips the root, up to the complete lifting of the root out of soil.
2. On the basis of the kinematic and dynamic Euler equations, the system of differential equations has been obtained for the three-dimensional oscillations of the root fixed in the soil as a rigid body in an elastic medium in the most general case—the case of asymmetric gripping of the root by the digging tool (gripping of the root by one share).

3. The mathematical model of oscillations of the root as a rigid body in an elastic medium during the symmetric gripping of the root by the digging tool (gripping of the root by both shares simultaneously) has been developed. The system of differential equations of the root's translational oscillations together with the soil surrounding it as well as the differential equation of the root's angular oscillations about the conventional point of its fixation in the soil have been set up. The solving of the obtained system of differential equations allows the law of the oscillatory process of the root in the soil during vibrational lifting, as well as the analytic expressions for the computation of the frequencies and amplitudes of the free and free accompanying oscillations and the amplitudes of the forced oscillations of the root as a rigid body in the soil, to be found. In accordance with the calculations, the root's centre of mass covers a distance of 50 mm along axis O_{x1} in 0.025 s at a perturbing force frequency of $v = 10$, 15 and 20 Hz along axis $Oz1$ at a perturbing force frequency of $v = 10$ Hz—a distance of 33 mm ($c_1 = 2 \cdot 105$ N·m^{-2}), a distance of 21 mm ($c_1 = 3 \cdot 105$ N·m^{-2}) or a distance of 13 mm ($c_1 = 4 \cdot 105$ N·m^{-2}), at $v = 15$ Hz—a distance of 35 mm ($c_1 = 2 \cdot 105$ N·m^{-2}), a distance of 25 mm ($c_1 = 3 \cdot 105$ N·m^{-2}), a distance of 15 mm ($c_1 = 4 \cdot 105$ N·m^{-2}), at $v = 20$ Hz—a distance of 40 mm ($c_1 = 2 \cdot 105$ N·m^{-2}), a distance of 30 mm ($c_1 = 3 \cdot 105$ N·m^{-2}), and a distance of 20 mm ($c_1 = 4 \cdot 105$ N·m^{-2}). The obtained theoretical values of the amplitudes of oscillations of the root as a rigid body under the analysed kinematic parameters ensure the full breaking of the bonds between the root and the soil and establish the conditions for the direct lifting of the root.

4. The mathematical model of direct lifting of the root from the soil by the vibrating digging tool has been generated. The system of differential equations of the root's plane-parallel motion during its direct lifting from the soil has been obtained. The solving of the mentioned system of differential equations has allowed the law of the motion of the root's centre of mass during its direct lifting from the soil to be found in the analytical form. The calculations performed with the use of the PC have allowed the duration of the direct lifting of the root from the soil to be found and the analysis of the effect that the design parameters of the digging tool and the kinematic parameters of the performed work process have on the duration of the lifting of the root from the soil.

Thus, at a perturbing force amplitude of $H = 500$ N and a transverse moving force of $P_1 = 400$ N, the soil resistance forces along axis Ox_1 and Oz_1, $Rx = 100$, with a perturbing force frequency of $v = 10$ Hz, and time of root lifting from the soil of 0.032 s. When the perturbing force amplitude varies within a range of 100–700 N (at a transverse moving force of $P_1 = 400$ N and a perturbing force frequency of $v = 10$ Hz), the time of beet root lifting from the soil varies within a range of 0.053–0.028 s.

When the transverse moving force varies within a range of $P_1 = 100$–700 N (at a perturbing force amplitude of $H = 500$ N and a perturbing force frequency of 10 Hz), the time of beet root lifting from the soil varies within a range of 0.043–0.026 s.

The achieved results of the theoretical research provide the possibility to determine the optimal kinematic modes of operation and vibrational lifting tool design parameters, proceeding from the requirement of keeping sugar beet roots intact when harvesting them.

6. Theory of Impact Interaction between Vibrational Lifting Tool and Sugar Beet Root

6.1. Impact Interaction at One Point

In any work process, the required conditions include providing sufficient productivity, reducing the energy consumption and increasing the quality of performance of the work process.

As regards beet harvesters, in order to ensure the quality of performance of their work process, it is necessary, first of all, to prevent damaging roots during their lifting. Meanwhile, the highest probability of damaging the lifted roots occurs in the case of impact interaction between the beet harvester digging tool and the root body fixed in the soil. It is quite obvious that at high velocities of the translational motion of modern beet harvesters as well as high rates of the oscillatory motion of vibrational lifting tools, it is possible to expect, especially when operating in dry and hard soil, the impact interaction between the digging shares and the root body at the instant when the lifting tool runs into the root.

This highlights the need to theoretically investigate the mentioned impact interaction and use the results obtained from the investigations the determine the kinematic and design parameters of the lifting tools that meet the condition of not damaging the roots in the impact interaction and comparing them with the kinematic parameters obtained in Section 4.

Since the roots are rather often positioned with an offset with respect to the row centreline, in many cases the impact interaction between the root and the tool takes place at one point—i.e., the interaction involves only one of the wedges. This is the case under consideration in the current subsection.

As the vibrating digging tool approaches the root, the loosened soil between the shares and the root almost does not accumulate due to the oscillation of the shares; therefore, the initial contact between the shares and the root's surface is immediate or through a rather thin layer of soil. Thereby, when the shares of the digging tool run into the root, they impact the root, which, as is known, features a significant impact impulse. As the impact impulse has a certain finite value and is effective within a very short time interval, the respective impact force is rather great; in fact, its magnitude significantly exceeds the values of all other forces acting on the root at the same time. However, since the root is still rigidly fixed in the soil, a danger of it breaking off or tearing apart arises. It is common practice to assume that the duration of the impact is equal to zero, which implies the assumption that the velocities of

177

the colliding bodies vary instantaneously by a finite value. At the same time, the positions of the bodies do not change; therefore, the presence of elastic constraints in the mechanical system has no effect on the progress of the impact process. This is due to the fact that no deformation arises in the mentioned constraints within the time of impact—accordingly, the constraints do not generate any reaction forces. If the mechanical system contains viscous elements, the reactions are generated in them during the impact; nevertheless, these reaction forces have finite magnitudes (as the velocities are finite)—hence, their impulses within the time of impact are equal to zero [33].

Usually, the further motion (after the impact) develops in different ways, depending on the presence or absence of elastic or viscous constraints. When the digging tool runs into the root, the soil at the lower part of the root remains unbroken (the root's tail part is fixed in this soil layer); therefore, said soil during the impact acts as an elastic or viscous (depending on the mechanical makeup and moisture content of the soil) shock absorber. Certainly, the harder and drier the soil is, the more adequate the above description is for the real impact process.

Further, taking into account the fact that the breaking off or tearing apart of the root is more probable in the case when the root is fixed in hard and dry soil, it is necessary to investigate such a case. First of all, the equivalent schematic model of the impact interaction between the vibrational lifting tool and the root body that takes place when the tool runs into the root is to be set up. For this purpose, the vibrating digging tool is represented as the two wedges $A_1B_1C_1$ and $A_2B_2C_2$, each of them having three-dimensional inclinations at angles of α, β, γ and both of them are positioned with respect to each other in such a way that a working channel necking rearwards is created (Figure 6.1). The mentioned wedges perform oscillatory motions in the longitudinal and vertical plane; the line of the translational motion of the vibrating digging tool is shown by an arrow.

It is assumed that the root approximated by a cone-shaped body only impacts with the face of wedge $A_1B_1C_1$ at point K_1 (Figure 6.1).

Moreover, the impact contact can take place either in the form of direct contact or contact via the thin layer of soil between the wedge face and the root.

In order to describe the impact process, it is necessary to set up the system of coordinates. For this purpose, the vibrational lifting tool is associated with the orthogonal Cartesian coordinate system $Oxyz$, where the centre O of which is placed in the middle of the lifter's necked passage, axis Ox is in line with the direction of the lifter's translational movement, axis Oz pointing vertically up, and axis Oy points to the lifter's right side (Figure 6.1).

Further, the forces generated by the interaction between the vibrational lifting tool and the root have to be presented (Figure 6.1).
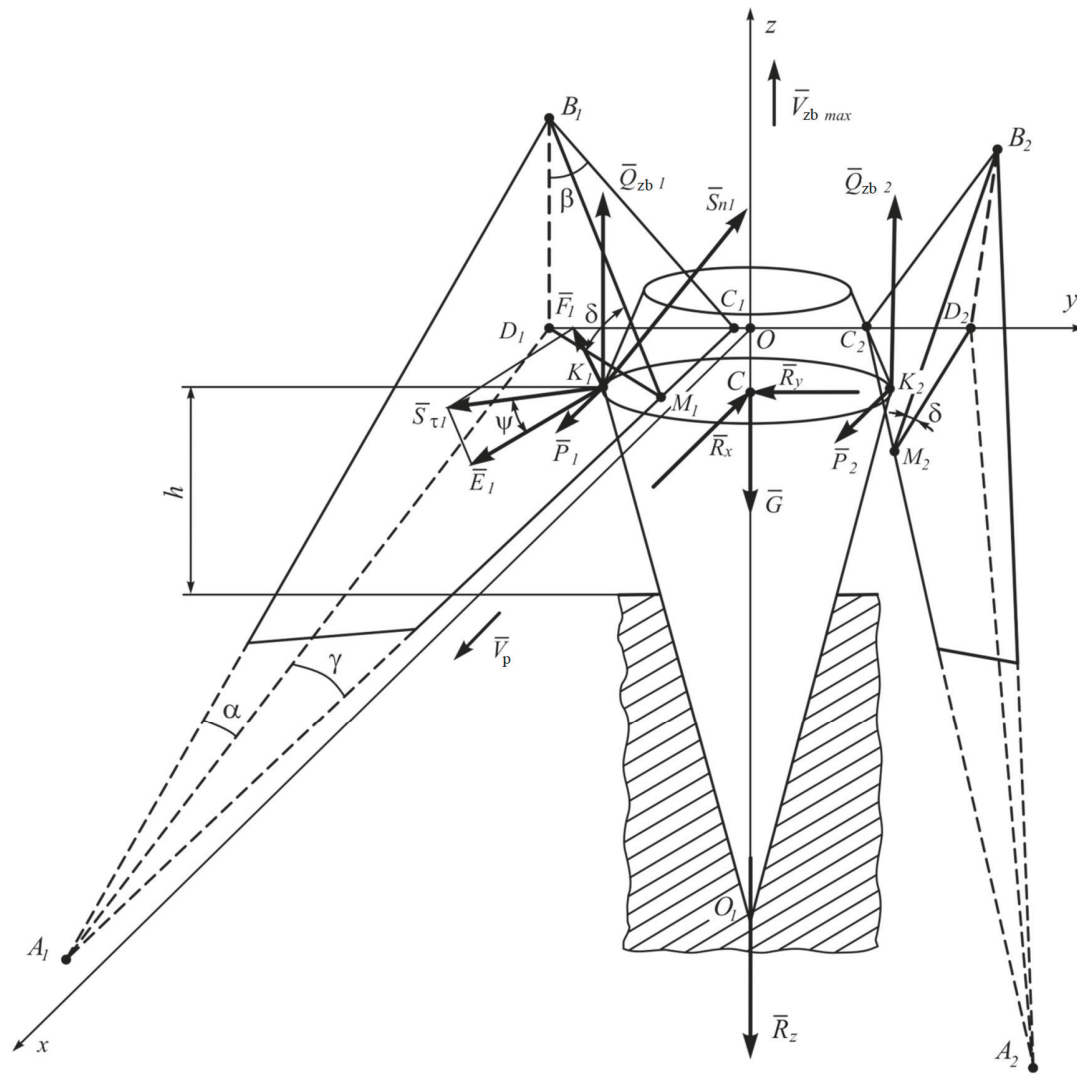
Figure 6.1. Equivalent schematic model of impact interaction at one point between vibrational lifting tool and root body fixed in soil.

It is assumed that the vibrational lifting tool exerts the vertical perturbing force $\overline{Q}_{zb.}$, which varies according to the following harmonic law:

$$Q_{zb.} = H \sin \omega t \qquad (6.1)$$

where H—amplitude of perturbing force (N); ω—angular frequency of perturbing force (s^{-1}).

Said perturbing force is applied to the root simultaneously by both the wedges; therefore, it is represented in the equivalent schematic model by its two components $\overline{Q}_{zb.1}$ and $\overline{Q}_{zb.2}$, applied at points K_1 and K_2, respectively, at a distance of h from the conditional fixation point O_1.

Therefore, the following relation is observed:

$$Q_{zb.1} = Q_{zb.2} = 0.5H \sin \omega t \tag{6.2}$$

As the vibrational lifting tool advances linearly along axis Ox, there are also propulsive forces $\overline{P}_1$ and $\overline{P}_2$ acting along axis Ox and applied at points K_1 and K_2, respectively.

In addition to this, at the contact point K_1, the friction force is applied, which counteracts the slipping of the root on the working face of wedge $A_1B_1C_1$. At the root's centre of mass (point$C$), the root weight force G_k is applied. The forces of bonding between the root and the soil that act along axes Ox, Oy and Oz are designated as $\overline{R}_x$, $\overline{R}_y$ and $\overline{R}_z$, respectively. Further, during the impact the root is subjected to the impact impulse $\overline{S}_{n1}$ generated by the vibrational lifting tool and applied at point K_1. Said impact impulse is vectored normally to the work face of the share—i.e., plane $A_1B_1C_1$.

Moreover, the tangential impact impulse $\overline{S}_{\tau 1}$ acts on the surface of the wedge. According to the Routh hypothesis, the relation between the magnitudes of the tangential and normal impact impulses is similar to Coulomb's law of friction—that is [34]:

$$S_\tau \leq fS_n \tag{6.3}$$

where f—dynamic coefficient that specifies the properties of the surfaces of the colliding bodies. In the general case, this coefficient can differ from the coefficient of friction for the bodies slipping relative to each other in continuous contact.

The sign of inequality represents the case when the tangential impulse is so small that no slipping takes place between the bodies. Only when the slipping is present, should the equality sign be applied.

The impulse $\overline{S}_{n1}$ has to be decomposed into component $\overline{F}_1$ that is at a right angle to the right line A_1C_1 and component $\overline{E}_1$ that is parallel to the right line A_1C_1 (Figure 6.1). That appears as follows:

$$\overline{S}_{\tau 1} = \overline{F}_1 + \overline{E}_1 \tag{6.4}$$

It is obvious that angle ψ between component $\overline{E}_1$ and vector $\overline{S}_{\tau 1}$ in a first approximation depends on the ratio $\frac{V_{zb.max}}{V_p}$.

Vector $\overline{S}_{\tau 1}$ in such a representation will allow finding its projections on axes Ox, Oy and Oz later.

The magnitude of the impact impulse can be different depending on the rate of the digging tool's oscillatory motion in the vertical plane at the instant when it runs into the root. Moreover, in view of the fact that the root has a conical shape when the vibrational lifting tool moves downwards, the vertical component of the impact

impulse is virtually absent. In such a case, the impact impulse is created only by the translational motion of the lifter.

The next step is to analyse in detail the oscillatory motion of the vibrational lifting tool. It is assumed that the digging tool moves upwards from its lowest position $-a$ to its highest position a, where a is the amplitude of oscillations of the tool; then, the digging tool moves downwards from the highest position a to the lowest position $-a$. Hence, the oscillations of the tool will take place in accordance with the following harmonic law:

$$z_k = -a \cos \omega t \tag{6.5}$$

where z_k—displacement of the tool from the horizontal axis, about which the oscillations take place (m); ω—angular frequency of oscillations of the digging tool (s^{-1}).

Hence, the digging tool's oscillatory motion velocity $V_{3\delta}$ at any instant of time t is equal to:

$$V_{zb.} = a\omega \sin \omega t \tag{6.6}$$

The maximum value of the velocity is equal to:

$$V_{zb.max} = a\omega \tag{6.7}$$

Therefore, it is necessary to investigate the impact interaction case where the impact impulse reaches its maximum. Such a case is observed at the moment when the vibrational lifting tool runs into the root if the tool is moving at that moment upwards at a velocity of $V_{zb.max}$.

In view of the fact that all the forces shown in Figure 6.1 have finite magnitudes, the impulses of these forces within the time of impact are virtually equal to zero. Only the impact impulses S_{n1} and $S_{\tau1}$ have nonzero values.

Further, the impulse-momentum theorem for the case of an impact is to be applied [32]:

$$m\left(\overline{U} - \overline{V}\right) = \overline{S}_{n1} + \overline{S}_{\tau1} \tag{6.8}$$

where $\overline{V}$—velocity of the digging tool before the impact; $\overline{U}$—velocity of the digging tool after the impact; m—mass of the reduced digging tool to the point of impact.

At the same time:

$$\overline{V} = \overline{V}_p + \overline{V}_{zb.max} \tag{6.9}$$

where $\overline{V}_p$—velocity of the translational motion of the lifter; $\overline{V}_{zb.max}$—maximum velocity of the oscillatory motion of the digging tool.

The vector of the lifter's translational motion velocity $\overline{V}_p$ is directed along axis Ox, while the vector of the digging tool's oscillatory motion velocity $\overline{V}_{zb.max}$—along axis Oz upwards. Taking into account (6.3), (6.8) acquires the following form:

$$m\left(\overline{U} - \overline{V}\right) = \overline{S}_{n1} + f\overline{S}_{n1} \tag{6.10}$$

(6.10) has to be written in the form of its projections on the axes of the Cartesian coordinate system $Oxyz$.

First, it is necessary to determine the projections of the vectors in Equation (5.10) on axis Ox.

It is obvious that:

$$V_x = V_p \tag{6.11}$$

As the vector $\overline{S}_{n1}$ is directed along the normal line to the wedge surface, in accordance with (3.12) the following is obtained:

$$S_{n1x} = \frac{S_{n1} \tan \gamma}{\sqrt{\tan^2 \gamma + 1 + \tan^2 \beta}} \tag{6.12}$$

As can be seen from Figure 6.1, the projections of the vectors $\overline{E}_1$ and $\overline{F}_1$ on axis Ox are equal to:

$$E_{1x} = E_1 \cos \gamma = S_{\tau 1} \cos \psi \cdot \cos \gamma \tag{6.13}$$

$$F_{1x} = F_1 \cos \delta \cdot \sin \gamma = S_{\tau 1} \sin \psi \cdot \cos \delta \cdot \sin \gamma \tag{6.14}$$

The projections of the vectors on axis Oy are found in a similar way.
Using (2.12), the following is obtained:

$$S_{n1y} = \frac{S_{n1}}{\sqrt{\tan^2 \gamma + 1 + \tan^2 \beta}} \tag{6.15}$$

As is clear from Figure 6.1,

$$E_{1y} = -E_1 \sin \gamma = -S_{\tau 1} \cos \psi \cdot \sin \gamma \tag{6.16}$$

$$F_{1y} = -F_1 \cos \delta \cdot \cos \gamma = -S_{\tau 1} \sin \psi \cdot \cos \delta \cdot \cos \gamma \tag{6.17}$$

It is obvious that:

$$V_y = 0 \tag{6.18}$$

Next, the projections of the vectors on axis Oz will be found.
It is obvious that:

$$V_z = V_{zb.max} \tag{6.19}$$

In accordance with Expression (3.12), the following is arrived at:

$$S_{n1z} = \frac{S_{n1} \tan \beta}{\sqrt{\tan^2 \gamma + 1 + \tan^2 \beta}} \tag{6.20}$$

Moreover,

$$E_{1z} = 0 \tag{6.21}$$

$$F_{1z} = F_1 \sin \delta = S_{\tau 1} \sin \psi \cdot \sin \delta \tag{6.22}$$

Taking into account (6.11)–(6.22), (6.10) is resolved into the following system of equations:

$$\left. \begin{aligned} m\left(U_x - V_p\right) &= \frac{S_{n1} \tan \gamma}{\sqrt{\tan^2 \gamma + 1 + \tan^2 \beta}} + f S_{n1} \cos \psi \cdot \cos \gamma - f S_{n1} \sin \psi \cdot \cos \delta \cdot \sin \gamma, \\ m U_y &= \frac{S_{n1}}{\sqrt{\tan^2 \gamma + 1 + \tan^2 \beta}} - f S_{n1} \cos \psi \cdot \sin \gamma - f S_{n1} \sin \psi \cdot \cos \delta \cdot \cos \gamma, \\ m\left(U_z - V_{zb.max}\right) &= \frac{S_{n1} \tan \beta}{\sqrt{\tan^2 \gamma + 1 + \tan^2 \beta}} + f S_{n1} \sin \psi \cdot \sin \delta. \end{aligned} \right\} \tag{6.23}$$

Thus, a system of three equations with the four unknown quantities S_{n1}, U_x, U_y, U_z has been obtained. The necessary fourth equation can be obtained using Newton's hypothesis about the collision of two bodies [32].

The relation between the digging tool velocities prior to and after the impact can be expressed with the use of the coefficient of restitution ε—that is:

$$U_n = -\varepsilon V_n \tag{6.24}$$

where U_n—projection of the tool velocity after the impact on the normal line to the wedge surface; V_n—projection of the tool velocity before the impact on the wedge surface's normal line.

Considering that $\overline{U} = \overline{U}_x + \overline{U}_y + \overline{U}_z$ and $\overline{V} = \overline{V}_p + \overline{V}_{zb.max}$ and taking into account (3.12), the following is obtained:

$$U_n = \frac{U_x \tan \gamma + U_y + U_z \tan \beta}{\sqrt{\tan^2 \gamma + 1 + \tan^2 \beta}} \tag{6.25}$$

$$V_n = \frac{V_p \tan \gamma + V_{zb.max} \tan \beta}{\sqrt{\tan^2 \gamma + 1 + \tan^2 \beta}} \tag{6.26}$$

By substituting (6.25) and (6.26) into (6.24), the needed fourth equation is obtained:

$$U_x \tan \gamma + U_y U_z \tan \beta = -\varepsilon\left(V_p \tan \gamma + V_{zb.max} \tan \beta\right) \tag{6.27}$$

Thus, the system of four linear equations of the following form is arrived at:

$$
\left.\begin{aligned}
m\left(U_x - V_p\right) &= \frac{S_{n1}\tan\gamma}{\sqrt{\tan^2\gamma + 1 + \tan^2\beta}} + fS_{n1}\cos\psi\cdot\cos\gamma - fS_{n1}\sin\psi\cdot\cos\delta\cdot\sin\gamma, \\
mU_y &= \frac{S_{n1}}{\sqrt{\tan^2\gamma + 1 + \tan^2\beta}} - fS_{n1}\cos\psi\cdot\sin\gamma - fS_{n1}\sin\psi\cdot\cos\delta\cdot\cos\gamma, \\
m\left(U_z - V_{zb.max}\right) &= \frac{S_{n1}\tan\beta}{\sqrt{\tan^2\gamma + 1 + \tan^2\beta}} + fS_{n1}\sin\psi\cdot\sin\delta, \\
U_x\tan\gamma + U_y + U_z\tan\beta &= -\varepsilon\left(V_p\tan\gamma + V_{zb.max}\tan\beta\right).
\end{aligned}\right\}
\tag{6.28}
$$

(6.28) can be formulated in the following form, which is more appropriate for solving with the use of Cramer's rule:

$$
\left.\begin{aligned}
mU_x + 0U_y + 0U_z - \left(\frac{\tan\gamma}{\sqrt{\tan^2\gamma + 1 + \tan^2\beta}} + f\cos\psi\cos\gamma - f\sin\psi\cos\delta\sin\gamma\right)S_{n1} &= mV_p, \\
0U_x + mU_y + 0U_z - \left(\frac{1}{\sqrt{\tan^2\gamma + 1 + \tan^2\beta}} - f\cos\psi\sin\gamma - f\sin\psi\cos\delta\cos\gamma\right)S_{n1} &= 0, \\
0U_x + 0U_y + mU_z - \left(\frac{\tan\beta}{\sqrt{\tan^2\gamma + 1 + \tan^2\beta}} + f\sin\psi\sin\delta\right)S_{n1} &= mV_{zb.max}, \\
\tan\gamma U_x + U_y + \tan\beta U_z + 0S_{n1} &= -\varepsilon\left(V_p\tan\gamma + V_{zb.max}\tan\beta\right).
\end{aligned}\right\}
\tag{6.29}
$$

The next step is to write down the principal determinant of (6.29) and find its value:

$$
\Delta = \begin{vmatrix}
m & 0 & 0 & -\left(\dfrac{1}{\sqrt{\tan^2\gamma + 1 + \tan^2\beta}} + f\cos\psi\cdot\cos\gamma - f\sin\psi\cdot\cos\delta\cdot\sin\gamma\right) \\
0 & m & 0 & -\left(\dfrac{1}{\sqrt{\tan^2\gamma + 1 + \tan^2\beta}} - f\cos\psi\cdot\sin\gamma - f\sin\psi\cdot\cos\delta\cdot\cos\gamma\right) \\
0 & 0 & m & -\left(\dfrac{\tan\beta}{\sqrt{\tan^2\gamma + 1 + \tan^2\beta}} + f\sin\psi\cdot\sin\delta\right) \\
\tan\gamma & 1 & \tan\beta & 0
\end{vmatrix}
\tag{6.30}
$$

$$
= m^2\left(\frac{\tan\beta}{\sqrt{\tan^2\gamma + 1 + \tan^2\beta}} + f\sin\psi\cdot\sin\delta\right)\tan\beta
$$
$$
+ m^2\left(\frac{1}{\sqrt{\tan^2\gamma + 1 + \tan^2\beta}} + f\cos\psi\cdot\sin\gamma - f\sin\psi\cdot\cos\delta\cdot\cos\gamma\right)
$$
$$
+ m^2\left(\frac{\tan\gamma}{\sqrt{\tan^2\gamma + 1 + \tan^2\beta}} + f\cos\psi\cdot\cos\gamma - f\sin\psi\cdot\cos\delta\cdot\sin\gamma\right)\tan\gamma.
$$

Further, the determinant for finding the unknown quantity S_{n1} is to be written down and its value is to be found:

$$
\Delta_{S_{n1}} = \begin{vmatrix}
m & 0 & 0 & mV_\Pi \\
0 & m & 0 & 0 \\
0 & 0 & m & mV_{zb.max} \\
\tan\gamma & 1 & \tan\beta & -\varepsilon\left(V_p\tan\gamma + V_{zb.max}\tan\beta\right)
\end{vmatrix}
\tag{6.31}
$$
$$
= -m^3(1 + \varepsilon)\left(V_p\tan\gamma + V_{zb.max}\tan\beta\right).
$$

184

Thereafter, according to Cramer's rule:

$$S_{n1} = \frac{\Delta_{S_{n1}}}{\Delta} \tag{6.32}$$

After substituting (6.30) and (6.31) into (6.32) and making some transformations, the following is obtained:

$$S_{n1}$$
$$= -\frac{\dfrac{m(1+\varepsilon)\cdot\left(V_p \tan\gamma+V_{zb.max} \tan\beta\right)\cdot\sqrt{tan^2\gamma+1+tan^2\beta}}{tan^2\beta+f\sin\psi\cdot\sin\delta\cdot\tan\beta\sqrt{tan^2\gamma+1+tan^2\beta}+1-(f\cos\psi\cdot\sin\gamma+f\sin\psi\cdot\cos\delta\cdot\cos\gamma)}}{\dfrac{m(1+\varepsilon)\cdot\left(V_p \tan\gamma+V_{zb.max} \tan\beta\right)\cdot\sqrt{tan^2\gamma+1+tan^2\beta}}{\sqrt{tan^2\gamma+1+tan^2\beta}+tan^2\gamma+(f\cos\psi\cdot\cos\gamma-f\sin\psi\cdot\cos\delta\cdot\sin\gamma)\tan\gamma\sqrt{tan^2\gamma+1+tan^2\beta}}} \tag{6.33}$$

Thus, the normal component of the impact impulse generated during the impact interaction between one of the wedges and the root fixed in the soil has been determined. (6.33) represents the functional relation between the normal component S_{n1} of the impact impulse and the design and kinematic parameters of the vibrational lifting tool of the beet harvester.

The sign "−" in (6.33) designates the impact impulse S_{n1} applied by the root to the digging tool. The impact impulse applied by the digging tool to the root has a positive sign and the same magnitude.

If the total impact impulse applied by the digging tool to the root is denoted by $\overline{S}$, it is:

$$\overline{S} = \overline{S}_{n1} + \overline{S}_{\tau 1} \tag{6.34}$$

then, according to (6.23), its projections on axes O_x, O_y and O_z are, respectively, equal to:

$$S_x = \frac{S_{n1}\tan\gamma}{\sqrt{\tan^2\gamma+1+\tan^2\beta}} + fS_{n1}\cos\psi\cdot\cos\gamma - fS_{n1}\sin\psi\cdot\cos\delta\cdot\sin\gamma \tag{6.35}$$

$$S_y = \frac{S_{n1}}{\sqrt{\tan^2\gamma+1+\tan^2\beta}} - fS_{n1}\cos\psi\cdot\sin\gamma - fS_{n1}\sin\psi\cdot\cos\delta\cdot\cos\gamma \tag{6.36}$$

$$S_z = \frac{S_{n1}\tan\beta}{\sqrt{\tan^2\gamma+1+\tan^2\beta}} + fS_{n1}\sin\psi\cdot\sin\delta \tag{6.37}$$

where S_{n1} is determined in accordance with (6.33), but with a positive sign.

Hence, based on (6.35), (6.36), (6.37) and (6.33), it is possible to determine the total impact impulse applied by the digging tool to the root:

$$S = \sqrt{S_x^2 + S_y^2 + S_z^2} \tag{6.38}$$

However, the quantity of greater interest is the magnitude of the impact force, which is more important than the impact impulse, as a great number of indicators for the physical and mechanical properties of sugar beets are only related to the forces applied by the digging tool to the root. Generally, the law of the impact force variation is unknown, but it is known that said force in a very short time of $t_{ud.}$ rises from zero to a very high level, then again falls to zero. Its maximum magnitude is about twice as large as its mean value for a time interval of $t_{ud.}$ [32].

In view of the fact that $F_{ud.sr} = \frac{S}{t_{ud.}}$ where S is the impact impulse, $F_{ud.sr}$ is the mean value of the impact force and $t_{ud.}$ is the duration of the impact; it follows that

$$F_{ud.} = 2F_{ud.sr} = \frac{2S}{t_{ud.}} \tag{6.39}$$

where $F_{ud.}$—maximum value of the impact force.

Taking into account (6.35), (6.36), (6.37) and (6.39), it is possible to write down the formulae for the projections of force $F_{ud.}$ on axes O_x, O_y and O_z, respectively:

$$F_{ud.x} = \left(\frac{2\tan\gamma}{\sqrt{\tan^2\gamma + 1 + \tan^2\beta}} + 2f\cos\psi\cdot\cos\gamma - 2f\sin\psi\cdot\cos\delta\cdot\sin\gamma \right)\frac{S_{n1}}{t_{ud.}} \tag{6.40}$$

$$F_{ud.y} = \left(\frac{2}{\sqrt{\tan^2\gamma + 1 + \tan^2\beta}} - 2f\cos\psi\cdot\sin\gamma - 2f\sin\psi\cdot\cos\delta\cdot\cos\gamma \right)\frac{S_{n1}}{t_{ud.}} \tag{6.41}$$

$$F_{ud.z} = \left(\frac{2\tan\beta}{\sqrt{\tan^2\gamma + 1 + \tan^2\beta}} + 2f\sin\psi\cdot\sin\delta \right)\frac{S_{n1}}{t_{ud.}} \tag{6.42}$$

where the quantity S_{n1} is determined in accordance with (5.33), taking it with a positive sign.

The duration of impact t_{ud} can be determined only by experiment. According to [31], $t_{ud} \approx 0.6\cdot10^{-2}$ s.

The next step is to analyse the conditions that allow damage to the root to be avoided during its impact interaction with the digging tool.

If the root fixed in the soil is considered as a cantilevered beam, the root under the action of the moment created by the horizontal impact force $\overline{F}_{ud.xy} = \overline{F}_{ud.x} + \overline{F}_{ud.y}$ is

subjected to bending deformation. Therefore, if the permissible level of said moment is exceeded, the root can break. As mentioned earlier, such an event is most probable in the case of dry and hard soil. The effect is different in the case of humid and soft soil, where the root will more probably incline through an angle to the horizon under the action of the horizontal force. If the impact takes place at point K_1 situated at a distance of h from the wedge's lower edge (from the unbroken soil layer) (Figure 6.1), the moment of the impact force horizontal component about said point is equal to:

$$M_{o1}\left(\overline{F}_{ud.xy}\right) = F_{ud.xy}h \overset{F_{ud.xy} = \sqrt{F_{ud.x}^2 + F_{ud.y}^2}}{\Rightarrow} = h\sqrt{F_{ud.x}^2 + F_{ud.y}^2} \qquad (6.43)$$

where $F_{ud.x}$ and $F_{ud.y}$ are determined with (6.40) and (6.41), the above-mentioned moment is equal to:

Considering the conditions that allow for the root to not break off under the action of the moment created by the horizontal force $\overline{F}_{ud.xy}$, two cases are theoretically possible: $\left[M_{zg}\right] < M_{op}$ and $\left[M_{zg}\right] > M_{op}$ where $\left[M_{zg}\right]$ is the bending moment permissible for the root body, which does not cause the root to break off and M_{op} is the support moment of the unbroken soil, in which the root is fixed. Due to the fact that the equilibrium conditions always imply $M_{op} = M_{o1}\left(\overline{F}_{ud.xy}\right)$ where the quantity M_{op} has to be understood as the maximum (potential) support moment that can be provided by the restraint, i.e., the soil, in which the root is fixed, without disrupting the restraint.

The first case above reported is typical of dry and hard soil, the second one is typically related to humid and soft soil. In the first case, the root breaking off is possible under the condition $\left[M_{zg}\right] < M_{o1}\left(\overline{F}_{ud.xy}\right) \le M_{op}$, hence, the condition for the root not breaking off in the first case is, taking into account (6.43):

$$\sqrt{F_{ud.x}^2 + F_{ud.y}^2}\,h \le \left[M_{zg}\right] < M_{op} \qquad (6.45)$$

In the second case, the root breaking off is unlikely in general; the only possible effect is the root inclining through an angle.

Obviously, in this case the condition for the root inclining through an angle without breaking off is, taking into account (6.43):

$$M_{op} < \sqrt{F_{ud.x}^2 + F_{ud.y}^2}\,h < \left[M_{zg}\right] \qquad (6.46)$$

The second case the root will neither break off nor incline if the the following condition (considering (6.43)) is met:

$$\sqrt{F_{ud.x}^2 + F_{ud.y}^2}\,h \le M_{op} < \left[M_{zg}\right] \qquad (6.47)$$

On the basis of the condition that allows the root not to break off (6.45) in the case of impact interaction between the digging tool and the root, the limitation on the tool's velocity can be determined.

For this purpose, (6.45) can be expanded, taking into account (6.40) and (6.41), as follows:

$$\sqrt{\left(\frac{2\tan\gamma}{\sqrt{\tan^2\gamma+1+\tan^2\beta}}+2f\cos\psi\cdot\cos\gamma-2f\sin\psi\cdot\cos\delta\cdot\sin\gamma\right)+\left(\frac{2}{\sqrt{\tan^2\gamma+1+\tan^2\beta}}+2f\cos\psi\cdot\sin\gamma-2f\sin\psi\cdot\cos\delta\cdot\cos\gamma\right)^2}\cdot\frac{S_{n1}h}{t_{ud}}\leq\left[M_{zg}\right] \tag{6.48}$$

The following designations are to be introduced:

$$\sqrt{\left(\frac{2\tan\gamma}{\sqrt{\tan^2\gamma+1+\tan^2\beta}}+2f\cos\psi\cdot\cos\gamma-2f\sin\psi\cdot\cos\delta\cdot\cos\gamma\right)^2}+\sqrt{\left(\frac{2}{\sqrt{\tan^2\gamma+1+\tan^2\beta}}+2f\cos\psi\cdot\sin\gamma-2f\sin\psi\cdot\cos\delta\cdot\cos\gamma\right)^2}=A \tag{6.49}$$

$$\frac{\frac{\sqrt{\tan^2\gamma+1+\tan^2\beta}}{\tan^2\beta+f\ \sin\psi\cdot\sin\delta\cdot\tan\beta\ \sqrt{\tan^2\gamma+1+\tan^2\beta}+1-(f\cos\psi\cdot\sin\gamma+f\sin\psi\cdot\cos\delta\cdot\cos\gamma)}}{\frac{\sqrt{\tan^2\gamma+1+\tan^2\beta}}{\sqrt{\tan^2\gamma+1+\tan^2\beta}+\tan^2\gamma+(f\cos\psi\cdot\cos\gamma-f\sin\psi\cdot\cos\delta\cdot\sin\gamma)\tan\gamma\ \sqrt{\tan^2\gamma+1+\tan^2\beta}}}=B \tag{6.50}$$

Taking into account (6.49), (6.48) acquires the following form:

$$\frac{AS_{n1}h}{t_{ud.}}\leq\left[M_{zg}\right] \tag{6.51}$$

wherefrom the following is obtained:

$$S_{n1}\leq\frac{\left[M_{zg}\right]t_{ud}}{Ah} \tag{6.52}$$

In view of (6.33) and (6.50), (6.52) takes the following form:

$$Bm(1+\varepsilon)\cdot\left(V_p\tan\gamma+V_{zb.max}\tan\beta\right)\leq\frac{\left[M_{zg}\right]t_{ud}}{Ah} \tag{6.53}$$

Finally, the following is derived from (6.53):

$$V_p \tan \gamma + V_{zb.max} \tan \beta \leq \frac{[M_{zg}] t_{ud}}{ABhm(1 + \varepsilon)} \tag{6.54}$$

Thus, the limitation on the velocity of the lifting tool has been established, taking into account its design parameters and reduced mass as well as the root's strength and coefficient of restitution.

As the velocity of the unit has an effect on its productivity, it is necessary to investigate the case of the sign of equality in (6.54). If the beet harvester's translational motion velocity V_p is preset, it is possible to derive, from (6.54), the magnitude of the maximum velocity $V_{zb.max}$ of the oscillatory motion of the vibrational lifting tool:

$$V_{zb.max} = \frac{1}{\tan \beta} \left(\frac{[M_{zg}] t_{ud}}{ABhm(1 + \varepsilon)} - V_p \tan \gamma \right) \tag{6.55}$$

On the basis of (6.7), it is possible to determine the required angular frequency of the digging tool oscillations at the preset amplitude of the oscillations, subject to the condition of not damaging the root:

$$\omega = \frac{1}{a \tan \beta} \left(\frac{[M_{zg}] t_{ud}}{ABhm(1 + \varepsilon)} - V_p \tan \gamma \right) \tag{6.56}$$

Hence, the hertz frequency of the digging tool oscillations is equal to:

$$v = \frac{1}{2\pi a \tan \beta} \left(\frac{[M_{zg}] t_{ud}}{ABhm(1 + \varepsilon)} - V_p \tan \gamma \right) \tag{6.57}$$

Based on the developed theory of the impact interaction between the vibrating digging tool and the root, it is possible to define, subject to the condition of not breaking off the root, quite a wide range of acceptable digging tool oscillation frequencies at different values of the design and kinematic parameters of the vibrational lifting tool.

In order to carry out the calculations, it is necessary to specify the values of some of the parameters present in (6.57).

In the further considerations, it is assumed that the design parameters of the trihedral wedges of the lifting tool—in particular, angles γ and β (Figure 5.1) are preset: $\gamma = 14°–15°$, $\beta = 50°–55°$.

The dihedral angle δ between the wedge's working face and its lower face (Figure 6.1) is determined with the use of (3.63).

The dynamic coefficient of friction of steel on the surface of the root is assumed to be equal to $f = 0.45$ [7]. To a certain approximation, it is assumed that angle $\psi = 45°$.

The distance between the impact contact point K_1 and the lower edge of the wedge (i.e., the boundary of the unbroken soil layer) is $h = 0.05$ m.

The coefficient of restitution for the impact is assumed to be $\varepsilon = 0.72$.

The permissible bending moment $[M_{zg}]$ can be determined on the basis of the following considerations.

If z—depth at which digging tool runs in the soil, it is obvious that the root will most probably break off at that depth, as at the depths greater than z the root sits in unbroken soil, while at the depths less than z the root cross-section area is greater (since the root has a conical shape).

Considering that the diameter d_k of the root cross-section at a depth of z is $d_k = D_k - 2z \cdot \tan \gamma_k$ where D_k is the root diameter (m) and γ_k is the taper angle of the root (°).

Subsequently, starting from the theory of strength of materials $[M_{zg}] = [\sigma]_{d.} \frac{\pi d_k^3}{32}$ where $[\sigma]_{d.}$—modulus of rupture of the root under dynamic load (Pa). Taking into account the previous formula, the following is arrived at:

$$[M_{zg}] = [\sigma]_d \frac{\pi (D_k - 2z \tan \gamma_k)^3}{32} \tag{6.58}$$

According to [7], $D_k = 67$–122 mm, $\gamma_k = 9°$–$18°$, $[\sigma]_{d.} = 1.15 \cdot 10^6$ Pa.

For the calculations, it is assumed that $D_k = 100$ mm, $\gamma_k = 15°$.

One of the design parameters that is important in determining the impact interaction is the mass of the reduced digging tool to the point of impact. An indicative set of values for the reduced mass is obtained with (6.57) for the preset ranges of the digging tool oscillation amplitudes and frequencies as well as the translational motion velocities that are to be used in the experimental investigations. The mentioned parameter variation ranges are as follows:

- digging tool oscillation amplitude $a = 8$~24 mm;
- digging tool oscillation frequency $v = 7.5$~20.3 Hz;
- lifter translation velocity $V_p = 1.4$~2.2 m·s^{-1}.

The following expression for calculating the reduced mass can be derived from (6.57):

$$m = \frac{[M_{zg}] t_{ud}}{ABh(1 + \varepsilon)\left(2v\pi a \tan \beta + V_p \tan \gamma\right)} \tag{6.59}$$

The calculations will be carried out for various values of the digging tool running depth—in particular, for z = 0.08; 0.10; −0.14 m and at three values of the amplitude: a = 0.008, 0.016 and 0.024 m.

The value of the reduced mass is obtained in the form of a function of the digging tool oscillation frequency v and the lifter translation velocity V_p—i.e., $m = m(v, V_p)$.

The values of the reduced mass calculated in the described manner allow for the root not to be broken off in the case of impact interaction at specific values of the digging tool running depth, oscillation amplitude and frequency as well as specific values of the lifter translation velocity.

The calculation process results in obtaining, apart from the tables of reduced mass values, the graphs of the function $m = m(v, V_p)$ for various value sets of the digging tool running depth and oscillation frequency and the respective contour diagrams. Since the operational running depth of the lifting tool does not, in the majority of cases, exceed 0.10 m [31], the case of calculation for a depth of z = 0.10 m and an amplitude of a = 0.016 m will be presented as an example. For this case, the graph of the function $m = m(v, V_p)$ and the respective contour diagram are presented in Figure 6.2. The frequencies in the presented case vary within the range of v = 7.5~20.3 Hz and the lifter translation velocities—within the range of V_p =1.4~2.2 m·s^{-1}.

(a)   (b)
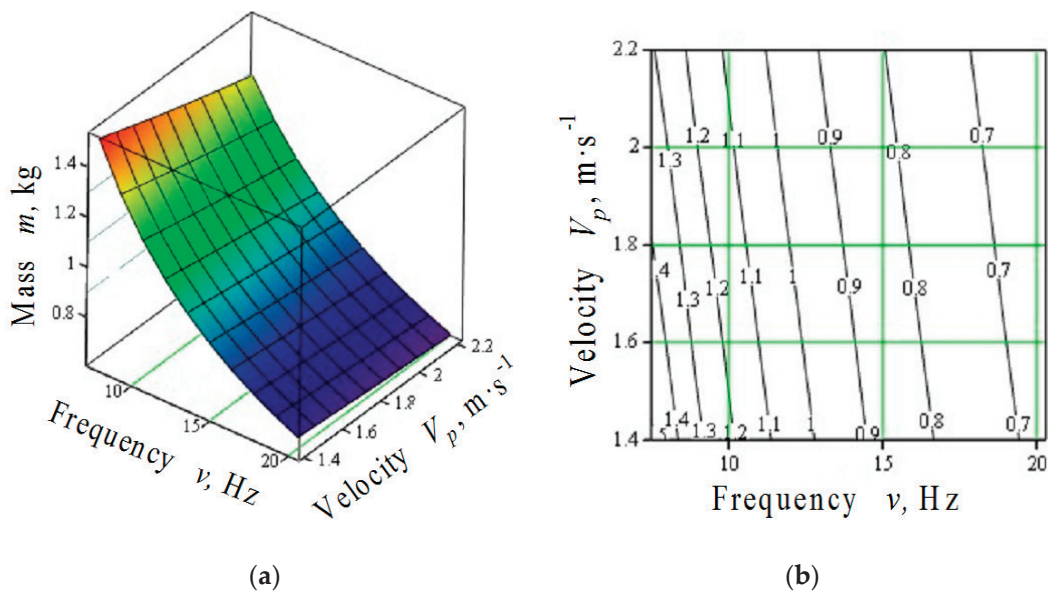
Figure 6.2. Surface (**a**) and contour diagrams (**b**) of values for digging tool mass reduced to point of impact $m = (v, V_p)$ (kg) (digging tool running depth z = 0.10 m; oscillation amplitude a = 0.016 m).

The trend of decreasing reduced mass is observed in the case of an increase in the digging tool oscillation amplitude. For example, at z = 0.10 m and an amplitude

of a = 0.008 m, the reduced mass varies within the range of m = 1.07~2.38 kg, but at z = 0.10 m and an amplitude of a = 0.024 m—within the range of m = 0.45~1.11 kg.

The reduced mass of the digging tool also decreases with the increase in its running depth. For example, at an amplitude of a = 0.016 m and a running depth of z = 0.10 m, the reduced mass varies within the range of 0.63~1.51 kg, but at the same amplitude and a running depth of z = 0.12 m—within the range of 0.29~0.69 kg.

The obtained diagram clearly displays the trend of the reduced digging tool mass decreasing with the increase in the tool oscillation frequency and the lifter translation velocity.

The results of the calculation of the reduced mass values for the frequency varying within the range of v= 7.5~20.3 Hz and the lifter translation velocity varying within the range of V_p = 1.4~2.2 m·s^{-1} are presented in Table 6.1.

Table 6.1. Ranges of variation of reduced mass against variation of tool oscillation frequency and lifter translation velocity.

Digging Tool Running Depth z (m)	Reduced Mass Value, m (kg)		
	a = 0.008 m	a = 0.016 m	a = 0.024 m
0.08	4.45~2.00	2.82~1.18	2.07~0.83
0.10	2.38~1.17	1.51~0.63	1.11~0.45
0.12	1.08~0.49	0.69~0.29	0.50~0.20

It has been established in the field experiments that the critical impact impulse energy that causes the root tail part (a diameter of 30~40 mm) to break off is equal to 2.5~3.0 J [31]. This corresponds to a digging tool running depth of 0.10~0.12 m.

In a first approximation, the impact impulse energy is equal to the kinetic energy of the digging tool prior to the impact. Based on this, the reduced mass that enables breaking off the root can be assumed to be $m = \frac{2T}{V_p^2}$ where m is the reduced mass of digging tool (kg); T is the kinetic energy of the digging tool prior to the impact (J)and V_p is the lifter translation velocity (m·s^{-1}).

At V_i = 1.4 m·s^{-1}, m = 2.55 kg; at V_p = 2.0 m·s^{-1}, m = 1.25 kg; at V_p = 2.2 m·s^{-1}, m = 1.03 kg. Hence, the obtained values are close to those presented in Table 6.1 at = 0.10 m.

Moreover, as is pointed out in [31], during the laboratory and field investigations, the impact impulse loads were created with the use of a pendulum impact machine, in which the hammer mass was 0.45~1.5 kg and impact velocity—1.0~2.5 m·s^{-1}. Thus, the mass of the hammer and the velocity of its motion were the same as the parameters mentioned in this paper.

Hence, the above-mentioned calculations have enabled obtaining quite a wide range of reduced mass values of the digging tool. Certainly, when developing

a specific vibrational lifting tool, a specific reduced mass value will be used. Nevertheless, by using the results of the described calculations, it is always possible to determine what kinematic parameters of the digging tool motion are stipulated by the specific reduced mass subject to the condition of not breaking off the roots. Moreover, if a specific reduced mass value is chosen from the obtained range of reduced mass values (or close to it), it is possible to calculate the permissible frequency values for a wider range of amplitudes, digging tool running depths and lifter translation velocities.

Said computation can be carried out using (6.57).

For example, a reduced mass value of m = 1.5 kg, which is within the range of reduced mass values m = 1.17~2.38 kg, is selected from Table 6.1 (digging tool running depth—0.10 m, oscillation amplitude—0.008 m). Using (6.57), the acceptable frequency of oscillations of the digging tool is calculated as a function of the lifter translation velocity and the digging tool oscillation amplitude—i.e., $v = (V_p, a)$. In this case, the lifter translation velocity varies within the range of 1.4~2.2 m·s^{-1} and the amplitude—within the range of 0.008–0.024 m. The results are in Table 6.2.

Table 6.2. Acceptable digging tool oscillation frequencies for reduced mass of m = 1.5 kg.

Digging Tool Running Depth, z (m)	Range of Variation of Digging Tool Oscillation Frequency, v (Hz)
0.08	33.08~9.97
0.10	15.17~4.01
0.12	3.89~0.243

As can be seen in Table 6.2, the frequency range v = 0.243–3.89 Hz ensures the roots are not broken off at a digging tool running depth of 0.12 m and less; the frequency range v = 4.01~15.17 Hz ensures the roots are not broken off at a digging tool running depth of 0.10 m and less; the frequency range v = 9.97~33.08 Hz—at a digging tool running depth of 0.08 m and less. Thereby, theoretically, it is possible to compute the digging tool oscillation frequency values that meet the condition of not breaking off the roots for quite a wide range of kinematic parameters of operation of the vibrational lifting tool.

The graph of the function $v = (V_p, a)$ and the contour diagram for a reduced digging tool mass of m = 1.5 kg and running depth of z = 0.10 m are presented below (Figure 6.3).

As can be concluded from the shown diagram, the acceptable frequency depends on the digging tool oscillation amplitude: as the oscillation amplitude goes up, the

permitted frequency sharply falls. It also decreases when the lifter translation velocity rises.

(a)   (b)
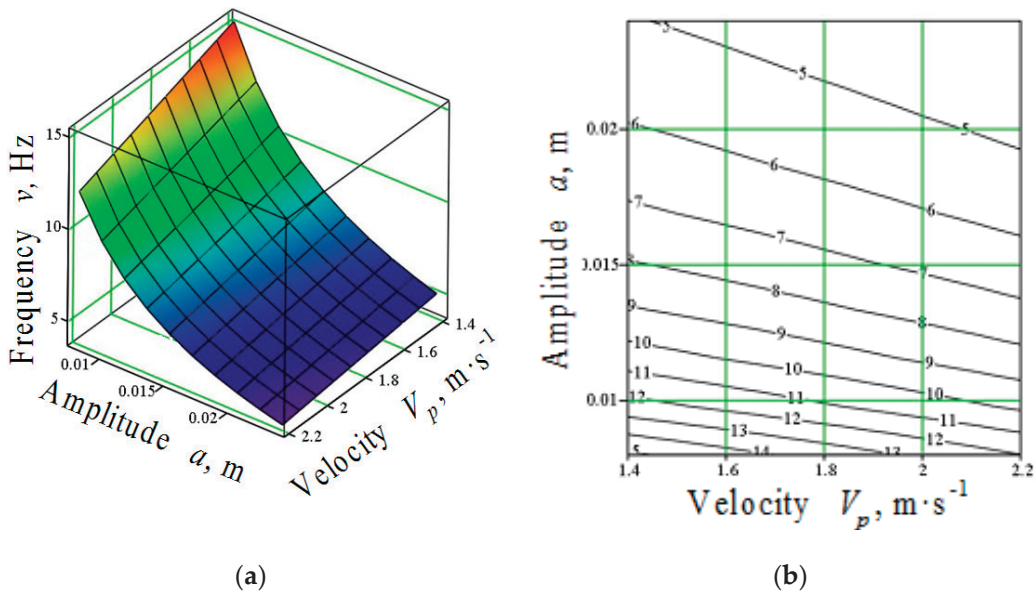
Figure 6.3. Surface (**a**) and contour diagrams (**b**) of values of digging tool oscillation frequency $v = (V_p, a)$ (Hz) acceptable subject to not breaking off roots during their impact interaction with digging tool (digging tool running depth $z = 0.10$ m; reduced digging tool mass $m = 1.5$ kg).

In the case of a running depth of $z = 0.14$ m, a reduced digging tool mass of $m = 1.5$ kg is unacceptable, since the permissible frequency values become, according to the calculations, negative, which makes no sense.

Similar calculations have been carried out for a reduced mass of $m = 1$ kg with the same ranges of the translational motion velocity and digging tool oscillation amplitude. The results of the calculations are shown in Table 6.3.

Table 6.3. Acceptable digging tool oscillation frequencies for reduced mass of $m = 1$ kg.

Digging Tool Running Depth, z (m)	Range of Variation of Digging Tool Oscillation Frequency, v (Hz)
0.08	52.38~16
0.10	25.52~7
0.12	8.60~1

The acceptable frequency values for a reduced mass of $m = 0.8$ kg are presented in Table 6.4.

Table 6.4. Acceptable digging tool oscillation frequencies for reduced mass of $m = 0.8$ kg.

Digging Tool Running Depth, z (m)	Range of Variation of Digging Tool Oscillation Frequency, v (Hz)
0.08	66.86~21.23
0.10	33.28~10.04
0.12	12.13~2.99

Additionally, the results of the calculations and the diagrams of acceptable frequencies for the digging tool with a reduced mass of $m = 2.0$ kg within the same ranges of the translational motion velocity and the oscillation amplitude are provided as an example. In particular, at $Z = 0.08$ m, the acceptable frequencies are within the range of $v = 6.76{\sim}23.43$ Hz, at $Z = 0.10$ m—within the range of $v = 2.28{\sim}10.00$ Hz.

It is rather convenient to determine the acceptable frequency value for each pair of values (V_p, a) with the use of the contour diagram shown in Figure 5.3b. The denser the coordinate grid is, the more accurately and conveniently the acceptable frequencies are determined.

As an example, the results of the calculation of the maximum acceptable oscillation frequency obtained for a reduced digging tool mass of $m = 1.5$ kg will be further analysed.

As the calculation results show, at a digging tool running depth of $z = 0.08$ m and an oscillation amplitude of $a = 0.008$ m, a maximum acceptable digging tool oscillation frequency of $v = 30$ Hz ensures breaking off of the root tail parts within the lifter translation velocity range of $1.4{\sim}2.2$ m·s^{-1}. For the same running depth and a digging tool oscillation amplitude of $a = 0.010$ m, a maximum acceptable oscillation frequency of $v = 24$ Hz ensures the root tail parts are not broken off within the above-mentioned lifter translation velocity range.

Under the same conditions, for an amplitude of $a = 0.012$ m, the maximum acceptable frequency is $v = 20$ Hz; for an amplitude of $a = 0.014$ m $-$ 17.1 Hz; for $a = 0.016$ m $-$ 15.0 Hz; $a = 0.018$ m $-$ 13.3 Hz; $a = 0.020$ m $-$ 12.0 Hz; $a = 0.022$ m $-$ 10.9 Hz; $a = 0.024$ m $-$ 10.0 Hz.

The above values of the vibrational tool oscillation frequency are the maximum acceptable values of the frequency subject to not breaking off the root tail parts during the impact interaction. Lower oscillation frequency values allow, to a greater extent, for not breaking off of the root tail parts. Nevertheless, as will be shown, the frequencies must be limited from below as well—i.e., there are minimum acceptable frequency values that ensure the guaranteed gripping of each root by the digging shares.

Meanwhile, the calculation has shown that the maximum acceptable frequency values for a digging tool running depth of $z = 0.10$ m are significantly lower. For example, at an oscillation amplitude of $a = 0.008$ m, a maximum acceptable oscillation frequency of $v = 12$ Hz allows the root tail parts to be not broken off within the lifter translation velocity range of $V = 1.4{\sim}2.2$ m·s^{-1}; at an oscillation amplitude of $a = 0.010$ m—the maximum acceptable frequency is $v = 9.6$ Hz; at an amplitude of $a = 0.012$ m—$v = 8$ Hz; at an amplitude of $a = 0.014$ m—$v = 6.9$ Hz.

In the case of greater values of the amplitude, the acceptable frequency values become even lower. When the frequency values fall below the minimum acceptable ones with regard to the guaranteed gripping of each root by the digging shares, the respective kinematic conditions must be rejected as they are technologically unacceptable.

For a reduced digging tool mass of $m = 1.5$ kg and a depth of running in the soil of 0.12 m, the maximum acceptable frequency values subject to the root tail parts not breaking off during the impact interaction are below 4 Hz. Hence, under the condition of the guaranteed gripping of the root by the digging shares, said frequency values are unacceptable.

It is quite obvious that the maximum acceptable frequency values for a reduced digging tool mass of $m = 1.5$ kg will meet the condition of not breaking off the root tail parts even more in the case of smaller reduced masses of the digging tool. Indeed, the maximum acceptable frequency values for the respective amplitudes and digging tool running depths will, in this case, be even higher. This is proved by the calculations for reduced digging tool masses of $m = 0.8$ kg and $m = 1.0$ kg. While the maximum acceptable frequency values for the digging tool's running depth of 0.12 m and its reduced mass of 1.5 kg are below 4 Hz, in the case of a reduced mass of $m = 1.0$ kg, said values are considerably higher. For example, at an amplitude of 0.008 m and a lifter translation velocity of $1.4{\sim}2.2$ m·s^{-1}, they stay within the range of $8.6{\sim}5.4$ Hz at an amplitude of 0.010 m; within the same translational motion velocity range—within the range of $6.8{\sim}4.4$ Hz; at an amplitude of 0.012 m—within the range of $5.7{\sim}3.6$ Hz.

For a reduced digging tool mass of $m = 0.8$ kg and a digging tool running depth of 0.12 m, the respective values of the maximum acceptable frequency are within the following ranges: at an amplitude of 0.008 m—$12.1{\sim}9.0$ Hz; at an amplitude of 0.010 m—$9.7{\sim}7.1$ Hz; at an amplitude of 0.012 m—$8.1{\sim}6.0$ Hz; at an amplitude of 0.014 m—$7.0{\sim}5.1$ Hz.

Hence, the above acceptable frequency values subject to the condition of the root tail parts not breaking off during the impact interaction with the digging shares have to be limited from below, proceeding from the condition of the guaranteed gripping of each root by the digging shares of the lifter.

Thus, the developed theory of impact interaction between the digging tool and the root fixed in the soil as well as the calculation algorithm generated on the basis of the theory facilitate computing with the use of the personal computer the kinematic operating conditions for a vibrational lifting tool within a sufficiently wide range taking into account its design and process parameters and proceeding from the condition of not breaking off the roots.

The algorithm of computing the acceptable oscillation frequency for a vibrational lifting tool subject to not damaging the roots during the impact interaction between them is presented below.

1. The permissible bending moment is found with (6.58).
2. Parameters A and B are found with (6.49) and (6.50), respectively.
3. The tentative set of the reduced mass values as the function $m = m(v, V_p)$ at different values of oscillation amplitude and digging tool running depth is computed with (6.59).
4. After selecting a specific value of the reduced mass m from the set of reduced mass values obtained in Step 3, the acceptable frequency is determined as the function $v = v(V_p, a)$ in accordance with (6.57) for various values of digging tool running depth.

Thereby, the theory of the impact interaction between the vibrational lifting tool and the root fixed in the soil produces rather a wide range of acceptable values for the digging tool oscillation frequency. However, it is necessary to place the acceptable values of frequency obtained above the limitations—from above and from below. The limitation from above is stipulated by the reliability of the digging tool oscillatory motion drive, as at excessively high frequencies the dynamic loads on the drive components sharply rise, which considerably reduces the reliability and durability of the drive. According to the results of experimental studies, the reliability of the drive sharply falls in the case of the existing drive designs when the digging tool oscillation frequency exceeds 20 Hz [7]. The limitation of the acceptable frequency values from below is imposed by the requirement to ensure the gripping of the root by the digging tool when the root is situated in the lifter's working channel. Therefore, it is important to analyse the relation between the number of the possible ways in which the root is gripped by the vibrational lifting tool over the time when the root resides in the lifter's working channel, and the following process parameters: the lifter's translational motion velocity, the length of its working channel and the frequency of oscillations of the working faces of the vibrational lifting tool.

As the extraction of roots during their vibrational lifting is possible only in the case of direct contact between the digging tool and the roots, an issue of importance is the length of the rear part of the lifter's working channel, which starts from the point of first contact with the root and extends until the end of the working channel

(i.e., the length over which the contact with the root and its final extraction from the soil take place). Of course, said length can be different (considering the variation of the design solutions that take into account the different root sizes, etc.); nevertheless, it must have an average value l, which can further be assumed as the design value.

The analytical relation between the number of oscillations that the vibrational lifting tool performs in its interaction with the root during the latter's stay in the rear part of the working channel, on the one hand, should be found, as should the length of the rear part of the working channel, the oscillation frequency and the lifter translation velocity, on the other hand.

If l—distance from the point of the first contact with the root to the end of the lifter's working channel and V_p—lifter translation velocity, the duration of stay of the root in the above-mentioned part of the working channel is equal to:

$$t_p = \frac{l}{V_p} \tag{6.60}$$

In that time, the digging tool performs the following number of oscillations:

$$k = v\frac{l}{V_p} \tag{6.61}$$

where v—frequency of oscillations of the vibrational lifting tool (Hz).

Hence, for example, if it is assumed, according to [7], that $V_p = 2\ \mathrm{m\cdot s^{-1}}\ \mathrm{m\cdot s^{-1}}$, $v = 20$ Hz, $l = 0.1$ m (the minimum possible value of the length), the following number of oscillations of the vibrational lifting tool is $k = \frac{20 \cdot 0.1}{2} = 1$ oscillation.

Then, knowing the number of oscillations performed by the vibrational lifting tool, it is necessary to find out how many times the tool grips the root in the time of the root's stay in the rear part of the channel at $k = 1$—i.e., in case the digging tool performs one full oscillation in said time.

In the situation under consideration, two cases are possible.

The first case: the digging tool meets the root (performs the first direct contact with the root) at the instant of time when the tool is moving up from its lowest position to its highest position. In further considerations, the digging tool oscillation period is denoted by τ. As the perturbing force in this case is vectored upwards, this first contact between the digging tool and the root will also be the first time when the digging tool grips the root and the process of breaking the bonds between the root and the soil begins. The gripping continues until the digging tool reaches its highest position. In further considerations, this time interval is denoted by $t_1 = s_1\tau$ where $0 \le s_1 \le 0.5$—a number that shows in what fraction of the oscillation period the first grip of the root by the digging tool takes place.

For example, if $s_1 = 0.5$ it means that the first grip starts at the lowest position; therefore, $t_1 = 0.5\tau$. However, if $s_1 = 0$, it means that the first contact starts at the highest position, which implies that $t_1 = 0$. All the other values of s_1 that comply with the above inequation, represent the start of the grip at any instant of time during the digging tool movement upwards from the lowest position to the highest one.

Having reached its highest position, the digging tool starts moving downwards. In this case, taking into account the conical shape of the root, the perturbing force stops acting on the root—this means that the root is not gripped anymore. However, the loss of contact between the root and the digging tool is rather unlikely in view of the translational motion of the lifter and the necking of its working channel. If the perturbing force stops acting on the root, the latter will try and return to the vertical position in view of the elasticity of the soil and its own elasticity. It is possible that at this stage the root has a slight tilt forward caused by the lifter's translational motion. Such circumstances remain present over the time of $t_2 = 0.5\,\tau$ as the digging tool moves from its highest position to the lowest one. After that, the digging tool repeats the upward movement from its lowest position to the highest one.

Thus, over the time of $t_3 = \tau - (t_1 + t_2)$, the second grip of the root by the digging tool takes place, which starts the process of the further disruption of bonds between the root and the soil right up to the complete extraction. Of course, if the duration of the root's stay in the rear part of the working channel (after the first contact) is not longer than τ, the second grip must end in the guaranteed complete extraction of the root from the soil; otherwise, the root will remain in the soil (that is, it will either be cut off by the shares or chock up the lifter's working channel).

In case the root is weakly fixed in the soil, it is not improbable that the extraction will take place during the first grip of it by the vibrational lifting tool.

The second case: the digging tool meets the root (performs the first direct contact with it) at the instant of time when the tool is moving down from its highest position to the lowest one. This contact will continue over the time of $t_1 = s_1\tau$, where $0 \le s_1 \le 0.5$.

In this period, no perturbing force from the vibrational lifting tool acts on the root. After reaching the lowest position, the digging tool starts moving in the opposite direction—i.e., from the lowest position to the highest one. In this period, the first grip of the root by the digging tool takes place and continues for $t_2 = 0.5\,\tau$ until the digging tool reaches its highest position. Next, the digging tool starts moving downwards and over the time of $t_3 = \tau - (t_1 + t_2)$, again, no perturbing force acts on the root—i.e., in this time interval no gripping of the root takes place.

Thus, in the second case, within the time interval of $t_1 + t_2 + t_3 = \tau$, the root is gripped by the digging tool only once. If in this case the time of the root staying in the rear part of the working channel (after the first contact) is no longer than τ,

then said single grip must result in the complete extraction of the root from the soil; otherwise, the root will remain in the soil.

Of course, one grip can be insufficient for the extraction of the root tightly bonded with the soil. In this case, obviously, it is necessary to increase considerably the gripping force, but this can result in the breaking off or tearing apart of the root body. Nonetheless, it is quite evident that even one grip of the root at a certain depth that allows it to be forced out of the surrounding and restraining soil and the following travel of the root in the lifter's necked working channel on the inclined faces of the shares are sufficient for the complete extraction of the root.

Thus, at $k = 1$ in the first case, it is appropriate to analyse two phases of the extraction process—the first phase and the third one, as during the first grip the perturbation of the root takes place; then, in the interval between the first and second grips, the root restores its position under the action of the elastic force of the soil and the root's own elasticity. During the second grip, the final extraction of the root from the soil takes place. In the second case, the extraction must be completed during one grip—i.e., the third phase of lifting takes place.

At $k < 1$ (the digging tool cannot complete one full oscillation within the time of stay of the root in the rear part of the lifter's working channel), in the first case only one grip of the root by the digging tool can take place; in the second case—no grip occurs. Indeed, the root must be lifted in one grip by the digging tool or, in an extreme case, by the necked working channel of the lifter due to the lifter's translational motion (as happens in the usual share lifter). However, the lifting of the root rigidly fixed in the soil by the necked channel due to the lifter's translational motion can result in the sharp tilting of the root along the lifter's motion and its breaking off. Moreover, at $k < 1$, the root rigidly fixed in the soil may still not be lifted even after one grip by the vibrational lifting tool.

Thereby, the correlation between the digging tool oscillation frequency, the lifter's translational motion velocity and the working channel length must allow the digging tool to perform more than one oscillation over the time of its stay in the rear part of the working channel—i.e., it is necessary to ensure that $k > 1$.

If, for example, $k = 2$ (when the length of the rear part of the lifter's working channel l is equal to 0.2 m) and the first case is under consideration (i.e., the first contact between the digging tool and the root takes place during the upward movement of the digging tool), then within the first oscillation period, the digging tool performs two grips of the root; within the second oscillation period—one grip. However, if the second case is under consideration (i.e., the first contact between the digging tool and the root takes place during the downward movement of the digging tool), then within the first and the second oscillation periods the digging tool performs one grip of the root per period. Hence, at $k = 2$ either three or, in the worst case, two grips of the root are guaranteed.

Thereby, at $k = 2$ in the first case, three phases of lifting have to be taken into consideration: the first phase—during the first grip, when the perturbing force acts on the root firmly bonded with the soil, and in the time interval between the first and second grips, when the root restores to its initial position; the second phase—during the second grip, when the perturbing force acts on the root in already loosened soil, and in the time interval between the second and third grips, when the root restores to its previous position; the third phase—during the third grip, when the final extraction of the root from the soil is performed. In the second case, two phases of lifting have to be analysed: the first and the third. Of course, such division into phases is rather conventional.

In general, for $k = n$ where n is a natural number, as can be concluded from the above considerations, the digging tool can complete $n + 1$ or n grips of the root.

Certainly, the greater k is, the smoother the process and the higher the quality of root extraction from the soil by the vibrational lifting tool, as with a greater number of oscillations used for one root, it is possible to apply a smaller perturbing force to lift the root, which means reducing the probability of breaking the root body. Moreover, the greater k is, the more oscillations the root performs together with the digging tool in the first and second phases of extraction, which means better cleaning of the root from the caked soil.

The growth of the number k can be achieved by either increasing the digging tool oscillation frequency and the length of its working channel or decreasing the lifter's translational motion velocity. In summary, even at $k = 1$, when the digging tool performs only two grips of the root in the time of the latter's stay in the rear part of the lifter, an oscillatory process takes place in the first phase of lifting (the first gripping of the root and the return of the root to its initial position in the time interval between the first and second grips) and the perturbation of the root under the action of the perturbing force and its return to the initial position under the action of the restoring forces (the elastic force of the soil and the root's own elastic force) occur. Even more so, at $k > 1$ an oscillatory process takes place that facilitates the guaranteed extraction of the root from the soil.

Hence, having specified the number $k(k \geq 1)$ of the digging tool oscillations performed together with one root during the latter's stay in the lifter's working channel, it is always possible to find the relation between the parameters v, l and V_p in accordance with (6.61). In particular, for specific values of l and V_p, the following is found from (6.61):

$$v = \frac{k V_p}{l} \tag{6.62}$$

In this way, the minimum digging tool oscillation frequency that ensures the rational conditions of the vibrational lifting of roots is determined. If = 1 (one

oscillation of the digging tool per root is performed), the following is obtained from (6.62):

$$v = \frac{V_p}{l} \qquad (6.63)$$

If the digging tool oscillation frequency is below the value found in (6.63), the proper conditions for the vibrational root lifting are not provided. This means that some of the roots will not be gripped by the digging tool in the vibrational process and, therefore, will not be extracted or will be broken in their tail parts. All this results in the undesirable loss of roots during their lifting.

Thus, the unjustified relation between the parameters k, v, l and V_p is one of the main causes of the loss of part of the roots during their vibrational lifting by the existing beet harvesters.

The next step is to plot the graphs (Figure 6.4) of the relation between the minimum acceptable frequency v and the lifter's translational motion velocity V_p at $k = 1$ and $l = 0.10$ m, $l = 0.15$ m and $= 0.20$ m as stated by (6.63).
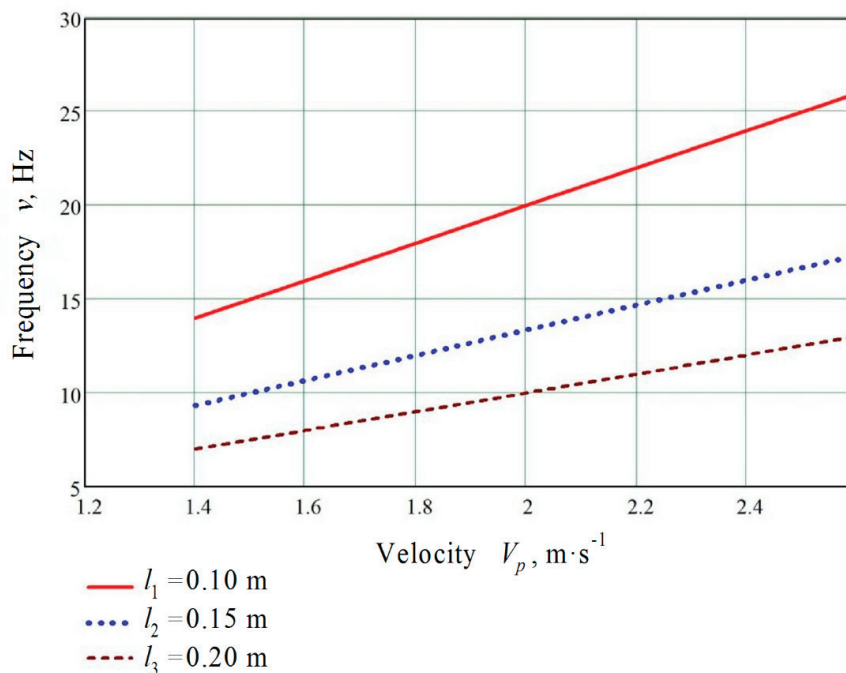
Figure 6.4. Graphs of relation between minimum acceptable frequency v of vibrational lifting tool and lifter's translational motion velocity V_p at lengths of $l = 0.10$ m; 0.15 m; 0.20 m for the rear part of the working channel.

As may be inferred from the obtained graphs (Figure 6.4), the growth of the lifter's translational motion velocity entails the increase in the minimum acceptable frequency of the digging tool oscillations, which guarantees the occurrence of one grip of the root by the digging tool.

Thereby, for each set of values of the lifter's translational motion velocity V_p and the length l of the rear part of its working channel, a specific minimum frequency value exists, below which the process of the vibrational lifting of roots is impaired in the sense that some roots are not lifted by the vibrational lifting tool. As is evident from the graph, at $l = 0.1$ m, a frequency of $v = 20$ Hz ensures the proper performance of the vibrational root lifting process at all values of the lifter's translational motion velocity V_{Π} below 2.0 m·s^{-1}, while at $l = 0.15$ m, a frequency of 20 Hz—at all values below 3.0 m·s^{-1}. Hence, at $l = 0.1$ m, when it is necessary to facilitate a lifter translation velocity of $V_p = 2.0$ m·s^{-1}, all the ranges of the acceptable frequency obtained under the condition of not damaging the roots during their impact interaction with the digging tool must be limited from below by a frequency value of $v = 20$ Hz.

This implies that in the case of some of the above-mentioned kinematic conditions, with values below $v = 20$ Hz having been obtained for the frequencies acceptable in the impact interaction, they are automatically out of compliance with the conditions required for the normal progress of the vibrational root lifting process at a length of $l = 0.1$ m for the rear part of the working channel and a lifter translation velocity of $V_p = 2.0$ m·s^{-1}.

On the other hand, if the acceptable frequency values obtained under the condition of not damaging the roots during the impact interaction are above 20 Hz, their applicability has to be assessed with regard to the reliability and durability of the drive that actuates the oscillatory motion of the digging tool.

The above theoretical considerations are supported rather accurately by the experimental studies on the mass of the lost sugar beet roots described in Section 6. For example, at a lifter translation velocity of $V_p = 2.1$ m·s^{-1} and a digging tool oscillation frequency of $v = 20.3$ Hz, the mass of the lost roots amounts to 0.64%, at a frequency of $v = 15.7$ Hz—2.2%, while at a frequency of 8.5 Hz—3.48% (Table 6.1).

Thereby, at a translation velocity of $V_p = 2.1$ m·s^{-1}, an oscillation frequency of $v = 20.3$ Hz allows for the normal conditions of the vibrational root lifting process, but frequencies of $v = 15.7$ Hz and $v = 8.5$ Hz are insufficient—i.e., some roots are not lifted by the digging tool or broken in their tail parts. This is confirmed by the calculations made with (6.63).

The same patterns are observed at lifter translation velocities of $V_p = 1.3; 1.75; 2.55$ m·s^{-1} (Table 6.1).

At a translation velocity of $V_p = 1.3$ m·s^{-1} and an oscillation frequency of $v = 20.3$ Hz, the mass of the lost roots amounts to 0.38%; at a frequency of $v = 15.7$ Hz—1.78%; at a frequency of $v = 8.5$ Hz—2.74%. Hence, frequencies of $v = 20.3$ Hz and $v = 15.7$ Hz allow for normal conditions of the vibrational root lifting process, but a frequency of $v = 8.5$ Hz is insufficient for this.

At a translation velocity of $V_p = 1.75 \text{ m·s}^{-1}$, a depth of running in the soil of 0.06 m and an oscillation frequency of $v = 20.3$ Hz, the mass of the lost roots amounts to 0.42%; at a frequency of $v = 15.7$ Hz—1.9%; at a frequency of $v = 8.5$ Hz—2.96%.

At a translation velocity of $V_p = 2.55 \text{ m·s}^{-1}$, the same lifter running depth and an oscillation frequency of $v = 20.3$ Hz, the mass of the lost roots amounts to 1.14%; at a frequency of $v = 15.7$ Hz—2.44%; at a frequency of—4.3%.

The described pattern rather accurately shows up in the results of the experimental studies presented in Table 6.4, where the mass of the lost roots (%) is determined at a digging tool oscillation frequency of $v = 8.5$ Hz.

For example, at a digging tool running depth in the soil of 0.06 m, the lost root mass is equal to (mean value):

at $V_p = 1.4 \text{ m·s}^{-1} - 1.2\%$;
at $V_p = 1.65 \text{ m·s}^{-1} - 4.9\%$;
at $V_p = 2.1 \text{ m·s}^{-1} - 6.2\%$.

At a digging tool running depth in the soil of 0.08 m, the following results have been obtained:

at $V_p = 1.4 \text{ m·s}^{-1} - 1.2\%$;
at $V_p = 1.65 \text{ m·s}^{-1} - 2.1\%$;
at $V_p = 2.1 \text{ m·s}^{-1} - 4.2\%$.

The losses are caused by the breaking off of root tail parts and the complete leaving in the soil of part of the roots due to the fact that a digging tool oscillation frequency of $v = 8.5$ Hz does not ensure the gripping of each root by the digging shares.

It is obvious that the root loss rate is higher at a digging tool running depth in the soil of 0.06 m than in the case of a running depth of 0.08 m, due to the increased number of the roots not lifted from the soil.

According to [31], in the process of the active improvement of the vibrational lifting tools mounted on the beet harvesters produced by the leading European manufacturers, the digging tool oscillation frequencies have risen from 3.3~6.0 Hz to 10 Hz, but it is not yet possible to achieve oscillation frequencies above 10 Hz in large-scale production conditions due to the inadequate reliability of the mechanism that drives the digging tool in its oscillatory motion. Taking into account that circumstance and based on the above calculations, the following conclusion is arrived at: in order to provide for the normal conditions of the vibrational root lifting process at a lifter translation velocity of $V_p = 2.0 \text{ m·s}^{-1}$ and a digging tool oscillation frequency of $v = 10.0$ Hz, it is necessary to have such proportions between the geometric parameters of the digging tool to ensure the length of the end part of the lifter's working channel (distance from the point of the first contact between the digging tool and the root to the end of the working channel) that meets the condition

$l \geq 0.2$ m. Otherwise, at a velocity of $V_p = 2.0$ m·s^{-1}, the required conditions of vibrational lifting are not complied with.

The next step is to select from the results obtained by numerical calculations the acceptable values of the digging tool oscillation frequency, which can be recommended for use within the translational motion velocity range of 1.3~2.2 m·s^{-1}, taking into account the limitation imposed on the digging tool oscillation frequency by the requirement to guarantee the gripping of each root by the digging shares:

- For a reduced digging tool mass of $m = 0.8$ kg: at a depth of running in the soil of 0.08 m and an oscillation amplitude of 0.008–0.024 m, the acceptable oscillation frequency is 21.2 Hz; at a running depth of 0.10 m—10.0 Hz; at a running depth of 0.12 m—9.0 Hz;
- For a reduced digging tool mass of $m = 1.0$ kg: at a depth of running in the soil of 0.08 m and an oscillation amplitude of 0.008–0.024 m, the acceptable oscillation frequency is 16.4 Hz; at a running depth of 0.10 m and an oscillation amplitude of 0.008–0.018 m, the acceptable oscillation frequency is 10.0 Hz; at an amplitude of 0.020–0.024 m—8.3 Hz;
- For a reduced digging tool mass of $m = 1.5$ kg: at a depth of running in the soil of 0.08 m and an oscillation amplitude of 0.008–0.024 m, the acceptable oscillation frequency is 10.0 Hz; at a running depth of 0.10 m and an oscillation amplitude of 0.008–0.010 m, the acceptable oscillation frequency is 10.0 Hz; at an amplitude of 0.012 m—8.0 Hz;
- For a reduced digging tool mass of $= 2.0$ kg: at a depth of running in the soil of 0.08 m and an oscillation amplitude of 0.008–0.016 m, the acceptable oscillation frequency is 10.0 Hz; at an oscillation amplitude of 0.018–0.020 m—8.1 Hz.

The recommended digging tool oscillation frequencies are summarised in Table 6.5.

Table 6.5. The recommended digging tool oscillation frequencies, ν (Hz).

Reduced Mass of Digging Tool, m (kg)	Running Depth of Digging Tool, z (mm)								
	0.08			0.10					0.12
	Oscillation Amplitude (m)								
	from 0.008 to 0.016	from 0.018 to 0.020	from 0.008 to 0.024	from 0.008 to 0.024	from 0.008 to 0.018	from 0.020 to 0.024	from 0.008 to 0.010	0.012	from 0.008 to 0.024
0.8	–	–	21.2	10.0	–	–	–	–	9.0
1.0	–	–	16.4	–	10.0	8.3	–	–	–
1.5	–	–	10.0	–	–	–	10.0	8.0	–
2.0	10.0	8.1	–	–	–	–	–	–	–

6.2. Impact Interaction at Two Points

In this subsection, the impact interaction between the vibrational lifting tool and the root at two points, i.e., in the case of both shares simultaneously running into the root fixed in the soil, is under investigation.

The first step is to set up the equivalent schematic model of said impact interaction between the vibrational lifting tool and the root body that takes place when the tool runs into the root (Figure 6.5).
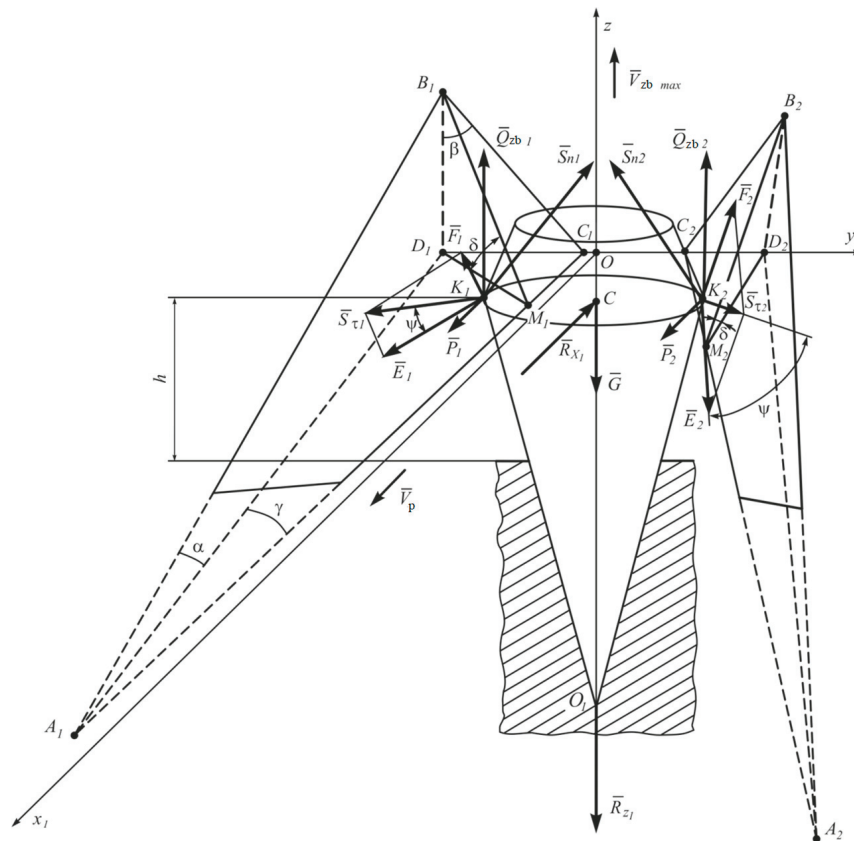
Figure 6.5. Equivalent schematic model of impact interaction at two points between vibrational lifting tool and root body fixed in soil.

It is assumed that the impact interaction between the root and the faces of wedges $A_1B_1C_1$ and $A_2B_2C_2$ takes place at points K_1 and K_2, respectively.

Moreover, the impact contact can take place either in the form of a direct contact or via a thin layer of soil between the wedge faces and the root.

In order to describe the impact process, it is necessary to set up the system of coordinates as the same as in Section 6.1. The schematic model of forces is similar to that in the previous subsection and differs only in that the root during the impact is subjected to the action of two impact impulses, $\overline{S}_{n1}$ and $\overline{S}_{n2}$, generated by the vibrating digging tool and applied at points K_1 and K_2, respectively, while $S_{n1} = S_{n2}$.

Said impact impulses are vectored normally to the work faces of the shares—i.e., to planes $A_1B_1C_1$ and $A_2B_2C_2$, respectively.

Moreover, on the surfaces of the wedges, the tangential impact impulses $\bar{S}_{\tau\,1}$ and $\bar{S}_{\tau\,2}$ act, while $\bar{S}_{\tau\,1} = \bar{S}_{\tau\,2}$ (Figure 6.5). The relation between the magnitudes of the tangential and normal impact impulses is defined in accordance with the Routh hypothesis, as was stated in Section 6.1.

The impulses $\bar{S}_{\tau\,1}$ and $\bar{S}_{\tau\,2}$ have to be decomposed into components $\bar{F}_1$ and $\bar{F}_2$, which are at right angles to the right lines A_1C_1 and A_2C_2, respectively, and components $\bar{E}_1$ and $\bar{E}_2$, which are parallel to the right lines A_1C_1 and A_2C_2, respectively (Figure 6.5).

The following is obtained:

$$\bar{S}_{\tau\,i} = \bar{F}_i + \bar{E}_i, i = 1,\ 2. \tag{6.64}$$

Vectors $\bar{S}_{\tau 1}$ and $\bar{S}_{\tau 2}$ in such a representation will later allow finding their projections on axes Ox and Oy.

The magnitude of the impact impulse can vary depending on the rate of the digging tool's oscillatory motion in the vertical plane. Moreover, in view of the fact that the root has a conical shape, when the vibrational lifting tool moves downwards, the vertical component of the impact impulse is virtually absent. In such a case, the impact impulse is created only by the translational motion of the lifter.

It is assumed that the oscillations of the tool are performed in accordance with the harmonic law (6.5).

Hence, the digging tool's oscillatory motion velocity V_{zb} at any instant of time t is determined according to (6.6), and the maximum value of said velocity is in accordance with (6.7).

Therefore, similar to the previous subsection, it is necessary to investigate the impact interaction case, where the impact impulse reaches its maximum. Such a case is observed at the moment when the vibrational lifting tool runs into the root if the tool is moving at that moment upwards at a maximum velocity of $V_{zb.max}$.

In view of the fact that all the forces shown in Figure 6.5 have finite magnitudes, the impulses of these forces within the time of impact are equal to zero. Only the impact impulses S_{n1} and S_{n2} have nonzero values, while it is obvious that $S_{n1} = S_{n2}$ (the impact is symmetric).

Further, the impulse-momentum theorem for the case of an impact is to be applied [32]:

$$m(\overline{U} - \overline{V}) = \bar{S}_{n1} + \bar{S}_{n2} + f\bar{S}_{\tau 1} + f\bar{S}_{\tau 2} \tag{6.65}$$

where $\overline{V}$—velocity of the digging tool before the impact; $\overline{U}$—velocity of the digging tool after the impact; m—reduced mass of the digging tool.

At the same time:

$$\overline{V} = \overline{V}_p + \overline{V}_{zb.max} \tag{6.66}$$

where $\overline{V}_p$—velocity of the translational motion of the lifter; $\overline{V}_{zb.max}$—maximum velocity of the oscillatory motion of the digging tool.

The vector of the lifter's translational motion velocity $\overline{V}_p$ is directed along axis Ox, while the vector of the digging tool's oscillatory motion velocity $\overline{V}_{zb.max}$—along axis Oz upwards. Taking into account (6.3), (6.65) acquires the following form:

$$m\left(\overline{U} - \overline{V}\right) = \overline{S}_{n1} + \overline{S}_{n2} + f\overline{S}_{n1} + f\overline{S}_{n2} \tag{6.67}$$

(6.67) has to be written in the form of its projections on the axes of the Cartesian coordinate system $Oxyz$.

Since the impact is symmetric with respect to plane xOz, (6.67) is resolved into the system of two equations in the projections on axes Ox and Oz.

It is necessary to determine the required projections of the vectors that are present in Equation (6.67).

It is obvious that,

$$V_x = V_p \tag{6.68}$$

As the vectors $\overline{S}_{n1}$ and $\overline{S}_{n2}$ are directed along the normal lines to the wedge surfaces, then, in accordance with (3.12), the following is obtained:

$$S_{n1x} = S_{n2x} = \frac{S_{n1}\tan\gamma}{\sqrt{\tan^2\gamma + 1 + \tan^2\beta}} \tag{6.69}$$

As can be seen from Figure 6.5, the projections of the vectors $\overline{E}_1, \overline{E}_2$ and $\overline{F}_1, \overline{F}_2$ on axis Ox are equal to:

$$E_{1x} = E_{2x} = E_1\cos\gamma = S_{\tau 1}\cos\psi\cdot\cos\gamma \tag{6.70}$$

$$F_{1x} = F_{2x} = F_1\cos\delta\cdot\sin\gamma = S_{\tau 1}\sin\psi\cdot\cos\delta\cdot\sin\gamma \tag{6.71}$$

It is also obvious that,

$$V_z = V_{zb.max} \tag{6.72}$$

In accordance with (3.12), the following is arrived at:

$$S_{n1z} = S_{n2z} = \frac{2S_{n1}\tan\beta}{\sqrt{\tan^2\gamma + 1 + \tan^2\beta}} \tag{6.73}$$

Moreover:

$$E_{1z} = E_{2z} = 0 \tag{6.74}$$

$$F_{1z} = F_{2z} = F_1 \sin\delta = S_{\tau 1}\, \sin\psi \cdot \sin\delta \tag{6.75}$$

Taking into account (6.68)–(6.75), (6.67) is resolved into the following system of equations:

$$\left. \begin{aligned}
m\left(U_x - V_p\right) &= \frac{2S_{n1}\tan\gamma}{\sqrt{\tan^2\gamma + 1 + \tan^2\beta}} + 2fS_{n1}\cos\psi \cdot \cos\gamma - 2f\sin\psi \cdot \cos\delta \cdot \sin\gamma, \\
m(U_z - V_{zb.max}) &= \frac{2S_{n1}\tan\beta}{\sqrt{\tan^2\gamma + 1 + \tan^2\beta}} + 2fS_{n1}\sin\psi \cdot \sin\delta
\end{aligned} \right\} \tag{6.76}$$

Thus, a system of two equations with three unknown quantities, S_{n1}, U_x, U_z, has been obtained. The necessary third equation can be obtained using Newton's hypothesis about the collision of two bodies [32].

The relation between the digging tool velocities prior to and after the impact can be expressed with the use of the coefficient of restitution ε, in accordance with (6.24).

Since $\overline{U} = \overline{U}_x + \overline{U}_z$, $\overline{V} = \overline{V}_p + \overline{V}_{zb.max}$, and taking into account (3.12), the following is obtained:

$$U_n = \frac{U_x \tan\gamma + U_z \tan\beta}{\sqrt{\tan^2\gamma + 1 + \tan^2\beta}} \tag{6.77}$$

$$V_n = \frac{V_p \tan\gamma + V_{zb.max} \tan\beta}{\sqrt{\tan^2\gamma + 1 + \tan^2\beta}} \tag{6.78}$$

By substituting (6.77) and (6.78) into (6.24), the third equation is obtained:

$$U_x \tan\gamma + U_z \tan\beta = -\varepsilon\left(V_p \tan\gamma + V_{zb.max} \tan\beta\right) \tag{6.79}$$

Thus, the system of three linear equations of the following form is arrived at:

$$\left. \begin{aligned}
m\left(U_x - V_p\right) &= \frac{2S_{n1}\tan\gamma}{\sqrt{\tan^2\gamma + 1 + \tan^2\beta}} + 2fS_{n1}\cos\psi \cdot \cos\gamma - 2f\sin\psi \cdot \cos\delta \cdot \sin\gamma, \\
m(U_z - V_{zb.max}) &= \frac{2S_{n1}\tan\beta}{\sqrt{\tan^2\gamma + 1 + \tan^2\beta}} + 2fS_{n1}\sin\psi \cdot \sin\delta, \\
U_x \tan\gamma + U_z \tan\beta &= -\varepsilon\left(V_p \tan\gamma + V_{zb.max} \tan\beta\right).
\end{aligned} \right\} \tag{6.80}$$

(6.80) can be formulated in the following form, which is more appropriate for solving with the use of Cramer's rule:

$$\left. \begin{aligned}
mU_x + 0U_z - \left(\frac{2\tan\gamma}{\sqrt{\tan^2\gamma + 1 + \tan^2\beta}} + 2f\cos\psi \cdot \cos\gamma - 2f\sin\psi \cdot \cos\delta \cdot \sin\gamma\right)S_{n1} &= mV_p, \\
0U_x + mU_z - \left(\frac{2\tan\beta}{\sqrt{\tan^2\gamma + 1 + \tan^2\beta}} + 2f\sin\psi \cdot \sin\delta\right)S_{n1} &= mV_{zb.max}, \\
\tan\gamma\, U_x + \tan\beta\, U_z &= -\varepsilon\left(V_p \tan\gamma + V_{zb.max} \tan\beta\right).
\end{aligned} \right\} \tag{6.81}$$

The next step is to write down the principal determinant of (6.81) and find its value:

$$\Delta = \begin{vmatrix} m & 0 & -\left(\dfrac{2\tan\gamma}{\sqrt{\tan^2\gamma+1+\tan^2\beta}} + 2f\cos\psi\cdot\cos\gamma - 2f\sin\psi\cdot\cos\delta\cdot\sin\gamma\right) \\ 0 & m & -\left(\dfrac{2\tan\beta}{\sqrt{\tan^2\gamma+1+\tan^2\beta}} + 2\sin\psi\cdot\sin\delta\right) \\ \tan\gamma & \tan\beta & 0 \end{vmatrix}$$

$$= m\left(\dfrac{2\tan\beta}{\sqrt{\tan^2\gamma+1+\tan^2\beta}} + 2f\sin\psi\cdot\sin\delta\right)\tan\beta$$

$$+m\left(\dfrac{2\tan\gamma}{\sqrt{\tan^2\gamma+1+\tan^2\beta}} + 2f\cos\psi\cdot\cos\gamma - 2f\sin\psi\cdot\cos\delta\cdot\sin\gamma\right)\tan\gamma \qquad (6.82)$$

Further, the determinant for finding the unknown quantity S_{n1} is to be written down and its value is to be found:

$$\Delta_{Sn1} = \begin{vmatrix} m & 0 & mV_p \\ 0 & m & mV_{zb.max} \\ \tan\gamma & \tan\beta & -\varepsilon\left(V_p\tan\gamma + V_{zb.max}\tan\beta\right) \end{vmatrix}$$

$$= -\left[m^2\varepsilon\left(V_p\tan\gamma + + V_{zb.max}\tan\beta\right) + m^2\tan\beta V_{zb.max}\right] - m^2 V_p\tan\gamma \qquad (6.83)$$

Thereafter, according to Cramer's rule:

$$S_{n1} = \dfrac{\Delta_{Sn1}}{\Delta} \qquad (6.84)$$

After substituting (6.82) and (6.83) into (6.84) and making some transformations, the following is obtained:

$$S_{n1}$$
$$= -\dfrac{\dfrac{m(1+\varepsilon)\left(V_p\tan\gamma+V_{zb.max}\cdot\tan\beta\right)\cdot\sqrt{\tan^2\gamma+1+\tan^2\beta}}{2\tan^2\beta+2f\sin\psi\cdot\sin\delta\cdot\tan\beta\sqrt{\tan^2\gamma+1+\tan^2\beta}+2\tan^2\gamma}}{\dfrac{m(1+\varepsilon)\left(V_p\tan\gamma+V_{zb.max}\cdot\tan\beta\right)\cdot\sqrt{\tan^2\gamma+1+\tan^2\beta}}{+(2f\cos\psi\cdot\cos\gamma-2f\sin\psi\cdot\cos\delta\cdot\sin\gamma)\tan\gamma\sqrt{\tan^2\gamma+1+\tan^2\beta}}} \qquad (6.85)$$

Thus, the normal component of the impact impulse arising during the impact interaction between one of the wedges and the root fixed in the soil has been determined. (6.85) represents the functional relation between the normal component S_{n1} of the impact impulse and the design and kinematic parameters of the vibrational lifting tool of the beet harvester.

The sign "−" in (6.85) designates the impact impulse S_{n1} applied by the root to the digging tool. The impact impulse applied by the digging tool to the root has a positive sign and the same magnitude.

If the total impact impulse applied by the digging tool (from both the wedges) to the root is denoted by $\overline{S}$:

$$\overline{S} = \overline{S}_{n1} + \overline{S}_{n2} + \overline{S}_{\tau 1} + \overline{S}_{\tau 2}, \tag{6.86}$$

then, according to (6.76), its projections on axes Ox and Oz are equal to, respectively:

$$S_x = \frac{2S_{n1}\tan\gamma}{\sqrt{\tan^2\gamma + 1 + \tan^2\beta}} + 2fS_{n1}\cos\psi\cdot\cos\gamma - 2fS_{n1}\sin\psi\cdot\cos\delta\cdot\sin\gamma \tag{6.87}$$

$$S_z = \frac{2S_{n1}\tan\beta}{\sqrt{\tan^2\gamma + 1 + \tan^2\beta}} + 2fS_{n1}\sin\psi\cdot\sin\delta \tag{6.88}$$

where S_{n1} is determined in accordance with (6.85), but with a positive sign.

Hence, based on (6.87), (6.88) and (6.85), it is possible to determine the total impact impulse applied by the digging tool to the root:

$$S = \sqrt{S_x^2 + S_z^2} \tag{6.89}$$

It is obvious that vector $\overline{S}$ lies in plane xOz, the same plane where the projections S_x and S_z lie.

Taking into account (6.87), (6.88) and (6.39), it is possible to write down the formulae for the projections of force $F_{ud.}$ on axes Ox and Oz, respectively:

$$F_{ud.x} = \left(\frac{4\tan\gamma}{\sqrt{\tan^2\gamma + 1 + \tan^2\beta}} + 4f\cos\psi\cdot\cos\gamma - 4f\sin\psi\cdot\cos\delta\cdot\sin\gamma\right)\frac{S_{n1}}{t_{ud.}} \tag{6.90}$$

$$F_{ud.z} = \left(\frac{4\tan\beta}{\sqrt{\tan^2\gamma + 1 + \tan^2\beta}} + 4f\sin\psi\cdot\sin\delta\right)\frac{S_{n1}}{t_{ud.}} \tag{6.91}$$

where the quantity S_{n1} is determined in accordance with Expression (6.85) and has a positive sign.

The duration of the impact $t_{ud.}$ can be determined only by experiment. According to [31], $t_{ud.} \approx 0.6\cdot10^{-2}$ s.

The next step is to analyse the conditions for avoiding damage to the root during its impact interaction with the digging tool.

If the root fixed in the soil is considered as a cantilevered beam, the root under the action of the moment created by the impact force $\overline{F}_{ud.x}$ is subjected to bending deformation, under the action of the impact force $\overline{F}_{ud.z}$—to tensile deformation.

Therefore, if the permissible levels of said forces are exceeded, the root can break or be torn apart. As mentioned earlier, such an event is most probable in the case of dry and hard soil. The effect is different in the case of humid and soft soil, where the root will more probably incline through an angle to the horizon under the action of the horizontal force and be pulled out under the action of the vertical force. If the impact takes place at points K_1 and K_2 situated at a distance of h from the conventional point of fixation O_1 (Figure 6.5), the moment of the horizontal component of the impact force about said point is (taking into account (6.90)) equal to:

$$M_{o1}(F_{ud.x}) = \left(\frac{4 \tan \gamma}{\sqrt{\tan^2 \gamma + 1 + \tan^2 \beta}} + 4f \cos \psi \cdot \cos \gamma - 4f \sin \psi \cdot \cos \delta \cdot \sin \gamma \right) \frac{S_{n1}h}{t_{ud.}} \tag{6.92}$$

Considering the conditions for the root not breaking under the action of the horizontal force $\overline{F}_{ud.x}$, two cases are theoretically possible the first one when $\left[M_{zg} \right] < M_{op}$ and the second when $\left[M_{zg} \right] > M_{op}$ where $\left[M_{zg} \right]$ is the bending moment permissible for the root body, which does not cause the root breaking off and M_{op} is the support moment of the unbroken soil, in which the root is fixed.

Equilibrium conditions always imply $M_{on} = M_{o1}(\overline{F}_{ud.x})$ where M_{op} has to be understood as the maximum (potential) support moment that can be provided by the restraint, i.e., the soil, in which the root is fixed, without disrupting the restraint.

The first case stated above is typical of dry and hard soil; the second one is typically related to of humid and soft soil.

In the first case, the root breaking off is possible, considering (6.92), under the following condition:

$$\left[M_{zg} \right] < \left(\frac{4 \tan \gamma}{\sqrt{\tan^2 \gamma + 1 + \tan^2 \beta}} + 4f \cos \psi \cdot \cos \gamma - 4f \sin \psi \cdot \cos \delta \cdot \sin \gamma \right) \frac{S_{n1}h}{t_{ud}} \leq M_{on} \tag{6.93}$$

Hence, the condition for the root not breaking off in the first case, considering (6.92) is as follows:

$$\left(\frac{4 \tan \gamma}{\sqrt{\tan^2 \gamma + 1 + \tan^2 \beta}} + 4f \cos \psi \cdot \cos \gamma - 4f \sin \psi \cdot \cos \delta \cdot \sin \gamma \right) \frac{S_{n1}h}{t_{ud}} < \left[M_{zg} \right] < M_{op} \tag{6.94}$$

In the second case, the root breaking off is unlikely in general; the only possible effect is the root inclining through an angle and, in this case, the condition for the root inclining without breaking off is, considering (6.92):

$$M_{op} < \left(\frac{4 \tan \gamma}{\sqrt{\tan^2 \gamma + 1 + \tan^2 \beta}} + 4f \cos \psi \cdot \cos \gamma - 4f \sin \psi \cdot \cos \delta \cdot \sin \gamma \right) \frac{S_{n1}h}{t_{ud}} < \left[M_{zg} \right] \tag{6.95}$$

Finally, in the second case, the root will neither break off nor incline subject to the following, considering (6.92), condition:

$$\left(\frac{4\tan\gamma}{\sqrt{\tan^2\gamma + 1 + \tan^2\beta}} + 4f\cos\psi\cdot\cos\gamma - 4f\sin\psi\cdot\cos\delta\cdot\sin\gamma \right)\frac{S_{n1}h}{t_{ud}} \leq M_{op} < \left[M_{zg}\right] \qquad (6.96)$$

Considering the conditions for the root not being torn apart under the action of the vertical force $\overline{F}_{ud.z}$, again, two cases are theoretically possible: $[F_{ro}] < R_z$ and $[F_{ro}] > R_z$ where $[F_{ro}]$ is the force permissible for the root body, which does not cause the root to tear apart and R_z is the vertical force of bonding between the root and the soil. Here, again, the quantity R_z has to be understood as the maximum (potential) bonding force that can be provided by the restraint without disrupting the restraint.

The first case is, again, typical of dry and hard soil; the second one is typically related to humid and soft soil.

In the first case, tearing the root apart is possible, considering (6.91), under the following condition:

$$[F_{ro}] < \left(\frac{4\tan\beta}{\sqrt{\tan^2\gamma + 1 + \tan^2\beta}} + 4f\sin\psi\cdot\sin\delta \right)\frac{S_{n1}}{t_{ud}} \leq R_z \qquad (6.97)$$

Hence, the condition for not tearing the root apart in the first case is, always considering (6.91) as follows:

$$\left(\frac{4\tan\beta}{\sqrt{\tan^2\gamma + 1 + \tan^2\beta}} + 4f\sin\psi\cdot\sin\delta \right)\frac{S_{n1}}{t_{ud}} \leq [F_{ro}] < R_z \qquad (6.98)$$

In the second case, tearing the root apart is unlikely. The only possible event is pulling the root out of the soil without tearing it apart.

The condition for the root being pulled out of the soil is, taking into account (6.91), as follows:

$$R_z < \left(\frac{4\tan\beta}{\sqrt{\tan^2\gamma + 1 + \tan^2\beta}} + 4f\sin\psi\cdot\sin\delta \right)\frac{S_{n1}}{t_{ud}} < [F_{ro}] \qquad (6.99)$$

The root will not be pulled out of the soil in case the following condition is met, which consider (6.91):

$$\left(\frac{4\tan\beta}{\sqrt{\tan^2\gamma + 1 + \tan^2\beta}} + 4f\sin\psi\cdot\sin\delta\right)\frac{S_{n1}}{t_{ud}} \leq R_z < [F_{ro}] \tag{6.100}$$

On the basis of the condition for the root not breaking off (6.94) and the condition for not tearing the root apart (6.99) in the case of impact interaction between the digging tool and the root, the limitation on the tool's velocity can be determined. For this purpose, the following is obtained from (6.94):

$$S_{n1} \leq \frac{[M_{zg}]t_{ud}\sqrt{\tan^2\gamma + 1 + \tan^2\beta}}{h\left[4\tan\gamma + (4f\cos\psi\cdot\cos\gamma - 4f\sin\psi\cdot\cos\delta\cdot\sin\gamma)\sqrt{\tan^2\gamma + 1 + \tan^2\beta}\right]} \tag{6.101}$$

and the following is derived from (6.98):

$$S_{n1} \leq \frac{[F_{ro}]t_{ud}\sqrt{\tan^2\gamma + 1 + \tan^2\beta}}{4\tan\beta + 4f\sin\psi\cdot\sin\delta\sqrt{\tan^2\gamma + 1 + \tan^2\beta}} \tag{6.102}$$

In order to provide for the convenience and abbreviation in the further writing down of expressions, the following designations are introduced:

$$\frac{\sqrt{\tan^2\gamma + 1 + \tan^2\beta}}{4\tan\gamma + (4f\cos\psi\cdot\cos\gamma - 4f\sin\psi\cdot\cos\delta\cdot\sin\gamma)\sqrt{\tan^2\gamma + 1 + \tan^2\beta}} = A \tag{6.103}$$

$$\frac{\sqrt{\tan^2\gamma + 1 + \tan^2\beta}}{4\tan\beta + 4f\sin\psi\cdot\sin\delta\sqrt{\tan^2\gamma + 1 + \tan^2\beta}} = B \tag{6.104}$$

$$\frac{\sqrt{\tan^2\gamma + 1 + \tan^2\beta}}{2\tan^2\beta + 2f\sin\psi\cdot\sin\delta\tan\beta\sqrt{\tan^2\gamma + 1 + \tan^2\beta} + 2\tan^2\gamma + (2f\cos\psi\cos\gamma - 2f\sin\psi\cos\delta\sin\gamma)\tan\gamma\sqrt{\tan^2\gamma + 1 + \tan^2\beta}} = C \tag{6.105}$$

Then, (6.85), (6.101) and (6.102) acquire the following form:

$$S_{n1} = Cm(1 + \varepsilon)(V_p\tan\gamma + V_{zb.max}\tan\beta) \tag{6.106}$$

$$S_{n1} \leq \frac{A[M_{zg}]t_{ud}}{h} \tag{6.107}$$

$$S_{n1} \leq B[F_{ro}]t_{ud} \tag{6.108}$$

where Expression (6.85) is taken with the positive sign.

Thereby, two expressions have been obtained for the limitation of the value of the impact impulse S_{n1}—that is, (6.107) and (6.108). As was noted in Section 6.1, the root as a cantilevered beam will most probably break off at the boundary between

the layers of broken and unbroken soil, the latter being the layer where the root's tail part is fixed. It was also noted that the tail part breaking off at the cross-section with a diameter of 30 ... 40 cm corresponds to a digging tool running depth of 10 ... 12 cm. It is obvious that breaking off due to bending is more probable at that cross-section than tearing apart due to stretching (tearing apart due to stretching can take place in the area below the cross-section, where the cross-section diameter is significantly smaller). Therefore, it is (6.107) that has to be used as the criterion in the estimation of the acceptable impact impulse value. This is despite the fact that, theoretically, the acceptable value of the impact impulse S_{n1} has to be determined using the following criterion:

$$S_{n1} \leq \min \left\{ \frac{A[M_{zg}]t_{ud}}{h}, B[F_{ro}]t_{ud} \right\} \tag{6.109}$$

Nevertheless, the above considerations imply that for the specific cross-section is true that $\min \left\{ \frac{A[M_{zg}]t_{ud}}{h}, B[F_{ro}]t_{ud} \right\} = \frac{A[M_{zg}]t_{ud}}{h}$.

From (6.106), the following is derived:

$$V_p \ \tan \gamma + V_{zb.max} \ \tan \beta = \frac{S_{n1}}{Cm \ (1 + \varepsilon)} \tag{6.110}$$

Finally, taking into account (6.107), the following inequation is arrived at:

$$V_p \ \tan \gamma + V_{zb.max} \ \tan \beta \leq \frac{A[M_{zg}]t_{ud}}{Cm \ (1 + \varepsilon)h} \tag{6.111}$$

Thus, the limitation on the velocity of the lifting tool taking into account its design parameters and mass as well as the root's strength and coefficient of restitution has been established.

As the velocity of the unit has an effect on its productivity, it is necessary to investigate the case of the sign of equality in (6.111). If the beet harvester's translational motion velocity V_p is preset, it is possible to derive from (6.111) the magnitude of the maximum velocity $V_{zb.max}$ of the oscillatory motion of the vibrational lifting tool:

$$V_{zb.max} = \frac{1}{\tan \beta} \left(\frac{A[M_{zg}]t_{ud}}{Cm \ (1 + \varepsilon)h} - V_p \tan \gamma \right) \tag{6.112}$$

Then, with (6.7), it is possible to determine, at the preset amplitude of the oscillations, the required angular frequency of the digging tool oscillations subject to the condition of not damaging the root:

$$\omega = \frac{1}{a \tan \beta}\left(\frac{A\left[M_{zg}\right]t_{ud}}{Cm\ (1+\varepsilon)h} - V_p \tan \gamma \right) \qquad (6.113)$$

The hertz frequency of the digging tool oscillations is equal to:

$$v = \frac{1}{2\pi a \ \tan \beta}\left(\frac{A\left[M_{zg}\right]t_{ud}}{Cm\ (1+\varepsilon)h} - V_p \ \tan \gamma \right) \qquad (6.114)$$

Based on the developed theory, the algorithm of calculations for finding the acceptable vibrational lifting tool oscillation frequency in relation to the lifter's translational motion velocity $\overline{V}_p$ and the digging tool oscillation amplitude at various depths of running of the digging tool can be developed.

The ranges of variation for the mentioned parameters are selected in the same way as in Section 6.1. The algorithm is comprised of the steps described below.

1. The permissible bending moment $\left[M_{zg}\right]$ is found with (6.58).
2. Parameters A and C are found with (6.103) and (6.105), respectively.
3. After selecting a specific value of the reduced mass m from the set of reduced mass values obtained in Section 6.1, the acceptable frequency is determined as the function $v = v\left(V_p, a\right)$ in accordance with (6.114).

Based on the developed theory of the impact interaction at two points, the calculation of the acceptable oscillation frequencies for the digging tool subject to the condition of not breaking off the root at different values of the design and kinematic parameters of the vibrational lifting tool has been accomplished for the reduced mass values presented in Section 6.1. All the design and kinematic parameters of the digging tool and the physical and mechanical properties of the roots required for the calculation have been assumed to be the same as in Section 5.1.

The ranges of variation of the acceptable frequencies obtained in the above-mentioned calculations are presented in Table 6.6.

Table 6.6. Acceptable digging tool oscillation frequencies for varying oscillation amplitudes (0.008–0.024 m) and lifter translation velocities (1.4–2.2 m·s^{-1}).

Digging Tool Running Depth (m)	Range of Variation of Acceptable Digging Tool Oscillation Frequency (Hz)		
	m = 0.8 kg	m = 1.0 kg	m = 1.5 kg
0.08	42.77~13.20	33.11~9.98	13.79~3.54
0.10	20.37~5.73	15.18~4.01	8.28~1.71
0.12	6.25~1.03	3.895–0.25	–

As may be inferred from Table 6.6, the values of the acceptable frequencies in the case of impact interaction between the digging tool and the root at two points are, under the same conditions, somewhat lower than in the case of an impact interaction at one point. Theoretically, it is necessary to select the acceptable frequency values as the intersection of the sets of acceptable frequency values for the impact interaction at one point and at two points. However, the probability of an impact simultaneously at two points is significantly lower than in the case of a one-point impact. Therefore, in the design of a specific lifting tool, it is sufficient to use the results obtained in Section 6.1.

The graph and the contour diagram of the function $v = v(V_p, a)$ for a reduced digging tool mass of m = 1.0 kg and running depth of z = 0.10 m are presented below (Figure 6.6).

(a) (b)
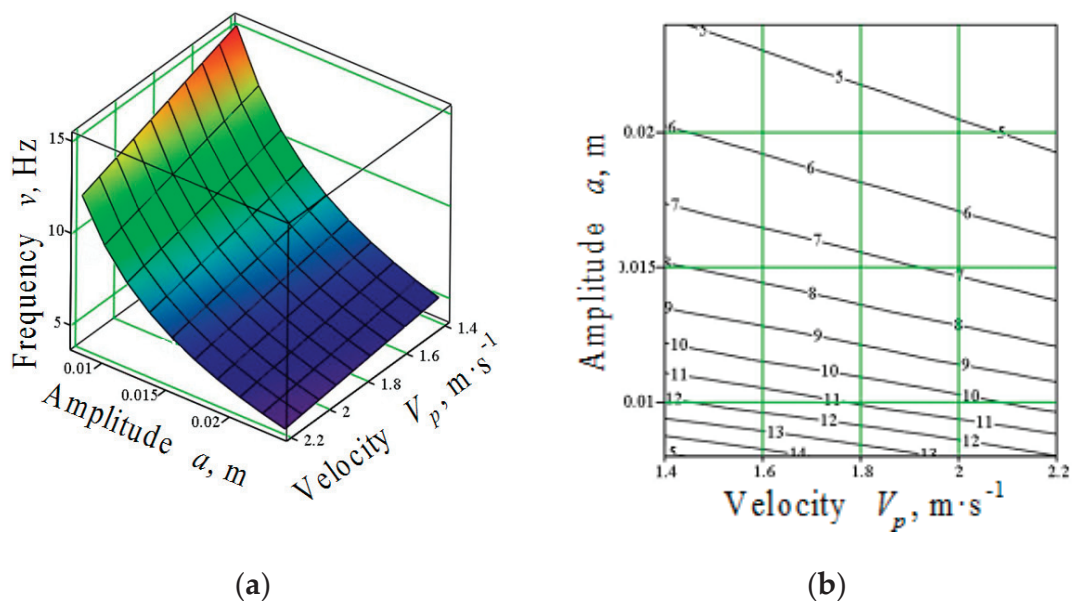
Figure 6.6. Surface (**a**) and contour diagrams (**b**) of values of digging tool oscillation frequency $v = v(V_p, a)$ (Hz) that are acceptable under condition of not damaging roots in the case of their impact interaction with digging tool at two points.

As can be concluded from the presented graph, the increase in the translational motion velocity and the digging tool oscillation amplitude results in the decrease in the acceptable oscillation frequency value. A decrease in acceptable frequency is also observed in the case where the depth of the digging tool running in the soil was increased.

The same as in Section 6.1, the obtained values of acceptable frequencies have to be limited from above taking into account the reliability of the digging tool oscillatory motion drive, as well as from below taking into account (6.63) or the graphs of the relation between the minimum acceptable frequency v on the one hand and the lifter's translational motion velocity and the length of the rear part of the lifter's working channel at which the normal conditions for the process of the vibrational lifting of sugar beet roots are ensured (Figure 6.4) on the other hand.

6.3. Conclusions

1. The principal scientific result produced in Section 6 is the developed theory of the impact interaction between the vibrational lifting tool and the sugar beet root fixed in the soil at the time when the digging tool runs into the root.
2. The mathematical model of the impact interaction between the digging tool and the root at one and two points has been generated. On the basis of the model, the theoretic conditions of not breaking off the tail parts of the roots during said interaction have been determined.
3. The algorithm of calculation for finding the acceptable frequency of oscillation of the vibrational lifting tool under the condition of not breaking off the roots during the impact interaction has been generated.
4. The ranges have been determined for the acceptable values of the digging tool mass reduced to the point of impact, the digging tool oscillation frequency and the lifter's translational motion velocity under the condition of not breaking off the roots during the impact, taking into account the design parameters of the vibrational lifting tool and the physical and mechanical properties of the sugar beet roots.
5. The theoretical values of the reduced mass have been obtained for the digging tool oscillation frequency varying within the range of $v = 7.5 \sim 20.3$ Hz and the lifter's translational motion velocity varying within the range of $V_{\Pi} = 1.4 \sim 2.2$ m·s^{-1} at different values of the depth of running of the digging tool (0.08~0.14 m) and different values of the digging tool oscillation amplitude (0.008, 0.016, 0.024 m). The theoretical values of the mass reduced to the point of impact are as follows:

   - For a digging tool running depth of 0.08 m:

     - At a digging tool oscillation amplitude of 0.008 m—4.45~2.00 kg;

- At a digging tool oscillation amplitude of 0.016 m—2.82~1.18 kg;
- At an oscillation amplitude of 0.024 m—2.07~0.83 kg.

- For a digging tool running depth of 0.10 m:

  - At an oscillation amplitude of 0.008 m—2.38~1.17 kg;
  - At an oscillation amplitude of 0.016 m—1.51~0.63 kg;
  - At an oscillation amplitude of 0.024 m—1.11~0.45 kg.

- For a digging tool running depth of 0.12 m:

  - At an oscillation amplitude of 0.008 m—2.38~1.17 kg;
  - At an oscillation amplitude of 0.016 m—0.69~0.29 kg;
  - At an oscillation amplitude of 0.024 m—0.50~0.20 kg.

6. The acceptable frequency of the digging tool oscillations is determined as a function of the lifter's translational motion velocity and the tool oscillation amplitude. In this case, the lifter's translational motion velocity varies within the range of 1.4~2.2 m·s^{-1}; the amplitude—within the range of 0.008~0.024 m. The calculations have been carried out for different values of the reduced mass (0.8, 1.0, 1.5, 2.0 kg) and different values of the digging tool running depth (0.08, 0.10, 0.12, 0.14 m). The following results have been obtained:

- For a reduced digging tool mass of 0.8 kg:

  - At a digging tool running depth of 0.08 m—66.86~21.23 Hz;
  - At a digging tool running depth of 0.10 m—33.28~10.04 Hz;
  - At a digging tool running depth of 0.12 m—12.13~2.29 Hz.

- For a reduced digging tool mass of 1.0 kg:

  - At a running depth of 0.08 m—52.38~16.41 Hz;
  - At a running depth of 0.10 m—25.52~7.45 Hz;
  - At a running depth of 0.12 m—8.60~1.81 Hz.

- For a reduced digging tool mass of 1.5 kg:

  - At a running depth of 0.08 m—33.08~9.97 Hz;
  - At a running depth of 0.10 m—15.7~4.01 Hz.

7. As may be inferred from the obtained theoretic results, at a reduced digging tool mass of m = 1.5 kg, a digging tool running depth of z = 0.08 m and an oscillation amplitude of a = 0.008 m, a maximum acceptable digging tool oscillation frequency of v = 30 Hz ensures the tail parts of the roots within the range of the lifter's translational motion velocity of 1.4~2.2 m·s^{-1} will not break off. At the same depth of running and a digging tool oscillation amplitude of a = 0.010 m, a maximum acceptable oscillation frequency of

$\nu = 24$ Hz ensures the tail parts of the roots within the above-mentioned range of the lifter's translational motion velocity will not break off. Under the same conditions, at an amplitude of $a = 0.012$ m, the maximum acceptable frequency is $\nu = 20$ Hz; at an amplitude of $a = 0.014$ m—17.1 Hz; at $a = 0.016$ m —15.0 Hz; $a = 0.018$ m—13.3 Hz; $a = 0.020$ m—12.0 Hz; $a = 0.022$ m—10.9 Hz; $a = 0.024$ m—10.0 Hz. The above-listed values of the digging tool oscillation frequency are the maximum acceptable frequency values subject to the condition of not breaking off the tail parts of the roots during the impact interaction. Lower values of the oscillation frequency guarantee, to a greater extent, that the tail parts of the roots will not break off. However, the frequencies have to be limited from below as well—that is, there are minimum acceptable frequency values that ensure the guaranteed gripping of each root by the digging shares. As has been proved by the calculation, the values of the maximum acceptable frequency are significantly lower at a digging tool running depth of $z = 0.10$ m. For example, at an oscillation amplitude of $a = 0.008$ m, a maximum acceptable oscillation frequency of $\nu = 12$ Hz ensures the tail parts of the roots within the range of the lifter's translational motion velocity of $V = 1.4{\sim}2.2$ m·s^{-1} will not break off; at an oscillation amplitude of $a = 0.010$ m, the maximum acceptable frequency is $\nu = 9.6$ Hz, at an amplitude of $a = 0.012$ m—$\nu = 8$ Hz; at an amplitude of $a = 0.014$ m—$\nu = 6.9$ Hz. At higher values of amplitude, the acceptable frequency values become even lower. If these frequency values fall below the minimum acceptable level under the condition of the guaranteed gripping of each root by the digging shares, the respective kinematic conditions of operation must be rejected as technologically unacceptable. At a reduced digging tool mass of $m = 1.5$ kg and a running depth of 0.12 m, the maximum acceptable frequency values subject to the condition of not breaking off the tail parts of the roots during the impact interaction are below 4 Hz. Under the condition of the guaranteed gripping of the root by the digging shares such frequency values are unacceptable. It is quite obvious that the frequency values that are maximum acceptable for a reduced digging tool mass of $m = 1.5$ kg are even more compliant with the condition of not breaking off the tail parts of the roots for lower values of the reduced digging tool mass. In effect, the maximum acceptable frequency values at the respective amplitudes and digging tool running depths are even higher. This is proved by the results of the calculations for reduced digging tool masses of $m = 0.8$ kg and $m = 1.0$ kg. While at a digging tool running depth of 0.12 m and a tool reduced mass of 1.5 kg, the maximum acceptable frequency values are below 4 Hz; in the case of a reduced mass of $m = 1.0$ kg, these values are considerably higher. For example, at an amplitude of 0.008 m and lifter translational motion velocities of 1.4~2.2 m·s^{-1}, they are within the range of 8.6–5.4 Hz, at an amplitude of 0.010 m and within the same

range of translational motion velocities—within the range of 6.8~4.4 Hz; at an amplitude of 0.012 m—within the range of 5.7~3.6 Hz. At a reduced digging tool mass of $m = 0.8$ kg and a digging tool running depth of 0.12 m, the respective values of the maximum acceptable frequency are within the following ranges:

- At an amplitude of 0.008 m—12.1~9.0 Hz;
- At an amplitude of 0.010 m—9.7~7.1 Hz;
- At an amplitude of 0.012 m—8.1~6.0 Hz;
- At an amplitude of 0.014 m—7.0~5.1 Hz.

8. The minimum acceptable digging tool oscillation frequencies that provide for the normal conditions of the vibrational root lifting process, i.e., the conditions that facilitate the guaranteed gripping of each root by the vibrational lifting tool, have been determined for the preset velocity of the lifter's translational motion and length of the rear part of the working channel. For example, at a length of $l = 0.1$ m lifter for the rear part of the working channel, a vibrational lifting tool oscillation frequency Hz guarantees gripping of each root by the digging tool at all values of the lifter translation velocity below or equal to 2.0 m·s^{-1}, while at $l = 0.15$ m, a frequency of $v = 20$ Hz is adequate at all values below or equal to 3.0 m·s^{-1} for the lifter translation velocity. At the same time, at $l = 0.15$ m, a digging tool oscillation frequency Hz provides for the guaranteed gripping of each root by the digging tool at all values of the lifter translation velocity below or equal to 2 m·s^{-1}. At $l = 0.2$ m, an oscillation frequency of $v = 10$ Hz provides for said conditions at all values of the translation velocity below or equal to 2 m·s^{-1}. If the frequency of oscillations of the digging tool does not allow for the gripping of each root by the digging shares, the root loss rate sharply rises due to breaking off of the root tail parts and due to not lifting the roots at all. The described theoretical results are rather accurately supported by the experimental studies of the mass of lost sugar beet roots. For example, at a lifter translation velocity of $V_p = 2.1$ m·s^{-1}, a depth of running in the soil of 0.06 m and a digging tool oscillation frequency of $v = 20.3$ Hz, the mass of lost roots amounts to 0.64%; at a frequency of $v = 15.7$ Hz—2.2%; at a frequency of 8.5 Hz—3.48%. At a lifter translation velocity of $V_p = 1.3$ m·s^{-1}, the losses are significantly lower. For example, at a frequency of = 20.3 Hz and a depth of running in the soil of 0.06 m, the mass of lost roots amounts to 0.38%; at an oscillation frequency of $v = 15.7$ Hz—1.78%; at an oscillation frequency of $v = 8.5$ Hz—2.74%. Thus, at a lifter translation velocity of $V_p = 1.3$ m·s^{-1}, the digging shares capture more roots than at a velocity of $V_p = 2.1$ m·s^{-1}. Moreover, the amount of the captured roots sharply rises when the digging tool oscillation frequency becomes higher, and, consequently, the lost root mass decreases.

9. We recommend using the following values of digging tool oscillation frequencies subject to the condition of not breaking off the tail parts of the roots during the impact interaction and the condition of the guaranteed gripping of each root by the digging tool when the translational motion velocity is within the range of 1.3~2.2 m·s^{-1} depending on digging tool's mass.

- $m = 0.8$ kg: at a depth in the soil of 0.08 m and an oscillation amplitude of 0.008–0.024 m, the acceptable oscillation frequency is 21.2 Hz; at a depth of 0.10 m—10.0 Hz; at a depth of 0.12 m—9.0 Hz.
- $m = 1.0$ kg: at a depth in the soil of 0.08 m and an oscillation amplitude of 0.008–0.024 m, the acceptable oscillation frequency is 16.4 Hz; at a depth of 0.10 m and an oscillation amplitude of 0.008–0.018 m, the acceptable oscillation frequency is 10.0 Hz; at an amplitude of 0.020–0.024 m—8.3 Hz.
- $m = 1.5$ kg: at a depth in the soil of 0.08 m and an oscillation amplitude of 0.008–0.024 m, the acceptable oscillation frequency is 10.0 Hz; at a depth of 0.10 m and an oscillation amplitude of 0.008–0.010 m, the acceptable oscillation frequency is 10.0 Hz; at an amplitude of 0.012 m—8.0 Hz.
- $m = 2.0$ kg: at a depth in the soil of 0.08 m and an oscillation amplitude of 0.008–0.016 m, the acceptable oscillation frequency is 10.0 Hz; at an oscillation amplitude of 0.018–0.020 m—8.1 Hz.

7. Experimental Research

7.1. Programme of Investigations

Following the completion of the analysis of the existing engineering developments, patent and literature sources, the special features in the operation of the developed vibrating digging tool, the sugar beet root harvesting work process and the agronomic requirements for it and in accordance with the set aims and tasks of research, the programme of experimental investigations is stipulated:

- Investigating the effect that the parameters and operation conditions of the vibrating digging tool have on the quality indicators of operation in order to verify the results of the theoretical research;
- Determining the energy and force parameters of the digging tool;
- Testing the root harvester with a vibrational lifting implement in field in order to verify the compliance of its performance with the agronomic requirements.

The engineering factors that had a substantial effect on the quality of the root digging included the digging tool oscillation frequency (Hz), the depth of running of the tool (m) and the velocity of translation of the harvester with vibrational lifting tools (m·s^{-1}).

The indicators that characterised the quality of work of the digging tool were the root loss mass rate (%) and the root damage mass rate (%).

The energy and force parameters were determined by measuring the tractive effort (kN), the power consumed by the drive of the vibrating digging tool (kW) and the torque generated on the power take-off shaft (N·m) at different travel speeds, digging tool vibration frequencies and depths of undercutting.

7.2. Technique of Laboratory and Field Experiment Investigations

In order to perform the experimental investigations of the process of the vibrational lifting of sugar beet roots from the soil, a new design of the vibrating digging tool was developed with the use of the design and kinematic parameters obtained in the theoretical investigations. The new design was supposed to ensure the required quality of the lifting of roots from dry and hard soil. The structural schematic model of the vibrational lifter is shown in Figure 7.1.
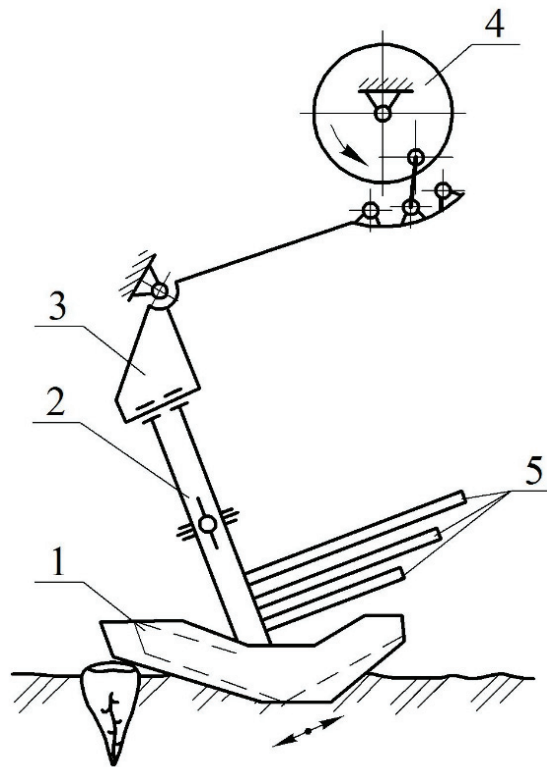
Figure 7.1. Schematic design and process model of vibrational lifting tool: 1—digging shares; 2—shanks; 3—share spacing adjustment mechanism; 4—vibration drive with share oscillation amplitude and frequency adjustment mechanism; 5—guide bars.

The lifter comprised the digging shares (1) mounted at the ends of the shanks (2), which were linked through the suspension brackets (3) with the drive mechanism (4) that forced the mentioned shares (1) to oscillate. The mechanism (4) was equipped with a device that could set (adjust) the frequency and amplitude of the shares' oscillatory motion over a wide range (frequency was controlled within the range of 8.5 to 20.3 Hz; amplitude—8 to 24 mm).

The bracket (3) for the suspension of the shanks (2) was equipped with an additional swivel joint, which provided for the free movement of the paired shanks (2) in the transverse-longitudinal plane within a small range. This facilitated the self-adjustment of the shares (1) during the vibrational lifter's translational motion.

In order to carry out the field and laboratory experiment investigations of the new vibrating digging tool under various parameters and conditions of the lifting tool's operation, a four-row trail-behind root harvesting implement (Figure 7.2) was manufactured.

<div style="text-align:center">(a)   (b)</div>
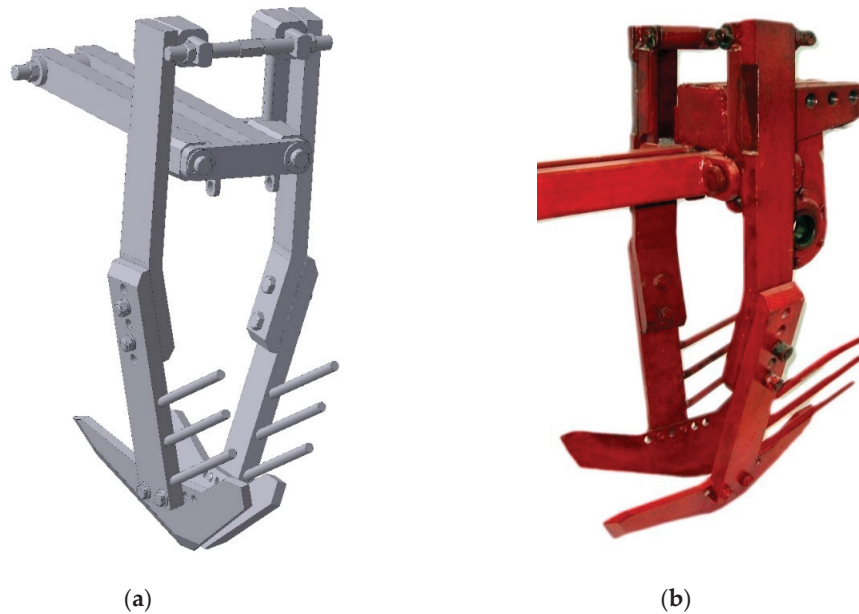
Figure 7.2. General view of vibrational lifting tool: (**a**)—3D-model in PC; (**b**)—photograph.

The experimental unit (Figure 7.3) comprised the main frame (1) supported by the axles with the rear wheels (2) and the front wheels (3), with the latter acting as feeler wheels. The unit was hitched to the tractor via the strain-gauge traction link. The front part of the frame (1) carried the vibrating digging tools (4) with the beater (5), the four-blade beater cleaner (6) was installed behind them. The vibrational lifting unit (4) comprised the crank drive (7) and the digging shares (8) with the beater shaft (5) positioned above them.

In order to determine the energy and force parameters, a strain-gauge traction link was attached to the unit, allowing for the simultaneous measurement of the horizontal and vertical components of the tractive effort applied to the towed apparatus. Foil strain gauges were installed on the shank (9) to measure the force of interaction between the share and the soil. All the tools of the experimental implement were driven by the power take-off shaft of the Class 1.4 tractor. An electric universal-joint recording dynamometer was installed between the tractor's power take-off shaft and the drive shaft of the experimental unit in order to determine the angular velocity, rotational torque and power transferred to the tools. The general appearance of the experimental implement is shown in Figure 7.4.

During the operation of the experimental unit, which occurred during the sugar beet harvesting season of the year 2016 near the village of Yaltushkov, Barsky district, Vinnytsia region (Ukraine), the digging share (8) was subjected to complex loads measured by the amount of bending of its shank (9) with the use of the affixed strain gauges. A track measuring wheel was attached to the frame to measure the experimental unit travel speed.

The cleaning and transporting tools of the root harvester were disconnected from the drive. Behind the vibrational lifting tools, a device was mounted, which reeled out canvas for collecting the sugar beet roots lifted from the soil in order to appraise the quality of their extraction in the process of in-field operation. The depth of running of the lifter in the soil was monitored by a measuring device.

The strain-gauge measurements required for assessing the energy characteristics of the vibrational lifting tools operating with the parameters under investigation were registered with the use of a strain-gauge station (mounted in a motorcar), which travelled during the experiments beside the experimental unit.
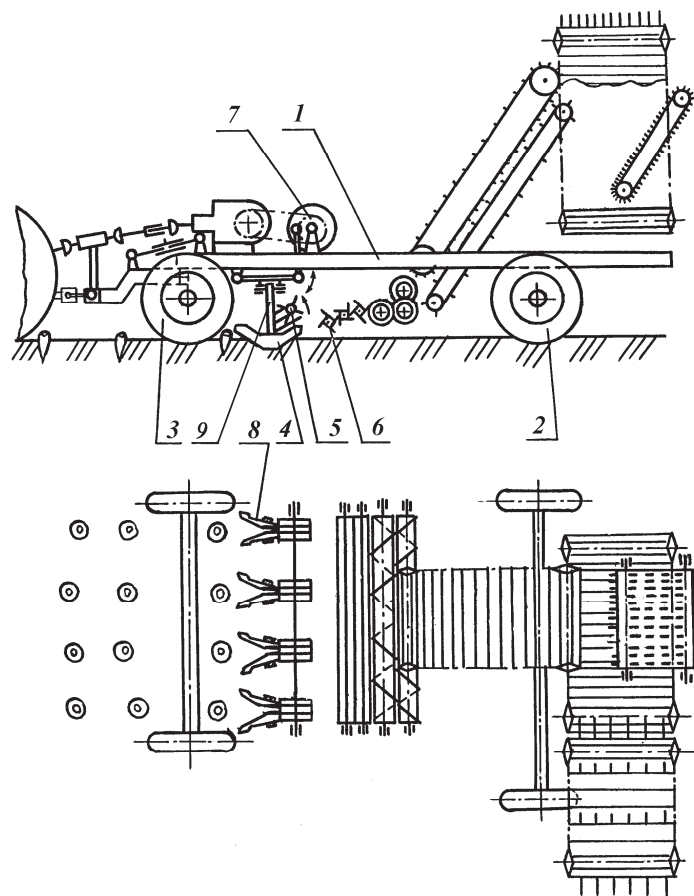
Figure 7.3. Schematic model of research prototype of root harvester with new vibrational lifting tools used for carrying out experimental investigations: 1—frame; 2—rear wheel axle; 3—front (feeler) wheel axle; 4—vibrational lifting tools; 5—beater; 6—four-blade beater cleaning machine; 7—crank drive of vibrational lifting device; 8—digging shares.

Figure 7.4. Experimental laboratory and field testing unit for investigating vibrational lifting tools.

During the development of the experimental unit, the principal requirement was to allow performing the laboratory and field experiment investigations in accordance with the specified programme and in full, implying that the design should allow changing the significant factors within sufficiently wide ranges by means of controlling and monitoring the factors.

Based on the completed analysis of the literary sources and the results of theoretical investigations, it was assumed that the rate of travel of the experimental unit would be set within the range of 1.3~2.55 m·s^{-1}, the depth of travel of the digging shares in the soil would vary within the range of 0.06~0.12 m, and the frequency of oscillation of the digging tool—8.5~20.3 Hz. In Figure 7.5, the vibrational lifting tools of the experimental unit are shown.

Figure 7.5. Vibrational lifting tools of experimental unit.

The agronomic indicators of the research plot of the field were determined in accordance with the conventional method and following the technique developed in UkrNDIPVT [35–37].

For the purpose of determining the indicators required for the agronomic appraisal, three accounted field plots with lengths of 20 m and widths of 2.7 m, i.e., six rows wide, were marked out lengthwise in the sugar beet plantation.

The rate of the weed infestation of the field plot was determined by using a rectangular frame measuring 90×111 cm (with an area of 1 m^2 in two adjacent rows and repositioning the frame five times along the diagonal of the field plot). The amount of weed was evaluated within the rectangular frame in total and separately in the area of one row within a 20 cm wide strip. The results of the counting were entered into the table of results.

Prior to starting the experimental investigations, the following mechanical and physical properties of the roots were determined in accordance with the technique of the research into the quality of operation of beet harvesters:

- Maximum diameter of root;
- Length of root;
- Mass of one root;
- Spacing between roots in row;
- Inter-row spacing;
- Height of root crown above soil surface;
- Offset of roots from conventional row centreline.

The statistical characteristics of the listed values were processed with the use of the standard formulae of the mathematical statistics:

Arithmetic mean $\bar{x}$:

$$\bar{x} = \frac{\sum x_i}{n} \tag{7.1}$$

where n—number of measurements.

Variance:

$$s^2 = \frac{\sum (x_i - \bar{x})^2}{n-1} \tag{7.2}$$

Root-mean-square deviation:

$$s = \sqrt{s^2} \tag{7.3}$$

Coefficient of variation:

$$v = \frac{s \cdot 100}{\bar{x}} \tag{7.4}$$

Absolute error of arithmetic mean:

$$s_{\overline{x}} = \frac{s}{\sqrt{n}} \qquad (7.5)$$

Confidence interval for arithmetic mean at a confidence coefficient of 0.95 and $(n - 1)$ degrees of freedom:

$$x = \overline{x} \pm t_{05}s_{\overline{x}} \qquad (7.6)$$

In each accounted field plot, all consecutive inter-row spaces within two working widths of a 12-row sowing unit were measured with the use of a tape measure. Measurements were made on the conventional row centrelines with a cumulative result.

It was decided to implement a multiple-factor experiment in the field testing of the root harvester. The main points of the multiple-factor experiment planning technique are provided in [38,39].

As is known, multiple-factor experiments offer many advantages, the most substantial of which are: a considerable reduction in the required number of experiments in comparison to the single-factor experiment; the possibility to generalise the research materials in the form of a mathematical model and conduct a statistical appraisal of them; the increased amount of information due to obtaining the data on the effect produced by the interaction between different factors.

On the basis of the theoretical investigations and the earlier testing of the machine, it has been established that the quality of the root extraction from the soil depended most of all on the following three factors: the rate of travel of the machine, the frequency of oscillation of the digging tools, the depth of running of the digging tools. The listed factors were independent of one another; therefore, it was possible to change their values independently.

Taking into account the results of the earlier testing of the root harvester and the theoretical investigations, the levels of variation of the factors were selected in such a way as to cover the range, within which the research into the machine operation was appropriate. When doing this, the following factors were taken into account: the range of the tractor's speed, within which the machine operation process is possible; the depth of root sitting in the soil; the amplitude and frequency of oscillation of the digging tool acceptable from the design point of view.

A comprehensive three-factor experiment to assess the effect that the above-mentioned factors had on the performance quality indicators was carried out by means of implementing the respective standard matrix.

The number of measurements for each experiment was determined in relation to its degree of variation, subject to the condition of obtaining the result with an error not exceeding 5% in accordance with the expression:

$$n_x = \frac{(tv)^2}{k^2} \tag{7.7}$$

where n_x—number of measurements necessary to provide for the required accuracy; t—table value of the Student criterion for the performed investigation; v—coefficient of variation of the parameter under investigation; k—experimental error ($k = 1.0 - 5.0\%$).

After substituting the data into the formula, it was found that the high adequacy of the obtained results and a nonsignificant error would be achieved in the case of five-time repetition of the tests.

The effect that the three factors have on the performance quality indicators can be described, following the results of processing of the data obtained in the experimental investigations, by regression equations in the form of a quadratic polynomial:

$$Y = b_0 + b_1 X_1 + b_{11} X_1^2 + b_2 X_2 + b_{22} X_2^2 + b_3 X_3 + b_{33} X_3^2 + b_{12} X_1 X_2 + b_{23} X_2 X_3 + b_{13} X_1 X_3, \tag{7.8}$$

where $b_0, b_1, b_2, b_3, b_{11}, b_{22}, b_{33}, b_{12}, b_{23}, b_{13}$—regression coefficients.

After implementing the experiment planning matrix with the use of the experimental unit, the problem of finding the coefficients of the variables and the effects of the interaction between them has to be solved. The problem can be solved with the use of the "STATISTIKA" software package for the PC by the Institute for Mechanisation and Electrification of Agriculture (IMESG).

Taking into account the fact that the matrix is orthogonal, the regression coefficients can also be determined independently of one another with the use of the following expression:

$$b_i = \frac{\sum_{j=1}^{N} x_{ij} y_i}{\sum_{j=1}^{N} x_{ij}^2} \tag{7.9}$$

where j—sequential number of the matrix column; x_{ij}—elements of the respective column.

The initial parameter в is determined and the specified levels of the factors are maintained with some errors. The statistical analysis of the equation at a preset probability of $\alpha = 0.95$ reveals whether the factor under consideration has a significant effect on the process. If the obtained absolute magnitude of coefficients b_i is greater than its error, the factor has an impact on the process. In the case where the factor has a negligible effect on the process, b_i is close to zero—i.e., the change in the process output y resulting from the change in the level of the respective factor is of the same

magnitude as the error in determining it. Such a factor can be excluded from the regression equation.

The statistical analysis of the regression equation, with the aim of determining the regression coefficients, was carried out in accordance with the technique described in [40]. The technique includes the following operations: finding the variance about the mean in the row; finding the mean variance in the repeatability of a single result throughout the experiment; finding the variance about the mean value of the process output (optimisation parameter); finding the variances of the regression equation coefficients; finding the errors and significance of the regression equation coefficients.

The regression equations obtained as a result of the factorial experiment correlate the levels of the factors with the process output in the area of the response surface for the response under investigation. At the same time, it is necessary to verify that the obtained equations describe the root lifting process with a sufficient degree of confidence. For this purpose, the dispersion is to be determined with the use of the formula [40]:

$$S^2_{ad} = \frac{\sum_{n=1}^{N}(\widetilde{y} - \overline{y})^2}{N - N'} \tag{7.10}$$

where $\widetilde{y}$—theoretical process output (after excluding the not significant regression coefficients from the equation); $\overline{y}$—process output realised in the matrix; N—N'—number of degrees of freedom, since only N' coefficients are determined with the use of the equation.

In this case, the Fisher criterion is determined by the following expression:

$$F_P = \frac{S^2_{ad}}{S^2_{\overline{y}}} \tag{7.11}$$

where $S^2_{\overline{y}}$—variance about the mean process output. The obtained value of the criterion is compared to the table value F_T. The criterion of adequacy of the regression equation is as follows:

$$F_T > F_P \tag{7.12}$$

In order to use the obtained equations expressed in terms of quadratic polynomials in the capacity of calculation formulae and for interpreting the experiment results, they have to be transformed into the form with denominate, i.e., decoded, quantities.

In order to carry out the strain-gauge measurements for the appraisal of vibrational lifting tools in terms of their energy characteristics, the mobile strain-gauge laboratory ChEK-1 (Figure 7.4) was used. The laboratory was capable of measuring and registering the force and velocity parameters and outputting immediately, after the completion of the tests, their mean values in six independent measuring channels.

Each force parameter measuring a channel was comprised of a strain-gauge transducer, a DC amplifier and an integrator. The measurement of the mean values of force parameters was carried out by way of integrating the amplified signals received from transducers over the duration of the experiment. In each measuring channel, its strain-gauge transducer was powered by a separate stabilised 12 VDC power supply source. Additionally, compact make-and-break devices or induction pulse transducers were provided for use in the velocity parameter transducers.

The strain-gauge system ChEK-1 facilitated measurements over discrete time intervals with durations of 7.5, 15, 30, 60, 120 and 240 s for the experiments. The measured values of the force and velocity parameters were output in the digital form.

7.3. Analysis of Results of Experimental Investigations on Effect That Lifter's Parameters and Operation Conditions Have on Operation Quality Indicators

The agricultural background of the experimental field plot was estimated as follows: type of soil—calcic chernozems, soil hardness—3.8~4.0 MPa; moisture content of soil—6~8% (soil elastic deformation coefficient $c = 1.5 \cdot 10^6$ N·m^{-3}); planting density of sugar beet roots—150.000 pcs·ha^{-1} (row spacing: 0.45 m; seeds distance in a row: 0.15 m); average dimensions of roots: diameter—0.094 m, length—0.24 m, weight—0.9 kg. These values are fully consistent with the agrotechnical standards of sugar beet cultivation and harvesting in Ukraine. Seeding of sugar beet (Beta Vulgaris cultivar) was carried out at the end of April, whereas experimental harvesting was conducted at the end of September. During the growing season, the weather conditions matched the average climatic conditions of the central part of Ukraine (Vinnytsia region): average temperature of 28 °C; rainfall not exceeding 320 mm. In accordance with the adopted programme of investigations, experiments for the investigation of the effect that the frequency of oscillation of the digging tools (X_1), depth of running of the digging tools (X_2) and the implement's translational motion velocity (X_3) have on the loss and damage of the roots were carried out. In the experiments, the ranges of variation for the kinematic parameters of the vibrational lifting tool were set on the basis of the accomplished theoretical investigations. The results are in Tables 7.1–7.5.

Table 7.1. Mass loss of sugar beet roots (%).

Velocity of Translation X_3 (m·s⁻¹)	Frequency of Oscillation X_1 (Hz)								
	8.5			15.7			20.3		
	Depth of Running in Soil X_2 (m)								
	0.06	0.09	0.12	0.06	0.09	0.12	0.06	0.09	0.12
1.3	2.7	2.7	1.9	1.7	0.5	0.4	0.4	0.1	0.2
	2.9	2.7	1.8	1.9	0.5	0.5	0.4	0.3	0.4
	2.8	2.8	1.9	1.7	0.4	0.5	0.3	0.4	0.4
	2.6	2.7	1.8	1.8	0.5	0.3	0.4	0.4	0.3
	2.7	2.6	1.8	1.8	0.6	0.4	0.4	0.5	0.4
1.75	2.9	1.8	2.0	1.9	0.4	0.6	0.3	0.4	0.5
	2.9	2.0	2.1	2.0	0.5	0.6	0.6	0.4	0.5
	3.0	1.9	2.6	1.9	0.5	0.7	0.5	0.5	0.6
	3.2	2.0	2.0	1.8	0.4	0.8	0.4	0.3	0.4
	2.8	1.9	2.4	1.9	0.5	0.7	0.3	0.4	0.5
(X_3)	(Y_1)								

Table 7.2. Mass of damaged sugar beet roots (%) (hardness of soil 4.0 MPa, moisture content of soil 6.0%).

Velocity of Translation X_3 (m·s⁻¹)	Frequency of Oscillation X_1 (Hz)								
	8.5			15.7			20.3		
	Depth of Running in Soil X_2 (m)								
	0.06	0.09	0.12	0.06	0.09	0.12	0.06	0.09	0.12
1.3	8.3	8.2	8.7	9.7	8.3	8.5	9.8	8.4	8.2
	8.3	8.2	8.4	9.4	8.3	8.2	9.9	8.4	8.0
	8.4	8.1	8.7	9.8	8.3	8.5	9.8	8.2	8.2
	8.2	8.3	8.6	9.8	8.1	8.4	9.7	8.3	8.4
	8.2	8.0	8.7	9.7	8.2	8.5	9.8	8.4	8.1
1.75	8.9	8.2	9.2	9.8	8.3	8.9	9.2	9.0	8.9
	9.2	8.1	9.0	9.4	8.4	8.8	9.2	8.9	8.7
	8.9	8.2	8.7	9.3	8.3	8.9	9.0	9.2	8.8
	8.7	8.3	8.9	9.4	8.3	9.0	9.3	9.1	8.9
	8.9	8.0	9.1	9.2	8.2	8.9	9.2	9.0	9.1
(X_3)	(Y_2)								

Table 7.3. Mass of damaged sugar beet roots (%) (hardness of soil 2.0 MPa, moisture content of soil 18.0%).

Velocity of Translation X_3 (m·s^{-1})	Frequency of Oscillation X_1 (Hz)								
	8.5			15.7			20.3		
	Depth of Running in Soil X_2 (m)								
	0.06	0.09	0.12	0.06	0.09	0.12	0.06	0.09	0.12
	4.9	3.3	3.8	4.3	3.8	4.1	4.2	4.0	4.3
	4.9	3.1	3.6	4.2	3.8	4.3	4.0	4.6	4.4
1.3	4.6	2.9	3.8	4.1	3.6	4.1	4.4	4.1	4.1
	4.7	3.0	3.8	4.1	3.7	4.2	4.2	4.0	4.3
	4.9	3.2	3.7	4.6	3.8	4.6	4.2	4.2	4.6
	5.1	3.0	4.7	5.1	3.4	4.7	4.6	4.7	4.8
	5.0	3.6	4.8	5.3	3.5	4.7	4.5	4.2	5.0
1.75	5.0	3.2	4.8	5.1	3.4	4.8	4.7	4.7	4.9
	5.1	3.4	4.7	5.2	3.4	4.6	4.7	4.8	5.0
	5.1	3.1	4.8	5.2	3.4	4.8	4.6	4.3	5.0
(X_3)				(Y_3)					

Table 7.4. Mass loss of sugar beet roots (%) at oscillation frequency of 8.5 Hz (hardness of soil 3.8 MPa, moisture content of soil 8.0%).

Velocity of Translation X_1 (m·s^{-1})	Depth of Running in Soil X_2 (m)			
	0.06	0.08	0.10	0.12
	3.0	1.0	0.0	0.0
	3.0	1.5	0.0	0.5
1.4	2.9	1.0	1.0	1.0
	3.1	1.2	0.0	0.0
	3.0	1.3	1.0	1.0
	5.0	2.0	0.0	0.0
	4.9	2.5	1.0	0.0
1.75	4.8	2.0	1.0	1.0
	4.9	2.0	0.0	0.0
	5.0	2.0	1.0	0.5
(X_1)		(Y_4)		

Table 7.5. Mass loss of sugar beet roots (%) at oscillation frequency of 8.5 Hz (hardness of soil 2.0 MPa, moisture content of soil 20.0%).

Velocity of Translation X_1 (m·s^{-1})	Depth of Running in Soil X_2 (m)			
	0.06	0.08	0.10	0.12
	2.0	2.0	2.0	0.0
	2.0	2.5	2.1	1.0
1.4	1.8	2.0	2.0	1.0
	1.5	2.3	2.3	1.2
	2.0	2.0	2.0	1.0
	4.0	3.0	0.0	0.0
	3.5	3.0	1.0	0.0
1.65	4.2	3.1	1.0	1.5
	4.0	3.2	1.5	1.2
	4.2	3.0	0.0	1.0
(X_1)		(Y_5)		

Based on the results of the accomplished experimental investigations, it has been established that with the increase in the digging tool oscillation frequency the root loss rate goes down, but at the same time the root damage rate slightly increases in the majority of cases.

The regression equation for the relation between the root loss rate (Y_1) and the digging tool oscillation frequency (X_1), depth of digging tool running in the soil (X_2) and velocity of translation (X_3) appears as follows:

$$Y_1 = 12.751 - 0.365X_1 - 175.545X_2 + 0.004X_1^2 + 0.912X_1X_2 \\ - + 884.748X_2^2 - 5.551X_2X_3 + 0.216X_3^2, \tag{7.13}$$

at a squared coefficient of correlation (coefficient of multiple determination) of $R^2 = 0.789$, a coefficient of multiple correlation of $R = 0.888$ and a standard error of $S_r = 0.508$. For this type of function, the nonsignificant coefficients are the regression coefficients of the factors X_3 and X_1X_3.

At the computing stage, the application software "STATISTICA 6" was used. In the environment of the software, based on the obtained model, the response surfaces for the response of the root loss rate to the digging tool's oscillation frequency and depth of running in the soil at the lifter translational motion velocity values of 1.3, 1.75, 2.1, 2.55 m·s^{-1} were plotted and their two-dimensional sections were obtained (Figures 7.6–7.13).
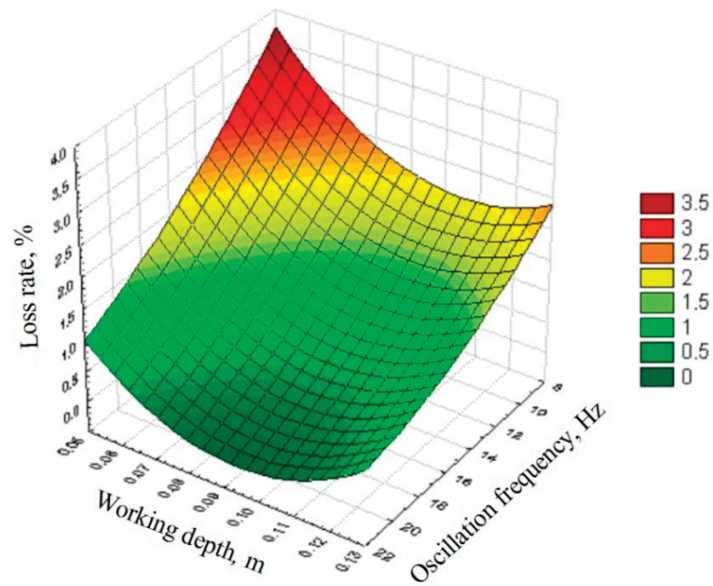
Figure 7.6. Quadratic response surface of root loss rate response to digging tool oscillation frequency and depth of its running in soil (at lifter translational motion velocity of 1.75 m·s^{-1}, soil hardness of 4.0 MPa, soil moisture content of 8.0 %, $c = 1.5 \cdot 10^6$ N·m^{-3}).
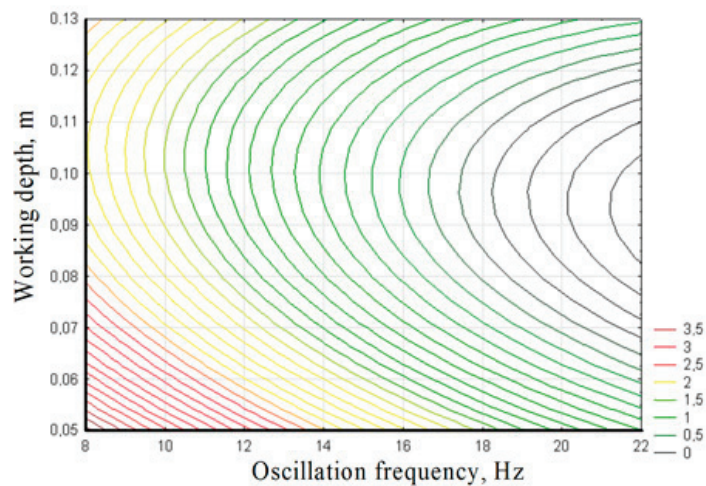
Figure 7.7. Two-dimensional sections of quadratic response surface of root loss rate response to digging tool oscillation frequency and depth of its running in soil (at lifter translational motion velocity of 1.75 m·s^{-1}, soil hardness of 4.0 MPa, soil moisture content of 8.0%, $c = 1.5 \cdot 10^6$ N·m^{-3}).
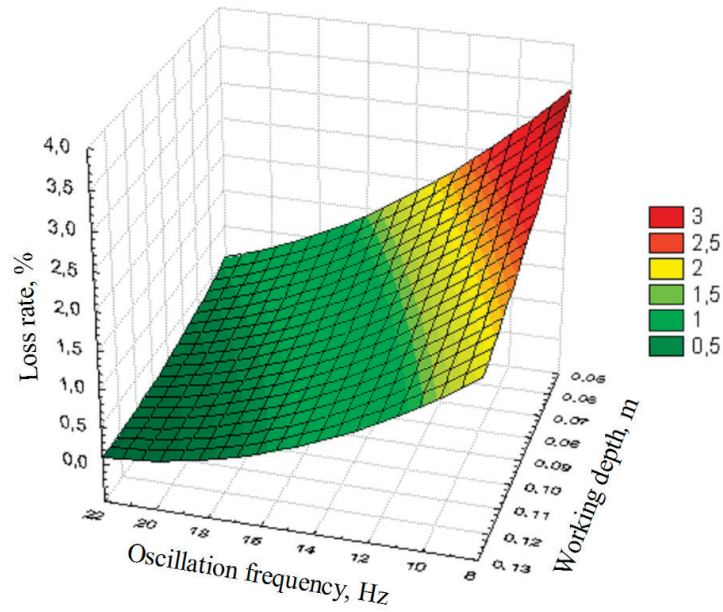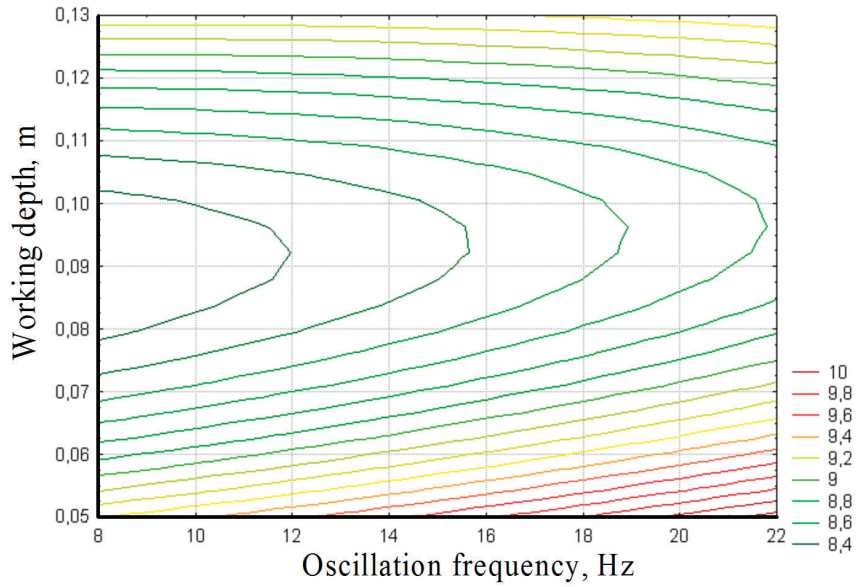
Figure 7.8. Quadratic response surface of root loss rate response to digging tool oscillation frequency and depth of its running in soil (at lifter translational motion velocity of 1.3 m·s^{-1}, soil hardness of 4.0 MPa, soil moisture content of 8.0%, $c = 1.5 \cdot 10^6$ N·m^{-3}).
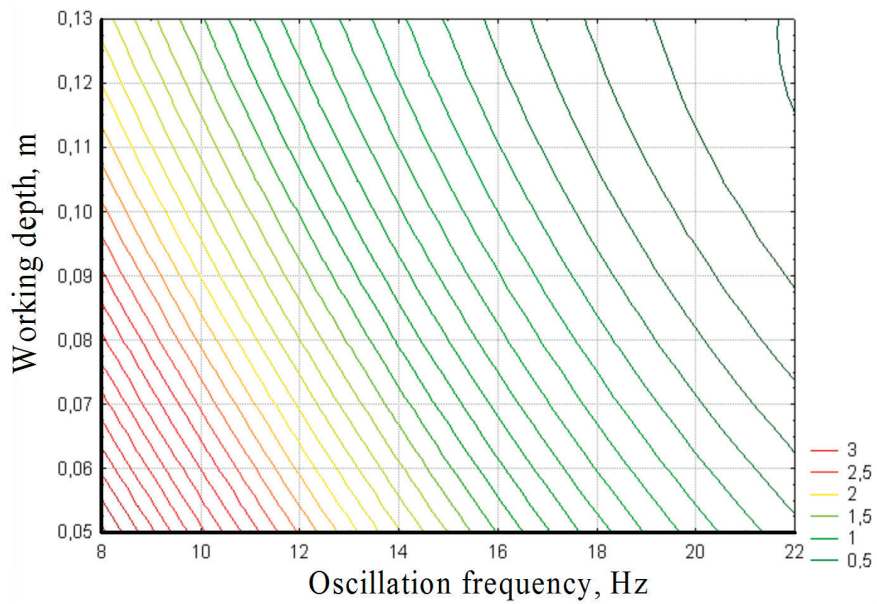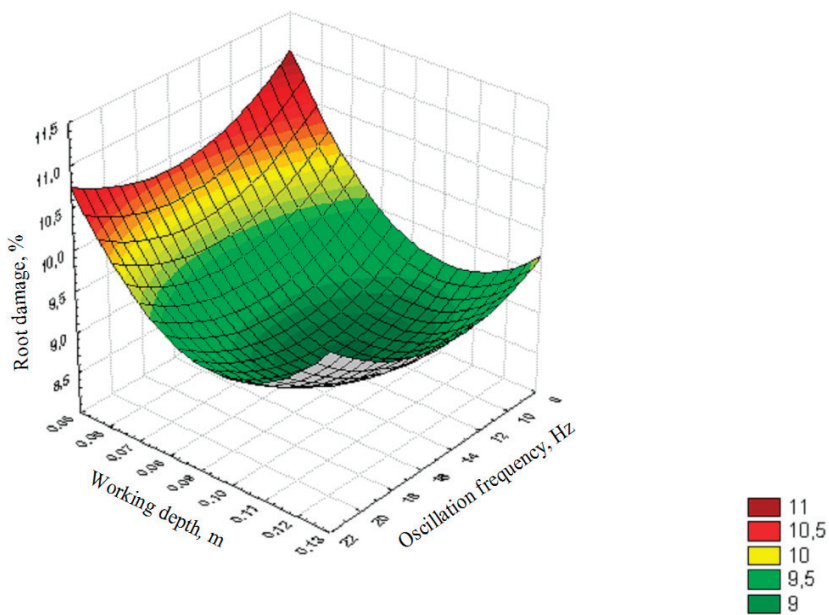

Figure 7.9. Two-dimensional sections of quadratic response surface of root loss rate response to digging tool oscillation frequency and depth of its running in soil (at lifter translational motion velocity of 1.3 m·s^{-1}, soil hardness of 4.0 MPa, soil moisture content of 8.0%, $c = 1.5 \cdot 10^6$ N·m^{-3}).
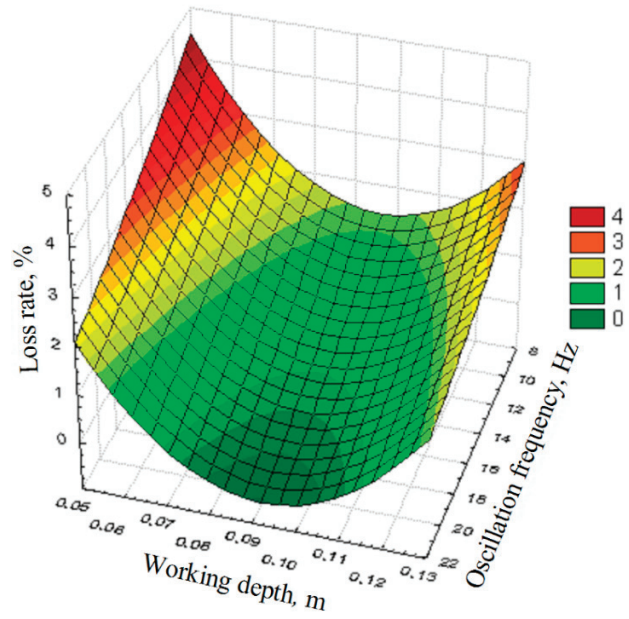
Figure 7.10. Quadratic response surface of root loss rate response to digging tool oscillation frequency and depth of its running in soil (at lifter translational motion velocity of 2.1 m·s^{-1}, soil hardness of 4.0 MPa, soil moisture content of 8.0%, $c = 1.5 \cdot 10^6$ N·m^{-3}).
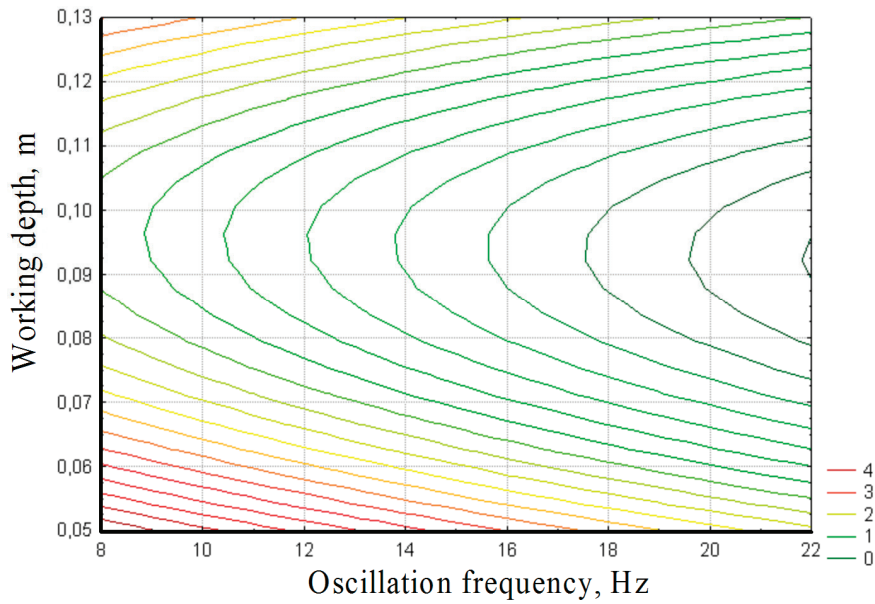
Figure 7.11. Two-dimensional sections of quadratic response surface of root loss rate response to digging tool oscillation frequency and depth of its running in soil (at lifter translational motion velocity of 2.1 m·s^{-1}, soil hardness of 4.0 MPa, soil moisture content of 8.0%, $c = 1.5 \cdot 10^6$ N·m^{-3}).
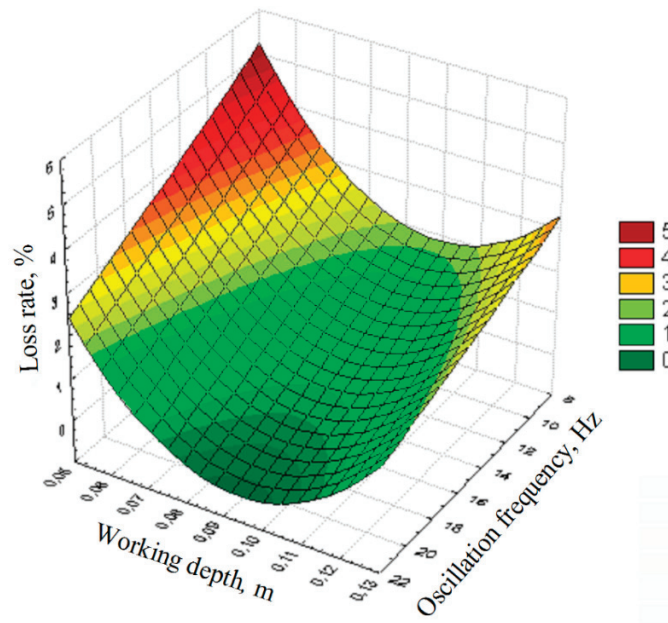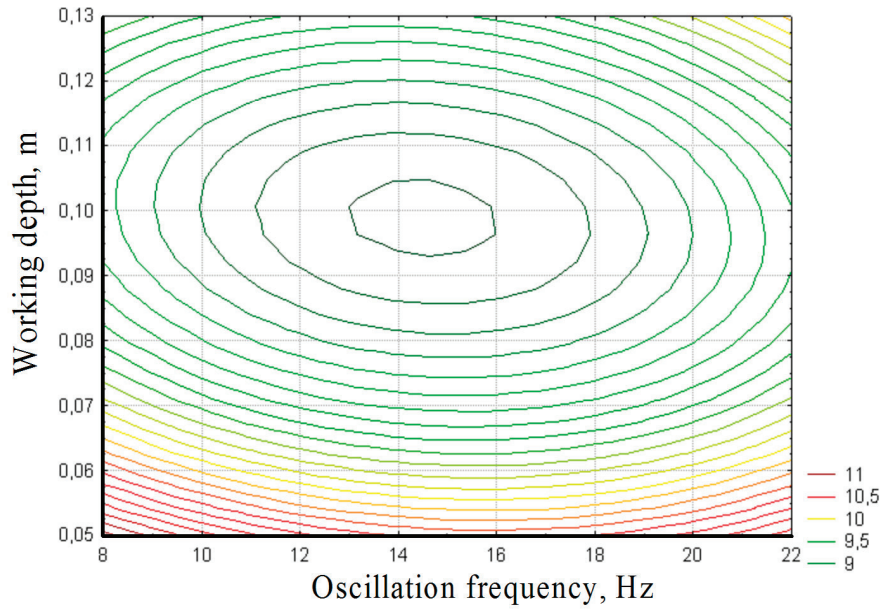
Figure 7.12. Quadratic response surface of root loss rate response to digging tool oscillation frequency and depth of its running in soil (at lifter translational motion velocity of 2.55 m·s^{-1}, soil hardness of 4.0 MPa, soil moisture content of 8.0%, $c = 1.5 \cdot 10^6$ N·m^{-3}).
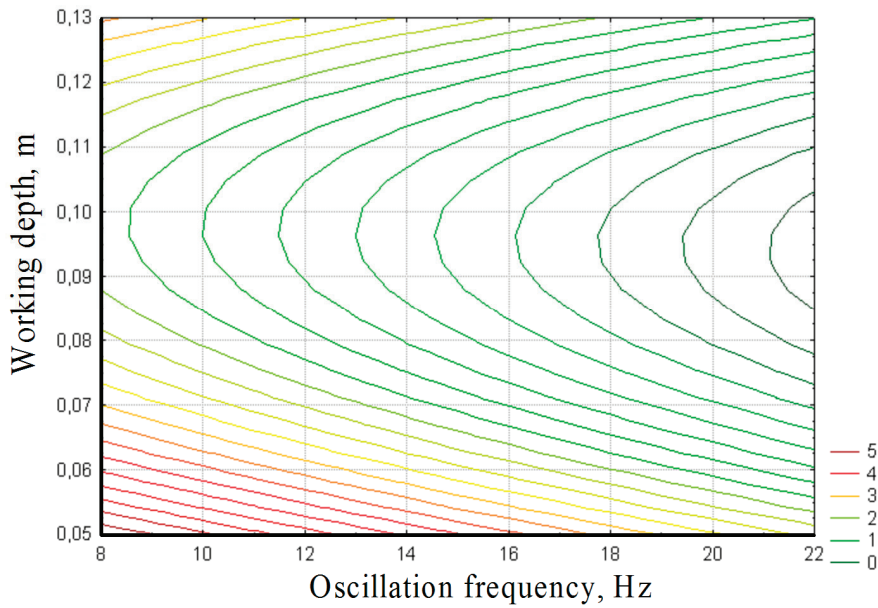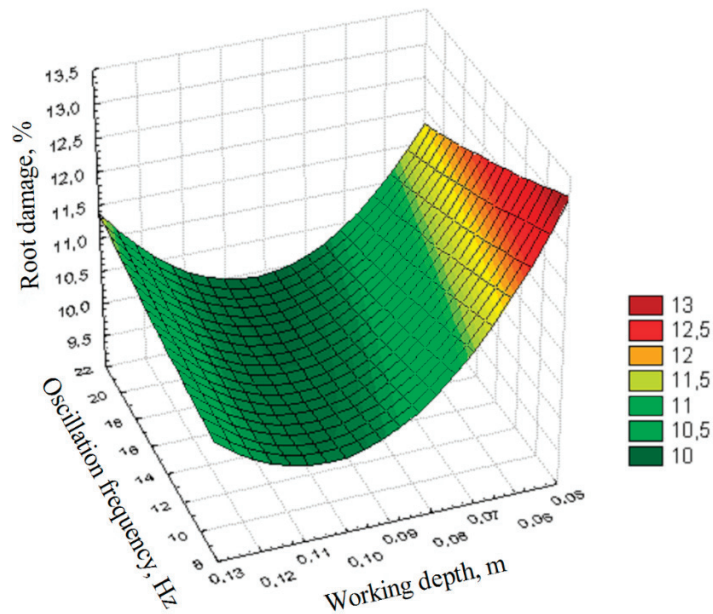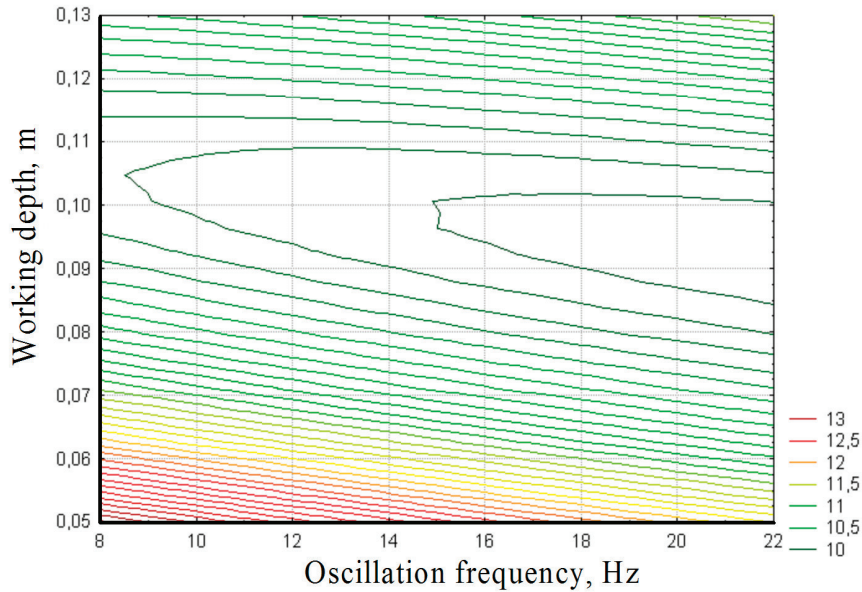

Figure 7.13. Two-dimensional sections of quadratic response surface of root loss rate response to digging tool oscillation frequency and depth of its running in soil (at lifter translational motion velocity of 2.55 m·s^{-1}, soil hardness of 4.0 MPa, soil moisture content of 8.0%, $c = 1.5 \cdot 10^6$ N·m^{-3}).

It follows from the presented relations that the loss of roots decreases when the digging tool oscillation frequency becomes greater, but the increase in the velocity of translation results in the greater loss of roots.

Moreover, at lifter translational motion velocities of 1.3~2.55 m·s^{-1}, minimum root loss is observed when the lifter runs in the soil at a depth of 0.09 Tm; at smaller and greater depths of lifter running, the loss rates increase.

This can be explained by the fact that at lifter running depths of less than 0.09 m, the loss rate increases on account of the roots not extracted at all, while running deeper than 0.09 m results in breaking off of the tail parts of the roots. Moreover, the described trend becomes more pronounced at greater velocities of the lifter's translational motion and lower frequencies of the digging tool's oscillation.

For example, at a lifter translational motion velocity of 1.3 m·s^{-1}, the mass percentage of the lost roots is within the range of 0.3~2.9%; at a velocity of 1.75 m·s^{-1}—within the range of 0.3~3.0%; at a velocity of 2.1 m·s^{-1}—within the range of 0.3~3.5%; at a velocity of 2.55 m·s^{-1}—within the range of 0.4~4.5%; moreover, the lower parts of the ranges correspond to a digging tool oscillation frequency of 20.3 Hz; the upper ones—a frequency of 8.5 Hz.

Hence, a digging tool oscillation frequency of 8.5 Hz is not compliant with the agronomic requirements with regard to the root losses (rates of up to 1.5% are acceptable), while the frequencies 15.7 and 20.3 Hz meet them.

The obtained experimental data have once again proved the theoretical conclusion about the existence of a minimum acceptable frequency of oscillation subject to the condition that each root must be captured by the digging tool; otherwise, either nonextraction of the root or the breaking off of its tail part takes place, as is observed at an oscillation frequency of 8.5 Hz.

It ought to be noted that in the case of lifting the roots by passive share lifters at a soil moisture content of 14~18%, the tail parts of the roots are broken off at a rate of 30~40% [31].

Further, the regression equation for the relation between the root damage rate (Y_2) and the digging tool oscillation frequency (X_1), depth of digging tool running in the soil (X_2), and translational motion velocity (X_3) appear as follows:

$$Y_2 = 15.427 + 0.121X_1 - 137.179X_2 - 2.69X_3 - 0.06X_1X_3 + 754.598X_2^2 - 5.691X_2X_3 + 1.491X_3^2 \quad (7.14)$$

at $R^2 = 0.822$; $R = 0.907$; $S_r = 0.442$. For this type of function, the nonsignificant coefficients are the regression coefficients of the factors X_1^2 and X_1X_2.

On the basis of the obtained model, the response surfaces for the response of the root damage rate to the digging tool's oscillation frequency and depth of its running in the soil at lifter translational motion velocity values of 1.3, 1.75, 2.1, and 2.55 m·s^{-1} were plotted and their two-dimensional sections were obtained (Figures 7.14–7.21).

It follows from the presented relations that there is no constant trend in the change in the root damage rate when digging tool oscillation frequency varies within the range of 8.5 to 20.3 Hz; nevertheless, it can be stated that the effect the frequency change has on the root damage rate is insignificant. The minimum root damage rate is observed when the digging tool runs in the soil at depths of 0.09~0.10 m. When the lifter translational motion velocity increases, the rate of root damage increases as well. For example, at the lifter translational motion velocity of 1.3 m·s^{-1}, the mass percentage of the damaged roots is within the range of 8.0~9.8%; at a velocity of 1.75 m·s^{-1}—8.1~ 9.8%; at a velocity of 2.1 m·s^{-1}—8.2~10.3%; at a velocity of 2.55 m·s^{-1}—10.5~12.8%.

Hence, velocities of the lifter's translational motion within the range of 1.3~2.1 m·s^{-1} are compliant with the agronomic requirements with regard to the root damage (rates up to 10% are acceptable), while a velocity of 2.55 m·s^{-1} does not meet the requirements (damage rates of up to 13%).
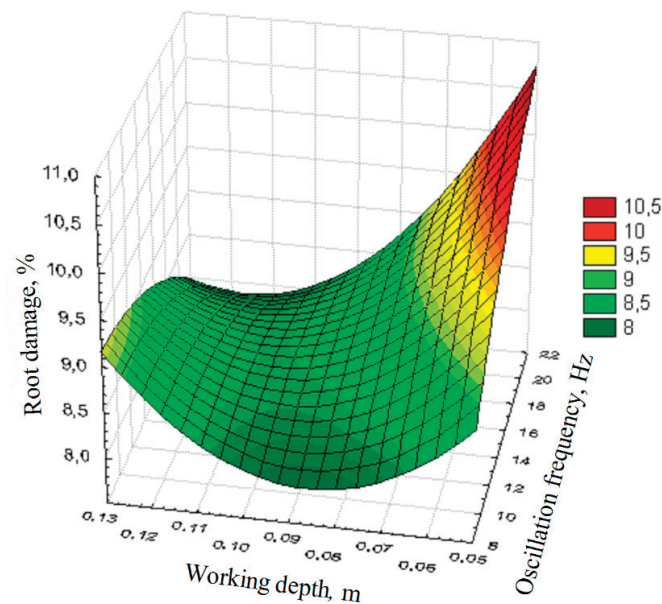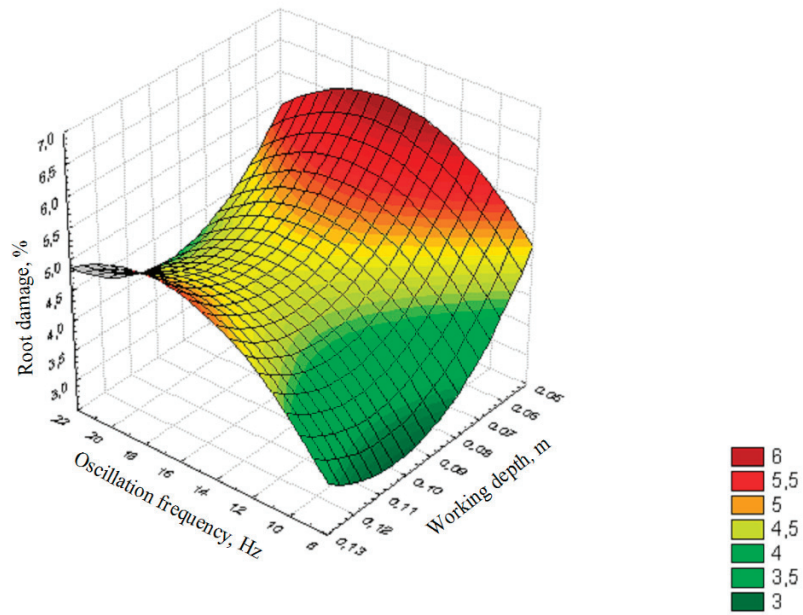

Figure 7.14. Quadratic response surface of root damage rate response to digging tool oscillation frequency and depth of its running in soil (at lifter translational motion velocity of 1.3 m·s^{-1}, soil hardness of 4.0 MPa, moisture content of 8.0%).
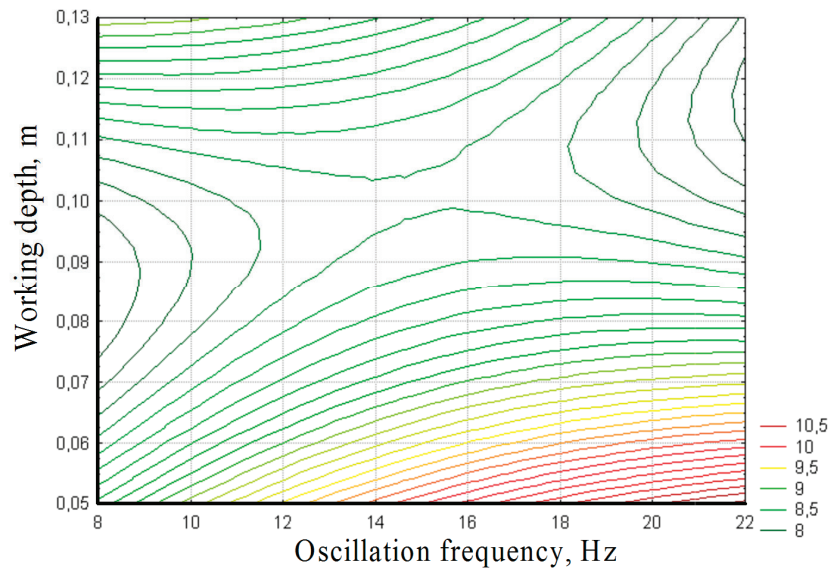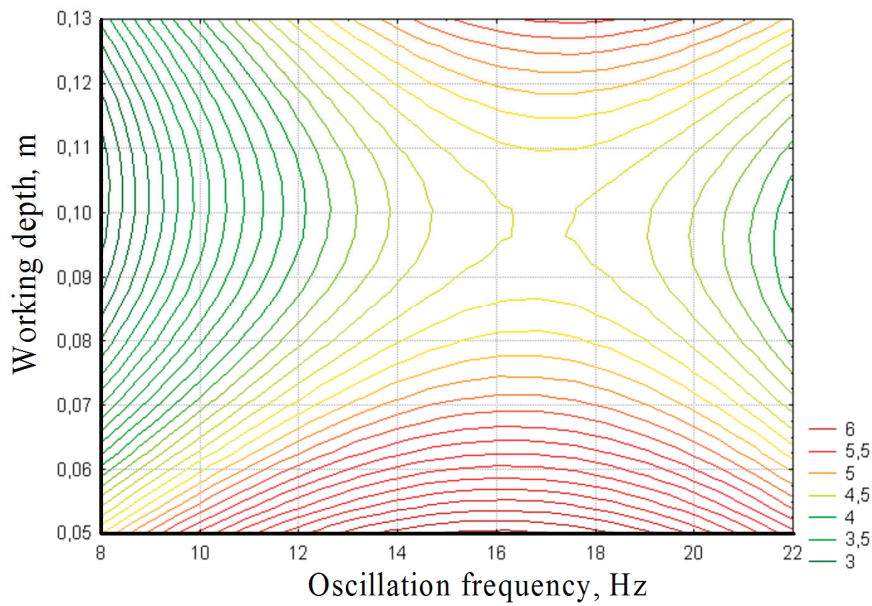
Figure 7.15. Two-dimensional sections of quadratic response surface of root damage rate response to digging tool oscillation frequency and depth of its running in soil (at lifter translational motion velocity of 1.3 m·s^{-1}, soil hardness of 4.0 MPa, moisture content of 8.0%).
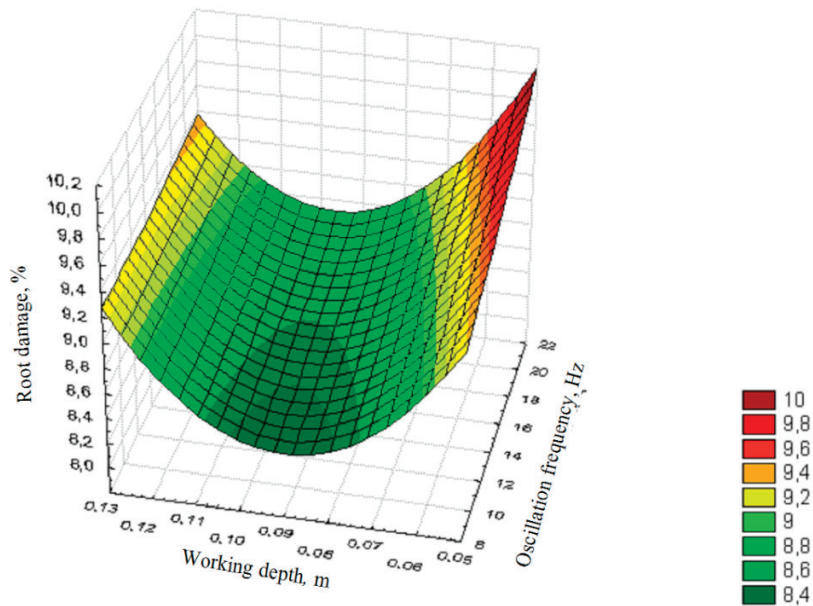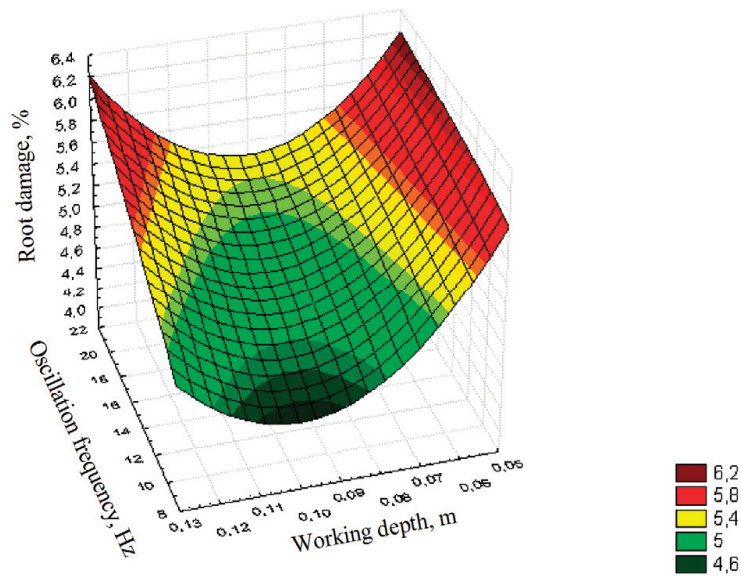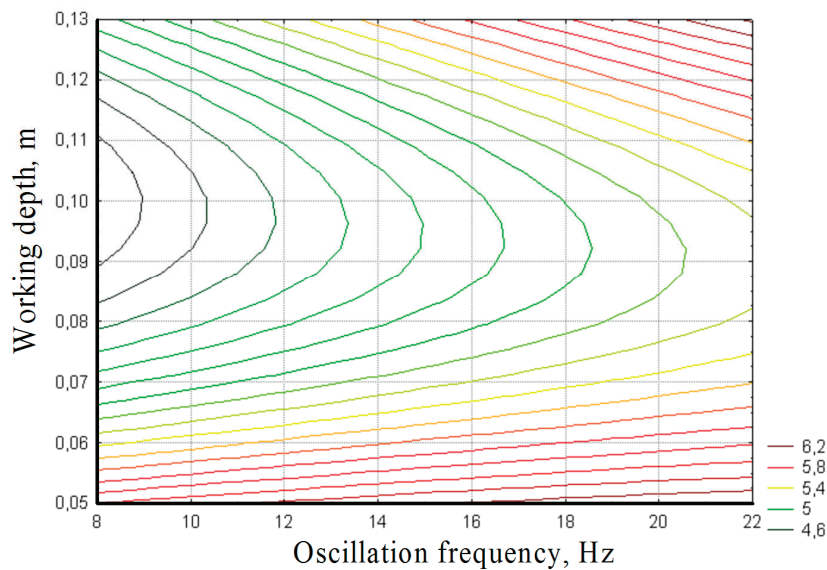

Figure 7.16. Quadratic response surface of root damage rate response to digging tool oscillation frequency and depth of its running in soil (at lifter translational motion velocity of 1.75 m·s^{-1}, soil hardness of 4.0 MPa, moisture content of 8.0%).

Figure 7.17. Two-dimensional sections of quadratic response surface of root damage rate response to digging tool oscillation frequency and depth of its running in soil (at lifter translational motion velocity of 1.75 m·s^{-1}, soil hardness of 4.0 MPa, moisture content of 8.0%).

Figure 7.18. Quadratic response surface of root damage rate response to digging tool oscillation frequency and depth of its running in soil (at lifter translational motion velocity of 2.1 m·s^{-1}, soil hardness of 4.0 MPa, moisture content of 8.0%).

Figure 7.19. Two-dimensional sections of quadratic response surface of root damage rate response to digging tool oscillation frequency and depth of its running in soil (at lifter translational motion velocity of 2.1 m·s^{-1}, soil hardness of 4.0 MPa, moisture content of 8.0%).

Figure 7.20. Quadratic response surface of root damage rate response to digging tool oscillation frequency and depth of its running in soil (at lifter translational motion velocity of 2.55 m·s^{-1}, soil hardness of 4.0 MPa, moisture content of 8.0%).

Figure 7.21. Two-dimensional sections of quadratic response surface of root damage rate response to digging tool oscillation frequency and depth of its running in soil (at lifter translational motion velocity of 2.55 m·s^{-1}, soil hardness of 4.0 MPa, moisture content of 8.0%).

The above investigations on the root damage in harvesting were carried out in the soil with a hardness of 4.0 MPa and moisture content of 8.0%. Similar research into the rates of root damage was undertaken at a soil hardness of 2.0 MPa and a soil moisture content of 18.0% ($c = 0.14 \cdot 10^6$ N·m^{-3}), which is rather typical of the sugar beet harvesting in Polesye (woodlands) and the Forest-Steppe zone (wood and grass lands) of Ukraine.

The results of said research are described by the following regression equation:

$$Y_3 = 12.2076 - 167.138X_2 - 1.577X_3 - 0.004X_1^2 + 1.083X_1X_2 + 0.04X_1X_3 + 802.733X_2^2 + 0.481X_3^2 \quad (7.15)$$

at $R^2 = 0.648$; $R = 0.805$; $S_r = 0.483$. For this type of function, the nonsignificant coefficients are the regression coefficients of the factors X_1 and X_1X_2.

On the basis of the obtained model, the response surfaces for the response of the root damage rate to the digging tool oscillation frequency and depth of its running in the soil at lifter translational motion velocity values of 1.3, 1.75, 2.1, and 2.55 m·s^{-1} were plotted and their two-dimensional sections were obtained (Figures 7.22–7.29).
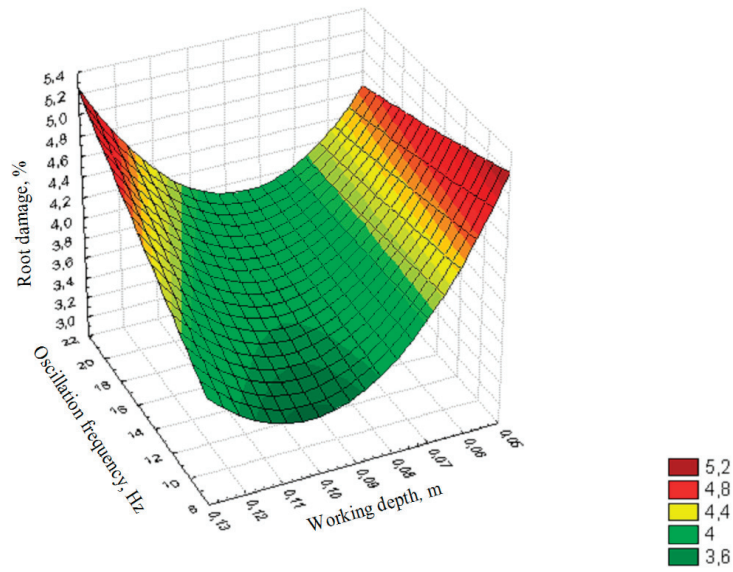
Figure 7.22. Quadratic response surface of root damage rate response to digging tool oscillation frequency and depth of its running in soil (at lifter translational motion velocity of 1.3 m·s^{-1}, soil hardness of 2.0 MPa, moisture content of 18.0%).
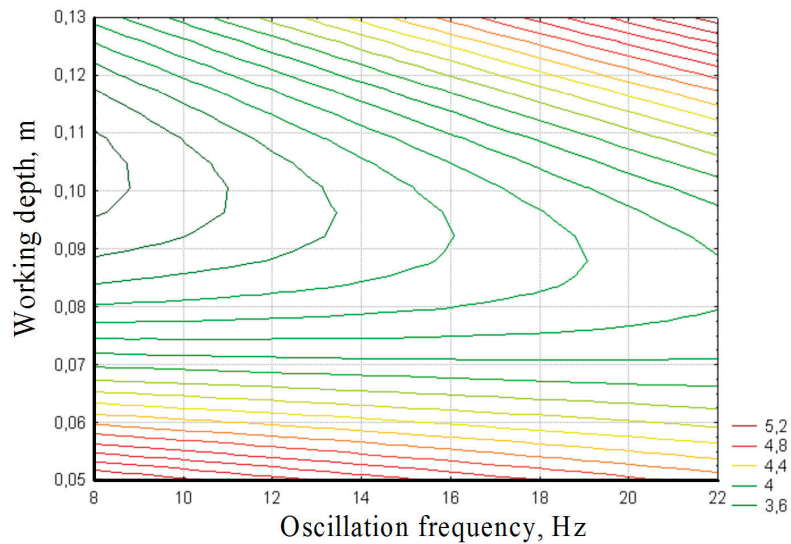
Figure 7.23. Two-dimensional sections of quadratic response surface of root damage rate response to digging tool oscillation frequency and depth of its running in soil (at lifter translational motion velocity of 1.3 m·s^{-1}, soil hardness of 2.0 MPa, moisture content of 18.0%).
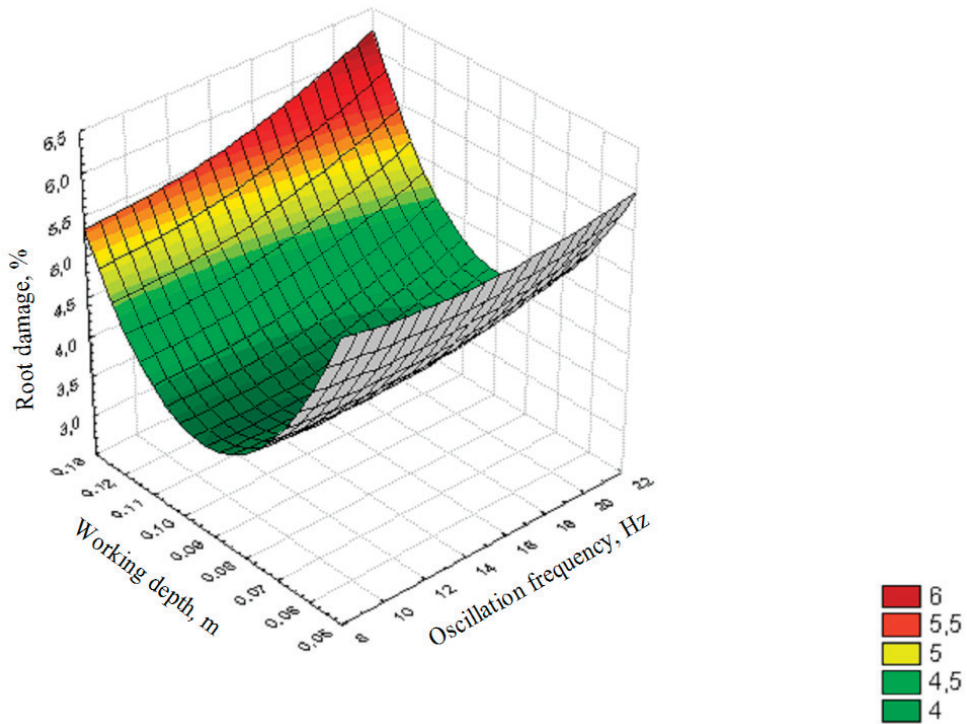
Figure 7.24. Quadratic response surface of root damage rate response to digging tool oscillation frequency and depth of its running in soil (at lifter translational motion velocity of 1.75 m·s^{-1}, soil hardness of 2.0 MPa, moisture content of 18.0%).
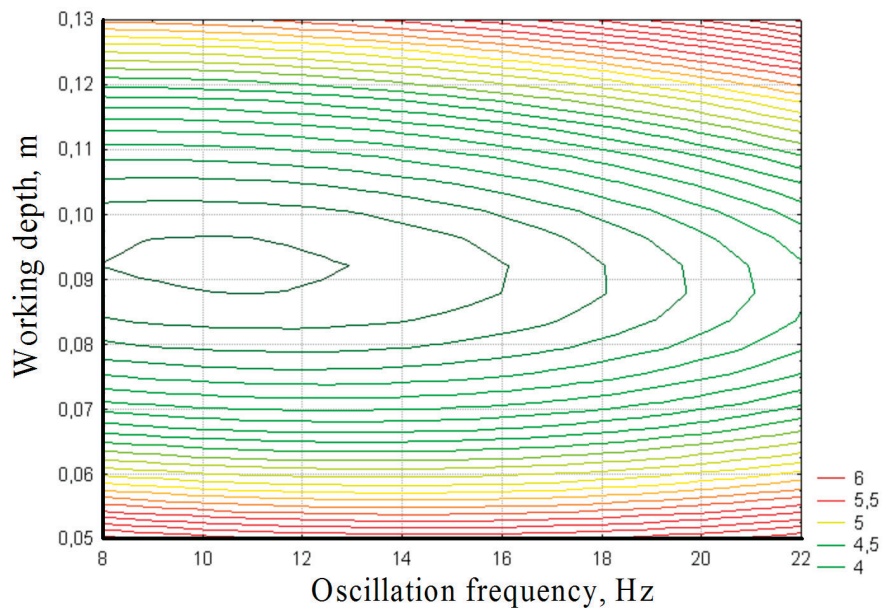
Figure 7.25. Two-dimensional sections of quadratic response surface of root damage rate response to digging tool oscillation frequency and depth of its running in soil (at lifter translational motion velocity of 1.75 m·s^{-1}, soil hardness of 2.0 MPa, moisture content of 18.0%).

Figure 7.26. Quadratic response surface of root damage rate response to digging tool oscillation frequency and depth of its running in soil (at lifter translational motion velocity of 2.1 m·s^{-1}, soil hardness of 2.0 MPa, moisture content of 18.0%).

Figure 7.27. Two-dimensional sections of quadratic response surface of root damage rate response to digging tool oscillation frequency and depth of its running in soil (at lifter translational motion velocity of 2.1 m·s^{-1}, soil hardness of 2.0 MPa, moisture content of 18.0%).

Figure 7.28. Quadratic response surface of root damage rate response to digging tool oscillation frequency and depth of its running in soil (at lifter translational motion velocity of 2.55 m·s^{-1}, soil hardness of 2.0 MPa, moisture content of 18.0%).

Figure 7.29. Two-dimensional sections of quadratic response surface of root damage rate response to digging tool oscillation frequency and depth of its running in soil (at lifter translational motion velocity of 2.55 m·s^{-1}, soil hardness of 2.0 MPa, moisture content of 18.0%).

As can be seen in the presented graphs (Figures 7.22–7.29), the mass percentage of the damaged roots increases within an insignificant range when the digging tool oscillation frequency and the lifter translational motion velocity go up—i.e., said parameters have no material effect on the root damage rate; additionally, in most

instances, the root damage rate reaches its minimum at a digging tool running depth of 0.09 m.

Thus, the experiments have proved that the range of the digging tool oscillation frequency of 8.5~20.3 Hz and the range of the lifter translational motion velocity of 1.3~2.55 m·s^{-1} at a soil hardness of 2.0 MPa and its moisture content of 18.0% meet the agronomic requirements with regard to the mass percentage of the damaged roots, as within these ranges said indicator stays within the range of 3.0~6.2%

It also ought to be noted that the mass of the damaged roots substantially depends on the hardness and moisture content of the soil. For example, at a hardness of 2 MPa and a moisture content of 18%, it stays within the range of 3.0~6.2%, while a hardness of 4 MPa and a moisture content of 8% shift it to the range of 8.0~13.0%

According to [41], in the case of lifting roots by passive share lifters, the amount of severely damaged roots equals 15~22%; contamination of the pile by soil amounts to 12~16%, while on dry (moisture content of 8~12%) and hard soils—30~40%.

Another important issue that needs investigation is the relation between the root loss rate and the soil hardness and moisture content in the vibrational lifting. For this purpose, the root harvester has to be tested at a digging tool oscillation frequency of 8.5 Hz, which is the frequency that causes the highest root loss rates, as shown above. Such an approach allows assessing the effect of the soil's hardness and moisture content on the root loss rate in the case of greater values of the loss rate. Based on the described set-up, the research has been carried out into the sugar beet root loss against the digging tool translational motion velocity (X_1) and depth of running (X_2) in different operation conditions.

The following regression equation has been obtained for a soil hardness of 3.8 MPa and a soil moisture content of 8.0%:

$$Y_4 = 0.40086 + 9.242X_1 - 131.572X_2 - 71.088X_1X_2 + 1015.235X_2^2 \qquad (7.16)$$

at $R^2 = 0.950$; $R = 0.975$; $S_r = 0.454$.

On the basis of the obtained model, the response surface (Figure 7.30) and its two-dimensional sections (Figure 7.31) have been generated.

As can be seen from the obtained graphs (Figures 7.30 and 7.31), the increase in the lifter translational motion velocity is accompanied by the growth of the losses; the increase in the depth of running in the soil results in their reduction. The reason for this is that the greater the lifter translational motion velocity is, the fewer the roots captured by the digging tool (as the translational velocity rises, the 8.5 Hz frequency progressively allows for less capturing) and the more roots remain or the more are broken at their tail parts. Obviously, the smaller the depth of the lifter running in the soil is, the higher the level, where the root tail part is broken off, is and/or the greater the number of the roots that are not extracted at all is, and, consequently, the higher

the observed losses are. When the lifter runs at a greater depth, the importance of the translational motion velocity for the root loss rate decreases, as the tail parts are broken off at a greater depth; therefore, the loss percentage becomes smaller and depends to a lesser extent on the lifter translational motion velocity. The losses are minimal at a depth of running in the soil of 0.11 m.
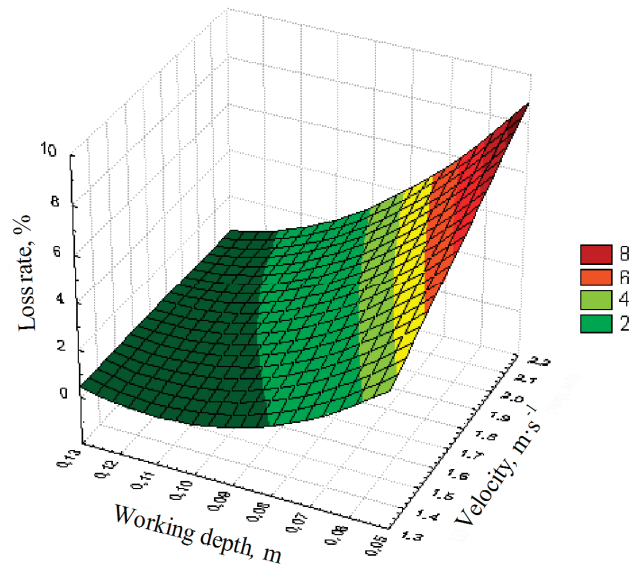
Figure 7.30. Quadratic response surface of root loss rate response to lifter translational motion velocity and depth of its running in soil (at digging tool oscillation frequency of 8.5 Hz, soil hardness of 3.8 MPa, soil moisture content of 8.0%).
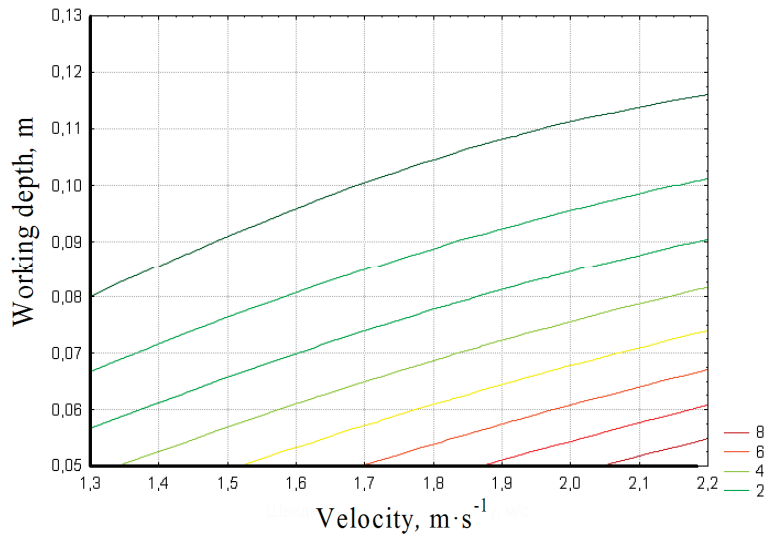
Figure 7.31. Two-dimensional sections of quadratic response surface of root loss rate response to lifter translational motion velocity and depth of its running in soil (at digging tool oscillation frequency of 8.5 Hz, soil hardness of 3.8 MPa, soil moisture content of 8.0%).

For the soil hardness of 2.0 MPa and moisture content of 20.0% the regression equation appears as follows:

$$Y_5 = -7.75 + 231.582X_2 + 3.301X_1^2 - 94.891X_1X_2 - 682.32X_2^2 \qquad (7.17)$$

The graphical representation of the root losses against the lifter translational motion velocity and the depth of its running in the soil under such conditions is given in Figures 7.32 and 7.33, respectively.

As can be seen in the presented graphs (Figures 7.32 and 7.33), at depths of the digging tool running in the soil within the range of 0.06~0.09 m, the loss rate rises together with the increase in the lifter translational motion velocity, while at the depths of running within the range of 0.10~0.12 m it shows no essential dependence on the velocity. The reasons for this are the same as in the preceding case. Additionally, as the depth of running of the digging tool in the soil increases, the losses decrease and reach their minimum at a depth of the digging tool running in the soil of 0.12 m.

As is evident from the obtained experimental data (Tables 6.4 and 6.5) as well as the graphs (Figures 7.31–7.33), in the soil (calcic chernozems) with a hardness of 3.8 MPa and a moisture content of 8%, the loss rate is 0.3~6.2%; in the soil (calcic chernozems) with a hardness of 2.0 MPa and a moisture content of 20%, the root loss rate is within the range of 0.3~ 5.8%. The experimental test occurred during the sugar beet harvesting season of the year 2016 near the village of Yaltushkov, Barsky district, Vinnytsia region (Ukraine).

Hence, in the last case, the variation of the soil conditions within the ranges of 2.0~3.8 MPa for hardness and 8~20% for moisture content has no significant effect on the root loss rate.

Thus, it has been established in the analysis of the data obtained by the statistical processing of the results of the research into the loss and damage of sugar beet roots that for each value of the lifter translational motion velocity the respective values of the oscillation frequency and the depth of running in the soil of the vibrating digging tool exist, which ensure the minimum root loss and damage rates. It has also been established that the extent of root damage depends on the conditions in which the work process of vibrational digging is performed (the soil hardness and moisture content). As the hardness of the soil increases and its moisture content declines, the mass of damaged roots rises.

Additionally, as a result of the completed experimental investigations, it has been established that the contamination of the roots lifted by vibrating digging tools of the new design by the soil is under 1%.

Based on the results of the experimental investigations, the root harvester was tested in the field with the aim of assessing its working capacity and the data needed for the calculation of its economic efficiency were determined.
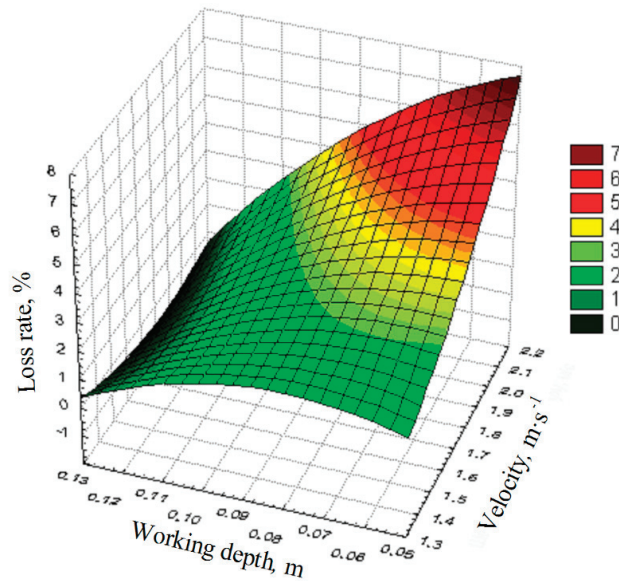
Figure 7.32. Quadratic response surface of root loss rate response to lifter translational motion velocity and depth of its running in soil (at digging tool oscillation frequency of 8.5 Hz, soil hardness of 2.0 MPa, soil moisture content of 20.0%).
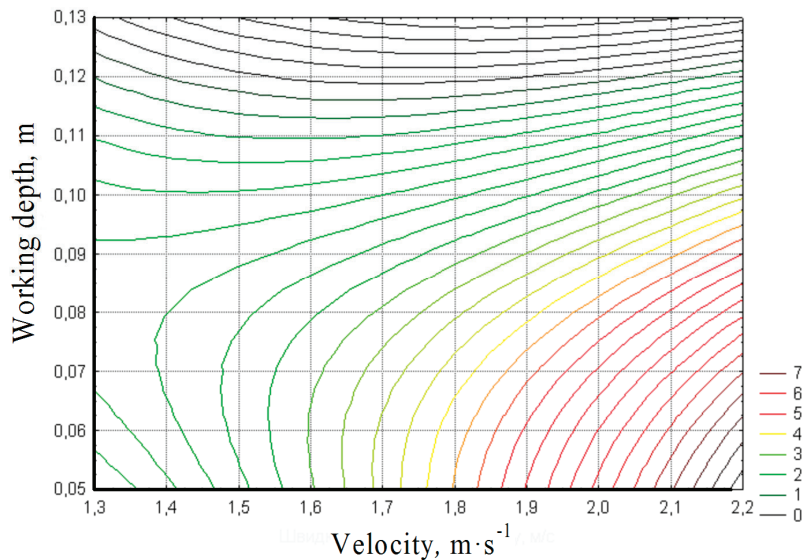
Figure 7.33. Two-dimensional sections of quadratic response surface of root loss rate response to lifter translational motion velocity and depth of its running in soil (at digging tool oscillation frequency of 8.5 Hz, soil hardness of 2.0 MPa, soil moisture content of 20.0%).

The working capacity of the root harvester with the new vibrating digging tools mounted on it under the justified rational operation conditions was estimated by its functioning and the duration of fault elimination breaks; its efficiency was evaluated by the agronomic indicators of the performed root harvesting. The conditions of

testing are presented in Table 7.6. Figure 7.34 shows the photograph of the sugar beet roots extracted by the vibrating digging tools during the experimental investigations.

Table 7.6. Agronomic indicators of experimental field plot.

Indicator	Acc. to TOR	Acc. to Test Results
Properties of crop:		
Offset of roots from theoretical row centreline (%)		
0 mm	N/A	8.4
±10 mm	N/A	12.7
±20 mm	N/A	23.1
±30 mm and more	N/A	31.5
Position of root crowns with respect to soil surface level (%)		
lower than −30 mm	N/A	0.0
−20 through −30 mm	N/A	0.0
0 through −20 mm	N/A	0.5
0 through +20 mm	N/A	41.7
above +20 mm through +40 mm	N/A	23.9
Planting density (thousand pcs·ha^{-1})	N/A	81.7
Biological yielding capacity of roots (t·ha^{-1})	70.0	53.6
Biological yielding capacity of leaves (t·ha^{-1})	20.00	19.2
Condition of tops on roots as regards shaping of leaves (%):		
rosette	N/A	19.2
semirosette	N/A	56.7
cone	N/A	24.1
Type of soil and its description with regard to its mechanical composition	N/A	calcic chernozems
Relief	Up to 7°	Level
Microrelief	N/A	Level
Soil moisture content (%):		
0–10 cm	20.0:23.0	22.5
10–20 cm	N/A	22.1
Soil hardness (MPa):		
0–10 cm	N/A	1.8
10–20 cm	N/A	2.6
Weed infestation:		
Weeds with height of up to 100 cm (pcs·m^{-2})	Not more than 5.0	4.0
Preceding crop and preceding soil preparation	N/A	Winter wheat, inter-row cultivation

It should be noted that the low yield of leaves reported in the table is due to the drought conditions in which the growing season of sugar beet took place.

It follows from the results of the completed investigations that it is advisable to use such designs of the vibrating digging tool that will deliver an oscillation frequency within the range of 10~18 Hz and a depth of running within the range of 0.08~0.10 m at a velocity of the lifter's translational motion within the range of 1.3~2.1 m·s^{-1}. The above-mentioned kinematic parameters of operation ensure the quality of performance of the work process of the vibrational lifting of sugar beet roots that meets the current agronomic requirements with regard to the rates of root loss and root damage.

Figure 7.34. Sugar beet roots lifted by vibrating digging tools during experimental investigations.

The results of the machine testing give evidence of the sufficiently high quality of performance of the work process of the vibrational lifting of sugar beet roots from the soil and the conformance of its indicators to the agronomic requirements for said work process.

7.4. Energy and Force Performance of Root Harvester with Vibrational Lifting Tools

The research into the energy parameters of the root harvester in the field was carried out by way of registering the readings of the strain-gauge transducers in different modes of operation of the harvester and at different parameters and in different modes of operation of the vibrating digging tools.

The agronomic indicators of the field plot, where the experimental investigations for determining the energy parameters were carried out, are presented in Table 7.6.

The graphical relations between the energy and force performance of the vibrational lifting tool and its translation velocity are presented in Figure 7.35.
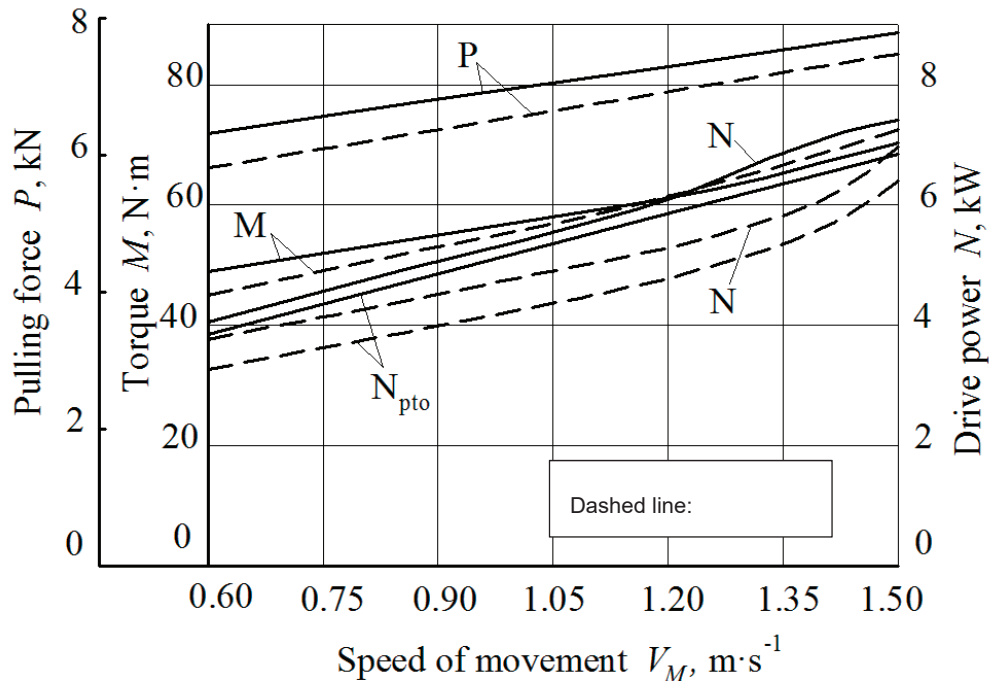
Figure 7.35. Energy and force performance of vibrational lifting tool (at share oscillation frequency of 8.5 Hz and depth of running in soil of 0.09 m).

Based on the completed analysis of the graphical relations, it has been established that within the range of velocities under investigation (0.6 to 1.4 m·s^{-1}), the tractive effort (P_L) varies within the range of 6.6 to 7.8 kN. Thus, it can be stated that changing the experimental unit translation velocity results in the increase in the tractive effort only within a small range.

As is stated in [31], in the case of implementing the vibrational lifting tool, the tractive resistance is reduced 2.5~3.5 times as compared to the resistance of the passive disk lifter. Moreover, when the velocity of translational motion increases, the resistance of the vibrational lifter rises less intensively than in the case of the passive disk lifter, and even more so in the case of the passive share lifter, which has been confirmed by the experimental results.

The power take-off shaft torque (M_{kr}) varies within the range of 50 to 70 N·m.

During the calculation of the traction power (N_T) and vibrational lifting tool drive power (N_{VVP}), the graphical relations were plotted. They indicate that the

values of N_T and N_{VVP} of the vibrational lifting tool vary within the range of 4.0 to 7.0 kW.

Additionally, the graphical relations were separately plotted for the power required for driving the oscillations of the vibrating digging tool as a function of the speed and depth of the digging shares running in the soil (Figure 7.36) as well as the velocity of translation and oscillation frequency of the tool (Figure 7.37).
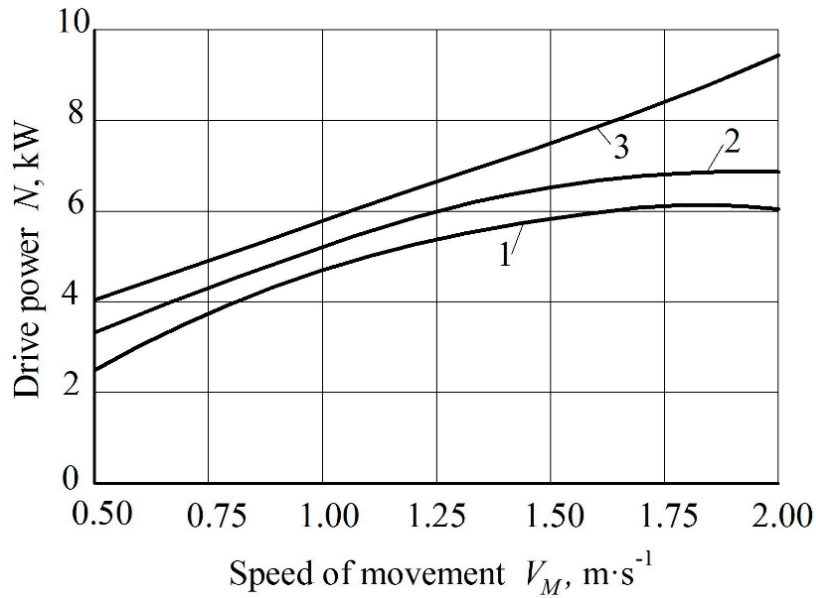
Figure 7.36. Relations between power needed to drive oscillations and digging share translation velocity and depth of running in soil (oscillation frequency of 8.5 Hz): 1—0.06 m; 2—0.09 m; 3—0.12 m.
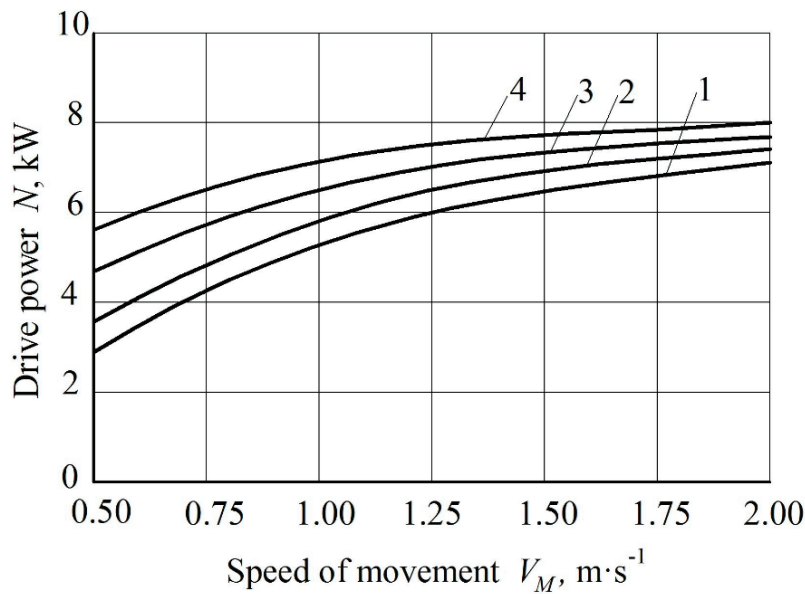
Figure 7.37. Relations between power needed to drive oscillations and digging share translation velocity and oscillation frequency (running depth of 0.09 m): 1—8.5 Hz; 2—11.0 Hz; 3—15.0 Hz; 4—20.3 Hz.

As is seen from the graphs, the lowest power consumed for driving the oscillations of the vibrating digging tools was observed at a frequency of 8.5 Hz and a depth of running in the soil of 0.06 m.

However, taking into account the fact that the minimum loss and damage of roots are observed when the lifter runs in the soil at a depth of 0.09 m, it is evident that the lifter's depth of running within the range of 0.08~0.10 m and the tool's oscillation frequency within the range of 10~18 Hz are more rational operation conditions.

7.5. Conclusions

1. On the basis of the adopted programme and technique, experimental research into the effect that the main design and process parameters of the vibrational lifting tool of the root harvester have on the quality performance of the sugar beet root harvesting work process has been carried out.

2. On the basis of the results of the experimental investigations, it has been established that the increase in the digging tool oscillation frequency results in the reduction in the root loss rate, while the higher velocity of translational motion makes the losses grow. Moreover, within the range of the lifter translational motion velocity of 1.3~2.55 m·s^{-1} the minimum loss rate was observed at a lifter running depth of 0.09 m, and at smaller or greater depths of the lifter translation the losses increase. It has been determined that at a soil hardness of 4.0 MPa, a soil moisture content of 8.0%, a depth of running in the soil of 0.09 m and translational motion velocity values within the range of the of 1.3~2.55 m·s^{-1},

a digging tool oscillation frequency of 8.5 Hz does not meet the agronomic requirements with regard to the root losses (the loss rate reaches 2.7%, while only values of up to 1.5% are acceptable); frequencies of 15.7 and 20.3 Hz are, on the contrary, acceptable (the loss rates amount to 0.5 and 0.4%, respectively).

3. It has been proved experimentally that the root damage rate at a soil hardness of 4.0 MPa, a soil moisture content of 8.0% and the digging tool oscillation frequency variation within the range of 8.5~20.3 Hz varies inconsistently; however, it has been shown that the frequency variation has little effect on the root damage rate. The minimum root damage rates are observed at digging tool running depths within the range of 0.09~0.10 m. When the lifter translational motion velocity increases, the root damage rate rises as well. For example, at a lifter translational motion velocity of 1.3 m·s^{-1}, the mass percentage of the damaged roots amounts to 8.0~9.8%; at a velocity of 1.75 m·s^{-1}—8.1~9.8%; at a velocity of 2.1 m·s^{-1}—8.2~10.3%; at a velocity of 2.55 m·s^{-1}—10.5~12.8%.

4. Velocities of the lifter's translational motion within the range of 1.3~2.1 m·s^{-1} meet the agronomic requirements with regard to the root damage rate (rates of up to 10% are acceptable), while a velocity of 2.55 m·s^{-1} is never compliant with said requirements.

5. It has been established that the mass percentage of the damaged roots essentially depends on the hardness and moisture content of the soil. For example, at a hardness of 2 MPa and a moisture content of 18% it varies within the range of 3.0~6.2%, but at a hardness of 4 MPa and a moisture content of 8%—within the range of 8.0~13.0%.

6. It has been found that changing the velocity of the lifter's translational motion causes the tractive effort to rise only within a small range; the power take-off shaft torque varies within the range of 50 to 70 N·m when the translational motion velocity is changed within the range of 0.5~1.4 m·s^{-1}. The lowest power consumption for driving vibrating digging tools (actuating their oscillations) corresponds to a digging tool oscillation frequency of 8.5 Hz and a depth of running in the soil of 0.06 m. Nevertheless, in view of the fact that the minimum root loss and damage rates are observed at a depth of the lifter running in the soil of 0.09 m, it is reasonable to assume that depths of the lifter running in the soil within the range of 0.08~0.10 m and digging tool oscillation frequencies within the range of 10~18 Hz are a more rational choice.

7. The results of the experimental investigations have proved that the theoretically obtained values of the kinematic parameters for the operation of the vibrational lifting tool, which allow for the complete extraction of the root from the soil subject to not breaking off the root's tail part during the impact interaction, are fully compliant with the agronomic requirements with regard to the loss and damage of the roots.

8. It has been discovered that it is more practical to use designs of the vibrational lifting tool that will, at a length within the range of 0.15–0.20 m for the rear section of the working channel, ensure an oscillation frequency within the range of 10~18 Hz and a running depth within the range of 0.08~0.10 m at a velocity within the range of 1.3~2.1 m·s^{-1} with regard to the lifter's translational motion.

8. Economic Efficiency and Application of Results of Scientific Research in Production

8.1. Calculation of Performance Indices for Evaluation of Economic Efficiency

The comparative appraisal of the economic efficiency of the KKP-3A root harvester equipped with the vibrational lifting tool developed on the basis of the results of scientific research has been carried out for the KKP-3 root harvester equipped with passive concave wheels assumed as the reference model.

The basis for the calculation of the economic efficiency indices is formed, according to [42], by the direct operating costs: the allocations for the renovation, major overhaul and running repairs, maintenance, the remuneration of labour, the cost of petroleum, oil, lubricants as well as the quality and amount of the product obtained with the use of the compared machines.

In the described case, the comparative appraisal is carried out based specifically on the quality of the output.

During the calculation of the economic characteristics, the additional economic benefit obtained by reducing the rates of the loss and severe damage of roots during their lifting is determined [43]. In this process, the productive capacity, the number of operating personnel and the fuel intensity of both machines are assumed to be equal.

The initial data for the calculation of the economic efficiency of the KKP-3A root harvester equipped with the new vibrational lifting tool are presented in Table 8.1.

Table 8.1. Initial data for calculation of economic efficiency of KPP-3A beet harvester.

Index Description	Unit	Advanced Model KKP-3A	Reference Model KKP-3
Operating capacity per hour of shift time	ha·h^{-1}	0.85	0.85
Annual planned work load	h	300	300
Average yield	t·ha^{-1}	37.3	37.3
Main quality indices:			
loss of roots	%	1.4	2.2
severe damage of roots		5.1	6.8

According to [43], the economic benefit provided by the reduction in the sugar beet root loss rate can be determined with the use of the following relation:

$$E_k = W_3 \cdot T_p \cdot U \cdot a \cdot c, \tag{8.1}$$

where W_3—machine's output per hour of shift time (ha·h^{-1}); T_p—annual planned work load of the machine (h); U—average yield of sugar beets (t·ha^{-1}); a—increase in sugar beet yield due to the reduction in losses by the machine under investigation as compared to the reference machine; c—purchasing price of sugar beets (USD·t^{-1}).

It is assumed that the average yield of sugar beets is 37.3 t·ha^{-1} [44], while the purchasing price of sugar beets is USD 6.85 t^{-1}.

The increase in sugar beet yield due to the reduction in losses amounts to:

$$a = \frac{2.2 - 1.4}{100} = 0.008. \tag{8.2}$$

By substituting the required values of the quantities present in (8.1), the following economic benefit due to the reduction in the loss of roots is obtained:

$$E_k = 0.85 \cdot 300 \cdot 37.3 \cdot 0.008 \cdot 6.85 = 521.23 \text{ USD} \tag{8.3}$$

The economic benefit per hectare of the harvested area is equal to:

$$E_k' = \frac{E_k}{W_3 T_p} = \frac{521.23}{0.85 \cdot 300} = 2.04 \text{ USDha}^{-1} \tag{8.4}$$

The additional economic benefit due to the reduction in the damage rate is determined with the use of the following relation:

$$E_{dod} = 0.95 \cdot 10^{-5}(x_1 - x_2)Qmtkc_1 - 10^{-4}(x_1 - x_2) \cdot [D_r - t(0.0104 + 0.00095x_2)]Qmtkc_2, \tag{8.5}$$

where x_1 and x_2 —number of severely damaged roots output by the reference and advanced model harvesters, respectively (%); Q—amount of sugar beet roots gathered per season (t); D_r—initial sugar content in roots (%) ($D_r = 17\% = 17\%$ [31]); m—part of the raw stock to be kept in store ($m = 0.4$); t—average period of storing beet roots in the sugar mill (days); k—correction factor; (c_1—wholesale price of sugar (USD·t^{-1}) ($c_1 = 122.8$ USD·t^{-1} [45]); c_2—direct costs of the production of 1 t of sugar ($c_2 = 41.0$ USD·t^{-1} [45]).

The number of roots gathered per season is determined with the use of the formula:

$$Q = UW_3T_p = 37.3 \cdot 0.85 \cdot 300 = 9512 \text{ t} \tag{8.6}$$

where U—average yield of sugar beets $(t \cdot ha^{-1})$; W_3—machine's output per hour of shift time $(ha \cdot h^{-1})$; T_p—annual planned work load of the machine (h).

The correction factor is defined as the following product of factors:

$$k = k_1 k_2 k_3, \tag{8.7}$$

where k_1—sugar beet procurement factor, $k_1 = 0.9$; k_2—factor of the sugar beet losses in the period from the delivery to the mill to the start of processing, $k_2 = 0.96$; k_3—factor of the sugar yield from the raw material, $k_3 = 0.75$.

Hence, $k = 0.9 \cdot 0.96 \cdot 0.75 = 0.648$.

The next step is to determine the additional economic benefit obtained by the reduction in the damage rate for different times of storing beet roots in the sugar mill:

At $t = 60$ days:

$$
\begin{aligned}
E_{dod} &= 0.95 \cdot 10^{-5} \cdot (6.8 - 5.1) \cdot 9512 \cdot 0.4 \cdot 60 \cdot 0.648 \cdot 122.8 - 10^{-4} \\
&\cdot (6.8 - 5.1) \cdot [17 - 60(0.0104 + 0.00095 \cdot 5.1)] \cdot 9512 \cdot 0.4 \cdot 0.648 \cdot 41.0 = 16.96 \text{ USD}
\end{aligned}
\tag{8.8}
$$

Hence, $E_{dod} = \text{USD}16.96$.

The additional economic benefit per hectare of the harvested area E'_{dod} is equal to:

$$E'_{dod} = \frac{E_{dod}}{W_3 \cdot T_p} = \frac{16.96}{0.85 \cdot 300} = 0.07 \text{ USD} \cdot ha^{-1} \tag{8.9}$$

Subsequently, the total economic benefit obtained by the reduction in the root loss and severe damage rates in this case amounts to:

$$E' = E'_k + E'_{dod} = 2.04 + 0.07 = 2.11 \text{ USD} \cdot ha^{-1} \tag{8.10}$$

The results of the described calculations for different times of storing beet roots in the sugar mill are presented in Table 8.2.

Table 8.2. Total economic benefit due to reduction in root loss and severe damage rates (amount of sugar beet roots gathered during season Q = 9512 t).

Time of Storing Roots in Sugar Mill, t (days)	Additional Economic Benefit Due to Reduced Damage Rate, E_{dod} (USD)	Specific Additional Economic Benefit Due to Reduced Damage Rate, E'_{dod} (USD·ha⁻¹)	Total Economic Benefit Due to Reduced Root Loss and Severe Damage Rates, E' (USD·ha⁻¹)
60	16.96	0.07	2.11
90	171.51	0.67	2.70
120	326.06	1.28	3.31
150	480.61	1.88	3.91
180	635.21	2.49	4.52

As is shown by the obtained calculation results, the economic benefit obtained by the reduction in the root damage rate increases together with the time of storing the roots in the sugar mill. This is due to the fact that roots without damage are better kept in storage and are less susceptible to rotting.

8.2. Application of Scientific Research Results in Production

On the basis of the results obtained in the accomplished scientific studies, the design and kinematic parameters of vibrational lifting tools have been established—in particular, the acceptable digging tool oscillation frequencies and amplitudes as well as lifter translation velocities subject to the condition of not damaging the tail parts of sugar beet roots that allow the process of lifting roots from the soil by means of vibrational digging. Additionally, the minimum acceptable values of the vibrational lifting tool oscillation frequency subject to the condition of the guaranteed gripping of each root by the digging shares have been established.

Based on the obtained scientific results, a new design of vibrational lifting tools has been developed. Tools of the new design have been manufactured and installed in root harvesters of the KKP-3A, MKP-6 types and in a trail-behind four-row root harvesting implement.

The undertaken scientific studies and engineering developments resulted in the obtaining of 10 patents for invention in Ukraine.

The theoretically and experimentally established parameters and modes of operation of lifting tools recommended in accordance with the results of the accomplished research investigations have been applied in the development of the new designs of lifting tools for root harvesters at OAO "Boreks" (Borodyanka, Ukraine) and OAO "Ternopol Combine Harvester Works". The developed designs of vibrational lifting tools have been industrially produced and passed the field testing.

8.3. Conclusions

1. An additional economic benefit is achieved by implementing vibrational lifting tools of the new design in the production process due to the substantial reduction in the rates of the loss and damage of sugar beet roots during vibrational lifting.
2. The additional economic benefit due to the reduced loss of roots in vibrational lifting as compared to the operation with the use of wheel lifters amounts to USD $2.04 \cdot \text{ha}^{-1}$.
3. The additional economic benefit due to the reduced damage of roots depends on the duration of storage in the sugar mill. If the storage period continues for 60 to 180 days, the benefit varies within the range of USD $0.07–2.49 \cdot \text{ha}^{-1}$.
4. The total economic benefit obtained by the reduction in the root loss and damage rates varies, depending on the time of storing roots in the sugar mill, within the range of USD $2.11–4.52 \cdot \text{ha}^{-1}$.

References

1. Vasilenko, P.M. *Introduction to Agricultural Mechanics*; Agricultural Education: Kiev, Ukraine, 1996.

2. Vasilenko, P.M. *Selected Issues in Methodology of Mathematical Investigations in Field of Agricultural Mechanics*; Ukrainian Research Institute of Mechanisation and Electrification in Agricultural Industry: Kiev, Ukraine, 1974.

3. Vasilenko, P.M. *On Methods of Mechanical and Mathematical Studies in Development of Agricultural Equipment*; VISKhOM: Kiev, Ucraine, 1962.

4. Vasilenko, P.M. *Theory of Motion of Particle on Rough Surfaces of Agricultural Machines*; Publishing House of Ukrainian Academy of Agricultural Sciences: Kiev, Ukraine, 1960.

5. Vasilenko, P.M.; Pogorely, L.V. *Fundamentals of Scientific Research: Textbook [for Higher Education Establishments]*; Higher School: Kiev, Ukraine, 1984; 266p, Mechanisation of production in agricultural industry.

6. Vasilenko, P.M.; Pogorely, L.V.; Brey, V.V. Vibrational Method of Harvesting Root Plants. *Mech. Electrif. Soc. Agric.* **1970**, 2, 9–13.

7. Pogorely, L.V.; Tatyanko, N.V.; Brei, V.V. *Sugar Beet Harvesting Machines (Design and Analysis)*; Pogorely, L.V., Ed.; Kiev Engineering: Kiev, Ukraine, 1983.

8. Bosoy, E.S.; Vernyaev, O.V.; Smirnov, I.I.; Sultan-Shakh, E.G. *Theory, Design and Calculations of Agricultural Machines: [Textbook for Universities of Agricultural Machinery]*, 2nd ed.; Mashinostroeniye: Moscow, Russia, 1978.

9. Gevko, R.B. *Digging and Cleaning Devices of Beet Harvesting Machines*; Design and Calculation Printer: Ternopol, Ukraine, 1997.

10. Gevko, R.B.; Tkatchenko, I.G.; Siny, S.V. *Trends in Development of Beet Harvesting Facilities*; Lutsk State Technical University: Lutsk, Ukraine, 1999.

11. Didenko, N.F.; Khvostov, V.A.; Medvedev, V.P. *Machines for Vegetable Harvesting*, 2nd ed.; Mechanical Engineering: Moscow, Russia, 1984.

12. Khvostov, V.A. *Root Crop and Onion Harvesters: Theory, Design, Calculation*; Khvostov, V.A., Reingart, E.S., Eds.; VISKhOM: Moscow, Russia, 1995.

13. Zavgorodny, A.F.; Kravchuk, V.I.; Yurchuk, V.P. *Geometric Design of Tools for Root Harvesters*; Pogorely, L.V., Ed.; Agrarian Science: Kiev, Ukraine, 2004.

14. Dubrovsky, A.A. *Vibrational Equipment in Agriculture*; State Mechanical Engineering: Moscow, Russia, 1968.

15. Bulgakov, V.M. *Theory of Beet Harvesting Machines: Monograph*; Publishing Centre of the National Agrarian University: Kiev, Ukraine, 2005; 352p.

16. Khelemsky, M. *On Determination of Process Qualities of Sugar Beets*; State Publishers Sugar Beet: Moscow, Russia, 1995; No. 1; pp. 12–13.

17. Bulgakov, V.; Pascuzzi, S.; Ivanovs, S.; Santoro, F.; Anifantis, A.S.; Ihnatiev, I. Performance Assessment of Front-Mounted Beet Topper Machine for Biomass Harvesting. *Energies* **2020**, *13*, 3524. [CrossRef]

18. Zazhigayev, L.S.; Kishyan, A.A. *Methods of Planning Physical Experiments and Processing Their Results*; State Nuclear Power Press: Moscow, Russia, 1978.

19. Gevko, R.B. *Substantiation of Design and Process Parameters of Tools in Beet Harvesting Machines: Author's Abstract of the Thesis for the Degree of Doctor Sc. Eng., Branch 05.05.11*; NAU: Kiev, Ukraine, 1999.

20. Burmistrova, M.F.; Komolkova, T.K.; Klemm, N.V. *Physical and Mechanical Properties of Agricultural Plants*; State Agriculture State Publishers: Moscow, Russia, 1956.

21. Bulgakov, V.M.; Holovach, I.V. Use of vibrational tools for lifting sugar beet roots. *Bull. Agrar. Sci.* **2004**, *2*, 40–45.

22. Bulgakov, V.M.; Holovach, I.V. *Theory of Vibrational Lifting of Roots*; Mechanisation of Production in Agricultural Industry: collection of scientific papers of National Agrarian University; NAU: Kiev, Ukraine, 2003; Volume XV, pp. 45–85.

23. Bulgakov, V.M.; Holovach, I.V. *Theory of Longitudinal Oscillations of Root during Its Vibrational Lifting from Soil*; Mechanisation of Production in Agricultural Industry: Bulletin of Kharkiv National Technical University of Agriculture of Petro Vasilenko: collection of scientific papers; KNTUA: Kharkiv, Ukraine, 2003; Volume 20, pp. 216–240.

24. Bulgakov, V.M.; Holovach, I.V. *About the Compelled Cross-Section Fluctuations of a Root Crop at Vibrating Excavation*; Bulletin of the Kharkiv national technical university of an agriculture of Peter Vasilenko: collection of scientific works; KNTUA: Kharkiv, Ukraine, 2005; Volume 39, pp. 23–39.

25. Bulgakov, V.M.; Holovach, I.V. *Theory of Transverse Oscillations of Root during Vibrational Lifting*; Studies of Tavria State Agricultural Technology Academy: collection of scientific papers; TSATA: Melitopol, Ukraine, 2004; Volume 18, pp. 33–48.

26. Privalov, I.I. *Analytical Geometry*; Physics and Mathematics State Publishers: Moscow, Russia, 1960.

27. Zayika, P.M. *Selected Problems of Agricultural Mechanics: Practical Guide*; Ukrainian Agriculture Academy Publishers: Kiev, Ukraine, 1992.

28. Zayika, P.M. *Theory of Agricultural Machines*; Oka: Kharkiv, Ukraine, 2001; Volume 1, Part 1.

29. Bertsekas, D. *Constrained Optimization and Lagrange Multiplier Methods*; Transl. from Eng.; Radio and Communications: Moscow, Russia, 1987.

30. Kurosh, A.G. *Course of Higher Algebra*; Science: Moscow, Russia, 1971.

31. Pogorely, L.V.; Tatyanko, N.V. *Beet-Harvesting Machines: History, Construction, Theory, Prognosis*; Kyiv Feniks: Kyiv, Ukraine, 2004.

32. Butenin, H.V.; Lunts, I.L.; Merkin, D.R. *A rate of theoretical mechanics*; Science: Moscow, Russia, 1985; Volume II, Dynamics.

33. Panovko, Y.G. *Elements of Applied Theory of Oscillations and Impact*; Polytechnics: Leningrad, Russia, 1990.

34. Panovko, Y.G. *Introduction to Theory of Mechanical Impact*; Science: Moscow, Russia, 1985.

35. Testing Agricultural Equipment. *Methods of Evaluation of Energy Factors: Guidance and Regulation Document 46.16.02.09-95*; Guidance and Regulation Documents; Official publication; FAO: Rome, Italy, 1995.

36. Testing Agricultural Equipment. *Principal Provisions: Guidance Document 46.16.01.05-93*; Guidance and Regulation Documents; Official Publication; FAO: Rome, Italy, 1995.

37. Zuyev, N.M. *Technique of Research into Quality of Operation of Sugar Beet Harvesting Machines*; Soviet National Research Institute of Sugar Beet: Kiev, Ukraine, 1989.

38. Adler, Y.P.; Markova, Y.V.; Granovsky, Y.V. *Design of Experiments in Search of Optimum Conditions*; Science: Moscow, Russia, 1971.

39. Dospekhov, B.A. *Technique of Field Experiment (Including Basic Principles of Statistical Analysis of Results of Experiment)*, 5th ed.; State Agricultural Industry Publishers: Moscow, Russia, 1985.

40. Draper, N.; Smith, H. *Applied Regression Analysis: in 2 Books*; transl. from Eng.; Finance and Statistics: Moscow, Russia, 1987; Book 1, 351p.; Book 2, 366p.

41. Pogorely, L.V.; Maksimchuk, V.P. Evaluation of Energy Performance of Sugar Beet Harvesting Machines. *Mech. Electrif. Soc. Agric. Ind.* **1971**, *8*, 22–25.

42. State Standards of USSR. *GOST 23.729-79: Agricultural Machinery. Economic Efficiency Methods*; State Standards Publishers: Moscow, Russia, 1970.

43. Vysotsky, A.A. *Dynamometer Testing of Agricultural Machines*; State Mechanical Engineering: Moscow, Russia, 1968; 290p.

44. Available online: http://www.sugarbeet.org.ua/node/39 (accessed on 4 February 2020).

45. Available online: http://www.sugarbeet.org.ua/node/33 (accessed on 4 February 2020).

46. Avanesov, Y.B. *Advanced Methods and Means of Mechanisation in Sugar Beet Harvesting*; VNIITEIagroprom: Moscow, Russia, 1987.

47. Avanesov, Y.B.; Bessarabov, B.I.; Rusanov, I.I. *Beet Harvesters*; Kolos: Moscow, Russia, 1979.

48. Anuryev, V.I. *Handbook for Design and Mechanical Engineers: 3 Parts*; Mashinostroeniye: Moscow, Russia, 1979–1982; Part 1., Part 2. & Part 3.

49. Arhangelski, Y.A. *Analytical Mechanics of Solids*; Science: Moscow, Russia, 1977.

50. Birger, I.A.; Shorr, B.F.; Yosilevich, G.B. *Strength Analysis of Machine Components: Handbook*, 3rd ed.; Mechanical Engineering: Moscow, Russia, 1979.

51. Brusilovsky, Y.R. Study on Work Process of Sugar Beet Root Lifting from Soil with Wheel Lifters. Ph.D. Thesis, Moscow Timiryazev Agricultural Academy, Moscow, Russia, 1966.

52. Babakov, I.M. *Theory of Oscillations*; Nauka: Moscow, Russia, 1968.

53. Brei, V.V. *Research and Development of Mechanised Process for Lifting Sugar Beet Roots from Soil: Thesis for the Degree of Candidate of Engineering, Branch 05.20.01*; NAU: Kiev, Ukraine, 1972.

54. Bulgakov, V.; Holovach, I. Mathematical modelling of vibrational root lifting process. In Proceedings of the Agricultural Engineering Problems: Proceedings Intern. Scient. Conf., Latvia, Jelgava, 2–3 June 2005; Latvia Univ. of Agriculture: Jelgava, Latvia, 2005; pp. 255–262.

55. Bulgakov, V.; Holovach, I. On transverse oscillations of beet root in soil during vibrational lifting. In Proceedings of the MOTROL: Motorization and Power Industry in Agriculture: proceedings V Intern. Research and Technical Conf., Lublin-Odessa, Ukraine, 20–22 September 2005; Polish Academy of Sciences Publisher: Warsaw, Poland; pp. 92–112.

56. Bulgakov, V.; Holovach, I. Theory of vibrational lifting of root crops. In Proceedings of the Agricultural Engineering Problems: Proceedings Intern. Scient. Conf., Latvia, Jelgava, 2–3 June 2005; Latvia Univ. of Agriculture: Jelgava, Latvia, 2005; pp. 247–254.

57. Bulgakov, V.; Holovach, I.; Novichok, Y. Research into process of vibrational lifting of roots from soil on the basis of Euler equations. In Proceedings of the MOTROL: Motorization and Power Industry in Agriculture: proceedings V Intern. Research and Technical Conf., Lublin, Poland, 19–21 September 2006; Polish Academy of Sciences Publisher: Warsaw, Poland; pp. 40–57.

58. Bulgakov, V.; Holovach, I.; Finko, S. Experimental research into energy performance of vibrational lifting tools. In Proceedings of the MOTROL: Motorization and Power Industry in Agriculture: Proceedings IV Intern Research and Technical Conf., Lublin-Kyiv: NAUU, Lublin, Poland & Kiev, Ukraine, 23–25 September 2003; Polish Academy of Sciences Publisher: Warsaw, Poland; pp. 32–40.

59. Bulgakov, V.M. *Development of Beet Root Harvesting Work Process and Machines: Author's Abstract of the Thesis for the Degree of Doctor Sc. Eng., Branch 05.05.11 in the Form of a Scientific Report*; VISKhOM: Moscow, Russia, 1993.

60. Bulgakov, V.M.; Holovach, I.V. Mathematical modelling of transverse oscillations of root during vibrational lifting from soil. *Vib. Eng. Technol.* **2003**, *1*, 11–14.

61. Bulgakov, V.M.; Kozibroda, Y.I. *Substantiation and Selection of Optimal Layout of Sugar Beet Harvester by Power Criterion*; Commission of Motorization and Energetics in Agriculture: Polish Academy of Sciences Branch in Lublin; WAR: Lublin, Poland, 2001; Volume 1, pp. 69–72.

62. Bulgakov, V.M.; Holovach, I.V. Differential equation of oscillations of solid body with one end fixed in elastic medium. *Ind. Hydraul. Pneum.* **2006**, *4*, 115–119.

63. Bulgakov, V.M.; Holovach, I.V.; Beryozovy, N.G. *Theoretical Study on Transverse Oscillations of Root Fixed in Soil*; Bulletin of Poltava State Academy of Agriculture: Collection of Scientific Papers; PSAA: Poltava, Ukraine, 2006; Volume 4, pp. 25–27.

64. Bulgakov, V.M.; Holovach, I.V. *Establishing Principal Moments of External Forces Acting on Root during Vibrational Lifting from Soil*; Bulletin of National Agrarian University: Collection of Scientific Papers; NAU: Kiev, Ukraine, 2005; Volume 2, pp. 199–211.

65. Bulgakov, V.M.; Holovach, I.V. Study on vibrational lifting of sugar beet root from soil with the use of Euler equations. *Electr. Eng. Mech.* **2006**, *2*, 67–75.

66. Bulgakov, V.M.; Holovach, I.V. *Application of Kinematic and Dynamic Euler EQUATIONS in Research into Vibrational Lifting of Roots*; Studies of Tavria State Agricultural Technology Academy: Collection of scientific papers; TSATA: Melitopol, Ukraine, 2005; Volume 27, pp. 3–27.

67. Bulgakov, V.M.; Holovach, I.V. *Mathematical Model of Lifting Root from Soil*; Mechanisation and automation of production processes: Bulletin of Sumy National Agrarian University: Collection of scientific papers; SNAU: Sumy, Ukraine, 2006; Volume 9, pp. 5–25.

68. Bulgakov, V.M.; Holovach, I.V. *Mathematical Model of Vibrational Lifting of Root from Soil*; Engineering-and-technology aspects of developing and testing new equipment

and technologies for agricultural industry of Ukraine: collection of scientific papers; UkrNDIPVT: Doslidnitske, Ukraine, 2004; Volume 7, pp. 77–90.

69. Bulgakov, V.M.; Holovach, I.V. *Mathematical Modelling of Lifting Sugar Beet Root from Soil*; Design, production and operation of agricultural machines: Nationwide interdepartmental research and technology paper collection; KNTU: Kirovograd, Ukraine, 2007; Issue 37, pp. 30–48.

70. Bulgakov, V.M.; Holovach, I.V. *Mathematical Modelling of Angular Oscillations of Root in Soil as in Elastic Medium during Vibrational Lifting*; Studies of Tavria State Agricultural Technology Academy: collection of scientific papers; TSATA: Melitopol, Ukraine, 2006; Issue 39, pp. 122–133.

71. Bulgakov, V.M.; Holovach, I.V. *Mathematical Modelling of Process of Vibrational Lifting of Root from Soil*; Bulletin of Agrarian Science; NAU: Kiev, Ukraine, 2007; pp. 44–46.

72. Bulgakov, V.M.; Holovach, I.V. *Modelling of Process of Vibrational Lifting of Sugar Beet Root from Soil*; Bulletin of National Agrarian University: collection of scientific papers; NAU: Kiev, Ukraine, 2005; Issue 80; Part I, pp. 313–324.

73. Bulgakov, V.M.; Holovach, I.V. *On Longitudinal Oscillations of Solid Elastic Body with One End Fixed*; Mechanisation of Agricultural Industry: Bulletin of Kharkiv National Technical University of Agriculture of Petro Vasilenko: collection of scientific papers; KNTUA: Kharkiv, Ukraine, 2007; Volume 49, pp. 218–228.

74. Bulgakov, V.M.; Holovach, I.V. *Generation of Mathematical Model of Lifting Root from Soil*; Agricultural engineering research: Bulletin of Lviv State Agrarian University: collection of scientific papers; LSAU: Lviv, Ukraine, 2006; Volume 10, pp. 162–173.

75. Bulgakov, V.M.; Holovach, I.V. *On Forced Transverse Oscillations of Root Body Fixed in Soil*; Vibration in engineering and technology; NAU: Kiev, Ukraine, 2004; No. 3; pp. 24–25.

76. Bulgakov, V.M.; Holovach, I.V. *On Forced Transverse Oscillations of Root Body during Vibrational Lifting*; Mechanisation and Electrification of Agricultural Industry: Interdepartmental topics scientific paper collection; NSRC IMEAI of UAAS: Glevakha, Ukraine, 2006; Volume 90, pp. 231–242.

77. Bulgakov, V.M.; Holovach, I.V. Analytical mathematical model of vibrational lifting of root from soil. *Vib. Eng. Technol.* **2004**, *3*, 34–46.

78. Bulgakov, V.M.; Holovach, I.V. *Development of Matematical Model of Withdrawal of a Root Crop from a Ground*; Technics of agrarian and industrial complex; NSRC IMEAI of UAAS: Glevakha, Ukraine, 2006; No. 6–7, pp. 36–38; No. 8, pp. 25–28; No. 9–10, pp. 47–49.

79. Bulgakov, V.M.; Holovach, I.V. *Theoretical Study on Lifting Roots from Soil with Share Lifter*; Zemes UKIO Inzinerija: LzUU Mokslo daRbai; UKIO: Raudondvaris, Lithuania, 2002; Volume 34, pp. 53–78.

80. Bulgakov, V.M.; Holovach, I.V. *Theoretical Study on Vibrational Lifting of Root Crops*; Materials of 6th International Symposium of Ukrainian Mechanical Engineers in Lviv; Publishing House of PE CME: Lviv, Ukraine, 2003; pp. 80–81.

81. Bulgakov, V.M.; Holovach, I.V. *Theoretical Study on Longitudinal Oscillations of Root in Soil as in Elastic Medium during Vibrational Lifting*; Bulletin of Kharkiv National Technical

University of Agriculture of Petro Vasilenko: collection of scientific papers; KNTUA: Kharkiv, Ukraine, 2006; Issue 44, Volume 2, pp. 131–155.

82. Bulgakov, V.M.; Holovach, I.V. *Theoretical and Experimental Studies on Kinematic and Energy Parameters of Vibrational Root Lifting Process*; Mechanisation and Electrification of Agricultural Industry: Interdepartmental topics scientific paper collection; NSRC IMEAI of UAAS: Glevakha Ukraine, 2003; Issue 87, pp. 41–57.

83. Bulgakov, V.M.; Holovach, I.V. *Theory of Vibrational Lifting of Sugar Beet Root from Soil*; Ulyanov Readings: Materials of International Science and Practice Conference, dedicated to 100th birthday of Prof. A.F. Ulyanov: "Maintenance and Electrification in Agriculture" section; SSU: Saratov, Russia, 2005; Part II; pp. 16–19.

84. Bulgakov, V.M.; Holovach, I.V. *Theory of Share Lifter*; Tractors and agricultural machinery; VISKhOM: Moscow, Russia, 2002; Part 1, Volume 10, pp. 25–29; Part 2, Volume 11, pp. 33–34.

85. Bulgakov, V.M.; Holovach, I.V. *Theory of Free Transverse Oscillations of Root Fixed in Soil during Its Vibrational Lifting*; Ulyanov Readings: Materials of International Science and Practice Conference, dedicated to 100th birthday of Prof. A.F. Ulyanov: "Maintenance and Electrification in Agriculture" section. Part II; SSU: Saratov, Russia, 2005; pp. 13–16.

86. Bulgakov, V.M.; Holovach, I.V. *Theory of Root Lifting*; Problems of reliability of machines and means of mechanisation in agricultural industry: Bulletin of Kharkiv National Technical University of Agriculture of Petro Vasilenko: collection of scientific papers; KNTUA: Kharkiv, Ukraine, 2007; Issue 51, pp. 363–376.

87. Bulgakov, V.M.; Holovach, I.V. *Theory of Lifting Roots with Share Lifter*; Mechanisation of Production in Agricultural Industry: collection of scientific papers of National Agrarian University; NAU: Kiev, Ukraine, 2002; Volume XII, pp. 3–20.

88. Bulgakov, V.M.; Holovach, I.V. *Theory of Vibrational Lifting of Root Crops Based on Kinematic and Dynamic Euler Equations*; Materials of Seventh International Symposium of Ukrainian Mechanical Engineers in Lviv; KINPATRI LTD: Lviv, Ukraine, 2005.

89. Bulgakov, V.M.; Holovach, I.V. *Specified Theory of Digging up Working Body of Share Type*; Bulletin of an agrarian science of Black Sea Coast: collection of scientific works; MNAU: Nikolaev, Ukraine, 2002; pp. 37–63.

90. Bulgakov, V.M.; Holovach, I.V. *Improved Theory of Vibrational Lifting of Beet Roots from Soil*; Technical Facilities of Agricultural Sector: Kiev, Ukraine, 2007; No. 8–9, pp. 54–55; No. 10, pp. 40–42; No. 11–12, pp. 48–51.

91. Bulgakov, V.M.; Holovach, I.V.; Beryozovy, N.G. *Vibrational Lifting Tool*; Scientists of Technical Institute in National Agrarian University—to Production Operations. Agrarian engineering in globalisation environment: collection of finished research projects; NAU: Kiev, Ukraine, 2008; pp. 56–57.

92. Bulgakov, V.M.; Holovach, I.V.; Beryozovy, N.G. *General-Purpose Set of Beet Harvesters for Farm. Enterprises – KPF-1.5; KKP-3A*; Scientists of Technical Institute in National Agrarian University—to Production Operations. Agrarian engineering in globalisation environment: collection of finished research projects; NAU: Kiev, Ukraine, 2008; pp. 60–61.

93. Bulgakov, V.M.; Holovach, I.V.; Burilko, A.V. *Theoretical Research into Process. of Vibrational Lifting of Sugar Beet Roots*; Mechanisation and Electrification of Agricultural Industry: Interdepartmental topics scientific paper collection; NSRC IMEAI of UAAS: Glevakha, Ukraine, 2005; Issue 89, pp. 61–73.

94. Bulgakov, V.M.; Holovach, I.V. Mathematical model of sugar beet root lifting. *Bull. Agrar. Sci.* **2002**, *9*, 51–54.

95. Bulgakov, V.M.; Holovach, I.V. *Modelling of Process. of Vibrational Lifting of Roots*; Studies of Tavria State Agricultural Technology Academy: collection of scientific papers; TSATA: Melitopol, Ukraine, 2006; Issue 39, pp. 26–32.

96. Bulgakov, V.M.; Holovach, I.V. *Analytical Mathematical Model. of Process. of Vibrational Lifting of Roots*; Studies of Tavria State Agricultural Technology Academy: collection of scientific papers; TSATA: Melitopol, Ukraine, 2004; Issue 17, pp. 11–24.

97. Bulgakov, V.M.; Holovach, I.V. Theoretical study on vibrational lifting of roots. *Vib. Eng. Technol.* **2004**, *3*, 18–23.

98. Bulgakov, V.M.; Holovach, I.V. *Theoretical Study on Longitudinal Oscillations of Root in Soil as in Elastic Medium during Vibrational Lifting*; Mechanisation of Agricultural Industry: Bulletin of National Agrarian University: collection of scientific papers; NAU: Kiev, Ukraine, 2006; Issue 101, pp. 160–173.

99. Bulgakov, V.M.; Holovach, I.V. *Theoretical Research into Forced Transverse Oscillations of Root Body*; Technical Facilities of Agricultural Sector: Kiev, Ukraine, 2005; No. 1; pp. 23–26.

100. Bulgakov, V.M.; Holovach, I.V. *Theoretical Research into Forced Transverse Oscillations of Root Body Fixed in Soil*; Design, production and operation of agricultural machines: Nationwide interdepartmental research and technology paper collection; KNTU: Kirovograd, Ukraine, 2005; Issue 35, pp. 3–20.

101. Bulgakov, V.M.; Holovach, I.V.; Finko, S.V. *Results of Experimental Investigation of Vibrational Beet Root Lifting*; Bulletin of National Agrarian University: collection of scientific papers; NAU: Kiev, Ukraine, 2003; Issue 60, pp. 86–92.

102. Bulgakov, V.M.; Holovach, I.V.; Datzishin, O.V. *Establishing External Force Factors in Vibrational Lifting of Roots from Soil*; Bulletin of National Agrarian University: collection of scientific papers; NAU: Kiev, Ukraine, 2005; Issue 92, Part 1, pp. 188–198.

103. Bulgakov, V.M.; Holovach, I.V.; Zykov, P.Y. *MKP-6 Trail-Behind Root Harvester with Advanced Cleaning and Conveying Tools*; Scientists of Technical Institute in National Agrarian University—to Production Operations. Agrarian engineering in globalisation environment: collection of finished research projects; NAU: Kiev, Ukraine, 2008; pp. 58–59.

104. Bulgakov, V.M.; Holovach, I.V.; Finko, S.V. *Mathematical Model of Vibrational Lifting of Roots from Soil*; Design, production and operation of agricultural machines: Nationwide interdepartmental research and technology paper collection; KNTU: Kirovograd, Ukraine, 2003; Issue 33, pp. 41–52.

105. Bulgakov, V.M.; Holovach, I.V.; Chernish, O.M. *Modelling and Analysis of Vibrational Beet Root Lifting Process*; Automation of production processes in mechanical engineering and instrument engineering: Ukrainian interdepartmental research and technology paper collection; LPNU: Lviv, Ukraine, 2006; No. 40; pp. 39–48.

106. Bulgakov, V.M.; Gurchenko, A.P. *KUM-3 Advanced Root Harvester*; Tractors and Agricultural Machines: Moscow, Russia, 1992; No. 8–9; pp. 32–34.

107. Bulgakov, V.M.; Zykov, P.Y. *Advanced Method of Beet Root Lifting*; Tractors and Agricultural Machines: Moscow, Russia, 1995; No. 11; pp. 31–33.

108. Bulgakov, V.M.; Finko, S.V.; Glukhovsky, V.S. *MKP-4 Root Harvester with Vibrational Lifting Tools*; State Publisher Sugar Beet: Moscow, Russia, 1995; No. 8; pp. 9–11.

109. Vasilenko, A.A. *Beet-Harvesting Machines. Theory, Construction and Calculation*; State Mechanical Engineering: Kharkiv-Kiev, Ukraine, 1937.

110. Lavendel, E.E. (Ed.) *Vibration in Engineering: Handbook*; State Mechanical Engineering: Kharkiv-Kiev, Ukraione, 1989; 420p.

111. *VISKhOM: Physical and Mechanical Properties of Plants, Soils and Fertilisers: Methods of Research, Instruments, Data*; State Publishers: Moscow, Russia, 1970.

112. Vovk, P.F. *Agrophysical Properties of Sugar Beet Roots as Regards Mechanisation of Their Harvesting*; Theory, design and production of agricultural machines: collection of scientific papers; Agriculture State Publishers: Leningrad, Russia, 1936; Volume 2, pp. 269–284.

113. Voityuk, D.G.; Tsarenko, A.N.; Yatsun, S.S. *Mechanical and Technological Properties of Agricultural Materials: Practical Course*; Agrarian Education: Kiev, Ukraine, 2000.

114. *Provisional Technique for Determining Additional Economic Benefit Due to Reduced Damage and Soiling of Roots When Testing Beet Harvester Pilot Models*; Regulatory and directive legal documents; Ukrainian Research Institute of Agricultural Machine Engineering: Kharkiv, Ukraine, 1986.

115. Gevko, B.M. *Scientific Basis for Development of Helical Conveying Mechanisms in Agricultural Machines: Author's Abstract of the Thesis for the Degree of Doctor Sc. Eng.*; Rostov Institute of Agricultural Machine Engineering: Rostov-on-Don, Russia, 1987.

116. Gevko, R.B. *Theoretical Substantiation of Motion of Root in Wheel Lifter*; Bulletin of Ternopol Instrument Engineering Institute: collection of scientific papers; TIEI: Ternopol, Ukraine, 1996; No. 2; pp. 100–108.

117. Gevko, R.B.; Polishchuk, V.A. *Selection of Parameters of Sugar Beet Combine Harvesters Subject to Not Damaging Roots*; Agricultural machines: collection of scientific papers; VV IAU: Lutsk, Ukraine, 1997; Issue 3, pp. 13–20.

118. Glukhovsky, V.S. *System Mechanisation of Sugar Beet Production*; Harvest: Kiev, Ukraine, 1976.

119. Glukhovsky, V.S.; Zuyev, N.M.; Yonitsoy, Y.S. *New Method of Sugar Beet Cultivation*; Sugar Beet: Moscow, Russia, 1994; No. 1; pp. 12–14.

120. Gernet, M.M. *Course in Theoretical Mechanics*; Higher School: Moscow, Russia, 1987.

121. Glevasky, I.V. *Sugar Beet Growing: Learning Aid*; Higher School: Kiev, Ukraine, 1991.

122. Holovach, I.; Zavgorodny, A.; Zavgorodny, O. *PC-Assisted Numerical Calculation of Amplitude of Forced Longitudinal Oscillations of Root Fixed in Soil*; MOTROL: Motorization and Power Industry in Agriculture: proceedings IV International Research and Technical Conf.; NAUU: Lublin-Kyiv, Ukraine, 2003; Volume 6, pp. 140–145.

123. Holovach, I.V.; Litvinov, O.I.; Baulin, A.M. *Generation of Model of Extracting Beet Root with Vibrational Lifting Tool*; Studies of Tavria State Agricultural Technology Academy: collection of scientific papers; TSATA: Melitopol, Ukraine, 2006; Issue 39, pp. 206–216.

124. Goldsmit, V. *Impact*; State Construction Publishers: Moscow, Russia, 1965.

125. Denisenko, I.I. *Study on Physical and Mechanical Properties of Sugar Beet and Mechanised Operations in Its Harvesting: Author's Abstract of the Thesis for the Degree of Candidate of Sc. Eng., Branch 05.20.01*; NAU: Kiev, Ukraine, 1965.

126. Germain, P. *Course of Continuum Mechanics*; Higher School: Moscow, Russia, 1983; 400p.

127. Bulgakov, V.; Pascuzzi, S.; Ivanovs, S.; Nadykto, V.; Nowak, J. Kinematic discrepancy between driving wheels evaluated for a modular traction device. *Biosyst. Eng.* **2020**, *196*, 88–96. [CrossRef]

128. Bulgakov, V.; Pascuzzi, S.; Nadykto, V.; Ivanovs, S.; Adamchuk, V. Experimental study of the implement-and-tractor aggregate used for laying tracks of permanent traffic lanes inside controlled traffic farming systems. *Soil Tillage Res.* **2021**, *208*, 104895. [CrossRef]

129. Bulgakov, V.; Pascuzzi, S. Mathematical model of the movement of a potato body along the surface of a spiral separator. *Acta Hortic.* **2021**, *1311*, 447–454. [CrossRef]

130. Pascuzzi, S.; Bulgakov, V. The theory of sifting the soil mass when cleaning potatoes on a spiral separator. *Acta Hortic.* **2021**, *1311*, 417–424. [CrossRef]

131. Pascuzzi, S.; Cerruto, E. Spray deposition in "tendone" vineyards when using a pneumatic electrostatic sprayer. *Crop Prot.* **2015**, *68*, 1–15. [CrossRef]

132. Pascuzzi, S. A multibody approach applied to the study of driver injures due to a narrow-track wheeled tractor rollover. *J. Agric. Eng.* **2015**, *46*, 105–114. [CrossRef]

133. Pascuzzi, S.; Cerruto, E. An innovative pneumatic electrostatic sprayer useful for tendone vineyards. *J. Agric. Eng.* **2015**, *46*, 123–127. [CrossRef]

134. Pascuzzi, S.; Blanco, I.; Anifantis, A.S.; Scarascia Mugnozza, G. Hazards assessment and technical actions due to the production of pressured hydrogen within a pilot photovoltaic-electrolyzer-fuel cell power system for agricultural equipment. *J. Agric. Eng.* **2016**, *47*, 89–93.

135. Anifantis, A.S.; Pascuzzi, S.; Scarascia Mugnozza, G. Geothermal source heat pump performance for a greenhouse heating system. An experimental study. *J. Agric. Eng.* **2016**, *47*, 164–170. [CrossRef]

136. Pascuzzi, S. Outcomes on the Spray Profiles Produced by the Feasible Adjustments of Commonly Used Sprayers in "Tendone" Vineyards of Apulia (Southern Italy). *Sustainability* **2016**, *8*, 1307. [CrossRef]

137. Pascuzzi, S.; Cerruto, E.; Manetto, G. Foliar spray deposition in a "tendone" vineyard as affected by airflow rate, volume rate and vegetative development. *Crop Prot.* **2017**, *91*, 34–48. [CrossRef]

138. Bulgakov, V.; Pascuzzi, S.; Ivanovs, S.; Kaletnik, G.; Yanovich, V. Angular oscillation model to predict the performance of a vibratory ball mill for the fine grinding of grain. *Biosyst. Eng.* **2018**, *171*, 155–164. [CrossRef]

139. Bulgakov, V.; Pascuzzi, S.; Nadykto, V.; Ivanovs, S. A mathematical model of the plane-parallel movement of an asymmetric machine-and-tractor aggregate. *Agriculture* **2018**, *8*, 151. [CrossRef]

140. Bulgakov, V.; Kutsenko, A.; Ivanovs, S.; Pascuzzi, S. Study on propagation regularity of harmonic waves in periodic structures of beam. *Eng. Rural Dev.* **2019**, *18*, 1053–1058.

141. Bulgakov, V.; Pascuzzi, S.; Adamchuk, V.; Kuvachov, V.; Nozdrovicky, L. Theoretical study of transverse offsets of wide span tractor working implements and their influence on damage to row crops. *Agriculture* **2019**, *9*, 144. [CrossRef]

142. Bulgakov, V.; Pascuzzi, S.; Beloev, H.; Ivanovs, S. Theoretical Investigations of the Headland Turning Agility of a Trailed Asymmetric Implement-and-Tractor Aggregate. *Agriculture* **2019**, *9*, 224. [CrossRef]

143. Bulgakov, V.; Pascuzzi, S.; Adamchuk, V.; Ivanovs, S.; Pylypaka, S. A theoretical study of the limit path of the movement of a layer of soil along the plough mouldboard. *Soil Tillage Res.* **2019**, *195*, 104406. [CrossRef]

144. Bulgakov, V.; Kaletnik, H.; Goncharuk, T.; Rucins, A.; Dukulis, I.; Pascuzzi, S. Research of the movement of agricultural aggregates using the methods of the movement stability theory. *Agron. Res.* **2019**, *17*, 1846–1860. [CrossRef]

145. Bulgakov, V.; Ivanovs, S.; Pascuzzi, S.; Boris, A.; Ihnatiev, Y. A mathematical model of the cutting process of the sugar beet leafy tops without a tracer. *INMATEH Agric. Eng.* **2019**, *59*, 33–40. [CrossRef]

146. Pascuzzi, S.; Sobczak, P.; Przywara, A.; Kachel MSantoro, F. Assessment of physical properties of pet-food based on wheat middlings and meat meal. In Proceedings of the 19th International Scientific Conference "Engineering for rural development" Proceedings, Jelgava, Latvia, 20–22 May 2020; Volume 19, pp. 198–203. [CrossRef]

147. Kraszkiewicz, A.; Sobczak, P.; Santoro, F.; Anifantis, A.S.; Pascuzzi, S. Co-firing of biomass with gas fuel in low–power boilers. In Proceedings of the 19th International Scientific Conference "Engineering for rural development" Proceedings, Jelgava, Latvia, 20–22 May 2020; Volume 19, pp. 76–81. [CrossRef]

148. Pascuzzi, S.; Bulgakov, V.; Santoro, F.; Anifantis, A.S.; Ivanovs, S.; Holovach, I. A Study on the Drift of Spray Droplets Dipped in Airflows with Different Directions. *Sustainability* **2020**, *12*, 4644. [CrossRef]

149. Pascuzzi, S.; Anifantis, A.S.; Santoro, F. The Concept of a Compact Profile Agricultural Tractor Suitable for Use on Specialised Tree Crops. *Agriculture* **2020**, *10*, 123. [CrossRef]

150. Parlavecchia, M.; Pascuzzi, S.; Anifantis, A.S.; Santoro, F.; Ruggiero, G. Use of GIS to Evaluate Minor Rural Buildings Distribution Compared to the Communication Routes in a Part of the Apulian Territory (Southern Italy). *Sustainability* **2019**, *11*, 4700. [CrossRef]

151. Anifantis, A.S.; Lorencowicz, E.; Przywara, A.; Pascuzzi, S.; Ruggiero, G.; Santoro, F. Common greenhouse conditioning plants compared with versatile geothermal system in Ames, Iowa". In Proceedings of the 18th International Scientific Conference "Engineering for rural development" Proceedings, Jelgava, Latvia, 22–24 May 2019; Volume 18, pp. 1325–1330. [CrossRef]

152. Bulgakov, V.; Pascuzzi, S.; Arak, M.; Santoro, F.; Anifantis, A.S.; Ihnatiev, Y.; Olt, J. An experimental investigation of performance levels in a new root crown cleaner. *Agron. Res.* **2019**, *17*, 358–370. [CrossRef]

153. Guerrieri, A.S.; Anifantis, A.S.; Santoro, F.; Pascuzzi, S. Study of a Large Square Baler with Innovative Technological Systems that Optimize the Baling Effectiveness. *Agriculture* **2019**, *9*, 86. [CrossRef]

154. Bulgakov, V.; Pascuzzi, S.; Santoro, F.; Anifantis, A.S. Mathematical Model of the Plane-Parallel Movement of the Self-Propelled Root-Harvesting Machine. *Sustainability* **2018**, *10*, 378. [CrossRef]

155. Pascuzzi, S.; Anifantis, A.S.; Cimino, V.; Santoro, F. Unmanned aerial vehicle used for remote sensing on an Apulian farm in southern Italy. In Proceedings of the 17th International Scientific Conference "Engineering for Rural Development" Proceedings, Jelgava, Latvia, 23–25 May 2018; Volume 17. [CrossRef]

156. Anifantis, A.S.; Przywara, A.; Pascuzzi, S.; Santoro, F. Performance of photovoltaic and ground source heat pump system for daytime cooling of mushroom greenhouse during summer: preliminary analysis. In Proceedings of the 17th International Scientific Conference "Engineering for rural development" Proceedings, Jelgava, Latvia, 23–25 May 2018; Volume 17. [CrossRef]

157. Anifantis, A.S.; Colantoni, A.; Pascuzzi, S.; Santoro, F. Photovoltaic and Hydrogen Plant Integrated with a Gas Heat Pump for Greenhouse Heating: A Mathematical Study. *Sustainability* **2018**, *10*, 378. [CrossRef]

158. Pascuzzi, S.; Santoro, F. Analysis of the Almond Harvesting and Hulling Mechanization Process: A Case Study. *Agriculture* **2017**, *7*, 100. [CrossRef]

159. Pascuzzi, S.; Santoro, F. Evaluation of farmers' OSH hazard in operation nearby mobile telephone radio base stations. In Proceedings of the 16th International Scientific Conference "Engineering for rural development" Proceedings, Jelgava, Latvia, 24–26 May 2017; Volume 16, pp. 748–755. [CrossRef]

160. Goryachkin, V.P. *Collected Works-Volume 2*, 2nd ed.; State Publishers: Moscow, Russia, 1968.

161. Goryachkin, V.P. *Collected Works-Volume 3*, 2nd ed.; State Publishers: Moscow, Russia, 1968.

162. Gurchenko, A.P. *Trends in Enhancement of Efficiency of Beet Harvesting Machinery*; Technical Facilities of Agricultural Sector: Kiev, Ukraine, 1997; No. 3.

163. Didenko, N.F.; Khvostov, V.A.; Medvedev, V.P. *Vegetable Harvesting Machines*; State Publishers Mechanical Engineering: Moscow, Russia, 1984.

164. Zeldovich, Y.B.; Myshkis, A.D. *Elements of Applied Mathematics*, 2nd ed.; State Publishers: Science: Moscow, Russia, 1967.

165. Zubenko, V.F. *Special Features of Industrial Engineering*; Sugar Beet: Moscow, Russia, 1980; No. 5; pp. 21–22.

166. Zubenko, V.F. *Sugar Beet*; Harvest: Kiev, Ukraine, 1979.

167. Zuyev, N.M. Study on Quality of Operation of Sugar Beet Combine Harvesters in Relation to Agrophysical Properties of Sugar Beet in Various Approaches to Forming Plantations. Ph.D. Thesis, V.N. Karazin Kharkiv National University, Kharkiv, Ukraine, 1971.

168. Zuyev, N.M. *Bonding Forces between Roots and Soil*; Mechanisation and Electrification of Socialist Agricultural Industry: Moscow, Russia, 1970; p. 10.

169. Myata, A.S.; Chumak, A.V. (Eds.) *Research into Tools of Agricultural Machines*; Collection of Research Papers of VISKhOM/sc.; Mechanical Engineering State Publishers: Moscow, Russia, 1954.

170. Ignatyeva, T. *How and When to Harvest Sugar Beets*; State Publishers Sugar Beet: Moscow, Russia, 2004; No. 8–9; pp. 24–25.

171. Kirnosov, V.I. *Measurement of Mechanical Characteristics of Materials*; State Standards Publishers: Moscow, Russia, 1976.

172. Kovalchuk, A.S.; Kravchuk, V.I.; Bulgakov, V.M. *On Future Lines of Development in Sugar Beet Harvesting*; Advanced technologies of growing and harvesting sugar beets: Bulletin of National Agrarian University; NAU: Kiev, Ukraine, 1997; Volume 2, pp. 3–8.

173. Kovtun, Y.I. *Density of Planting, Crop Yield and Quality of Harvesting*; Sugar Beet: Moscow, Russia, 1994; No. 6; pp. 6–7.

174. Kovtun, Y.I. *Development Trends in Beet Growing*; Sugar Beet Production and Processing: Moscow, Russia, 1991; No. 1; pp. 54–77.

175. Kovtun, Y.I. *Technological Capabilities of Facilities in Realization of Beet's Biological Potential*; Sugar Beet: Moscow, Russia, 1992; No. 3; pp. 25–31.

176. Kovtun, Y.I.; Minchin, G.G.; Dorodnykh, A.V. *Current Situation and Trends in Development of Machine Technology and Machine Design in Sugar Beet Growing Abroad*; State Publishers Central Information and Technical and Economic Research Institute of Tractor Agricultural Mechanical Engineering: Kiev, Ukraine, 1975.

177. Kozibroda, Y.I. *Development of Work Process and Machinery for Topping Sugar Beet Roots: Author's Abstract of the Thesis for the Degree of Candidate of Sc. Eng., Branch 05.05.11 in the form of a Scientific Report*; VISKhOM: Moscow, Russia, 1992; 21p.

178. Kozibroda, Y.I. *Trends in Development of Sugar Beet Harvesting Machines*; Zbruch: Ternopol, Ukraine, 1996; 92p.

179. Korn, G.; Korn, T. *Mathematical Handbook*; transl. from Eng.; Science: Moscow, Russia, 1970; 719p.

180. Letoshnev, M.N. *Agricultural Machines. Theory, Design, Engineering and Testing*; Moscow-Leningrad State Publishers of Agricultural Literature: Moscow, Russia, 1955; 764p.

181. Linnik, N.K.; Bulgakov, V.M. *Main Trends in Basic Research into Mechanisation of Sugar Beet Harvesting*; Problems and opportunities in development of sugar beet harvesting facilities: collection of scientific papers; VNTU: Vinnitsa, Ukraine, 1996; p. 1.

182. Lurye, A.B. *Modelling Agricultural Units*; Spike: Moscow, Russia, 1979.

183. Lurye, A.B. *Statistical Dynamics of Agricultural Units*; Spike: Moscow, Russia, 1981.

184. Manpil, L.I. *Determination of Coefficient of Instantaneous Friction of Root Tubers on Working Face*; Tractors and Agricultural Machines: Moscow, Russia, 1986; No. 12; pp. 28–30.

185. National Standards of Ukraine. *Sugar Beet Harvesting Machines: DSTU 2258-93 (GOST 7496-93): General Specifications (to Replace GOST 7496-84)*; State Standard of Ukraine: Kiev, Ukraine, 1993.

186. Makovetsky, O.A.; Brei, V.V.; Pogorely, L.V. *Mechanisation of Sugar Beet Production*; Harvest: Kiev, Ukraine, 1991.

187. Tsymbal, A.G.; Tatyanko, N.V.; Basin, V.S. *Machines for Sugar Beet Growing*; Mechanical Engineering: Moscow, Russia, 1976.

188. Pogorely, L.V. (Ed.) *Mechanisation of Sugar Beet Production*, 2nd ed.; rev. and enl.; Harvest: Kiev, Ukraine, 1991; 184p.

189. *Technique for Determining Economic Efficiency of Application of New Equipment, Inventions and Technical Innovations in Economy*; State Publishers Patent Information Research Institute of Russia: Moscow, Russia, 1982.

190. Myshkis, A.D. *Mathematics*; Special courses; Science: Moscow, Russia, 1971; 632p.

191. Melnichuk, D.A. (Ed.) *Scientific Foundations for the Sustainable Development of Agriculture in Woodland-and-Steppe area of Ukraine: Treatise [in 2 vol.]*; Cabinet of Ministers of Ukraine National Agrarian University; OOO «Alefa»: Kiev, Ukraine, 2003; Volume 1, 886p.

192. Yasenetsky, V.A. (Ed.) *New Agricultural Equipment*; Harvest: Kiev, Ukraine, 1991; 320p.

193. Orlov, V.P. *Engineering Analysis of Multi-Criterion Problems*; Science: Moscow, Russia, 1982; 98p.

194. Volkov, P.M.; Tenenbaum, M.M. (Eds.) *Elements of Theory and Analysis of Agricultural Machines with Regard to Strength and Reliability*; Mechanical Engineering: Moscow, Russia, 1977; 310p.

195. OST 70.8.6.-83: Testing Agricultural Equipment. In *Sugar Beet Harvesting Machines: Test Programme and Technique*; State Publishers USSR State Committee for Production and Engineering Support of Agricultural Equipment: Moscow, Russia, 1984.

196. Pavlovsky, M.A.; Putyata, T.V. *Theoretical Mechanics*; Higher School: Kiev, Ukraine, 1985; 318p.

197. Palkin, G. Harvesting beet roots in one run. *News Agric. Eng.* **2005**, *3*, 7.

198. Parlavecchia, M.; Pascuzzi, S.; Santoro, F.; Ruggiero, G. Minor rural building heritage and territorial features in local action group sud est barese area (southern italy). In Proceedings of the 20th International Scientific Conference Engineering for Rural Development, Jelgava, Latvia, 26–28 May 2021; Volume 20, pp. 1409–5976. [CrossRef]

199. Bulgakov, V.; Kuvachov, V.; Ivanovs, S.; Melnyk, V.; Santoro, F.; Olt, J. Operational and technological properties of ploughing block-modular machine-and-tractor aggregate. In Proceedings of the 20th International Scientific Conference Engineering for Rural Development, Jelgava, Latvia, 26–28 May 2021; Volume 20, pp. 650–656. [CrossRef]

200. Bulgakov, V.; Ivanovs, S.; Yaremenko, V.; Santoro, F. Research in dynamic transitional processes of functioning of combine harvester hydraulic drives. In Proceedings of the 20th International Scientific Conference Engineering for Rural Development, Jelgava, Latvia, 26–2 May 2021; Volume 20, pp. 643–649. [CrossRef]

201. Pascuzzi, S.; Guerrieri, A.S.; Vicino, F.; Santoro, F. Assessment of required torque and power by big square baler during the wrapping and baling process. In Proceedings of

the 20th International Scientific Conference Engineering for Rural Development, Jelgava, Latvia, 26–28 May 2021; Volume 20, pp. 298–302. [CrossRef]

202. Bulgakov, V.; Adamchuk, O.; Pascuzzi, S.; Santoro, F.; Olt, J. Research into engineering and operation parameters of mineral fertiliser application machine with new fertiliser spreading tools. *Agron. Res.* **2021**, *19*, 676–686. [CrossRef]

203. Bulgakov, V.; Adamchuk, O.; Pascuzzi, S.; Santoro, F.; Olt, J. Experimental research into uniformity in spreading mineral fertilizers with fertilizer spreader disc with tilted axis. *Agron. Res.* **2021**, *19*, 28–41. [CrossRef]

204. Bulgakov, V.; Pascuzzi, S.; Ivanovs, S.; Ruzhylo, Z.; Fedosiy, I.; Santoro, F. A New Spiral Potato Cleaner to Enhance the Removal of Impurities and Soil Clods in Potato Harvesting. *Sustainability* **2021**, *12*, 9788. [CrossRef]

205. Rydzak, L.; Kobus, Z.; Nadulski, R.; Wilczyński, K.; Pecyna, A.; Santoro, F.; Sagan, A.; Starek, A.; Krzywicka, M. Analysis of Selected Physicochemical Properties of Commercial Apple Juices. *Processes* **2020**, *8*, 1457. [CrossRef]

206. Przywara, A.; Santoro, F.; Kraszkiewicz, A.; Pecyna, A.; Pascuzzi, S. Experimental Study of Disc Fertilizer Spreader Performance. *Agriculture* **2020**, *10*, 467. [CrossRef]

207. Hassaan, M.A.; Pantaleo, A.; Santoro, F.; Elkatory, M.R.; De Mastro, G.; El Sikaily, A.; Ragab, S.; El Nemr, A. Techno-Economic Analysis of ZnO Nanoparticles Pretreatments for Biogas Production from Barley Straw. *Energies* **2020**, *13*, 5001. [CrossRef]

208. Coppola, G.; Costantini, M.; Orsi, L.; Facchinetti, D.; Santoro, F.; Pessina, D.; Bacenetti, J. A Comparative Cost-Benefit Analysis of Conventional and Organic Hazelnuts Production Systems in Center Italy. *Agriculture* **2020**, *10*, 409. [CrossRef]

209. Bulgakov, V.; Ivanovs, S.; Santoro, F.; Anifantis, A.S. Experimental research of energy-power parameters of vane cleaner of beet root heads with horizontal drive shafts. In Proceedings of the Engineering for Rural Development, Jelgava, Latvia, 20–22 May 2020; Volume 19, pp. 406–412. [CrossRef]

210. Santoro, F.; Przywara, A.; Sobczak, P.; Kraszkiewicz, A.; Anifantis, A.S. Lightning protection systems in stables. In Proceedings of the 19th International Scientific Conference "Engineering for rural development" Proceedings, Jelgava, Latvia, 20–22 May 2020; Volume 19, pp. 313–318. [CrossRef]

211. Rajabi Hamedani, S.; Villarini, M.; Colantoni, A.; Carlini, M.; Cecchini, M.; Santoro, F.; Pantaleo, A. Environmental and Economic Analysis of an Anaerobic Co-Digestion Power Plant Integrated with a Compost Plant. *Energies* **2020**, *13*, 2724. [CrossRef]

212. Pantaleo, A.; Villarini, M.; Colantoni, A.; Carlini, M.; Santoro, F.; Rajabi Hamedani, S. Techno-Economic Modeling of Biomass Pellet Routes: Feasibility in Italy. *Energies* **2020**, *13*, 1636. [CrossRef]

213. Zavadskiy, V.; Anifantis, A.S.; Santoro, F. Solving of renewable energy sources usable potential evaluation in remote rural area on example of Basilicata region (Southern Italy)—Case study. In Proceedings of the 18th International Scientific Conference "Engineering for rural development" Proceedings, Jelgava, Latvia, 22–24 May 2019; Volume 18, pp. 1401–1407. [CrossRef]

214. Bulgakov, V.; Ivanovs, S.; Santoro, F.; Anifantis, A.S. Experimental investigation of the energy-power characteristics of the cleaner of the root crop heads from the haulm. In Proceedings of the 18th International Scientific Conference "Engineering for rural development" Proceedings, Jelgava, Latvia, 22–24 May 2019; Volume 18, pp. 129–135. [CrossRef]

215. Kobus, Z.; Nadulski, R.; Anifantis, A.S.; Santoro, F. Effect of press construction on yield of pressing and selected quality characteristics of apple juice". In Proceedings of the 17th International Scientific Conference "Engineering for rural development" Proceedings, Jelgava, Latvia, 23–25 May 2018; Volume 17. [CrossRef]

216. Koszel, M.; Przywara, A.; Santoro, F.; Anifantis, A.S. Evaluation of use of biogas plant digestate as fertilizer in alfalfa and winter wheat. In Proceedings of the 17th International Scientific Conference "Engineering for rural development" Proceedings, Jelgava, Latvia, 23–25 May 2018; Volume 17. [CrossRef]

217. Przywara, A.; Koszel, M.; Santoro, F.; Anifantis, A.S. Comparison of selected physical parameters of rapeseed cultivars. In Proceedings of the 17th International Scientific Conference "Engineering for rural development" Proceedings, Jelgava, Latvia, 23–25 May 2018; Volume 17. [CrossRef]

218. Bianchi, B.; Tamborrino, A.; Santoro, F. "Assessment of the energy and separation efficiency of the decanter centrifuge with regulation capability of oil water ring in the industrial process line using a continuous method." In: "Proceedings of the 10th Conference of the Italian Society of Agricultural Engineering-Horizons in agricultural, forestry and biosystems engineering." Viterbo, Italy, 08-12/09/2013. *J. Agricu. Eng.* **2013**, *XLIV*, 278–282. [CrossRef]

219. Przywara, A.; Anifantis, A.S.; Pascuzzi, S.; Santoro, F.; Kraszkiewicz, A. Assessment of relationship between mean radius of mineral fertilizer spreading area and examined features. In Proceedings of the 19th International Scientific Conference "Engineering for rural development" Proceedings, Jelgava, Latvia, 20–22 May 2020; Volume 19, pp. 134–139. [CrossRef]

220. Anifantis, A.S.; Przywara, A.; Sobczak, P.; Pascuzzi, S.; Santoro, F. Energy performance comparison of two small scale combined geothermal heating plants for greenhouse heating. In Proceedings of the 19th International Scientific Conference "Engineering for rural development" Proceedings, Jelgava, Latvia, 20–22 May 2020; Volume 19, pp. 63–68. [CrossRef]

221. Bulgakov, V.; Holovach, I.; Kiurchev, S.; Pascuzzi, S.; Arak, M.; Santoro, F.; Anifantis, A.S.; Olt, J. The theory of vibrational wave movement in drying grain mixture. *Agron. Res.* **2020**, *18*, 360–375. [CrossRef]

222. Anifantis, A.S.; Camposeo, S.; Vivaldi, G.A.; Santoro, F.; Pascuzzi, S. Comparison of UAV Photogrammetry and 3D Modeling Techniques with Other Currently Used Methods for Estimation of the Tree Row Volume of a Super-High-Density Olive Orchard. *Agriculture* **2019**, *9*, 233. [CrossRef]

223. Bulgakov, V.; Pascuzzi, S.; Anifantis, A.S.; Santoro, F. Oscillations Analysis of Front-Mounted Beet Topper Machine for Biomass Harvesting. *Energies* **2019**, *12*, 2774. [CrossRef]

224. Pascuzzi, S.; Santoro, F.; Anifantis, A.S.; Cimino, V. Correlation analysis between vegetation index (NDVI) and canopy coverage (TOC) based on remote sensing by using UAV. In Proceedings of the 18th International Scientific Conference "Engineering for rural development" Proceedings, Jelgava, Latvia, 22–24 May 2019; Volume 18, pp. 214–220. [CrossRef]

225. Bulgakov, V.; Pascuzzi, S.; Nikolaenko, S.; Santoro, F.; Anifantis, A.S.; Olt, J. Theoretical study on sieving of potato heap elements in spiral separator. *Agron. Res.* **2019**, *17*, 33–48. [CrossRef]

226. Santoro, F.; Anifants, A.S.; Ruggiero, G.; Zavadskiy, V.; Pascuzzi, S. Lightning Protection Systems Suitable for Stables: A Case Study. *Agriculture* **2019**, *9*, 72. [CrossRef]

227. Pascuzzi, S.; Santoro, F.; Manetto, G.; Cerruto, E. Study of the correlation between foliar and patternator deposits in a "Tendone" vineyard. *Agric. Eng. Int. CIGR J.* **2018**, *20*, 97–107.

228. Cerruto, E.; Manetto, G.; Santoro, F.; Pascuzzi, S. Operator Dermal Exposure to Pesticides in Tomato and Strawberry Greenhouses from Hand-Held Sprayers. *Sustainability* **2018**, *10*, 2273. [CrossRef]

229. Anifantis, A.S.; Pascuzzi, S.; Santoro, F. Performance comparison between fuel cell coupled with geothermal source heat pump and geothermal source gas engine heat pump system for greenhouse heating: A mathematical study. In Proceedings of the 17th International Scientific Conference "Engineering for rural development" Proceedings, Jelgava, Latvia, 23–25 May 2018; Volume 17. [CrossRef]

230. Santoro, F.; Lorencowicz, E.; Anifantis, A.S.; Pascuzzi, S. Stability analysis of platforms for picking fruit according to forthcoming standard EN 16952: A case study. In Proceedings of the 17th International Scientific Conference "Engineering for rural development" Proceedings, Jelgava, Latvia, 23–25 May 2018; Volume 17. [CrossRef]

231. Pascuzzi, S.; Santoro, F. Analysis of Possible Noise Reduction Arrangements inside Olive Oil Mills: A Case Study. *Agriculture* **2017**, *7*, 88. [CrossRef]

232. Petrov, G.D.; Manpil, L.I.; Shakhotin, M.M. *Analytical Estimation of Kinetic Energy Loss in Case of Root Tubers Colliding with Plane*; Papers of VISKhOM; Research and Production Association VISKhOM: Moscow, Russia, 1976; pp. 21–24.

233. Petrov, G.D.; Orlov, P.E.; Starikov, V.M.; Karev, E.B. *Long-Term Trends in Development of Sugar Beet Harvesting Equipment*; Tractors and agricultural machines; State Press: Kiev, Ukraine, 1994; Volume 11, pp. 7–11.

234. Pogorely, L.V. *Engineering Methods of Agricultural Equipment Testing*; State Publishers Engineering: Kiev, Ukraine, 1991.

235. Pogorely, L.V. *Research and Development of Sugar Beet Root Topping Work Process: Author's Abstract of the Thesis for the Degree of Candidate of Sc. Eng., Branch 05.20.01*; Ukrainian Academy of Agriculture: Kiev, Ukraine, 1964.

236. Pogorely, L.V. *Raising Operation and Process Efficiency of Agricultural Equipment*; Kiev Engineering: Kiev, Ukraine, 1990.

237. Pogorely, L.V. *Process and Engineering Principles of Improvement of Mechanised Sugar Beet Harvesting Processes: Author's Abstract of the Thesis for the Degree of Doctor Sc. Eng., Branch 05.20.01*; Ukrainian Academy of Agriculture: Kiev, Ukraine, 1974.

238. Pogorely, L.V.; Bilsky, V.G.; Kononenko, N.P. *Scientific Basis for Improvement of Agricultural Equipment*; Harvest: Kiev, Ukraine, 1989.

239. Pogorely, L.V.; Pokusa, A.A.; Kuzminov, V.G. Trends in development of optimal range of sugar beet harvesting machines. *Eng. Agric.* **1988**, *6*, 43–45.

240. Pogorely, M.L. *Improvement of Technological Efficiency of Sugar Beet Harvesting Machines: Author's Abstract of the Thesis for the Degree of Candidate of Sc. Eng., Branch 05.05.11*; NAU: Kiev, Ukraine, 2001.

241. Agricultural Machines. *Elements of Theory and Analysis*; Higher Education: Kiev, Ukraine, 2005; 464p.

242. Pisarenko, G.S.; Yakovlev, A.P.; Matveyev, V.V. *Handbook on Strength of Materials*; Scientific Thought: Kiev, Ukraine, 1975.

243. Piskunov, N.S.; Calculus, N.S. *Piskunov*, 9th ed.; Science: Moscow, Russia, 1970; Volume 2.

244. Melnikov, S.V.; Aleshkin, V.R.; Roshchin, P.M. *Planning Experiments in Studies on Agricultural Processes*, 2nd ed.; Spike: Leningrad, Russia, 1980.

245. Pogrebnyak, S.P.; Rarog, G.P.; Ilyevich, S.V. *Improving Technology*; Sugar Beet Production and Processing: Moscow, Russia, 1990; No. 1; pp. 23–24.

246. Birger, I.A.; Panovko, Y.G. (Eds.) *Strength. Stability. Vibrations: Handbook: [in 3 vol.]*; State Publishers Mechanical Engineering: Moscow, Russia, 1968.

247. Revenko, I.I. *Machine Systems*; State Publishers Knowledge: Kiev, Ukraine, 1982.

248. Rogatinsky, R.M. Mechanical and Technological Elements of Interaction between Auger-Type Tools and Raw Stock in Agricultural Production. Ph.D. Thesis, National Agrarian University, Kiev, Ukraine, 1997.

249. Savchenko, K.A.; Zhukov, A.V.; Kovalyov, N.M. *Sugar Beet Production in USA*; State Publishers Sugar Beet: Moscow, Russia, 1982; No. 7; pp. 38–40.

250. Sedov, L.I. *Continuum Mechanics Volume 1 & 2*; Science: Moscow, Russia, 1984.

251. Noyabr, G.E.; Demidov, G.K.; Zonov, B.I. Agricultural and Melioration Machines. Noyabr, G.E, Ed.; Agricultural Industry Publishers: Moscow, Russia, 1986.

252. Kletskin, M.I. *Agricultural Machine Designer's Handbook: [in 4 vol.]*; Mechanical Engineering: Moscow, Russia, 1969.

253. Sukhanova, R.S. *Mechanisation of harvesting in Western Europe*; Sugar Beet: Moscow, Russia, 1986; No. 8; pp. 45–48.

254. *Tariff and Hourly Wages of Employees in Agricultural Industry: Decree of State Committee of Central Labour and Remuneration Agency of Ukraine of 01.11.1994*; State Publishers: Kiev, Ukraine, 1994; Regulatory and directive legal documents.

255. Timoshenko, S.P.; Young, D.H.; Weaver, W. *Vibration Problems in Engineering*; transl. from Eng.; Mechanical Engineering: Moscow, Russia, 1985.

256. Tkatchenko, O.M.; Royika, M.V. (Eds.) *Ukrainian Intensive Technology of Sugar Beet Growing*; Academy Press: Kiev, Ukraine, 1998.

257. Ferster, E.; Renz, B. *Methods of Correlation and Regression Analysis*; Finance and Statistics: Moscow, Russia, 1983.

258. *Physical and Mechanical Properties of Plants, Soils and Fertilisers*; Mechanical Engineering: Moscow, Russia, 1970.

259. Voronyuk, B.A.; Pyankov, A.I.; Maltseva, L.V. *Physical and Mechanical Properties of Plants, Soils and Fertilisers: Methods of Research, Instruments, Data*; Spike: Moscow, Russia, 1970.

260. Khailis, G.A. *Mechanics of Plant Materials*; UAAS: Kiev, Ukraine, 1994.

261. Khailis, G.A. *Elements of Theory and Analysis of Agricultural Machines*; Publishing House of Ukrainian Academy of Agriculture: Kiev, Ukraine, 1992.

262. Khelemendik, N.M. *Trends and Methods in Development of Tools for Agricultural Machines*; Agrarian Science: Kiev, Ukraine, 2001.

263. Khelemendik, N.M. *Improvement of Mechanical and Technological Efficiency of Labour-Intensive Processes in Sugar Beet Growing: Abstract of Thesis for the Degree of Doctor of Engineering Science: Speciality 05.20.01*; Ternopol Instrument Engineering Institute: Ternopol, Ukraine, 1996.

264. Khelemendik, N.M. *Study on work process and tools for sugar beet harvesting in Western Steppe of Ukrainian SSR. PhD thesis Branch 05.20.01*; Voronezh State University: Voronezh, Russia, 1968.

265. Haug, E.; Arora, J. *Applied Optimal Design: Mechanical and Structural Systems*; Mir: Moscow, Russia, 1997; 478p.

266. Tsurpal, I.A.; Bulgakov, V.M.; Finko, S.V. On development of new set of sugar beet harvesting machines for farm enterprises. In Proceedings of the Agrarian Science in Uman State Agrarian University: Problems, Research, Achievements: Materials of Scientific Conference, Kiev, Ukraine, 7 October 1993.

267. Shabalin, S.A. *Applied Metrology in Questions and Answers*; Standards Publishers: Moscow, Russia, 1990; 192p.

268. Schenck, H. *Theories of Engineering Experimentation*; Mir: Moscow, Russia, 1972; 374p.

269. Shpaar, D.; Kunze, A.; Mangraph, G. Advanced technologies in beet growing industry. *Sugar Beet* **1994**, *2*, 23–24.

270. Elsgoltz, L.E. *Differential Equations and Variational Calculus*; Science: Moscow, Russia, 1965; 235p.

271. Bulgakov, V.; Holovach, I. Mathematical model of vibrating excavation of the root crop from the ground. In Proceedings of the 5th Research and Development Conference of Central- and Eastern European Institutes of Agricultural Engineering, NAUU, Kiev, Ukraine 12–14 May 2007; pp. 199–209.

272. Bulgakov, V.; Holovach, I. Theoretical research of an extraction of roots of sugar beet. In Proceedings of the AGROTECH NITRA: 40 Years of Agricultural Engineering Study Branch and Its Effect on Agricultural Technical Sciences: Proceedings of Conf., Nitra, Slovenska Republika, 6 November 2002; pp. 52–72.

273. Bulgakov, V.; Holovach, I. *Longitudinal Oscillations of the Sugar Beet Root Crop Body at Vibrational Digging Up from Soil*; RES. AGR. ENG.; Czech Academy of Agricultural Sciences: Praha, Czhech Republic, 2005; pp. 93–98.

274. Bulgakov, V.; Holovach, I. Theory of the ploughshare digging out end-effectors for sugar beet root crops. In Proceedings of the International Science Conference of Materials Science and Manufacturing Technology, Prague, Czech Republic, 26–27 June 2007; pp. 273–289.

275. Bulgakov, V.; Holovach, I.; Berezovyy, M. Theory of the sugar beet root crops vibration digging up. In Proceedings of the TAE: Trends in Agricultural Engineering: Conference Proceedings 3rd International Conference, Prague, Czech Republic, 12–14 September 2007; pp. 84–91.

276. Bulgakov, V.; Holovach, I.; Nowak, J. *The Theory of Root Crops Vibrational Digging up Process*; MOTROL: Motorization and Power Industry in Agriculture; University of Life Science Lublin: Lublin, Poland, 2005; Volume VII, pp. 60–68.

277. Bulgakov, V.; Holovach, I.; Nowak, J. *Vibrating Way of Excavation of Root Crops of Sugar Beet*; MOTROL: Motorization and Power Industry in Agriculture; University of Life Science Lublin: Lublin, Poland, 2004; Volume VI, pp. 14–27.

278. Bulgakov, V.; Holovach, I.; Spokas, L. *Theoretical Investigation of a Root Crop cross Oscillations at Vibratinal Digging Up*; Agricultural Engineering: research papers; Raudondvaris: Kauno, Lithuania, 2005; pp. 19–35.

279. Bulgakov, V.; Holovach, I.; Szeptycki, A. Teoria dzialania lemieszowego zespolu podkopujacego w maszynach do zbioru burakow. *Sci. Pol. Acta Tech. Agrar.* **2003**, *2*, 67–74.

280. Bulgakov, V.; Holovach, I. *Build-Up of Mathematical Model of the Root Crop Vibrational Digging Up from Soil*; INZINERIJA Mokslo darbai; INZINERIJA Mokslo darbai Lituvos Mokslu Akademija: Vilnius, Lithuania, 2006; Volume 7, pp. 20–26.

281. Kesten, E. Entwicklungstendenzen in der Zuckerrubenernte. *Landtechnik* **1973**, *13*, 353–354.

282. Kromer, K.-H.; Schulze, P. Entwicklungder Mechnisierung Vou 1950 bis 2000. *Zuckerrube* **2001**, *4*, 254–259.

283. Kromer, K.-H.; Stratz, J.; Tschepe, M. Technischer Stand der Zuckerrubenernte–Rodertest Seligenstadt 2000. *Landtechnik* **2001**, *56*, 78–79.

284. Merkes, R. 50 Jahre Prodaktionstechnik im Zuckerrubenbau in Deutchland. *Zuckerrube* **2001**, *4*, 214–217.

285. Strum, R.D.; Kirk, D.E. *First Principles of Discrete Systems and Digital Signal Processing*; Addison-Wesley Publishing Company: Boston, MA, USA, 1988; 357p.

286. Thompson, J. Sugar Beet harvesting machine. *Br. Sugar Beet Rev.* **1987**, *58*, 59.

Index

relation between amplitude of oscillations and distance x of cross-section of conditional point of attachment *84*

relation between amplitude of oscillations/amplitude of disturbing force *85, 86*

scheme of forces having an action at time of gripping by vibration tool *60*

soil's elastic deformation coefficients *74*

values of first/second natural frequencies *73*

transverse 87–111

amplitude depends on distance from root's cross-section to conventional point of roots fixation in soil *106*

elastic deformation coefficient of soil *107, 108*

equivalent schematic model at moment when vibrational digging tool grips it 88

forced oscillations in soil 98–108

free oscillations in soil 87–98

relation between first natural frequency and soil's deformation coefficient c *97*

relation between second natural frequency and soil's deformation coefficient c *97*

values of first/second frequencies *96*

Ostrogradsky-Hamilton action see Hamilton-Ostrogradsky principle

Pascuzzi, S. 3
Petrov, G.D. 3
Pogorely, L.V. 3
Pogorely, M.L. 3
Progorely, L.V. 3

Ritz method 64–75, 76, 92–6, 110

Santoro, F. 3
scientific research, application of results in production 264
share lifters 14–18

analysis of force interaction with soil around root 37–9, *39, 40*

backup forces 16–17

conclusions 54–5

determination of projections of normal reactions on Cartesian coordinate 40–2

differential equation of motion of root during extraction 46–54

force interaction with working faces of shares during approach to/contact with root 42–6

geometrical parameters 15–17

physical model 17–18

schematic model of *15*

MDPI

MDPI